Université Lille Nord de France

Inserm

UNIVERSITÉ DROIT ET SANTÉ DE LILLE II

École Doctorale Biologie-Santé

THÈSE

Pour l'obtention du grade de

DOCTEUR DE L'UNIVERSITÉ DE LILLE II

Spécialité: Neurosciences

Morphological, molecular and genetic aspects of the GnRH neuronal migratory process in mice and humans

---

SAMUEL ANDREW MALONE

Thèse présentée et soutenue à Lille, le 20 octobre 2017

Composition du Jury:

Dr. Philippe CIOFI	Chargé de Recherche, INSERM U862, Bordeaux	Rapporteur
Pr. Ulrich BOEHM	Prof. Universität des Saarlandes, Germany	Rapporteur
Pr. Nelly PITTELOUD	Chef de service CHUV, Lausanne	Examinateur
Dr. Jenny VISSER	Group leader, Erasmus University, Rotterdam	Examinateur
Dr. Sophie CATTEAU-JONARD	PU-PH, Hôpital Jeanne de Flandre, Lille	Examinateur
Dr. Paolo GIACOBINI	Chargé de Recherche, INSERM U1172, Lille	Directeur de Thèse

To Jean Malone, who passed away
during the writing of this Thesis

Acknowledgments

To whomever is reading this, ok you don't get any credit for getting this far but once you're done with the acknowledgments I think you should stick around and read the rest, I think it's pretty cool. I'm also indebted to a lot of people for helping me reach the point where I could even attempt something like this. My mum for teaching me to read & write would be a good start... but skipping a few intervening years in which I grew and then lost a lot of hair, some other people snuck their way in there too.

Firstly, to the members of my thesis committee, Pr Nelly Pitteloud, Pr Ulrich Boehm, Dr Jenny Visser, Dr Philippe Ciofi *and* Dr Sophie Catteau-Jonard, *thank you for taking the time to evaluate this work and I hope the next time I see you we can share a nice wine (of course chosen by Philippe) and talk all about it!*

My dear supervisor Dr Paolo Giacobini, *I can't thank you enough for everything you've done for me. From meeting me at the station the very first time I arrived, through all the cigarette breaks, to this month of writing you've always been a great boss and friend. Your kindness has been instrumental to forging the atmosphere of the lab that is welcoming to everyone and makes us all feel like one big family. I couldn't have asked for a better mentor to guide me through this process and wish you every continued success for the future!*

Dr Vincent Prévot, *you answered a random email one fateful Thursday (I'm imagining there was rain lashing against the window and the roar of thunder) and four years later this is the result! It has been an honour and privilege to be a part of your lab, so thank you for giving me this opportunity. Considering our almost polar opposite sleep schedules, I feel I can now tell you that more than once I received an 'early' email from you as I was checking before going to bed, I've learnt a great deal from you and have always walked away from our conversations feeling enlightened and enthusiastic. I hope you've enjoyed it as much as I have and that I leave the lab a little better off than when I arrived!*

Béné, Ariane, David Blum; *To the bosses who have helped shape my project without ever taking any credit, thank you all for your helpful comments, expertise and insights (and chocolate).*

Anne et Danièle, vous êtes toutes les deux, le coeur du laboratoire sans qui nous serions tous perdus. Merci infiniment pour votre gentillesse et votre patience avec moi. Merci pour m'avoir appris comment travailler au laboratoire et pour toutes ces petites choses que vous faites pour nous tous quotidiennement. Vous êtes les meilleures!

Noury Noury Noury, *the girl with a heart the size of France. I almost can't imagine the lab before your smiles and laughter arrived. I don't really have anything funny to say (for once), just that I'm so so happy you came to the lab. They say friends are the family you choose, so I'm glad we chose each other. I know one day, not too far in the future, you're going to be where I am now, looking for something in a thesis... so remember, if you ever need it, you can come straight here to the very first page – you are amazing & we all believe you're going to do great things, never forget that!*

Giuli P, the Queen of Nonsense; '*It was the best of times, it was the worst of times'. Ok there's not really enough space or words to go full Dickens here about our theses, but suffice to say I couldn't imagine having done all this without you being here. I hope we've made each other better scientists and people*

through our time in Lille. Seeing you smile is always a delight, so whether you're off scubaqus-ing here or Sneakinson-ing there I wish you all the happiness & success you deserve Billy Baccalà!

Moni, *strangely it feels like this thesis wouldn't exist if you didn't. Very Murakami-esqe no? To all the secret bars we've discovered and have yet to discover, for all the Espanish I've learnt and have yet to learn, gracias tía*

Sarah, Madame la Gallet, *you know I think you're amazing, right?! If I'm ever half as composed as you I think I'll be doing pretty well all things considered! If I remember correctly (and I do, I wrote them down on a calendar) you were wrong about something a total of four times... in four years – that is ridiculous, I'm usually wrong about more than four things before lunch. Thank you for all your care and attention, bisous bisous.*

María María, *it's been fun in Lille getting to understand each other, I'd say we're getting closer... even if it's taken us years of being in the same office! Just next time let's do it in somewhere a little sunnier? I'm thinking by the sea, strolling down the street, enjoying a *changes accent* 'delicious café con leche' Thank you for all your friendship and jokes these past few years, I appreciate them all.*

Charlotte, *oh little* Charlottine. *How I have missed you and your sounds since you left us. The first French person I met when I arrived, the first person I ever saw eat a snail, the first friend I saw get married! You're irreplaceable in the lab and in my heart & definitely hold the distinction of introducing me to cursing in French. Keep doing great things & I know our paths will for sure cross many times in the future!*

Soon to be Dr Sara, *Science brought us together and it's led us on many adventures. I hope you're as excited as I am for the next ones! It never seemed to rain when you were around, I think you should come back soon...*

Ira, Pippo, Messins, Gustavo; *the original gang that took me in and made me feel like part of the family. I thought I had some experience with drinking beer before I arrived, until I received your education... You guys have always been there for me, whether it was to answer a scientific question, to put a roof over my head or food in my belly. I will always be indebted to you all. Mao*

Valerie, Sonal, Jerome, Manon, Emilie, Megane; *thanks for all the fun times in the lab! We made it, 64 is no longer just a number!!*

Morgane, *my hero(ine) – thank you so much for sharing your time & expertise these past two years, you were never too busy to answer any questions I had. We need to get you to Lille to celebrate soon!*

Emilie, Raphael, Claudia; *my go-to sources of wisdom and smiles from up the stairs. You always made me feel welcome, listened to me and always made me smile. These years in Lille wouldn't have been the same without knowing you all and reminding me that things happen outside of the World of our corridor!*

Luc, Celine, Sophie, Michele, Natalie, Delphine, Julien & Thomas; *the people who make the JPArc & animal facilities run. I know I'm prone to causing some headaches, hopefully they didn't extend to sleepless nights, thank you for all the help with the endless paperwork & your positivity.*

Meryem & Antonino, *thanks for all your help and support with my imaging and analysis, I hope we can do some cool stuff together soon.*

Domingo & JCM, *I owe so much of my enthusiasm for research to your great teaching abilities. You laid the groundwork and gave me the inspiration I needed to pursue my dreams.*

Spoon, Yvette, Laurent, Adam, *without whom I would never have finished a single year at University. I hope when you see this, it will make lending me all your notes seem a little more worthwhile; no-one, least of all me thought I would ever continue on in Science. I know everyone was jealous of us and how much fun we had/thought we were completely crazy back in the old anatomy days, you guys managed to convince me Science could be fun and just might lead me to some cool people. I'm so proud of us all for what we have achieved so far in such a short amount of time. I love you all and can't wait to see what comes next!*

Stephen & Daniel, *I know it's been hard for you both – you've missed me, at least this provides some proof that I was doing something other than being late for every single birthday and Christmas present for the past four years. We've been friends now for a quarter of a century, though we've left the days of the little yellow jumpers behind in favour of Mayo, Kerry & Dublin jerseys. Hopefully by the time this is published the days of suffering will finally be behind me... Sam for Mayo; Mayo for Sam!!*

Dr Greg, *I wish you were around more – so many projects that will never see the light of day... hope we get the chance to combine our creativity for the amusement of mankind one day. Thanks for all the random Science talks too! Less thankful for all the cat hair I have everywhere though.*

Family, *without you I really wouldn't be here. You've supported me in every way imaginable & I just hope I can make you all proud. We can argue forever about where I got all my bad habits and manners from, but at the end of the day I wouldn't change any of you for the World & I'm sure you feel the same.*

A special mention should go to Rachel, *God knows how long you've been putting up with all of us, but your support, never-ending ability to embrace change and pursue new interests has left a profound impact on my World view and what kind of person I would like to be. Thank you for everything!*

Ανθή *ήρθε η στιγμή να φορέσεις τα γυαλιά της πρεσβυωπίας σου.*

Ανθή *και* Αντώνη, *είμαι σίγουρος ότι αρχικά απορήσατε όταν γνωρίσατε στην Αθήνα τον ψηλό, καραφλό, Άγγλο φίλο της Νάντιας που μιλά πραγματικά γρήγορα. Απορήσατε όμως ακόμα περισσότερο όταν συνέχισε να επιστρέφει. Θα σας εκμυστηρευτώ κάτι..ήταν ξεκάθαρα για το φαγητό. Αισθάνθηκα ευπρόσδεκτος σαν να ήμουν μέλος της οικογένειας και το συναίσθημα αυτό είναι κάτι το απερίγραπτο. Σας ευχαριστώ για όλα όσα κάνατε για εμένα και ελπίζω να σας το ανταποδώσω και να ζήσουμε κι άλλες αξέχαστες στιγμές.*

Φρίξο, *μικρέ κατεργάρη. Πιστεύω πως ο μόνος λόγος που δεν μας έχεις καταβροχθίσει μέσα στη νύχτα είναι γιατί σε ταΐζουμε και χειριζόμαστε τα παιχνίδια σου.*

Μπου μου*! Ζήσαμε τόσα πολλά μαζί όλα αυτά τα χρόνια αλλά έχουμε και άλλα τόσα πολλά να ζήσουμε ακόμη. Δε φανταζόμουν ποτέ ότι θα έβρισκα την καλύτερη μου φίλη να ζει και να δουλεύει εδώ, τόσο κοντά μου. Δεν ξέρω πως θα μπορούσα να περάσω όλα αυτά τα χρόνια χωρίς την αληθινή σου φιλία. Λύπες και χαρές, όλα τα περάσαμε μαζί ...και με αλκοόλ φυσικά. Φτάνουμε γρήγορα στο τέλος αυτής της διαδρομής και μας περιμένει ένας τεράστιος κόσμος εκεί έξω να τον εξερευνήσουμε, μαζί για πάντα.*

Abstract

The control of reproduction is mediated by a hypothalamic network that regulates the periodic secretion of gonadotropin-releasing hormone (GnRH). GnRH neurons originate in the nose and enter the brain along vomeronasal and terminal axons during embryonic development. Alterations in the development of this system or in the secretion of GnRH are associated with congenital hypogonadotropic hypogonadism (CHH) and Kallmann syndrome (KS) in humans: characterised by a failure of sexual competence. This work provides evidence that Anti-Müllerian hormone (AMH), a hormone involved in male urogenital development is mutated in CHH and KS cohorts and suggests that defective AMH signalling may contribute to these pathologies through regulation of the migration of GnRH cells.

A further aim has been to provide new insights into the development of several body systems during human embryonic development by imaging whole embryos and foetuses at a cellular resolution. This allows for the first time, a true representation and appreciation of cells in their native, *in vivo* context. This approach has highlighted previously unknown features about the sexually dimorphic development of the urogenital system in humans, whilst also revealing that not only is the GnRH population in humans significantly higher than previously thought, but that GnRH cells target several extrahypothalamic brain regions in addition to the hypothalamus. Their presence in these areas raises the possibility that GnRH has non-reproductive roles, creating new avenues for research on GnRH functions in cognitive, behavioural and physiological processes.

Key Words:

GnRH, CHH, KS, AMH, DISCO, Development

Résumé Français

Le contrôle de la reproduction est médié par un réseau hypothalamique qui régule la sécrétion de la Gonadotropin Releasing Hormone (GnRH). Les neurones à GnRH naissent dans la placode olfactive et migrent vers le cerveau le long des axones vomeronasaux et terminaux au cours du développement embryonnaire. Des perturbations dans le développement ou dans la sécrétion de GnRH sont associées à l'hypogonadisme hypogonadotrope congénital (CHH) et au syndrome de Kallmann (KS). Ce travail révèle que l'hormone anti-Müllerienne (AMH), impliquée dans le développement urogénital masculin, est mutée dans les cohortes de patients atteints de CHH et KS et suggère que la perturbation de la signalisation de l'AMH pourrait contribuer à ces troubles à travers la régulation de la migration des neurones à GnRH.

L'imagerie de fœtus et embryons humains entiers à résolution cellulaire a dévoilé de nouveaux concepts sur le développement embryonnaire humain, permettant d'établir, pour la première fois une véritable représentation des neurones dans leur contexte natal, in vivo, ainsi que de mettre en évidence des caractéristiques inconnues sur le développement sexuellement dimorphique du système urogénital chez l'homme. Cette approche a révélé que non seulement le nombre de neurones à GnRH chez l'homme était significativement plus élevé que celui estimé auparavant, mais aussi que ces derniers migrent vers plusieurs régions du cerveau extra-hypothalamique, Leur présence dans ces régions soulève l'hypothèse qu'ils pourraient exercer des rôles non-reproductifs, créant de nouvelles pistes pour la recherche sur les fonctions du système GnRH dans les processus cognitifs, comportementaux et physiologiques.

Mots clés:

GnRH, CHH, KS, AMH, DISCO, Développement

Résumé Français Substantiel

Tout au long de l'histoire, le désir des scientifiques de comprendre la physiologie et la maladie en étudiant minutieusement les caractéristiques anatomiques a toujours été confronté à une contrainte insoluble: ils ne peuvent pas simplement voir à travers les tissus. La dissection a donc été le mode opératoire des anatomistes: des études pionnières de Galen, aux biologistes modernes qui sectionnent systématiquement les tissus pour étiqueter des structures pour une analyse microscopique.

Bien que ces méthodes aient formé une richesse de connaissances reliant la forme anatomique à la fonction, elles sont intrinsèquement erronées en raison d'une appréciation en 3 dimensions des structures perdues. Cela a été particulièrement problématique pour l'étude des processus de développement, où les structures évoluent continuellement et, par conséquent, une visualisation précise a été impossible à réaliser grâce aux méthodes traditionnelles et aux atlas anatomiques. De plus, la majorité de nos connaissances sur les systèmes de développement découlent d'études menées dans le poulet et le poisson zèbre; qui, bien que d'excellents modèles pour étudier ces processus, peuvent présenter des différences significatives par rapport aux humains. Associée aux difficultés d'accès aux tissus, notre compréhension du développement humain a progressé peut-être le processus biologique le plus lent depuis les années 1930; alors que dans certains cas, des observations de vertébrés inférieurs ont été appliquées de manière erronée à l'homme, ce qui a donné lieu à de fortes contradictions dans la littérature existante.

Sans une bonne compréhension du développement physiologique, nous n'avons pas les connaissances fondamentales requises pour que les cliniciens et les chercheurs s'attaquent aux syndromes de développement qui influèrent une grave charge de santé et un fardeau émotionnel pour la société. Les progrès récents dans les techniques d'imagerie in vivo non invasives, ont été très prometteurs pour détecter des anomalies congénitales et fournir des informations sur les caractéristiques topologiques brutes du développement fœtal; cependant, ils manquent d'une résolution suffisante pour informer les

biologistes du développement des caractéristiques actuellement inconnues de l'organogenèse. Cela a récemment été particulièrement souligné par la récente augmentation des infections par le virus Zika et les effets préjudiciables sur le développement céphalique.

La première méthode pour y remédier par des tissus «éclaircis optiquement» a été proposée et développée par l'anatomiste allemand Werner Spalteholtz; en fonction de la déshydratation des tissus afin d'obtenir une correspondance de l'indice de réfraction. Plus récemment, avec les progrès de la microscopie de fluorescence en feuille légère (LSFM), une variété de techniques de compensation optique ont été développées qui ont tous pour résultat un clouage de tissus par des principes similaires, malgré les différences sous-jacentes dans leurs approches chimiques. Chaque méthodologie a ses avantages et inconvénients respectifs, conçue pour répondre de manière idéale à différentes questions biologiques. L'un de ces protocoles, 3DISCO, basé sur la capacité des solvants organiques spécifiques à se déshydrater, à solvater les lipides et à provoquer une correspondance de l'indice de réfraction, entraîne également une réduction de 50% du volume total du tissu. Ces propriétés, en conjonction avec sa compatibilité avec une large gamme d'anticorps et la préservation du signal de fluorescence, signifient qu'il est idéal pour examiner le développement de plusieurs systèmes corporels pendant le premier trimestre du développement humain.

Au cours de l'embryogenèse, tous les processus de développement précoce continuent selon une trajectoire unique, indépendamment du sexe génétique, avec la différenciation des gonades embryonnaires formant la première signature moléculaire qui provoque une différenciation sexuelle. Avant l'expression des facteurs des testicules, la gonade existe dans un état bi potentiel, formé de deux conduits appariés, le conduit Wolffien capable de se différencier par le conduit masculin et Müllerian (MD) capable de former le tractus reproducteur féminin. Chez les mammifères, la présence de la région déterminant le sexe sur le gène Y (SRY) est nécessaire et suffisante pour déclencher une différenciation sexuelle de la gonade bi potentielle pour former des structures reproductrices masculines. L'expression SRY déclenche une cascade moléculaire impliquant l'expression d'un gène homologue 10 (SOX10) et une

expression du gène anti-Müllerian Hormone (AMH) liée à SRY à partir du testicule embryonnaire. AMH est un membre de la superfamille du facteur de croissance transformant-β (TGFß) qui initie la transition épithéliale-mésenchymateuse en régulant la régression du MD. Cette signalisation est régulée dans une fenêtre temporelle stricte, à l'extérieur de laquelle le MD est horriblement insensible et la régression ne peut pas se produire. En outre, les mutations génétiques dans l'AMH ou son récepteur AMHR2 entraînent la rétention des structures de MD à l'âge adulte dans les mâles 46XY, autrement normalement virilisés, ce qui provoque le syndrome du conduit de Müllerian persistant du syndrome d'infertilité (PMDS). Bien que ce processus par lequel un facteur testiculaire autre que la testostérone ait été responsable de la régression MG a été identifié en 1974 par le scientifique français Alfred Jost travaillant sur des lapins, la plupart de nos connaissances sur le processus ont ensuite été menées dans des modèles de rongeurs, en établissant une approche globale image qui doit encore être confirmée chez les humains.

L'acquisition de la compétence en matière de reproduction dépend du bon développement de plusieurs systèmes corporels distincts des gonades - l'hypophyse et le cerveau; qui forment ensemble l'axe hypothalamo hypophysaire gonadique. La communication entre chaque composante de l'axe est relayée par des messagers hormonaux sécrétés dans le sang, assurant que les fonctions de chacun et les sécrétions sont maintenues autour des points de consigne physiologiques. Bien que de nombreuses entrées externes et internes régulent la fertilité en fonction des besoins spécifiques de l'espèce, dans tous les vertébrés, les intrants convergent éventuellement sur une seule population de neurones qui synthétisent et sécrètent l'hormone de décapeptide gonadotrophine. Ces neurones forment un réseau neuronal dispersé avec des corps cellulaires généralement trouvés dispersés dans un continuum bilatéral de la bande dorsale de Broca à l'hypothalamus antérieur, typiquement entre environ 800 cellules chez la souris et plusieurs milliers chez les humains. Ces neurones envoient des projections à la zone externe de l'éminence médiane où ils sécrètent la GnRH dans le plexus primaire spécialisé de la circulation du porteur de l'hypothalamo-hypophysaire, pour être administré à l'hypophyse antérieure où elle régule la synthèse et la sécrétion des hormones gonadotrophines à l'hormone lutéinisante (LH) et l'hormone folliculo-stimulante (FSH).

L'invalidation génétique de la GnRH, comme dans la souris hypogonadique naturelle (Hpg) rend les animaux stériles, la fertilité pouvant être restaurée par transplantation de neurones GnRH immortalisés ou de cellules du cerveau embryonnaire contenant des neurones GnRH. Une perte de GnRH chez l'homme est typiquement congénitale (bien que dans de rares cas elle puisse être acquise) et forme un groupe de syndromes d'infertilité, collectivement connus sous le nom d'hypogonadismes hypogonadotropes congénitaux (CHH). Le séquençage génomique de plusieurs cohortes de CHH a révélé que plusieurs familles de gènes peuvent générer l'état et, actuellement, environ 50% des cas cliniques peuvent s'expliquer par ces mutations connues.

Les neurones de la GnRH sont inhabituels dans la mesure où ils naissent dans le compartiment nasal et doivent migrer le long d'une collection de fibres nerveuses olfactives et terminales à travers la plaque cribriforme pour entrer dans le cerveau et cibler l'hypothalamus. Bien que ce processus semble particulier, car toutes les autres hormones de libération hypophysiotropes sont nées dans l'hypothalamus en développement, elles sont à la base d'une relation évolutive profonde entre la reproduction et l'olfaction. Ceci est souligné par un autre syndrome d'infertilité humaine connu sous le nom de syndrome de Kallmann (KS) qui associe CHH et anosmie et les résultats en raison de la rupture de la migration embryonnaire des fibres olfactives qui servent de guide pour les neurones GnRH pendant le développement.

Bien que le comportement migratoire des cellules olfactives et de la GnRH ait été décrit initialement il y a près de 30 ans, une description complète et une cartographie anatomique de ces cellules dans l'embryologie humaine, en raison de raisons socioculturelles, religieuses ou morales, manquent encore. À l'heure actuelle, environ seulement 50% des cas cliniques de CHH ont expliqué des causes génétiques, la proportion restante étant attribuée à des mutations génétiques inconnues. Les données récentes provenant de notre laboratoire ont identifié AMH comme un stimulant puissant de la libération de GnRH, déclenchant la libération de LH in vivo et augmentant l'activité de tir électrique des neurones de GnRH.

Les auteurs ont également démontré que le récepteur AMH AMHR2 est exprimé par la migration des neurones GnRH pendant le développement chez les souris et les humains.

Les principaux objectifs de ce travail sont donc:

- Appliquer les progrès récents dans le domaine de la décoloration des tissus et de l'immunocoloration totale pour caractériser le développement des systèmes nerveux périphérique humain et urogénital pendant le premier trimestre de gestation
- Utiliser ces techniques en combinaison avec des méthodes histologiques traditionnelles pour fournir la première description détaillée de la migration de la GnRH dans le développement humain et créer un atlas 3D de leur répartition spatiale au début du développement
- Caractériser un rôle potentiel de la signalisation hormonale anti-Müllerienne dans le développement du système GnRH et sa contribution potentielle à la CHH.

La génération d'une cartographie cellulaire et moléculaire précise de l'embryon humain est essentielle pour comprendre les mécanismes de l'organogenèse dans des conditions normales et pathologiques. Ici, nous avons combiné l'immunocoloration intégrale, le décapage 3DISCO et l'imagerie feuille-lumière pour faire les premières étapes vers la construction d'une carte cellulaire tridimensionnelle du développement humain pendant le premier trimestre de gestation. Nous fournissons des images 3D à une résolution sans précédent des différents systèmes de développement, y compris le système nerveux périphérique et le système urogénital. Nous présentons des preuves d'une vascularisation différentielle des voies génitales masculine et féminine associée à la détermination du sexe. Ce travail ouvre la voie à un atlas de référence cellulaire et moléculaire des cellules humaines qui est essentiel à la compréhension des troubles du développement humain.

En outre, les résultats décrits dans les chapitres précédents aident à élucider plusieurs aspects morphologiques et fonctionnels importants du développement du système GnRH-1 chez les souris et les humains. Nous fournissons la première preuve de l'immunoréactivité de la GnRH au CS16, environ 39 jours de gestation, ce qui confirme que la naissance de cette population survient plusieurs jours plus tôt que précédemment. Notre quantification du nombre total de cellules GnRH présentes au cours du développement humain est le premier de son genre et suggère une augmentation rapide de la taille de la population entre les 39ème et 44ème jours de gestation, passant de 50 cellules à une moyenne d'environ 8 000 cellules quelques jours plus tard. Ce nombre est très susceptible d'être une représentation précise de la population totale, car l'ARNm de GnRH-1 a montré un profil d'expression très similaire et un nombre similaire dans les cerveaux adultes post-mortem.

La confirmation des résultats signalés il y a 20 ans dans les macaques rhésus d'une voie migratoire dorsale, conduisant à des populations extra-hypothalamiques de neurones exprimant GnRH ouvre la voie à de nouvelles découvertes scientifiques et cliniques sur le rôle de l'expression et la libération de la GnRH dans la physiologie de la reproduction humaine, le comportement olfactif et les processus cognitifs.

Longtemps considéré comme une hormone purement gonadique, nous rapportons que l'hormone anti-müllerienne s'exprime lors d'un développement embryonnaire précoce le long de la voie migratrice de GnRH et qu'elle régule la motilité de la GnRH par l'intermédiaire de l'hétérodimérisation AMHR2 / BMPR1b. L'invalidation de la signalisation AMH in vivo entraîne un développement défectueux du système olfactif périphérique et une migration embryonnaire altérée des cellules GnRH vers le cerveau antérieur basal, ce qui entraîne une réduction significative de la taille de la population de GnRH à l'âge adulte et un phénotype de type KS.

Ces nouveaux rapports sont étayés par un séquençage exhaustif d'une cohorte de 70 KS et de 43 nCHH probants, qui ont identifié plusieurs mutations hémisomeos hétérozygotes dans les gènes AMH et AMHR2 chez les individus KS et nCHH. La validation biochimique a révélé que plusieurs formes mutées

d'AMH ont entraîné une diminution de la motilité de la cellule GnRH et une diminution de la sécrétion de l'AMH par les cellules COS-7 transfectées, ce qui suggère fortement que ces variantes ont un effet pathogène. Nos résultats mettent en évidence un rôle nouveau pour l'AMH dans le développement et la fonction des neurones de la GnRH et indiquent que l'insuffisance de signalisation AMH contribue à la pathogenèse de la CHH.

En résumé, ce travail donne un aperçu de la base moléculaire de la signalisation AMH dépendant dans l'établissement correct du processus migratoire GnRH. En outre, ce travail implique des mutations AMH dans la pathophysiologie de la CHH en cohérence avec le rôle de ce gène dans le bon développement des neurones GnRH et supporte l'idée que les défauts migratoires de la population GnRH sont exclusivement réservés à KS et ne se produisent pas dans les conditions de nCHH.

Curriculum Vitae

Education

Degree	Field of study	Institution	Supervisor	Years
Ph.D	Neuroscience	Université Lille 2, INSERM U1172, France	Dr. Paolo Giacobini	2014–2017
M.Sc	Neuroscience	Université Lille 2, INSERM U1172, France	Dr. Paolo Giacobini	2013–2014
B.Sc	Anatomical Science & Physiology	University of Bristol, UK	Dr. Domingo Tortonese, Dr. David Bates	2009–2012

Position

Name and Type	Institution and location	Years
Doctoral Fellowship	Université Lille 2, INSERM U1172, France	2014–2017
Master Fellowship	Université Lille 2, INSERM U1172, France	2013–2014
Research Contract	University of Bristol, Anatomy Dept, UK	2012–2012

Publications

- **Malone SA**, Papadakis G, Cassatella D, Cimino I, Acierno J, Cui X, Mimouni N, Messina A, Pitteloud N, Giacobini P. Defective Anti-Müllerian Hormone Signalling Alters the Development of the GnRH/Olfactory systems & Contributes to Congenital Hypogonadic Hypogonadism. *In preparation*

- Chachlaki K, **Malone SA**, Qualls-Creekmore E, Hrabovszky E, Munzberg H, Giacobini P, Ango F, Prevot V. Phenotyping of nNOS Neurons in the Postnatal and Adult Female Mouse Hypothalamus. *J Comp Neurol*, 2017. doi:10.1002/cne.24257

- Belle M, Godefroy D, Couly G, **Malone SA**, Collier F, Giacobini P, Chédotal A. Tridimensional Visualization and Analysis of Early Human Development. *Cell*. 2017. doi:10.1016/j.cell.2017.03.008

- Casoni F*, **Malone SA***, Belle M, Luzzati F, Collier F, Allet C, Hrabovszky E, Rasika S, Prevot V, Chédotal V, Giacobini P. Development of The Neurons Controlling Fertility in Humans: New Insights from 3D Imaging & Transparent Fetal Brains. *Development*. 2016 143: 3969–3981; doi: 10.1242/dev.139444

- Parkash J, Messina A, Langlet F, Cimino I, Loyens A, Mazur D, Gallet S, Balland E, **Malone SA**, Pralong FP, Cagnoni G, Schellino R, De Marchis S, Mazzone M, Pasterkamp JR, Tamagnone L, Prevot V, Giacobini P. Semaphorin7A Regulates Neuroglial Plasticity at the Adult Hypothalamic Median Eminence. *Nature Communications*. 2015, 6:6385 doi:10.1038/ncomms7385.

- **Core organising committee** for 4th joint meeting of the British (BSN) and French (SNE) Neuroendocrine Societies, Lille, France, 2015. Webmaster, participant registrations, management of abstract book.

- **Malone SA**, Papadakis G, Cassatella D, Cimino I, Acierno J, Cui X, Mimouni N, Messina A, Pitteloud N, Giacobini P. A novel role for Anti-Müllerian hormone in regulating the development of the gonadotropin releasing hormone network
  Poster
  French Society for Neuroscience
  Bordeaux, France, May 2017

- **Malone SA**, Papadakis G, Cassatella D, Cimino I, Acierno J, Cui X, Mimouni N, Messina A, Pitteloud N, Giacobini P. A novel role for Anti-Müllerian hormone in regulating the development of the gonadotropin releasing hormone network
  Poster
  Society for Neuroscience
  San Diego, USA, November 2016

- **Malone SA**, Papadakis G, Cassatella D, Cimino I, Acierno J, Cui X, Mimouni N, Messina A, Pitteloud N, Giacobini P. A novel role for Anti-Müllerian hormone in regulating the development of the gonadotropin releasing hormone network
  Scientific meeting of the European GnRH network
  Poster
  Budapest, Hungary, March 2016

- **Malone SA**, Papadakis G, Cassatella D, Cimino I, Acierno J, Cui X, Mimouni N, Messina A, Pitteloud N, Giacobini P. A novel role for Anti-Müllerian hormone in regulating the development of the gonadotropin releasing hormone network
  Journée Andre Vaubert
  Poster ***won best use of imaging**
  Lille, France, September 2015

- **Malone SA**, Papadakis G, Cassatella D, Cimino I, Acierno J, Cui X, Mimouni N, Messina A, Pitteloud N, Giacobini P. A novel role for Anti-Müllerian hormone in regulating the development of the gonadotropin releasing hormone network
  Scientific meeting of the European GnRH network
  Poster
  Prato, Italy, March 2015

- **Malone SA**, Papadakis G, Cassatella D, Cimino I, Acierno J, Cui X, Mimouni N, Messina A, Pitteloud N, Giacobini P. A novel role for Anti-Müllerian hormone in regulating the development of the gonadotropin releasing hormone network
  European Conference of Clinical Endocrinology
  Poster ***won best poster**
  Rouen, France, August 2014

Abbreviations

° C	Degrees Celsius
3DISCO	3-Dimensional imaging of solvent cleared organs
Acv	Activin
ALK	Activin like kinase
AMH	Anti-Müllerian hormone
AMHR2	AMH receptor 2
AMPA	α-amino-3-hydroxy-5-methyl-4-isoxazolepropionic acid
ANOVA	Analysis of variance
AR	Androgen receptor
ß3GnT1	ß1,3-N acetylglucosaminyltransferase-1
BBB	Blood-brain-barrier
BMP	Bone morphogenic protein
bp	Base pair
BrDU	5'-bromo-2-deoxyuridine
BS	Binding site
CCD	Charge coupled device
CCK	Cholecystokinin
CDGP	Constitutional delay of growth and/or puberty
CHARGE	Coloboma of the eye, heart defect, choanal atresia, retarded growth and development, genital hypoplasia, external ear anomalies and deafness
ChAT	Acetyl choline transferase
CHH	Congenital hypogonadotropic hypogonadism
CN	Cranial nerve
CNC	Cranial neural crest
CNS	Central nervous system
COS	CV-1 in origin, carrying SV40 genetic material
CRH	Corticotropin releasing hormone
cRNA	Complementary RNA
CS	Carnegie stage
cVNN	Caudal branch of the VNN
Da	Dalton
DAX1	Dosage-sensitive sex reversal, adrenal hypoplasia critical region on chromosome X, gene 1
DBB	Dorsal band of Broca
DBE	Dibenzyl ether
DCC	Deleted in colorectal cancer
DCM	Dichloromethane
DCX	Doublecortin
DEPC	Diethyl pyrocarbonate
Dig	Digoxigenin-11-UTP
DMEM	Dulbecco's modified Eagle's medium
DMSO	Dimethyl sulfoxide
DNA	Deoxyribonucleic acid
DNER	Delta and notch-like epidermal growth factor-related receptor

dNTP	Deoxyribo-nucleoside triphosphate
DPBS	Dulbecco's PBS
DSCAM	Down syndrome cell adhesion molecule
DTT	Dithiothreitol
EDTA	Ethylenediaminetetraacetic acid
EGTA	Egtazic acid
Eph	Ephrin
ERK	Extracellular signal-regulated kinase
FACS	Fluorescence-activated cell sorting
FGF	Fibroblast growth factor
FGFR	FGF receptor
FISH	Fluorescent ISH
Foxl2	Forkhead box L2
FSH	Follicle stimulating hormone
g	Gram
GABA	γ-aminobutyric acid
GAD	Glutamate decarboxylase
GAP1	GnRH1 associated peptide
GDF	Growth and differentiation factors
GFP	Green fluorescent protein
GHRH	Growth hormone releasing hormone
GnRH	Gonadotropin-releasing hormone
GnRHR	GnRH receptor
GPCR	G-protein coupled receptor
GW	Gestational weeks
h	Hour
HCG	Human chorionic gonadotropin
HCl	Hydrochloric acid
HGF	Hepatocyte growth factor
HH	Hypogonadotropic hypogonadism
HPG	Hypothalamo-hypophyseal-gonadal
Hpg	Hypogonadic
HS6ST1	Heparan sulphate 6-O-sulftransferase enzyme
Ig	Immunoglobulin
IKK	IkB kinase
iq	Interquartile
ISH	*in situ* hybridisation
k	Kilo
KNDy	Kisspeptin, neurokininB, dynorphin
KS	Kallmann Syndrome
L	Litre
LH	Luteinising hormone
LHA	Lateral hypothalamic area
LHR	Luteinising hormone receptor
LHRH	Luteinising hormone releasing hormone

LNC	Long non-coding
LRF	Luteinising hormone releasing factor
LSFM	Light sheet fluorescence microscopy
MAPK	Mitogen activated protein kinase
MAP3K	MAPK kinase kinase
MCH	Melanocortin concentrating hormone
MHC	Myosin heavy chain
MIS	Müllerian inhibiting substance
mL	Millilitre
MM	Migratory mass
MOS	Metal oxide semiconductor
mRNA	messenger RNA
NA	Numerical aperture
N/FbJ	Nasal/forebrain junction
NC	Neural crest
NCAM	Neural cell adhesion molecule
nCHH	Normosmic CHH
NELF	Nasal embryonic LHRH factor
NF-kB	Nuclear factor k-light-chain-enhancer of activated B cells
NGS	Next generation sequencing
nm	nanometre
NMDA	*N*-methyl-D,L-aspartate
Nrp	Neuropilin
NGS	Next generation sequencing
OB	Olfactory bulb
OCT	Optimal cutting temperature
OEC	Olfactory ensheathing cells
OMIM	Online Mendelian inheritance in man
OMP	Olfactory marker protein
OP	Olfactory placode
OSN	Olfactory sensory neurons
OVLT	Organum vasculosum laminae terminalis
PAX6	Paired box 6
PBS	Phosphate buffered saline
PC	Prohormone convertase
PCOS	Polycystic ovary syndrome
PDMS	Polydimethylsiloxane
PFA	Paraformaldehyde
PLVAP	Plasmolemma vesicle associated protein
POI	Primary ovarian insufficiency
pM	Picomolar
PMDS	Persistent Müllerian Duct Syndrome
PMSF	Pemoihenylmethane sulfonyl fluoride
PNS	Peripheral nervous system
POA	Pre-optic area

PSA	Polysialic acid
PVDF	Polyvinylidene fluoride
pVNO	Presumptive VNO
RNA	Ribonucleic acid
rPOA	Rostral POA
Rspo1	R-spondin homolog (*xenopus laevis*)
RT	Room temperature
SBE	SMAD binding element
S.E.M	Standard error of the mean
SBE	Smad binding element
SD	Standard deviation
Sema	Semaphorin
SEF	Similar expression to FGFs
SF-1	Steroidogenic factor 1
SFM	Serum free medium
siRNA	Small inhibitory RNA
SOX	SRY-related homolg box protein
SRY	Sex-determining region Y
SSC	Saline sodium citrate
SV	Simian virus
SYBR	N', N'-dimethyl-N-[4-[(E)-(3-methyl-1,3-benzothiazol-2-ylidene)methyl]-1-phenylquinolin-1-ium-2-yl]-N-propylpropane-1,3-diamine
$t_{1/2}$	Half life
TAG-1	Transient axonal glycoprotein/contactin-2
TBS	Tris-buffered saline
TESCO	Testis-specific enhancer of SOX9
TGF	Transforming growth fact0r
THF	Tetrahydrofuran
Tlx-2	T-cell leukaemia homeobox 2
TN	*Nervus terminalis,* CN-0, CN-N
TNF	Tumour necrosis factor
tPA	Tissue plasminogen
TRH	Thyrotropin releasing hormone
tRNA	Transfer RNA
TSA	Tyramide signal amplification
µg	Microgram
µm	Micrometre
uPA	Uroplasminogen
V	Volt
vFB	Ventral forebrain
VNN	Vomeronasal nerve
VNO	Vomeronasal organ
WES	Whole exome sequencing
WNT4	Wingless-type MMTV integration site family member 4
WT1	Wilms' tumour suppresor-1

Index

Figures & Tables

CHAPTER 1

An Overview of Hypothalamic Anatomy & Function

1.1 A Historical Overview of the Neuroendocrine Hypothalamus

Some of the earliest reports of endocrine function and hormonal signalling originate from the early 18th century observations of choirboys who, when castrated before puberty maintained a soprano voice and developed an enlarged lung capacity. While these were desirable attributes for a chorus member or soloist to possess, the procedure also rendered the Castrati infertile and it was observed that they maintained their youthful appearance well past pubertal age as their bodies grew disproportionately to other men. That the testes could be essential to not only reproductive capacity but also to several seemingly unconnected body systems and processes, whilst keenly observed, would not be fully appreciated or explained for several centuries. This idea of non-neuronal connections between organs, implying a form of communication at distance, would eventually be given a name by Ernest Starling: hormones (Starling I-IV, 1905). Hormones form a family of chemical messengers secreted into the blood with target tissues in distal regions of the organism and as such play a role in the regulation of the organism's development, homeostasis, behaviour, reproductive capacity and the overall modulation of physiological circuits.

Perhaps the earliest experiments that significantly contributed to our understanding of hormonal regulation in humans were those of British physician Victor Horsley (also credited with co-inventing the first stereotaxic apparatus alongside Clarke), who initially noted that thyroidectomy induced myxoedema and cretinism. Subsequent re-implantation of ovine thyroid glands resulted in amelioration of his patients' symptoms and injections of liquidised porcine thyroid glands by his one-time student Dr George Murray became the first true treatment for a hormonal imbalance: a disorder that today is completely curable thanks to their pioneering efforts.

We now know that there exist tripartite axes regulating many hormonal processes, formed from feedforward and feedback loops of varying complexity involving the hypothalamus, hypophysis and peripheral target tissues (**Figure 1**). Whilst the effects of removing these target endocrine tissues such as the pancreas, thyroid or gonads is a relatively recent discovery in terms of the

history of medicine, the basic principle of body systems signalling through the blood, to be processed by the brain and transported through the infundibulum to the hypophysis is close to 2000 years old.

According to the most prominent medical researcher of antiquity Κλαύδιος Γαληνός (Galen of Pergamon, AD129–200),

> '*the vital spirit changed into the animal spirit in the blood from the heart, at the rete mirabile*'

the *rete mirabile* – the plexus covering the surface of the median eminence. Although this deduction was based solely on the anatomical structure and positioning of the hypophysis at the base of the brain in oxen, monkeys, goats and pigs; and rooted in the belief of the Hippocratic humours, by the mid 17th century this idea had survived the anatomical revolutions of Andries van Wesel (Andreas Vesalius, 1514–1564) and led Thomas Willis in 1664 to remark,

> "*a discharge of humours is effected into its aperture from every angle and recess of the interior cerebrum, and its appendage; and while in the various animals the shape and the situation of the ventricles differ, nevertheless in every one of them all the ventricles, of whatever kind they be, have apertures opening in the direction of the infundibulum*"

Through several centuries of often contentious scientific experimentation, this 'animal spirit' that was present in the vascular plexus described by Galen has been shown to carry a variety of neurohormones released from parvocellular hypothalamic neurons, regulating the endocrine output of the adenohypophysis including: lactation, stress, growth and reproduction – certainly processes that we think of animalistic in nature even now. The anatomical conservation of structure noted by Willis underlies a very ancient and evolutionarily conserved form of cellular communication, that as previously mentioned forms feedback axes, which today inform the study of neuroendocrinology.

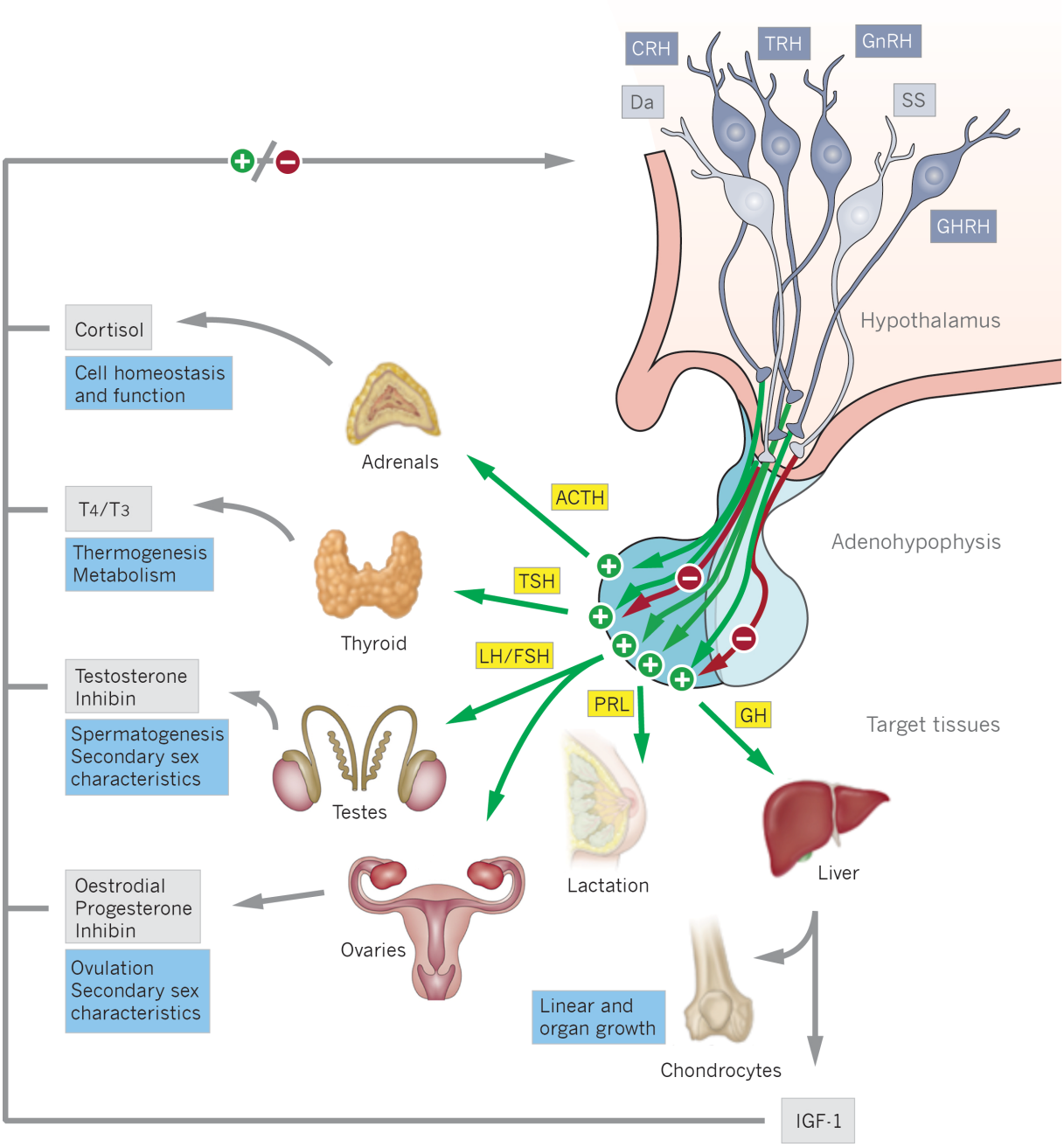

Figure 1. Hypothalamo–adenohypophyseal axes

Schematic illustrating the hypothalamic hormones that regulate adenohypophyseal tropic hormones, which in turn determine target gland secretions. These peripheral secretions feedback to regulate hypothalamic and adenohypophysis function. Abbreviations: ACTH: Adrenocorticotropic hormone; CRH: Corticotropin releasing hormone; DA: Dopamine; FSH: Follicle stimulating hormone; GH: Growth hormone; GnRH: Gonadotropin releasing hormone; IGF-1: Insulin like growth factor-1; LH: Luteinising hormone; PRL: Prolactin; SS: Somatostatin; TRH: Thyrotropin releasing hormone; TSH: Thryotropin stimulating hormone; T_4/T_3: Thyroid hormone. Schematic made by Malone SA

This idea resurfaced in the 1950's as a topic of great interest, a period when many of the discoveries that shape neuroscience as we know it today were made. Chemical neurotransmission at motoneuron synapses (Brok et al., 1952), the ionic basis for action potential propagation (Hodgkin & Huxley, 1952), the first visualisation of the synapse by electron microscopy (Palade & Palay, 1954) and the first tracer of neuronal pathways (Nauta & Gygax, 1954) all immediately preceded Geoffrey Harris' influential *Neural control of the Pituitary Gland* (1955). Here Harris outlined three key properties that a hypophysiotropic releasing factor should satisfy in order for the hypothalamus to regulate hypophyseal function:

- The substance must be present in the hypophyseal portal vessels at a concentration greater than the systemic circulation
- The concentration within the portal circulation should vary in accordance with electrical activation of hypothalamic nerves
- The activity of the adenohypophysis should correlate with these varying concentrations

To fully satisfy of all Harris' criteria would require twenty years of experimentation, with gonadotropin releasing hormone (GnRH) becoming the first fully recognised hypothalamic releasing factor (Fink, 1976; Sarkar et al., 1976), placing it centrally as the controller of the hypothalamo–hypophyseal–gonadal (HPG) axis (Section 1.4).

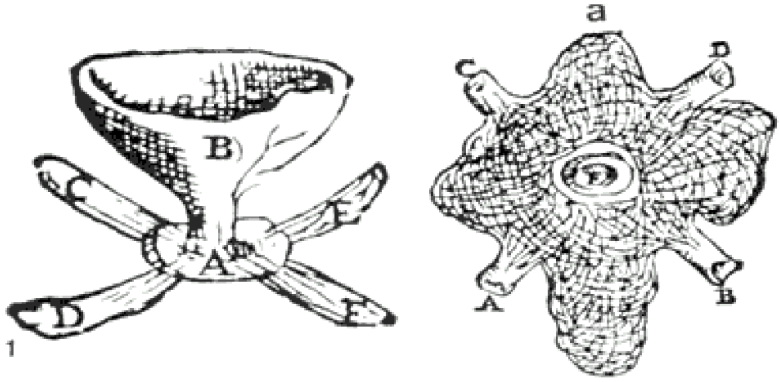

Figure 2. Classical drawings of the ventral surface of the brain relating to the adenohypophysis. Vesalius' representation of the infundibulum, depicting a cup set upright (representing the hypothalamus) through which it was thought that the pituita of the brain was carried to the adenohpophysis. The second drawing illustrates the rete mirabile, the intricate branching of blood vessels seen after careful dissection of the ventral surface of the brain. Ref. Saunders & O'Malley, 1950, p19

1.2 Development of the hypothalamus

The evolutionary origins of the hypothalamus can be traced to the murky waters that are home to the last common ancestor of vertebrates, flies and worms. The annelid worm *Platynereis dumerilii* shares almost identical development of RF-amide and vasotocin (a hormone that shares a largely similar functional role to vasopressin and oxytocin in regulating reproduction and water balance) neurons with zebrafish *danio rerio* (Tessmar-Raible et al., 2007), suggesting that these neurons that would eventually cluster together to form the vertebrate hypothalamus, may have already been present in Urbilateria (the hypothetical last common ancestor of animals possessing a bilateral symmetry). Furthermore, hypothalamic related neuropeptides have been identified in ganglions of lower evolutionary animals such as corals and clams (Twan et al., 2006; Takayanagi and Onaka, 2010) confirming a very ancient evolutionary origin.

Despite its obvious importance to physiology as a whole, study into the development of the hypothalamus lags well behind research into other, more easily segmented regions of the brain such as the hippocampus or cerebellum. Wilhem His, the founder of the topological embryologic school of thought "*Entwicklungsmechanik*" coined the term hypothalamus in his work on the development of the human brain (His, 1893a, 1893b), however, its development still continues to be an active field of research.

Two main schools of thought have dominated our understanding of hypothalamic embryology since the time of His, with the most popular, the 'columnar diencephalic model' of Herrick (1910) (largely based on work in chick embryos), recently falling out of favour as the application of more sophisticated tools, and substantial accrual of data has led to the re-adoption of the 'prosomeric model' of brain development (recently updated by Puelles & Rubenstein, 2015). Indeed, using a genoarchitectural approach, Domínguez and colleagues (2015) identified shared genetic traits between reptiles and amphibians, highlighting an important milestone in the anamniote/amniote transition; whilst a further study into the neurodevelopment of the cat shark *Scyliorhinus canicula* supported a prosomeric developmental architecture of the hypothalamus (Santos-Durán et al., 2015) and making it likely that the

proposed subdivisions are ancestral to jawed vertebrates.

The model proposes that the hypothalamus originates as the rostralmost part of the neural tube, since the developmental forebrain length axis ends in the terminal wall of the hypothalamus. The neural tube itself is a derivative of the dorsal ectoderm that is specified to become neural ectoderm (forming the neural plate) during the third week of human gestation. It should also be recognised at this point that another ectodermal derivative, the neural crest, is distinct from the neural tube, forming at the site of dorsal closure of the tube and gives rise to several important cell lineages including the peripheral nervous system (including neuroglial cells) as well as the dentine of the teeth (**Figure 3**).

As the neural tube fuses, the brain and spinal cord are recognisable and the brain becomes subdivided into a forebrain (prosencephalon), midbrain (mesencephalon) and hindbrain (rhombencephalon) (**Figure 4**). By the end of the fifth week the prosencephalon becomes further subdivided to form the telencephalon and diencephalon (Moore & Persaud, 1993 – Developmental biology, 6th edition, S. Gilbert).

Neurogenesis in the neural tube begins in the ventral hindbrain behind the cephalic flexure, with the neurogenic zone surrounding the ventricle. In the human (Gilbert, 1935) and mouse (Croizier et al., 2011), neurogenesis begins in a column of cells referred to by Gilbert as the 'cell cord'. Following neurogenesis, neuronal migration is essential to the correct development of the nervous system and has been shown to occur through two distinct processes. Radial migration is the principle mode of neuronal migration in the developing brain and occurs along a scaffold of radial glial cell cells via complex cell–cell interactions to direct the positioning of neurons and is responsible for the majority of initial histogenesis of neural tube–derived brain regions (Pearlman et al., 1998; Rakic, 1990). In contrast, tangential migration occurs perpendicular to the direction of radial migration and depends on the interaction of neurons with gradients of diffusible molecules, that act as chemoattractants and repellents (Pearlman et al., 1998). This cell cord gives rise to the first generated hypothalamic neurons that will ultimately form the post–chiasmatic lateral hypothalamus and include MCH expressing cells (Croizier et al., 2011).

Neurogenesis in the hypothalamus is described as involving three stages: an early stage that produces only the lateral zone; a second that is concomitant to neurogenesis in the telencephalon and produces neurons in all hypothalamic longitudinal zones, but mostly the medial; and a late third stage that concerns mainly periventricular zone neurons. Interestingly several studies have found an important lateral–medial migration pattern in the developing hypothalamus (**Figure 5**) (Crozier et al., 2015), beginning structural organisation at E11 in rats, with the organisation of the hypothalamus proper completed by E16. The hypothalamus appears to have an intrinsic dorsal/ventral patterning consistent with the alar, basal and floor plate territories of the developing neural tube, whilst anterior/posterior zones appear to be organized according to local environmental signals (Kapsimali et al., 2004; Muthu et al., 2016).

Morales–Delgado and colleagues (2014) characterised progenitor domains in the early hypothalamic ventricular zone of the mouse, mapping the migration of peptide–expressing neuronal subpopulations to their final settling place. The authors found intricate tangential and radial migration routes as well as a considerable degree of intermixing between the subpopulations underlie the complex adult anatomy of the hypothalamus. The general organisation of the vertebrate brain is evolutionarily conserved, however several events during tetrapod and mammalian evolution have led to neuroanatomical changes (Suárez et al., 2014). Importantly, it has been shown that key genetic factors driving the patterning and specification of major hypothalamic nuclei are evolutionarily conserved (Tessmar–Raible et al., 2007).

Based on the accumulated wealth of embryological transcription factor data, and a prosomeric model that explains the anatomical positioning of nuclei based on data, rather than undefined anatomical landmarks, it is perhaps useful to topologically view the hypothalamus as the hypo*telencephalon* (**Figure 5**).

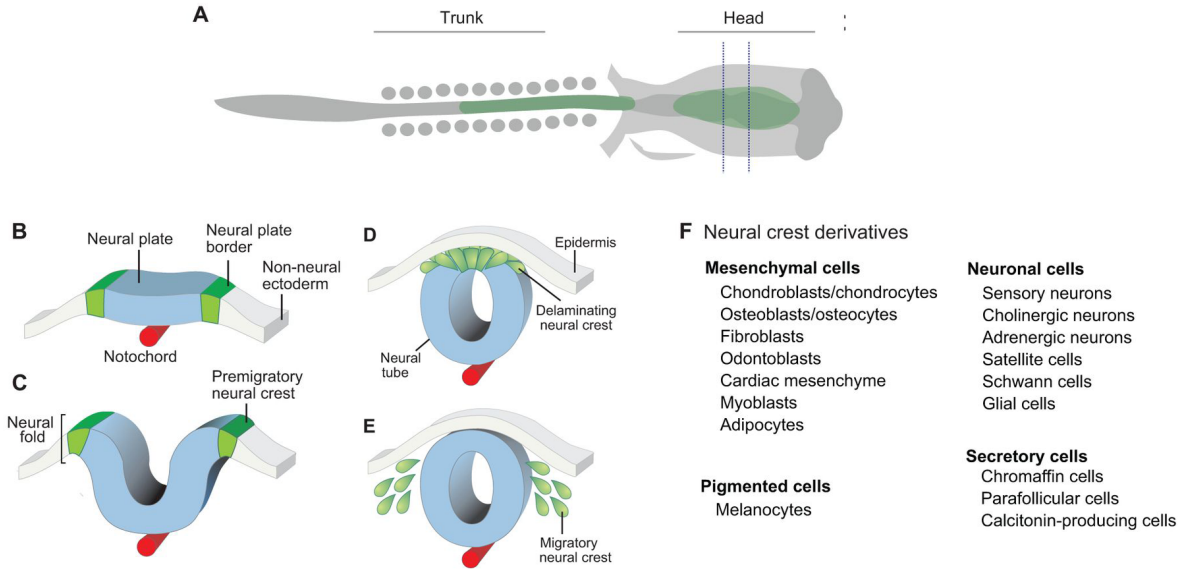

Figure 3. Embryonic development of the neural tube and neural crest.
(A) Schematic representation of the dorsal view of ten somite chick embryo showing the neural crest at the midline, with dotted lines indicating the regions represented in (B–E). (B) Development of the neural crest begins at the gastrula stage, with the specification of the neural plate border at the edges of the neural plate. (C) As the neural plate closes to form the neural tube, the neural crest progenitors are specified in the dorsal part of the neural folds. (D) After specification, the neural crest cells undergo EMT and delaminate from the neural tube. (E) Migratory neural crest cells follow stereotypical pathways to diverse destinations, where they will give rise to distinct derivatives. (F) The neural crest is multipotent and has the capacity to give rise to diverse cell types, including cells of mesenchymal, neuronal, secretory and pigmented identity. Adapted from, Simões-Costa & Bronner. Development 2015 142: 242-257; doi: 10.1242/dev.105445

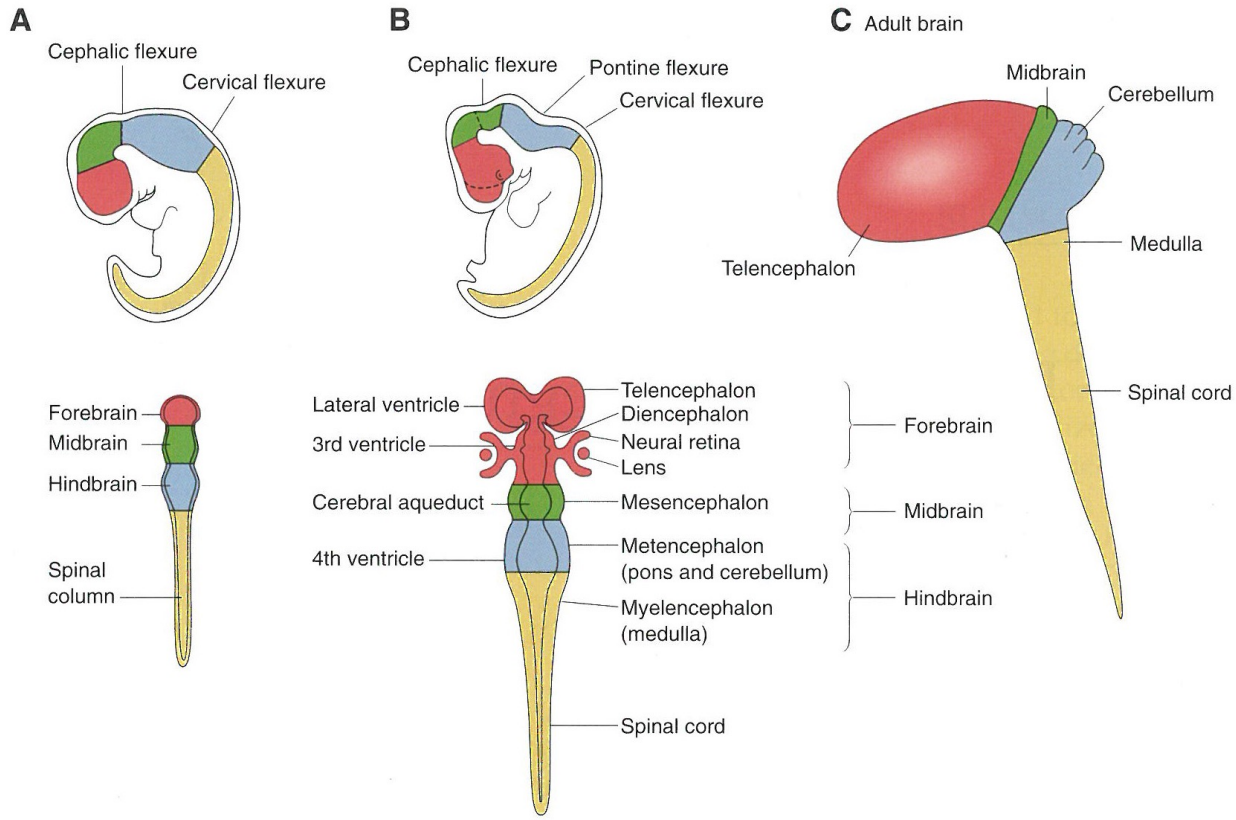

Figure 4. The neural tube forms the vertebrate brain and spinal cord.

Lateral (upper) and dorsal (lower panels) vies of human embryos at successively older stages of human development. (A) The primary three divisions of the brain. (B) Further development leads to the forebrain vesicle subdividing into paired telencephalic vesicles and the diencephalon. (C) Simplified organisation of the adult brain, showing the embryonic origins of each region. Taken from Figure 2.1 page 30, Sanes et al., Development of the Nervous System. 2nd Edition, 2006

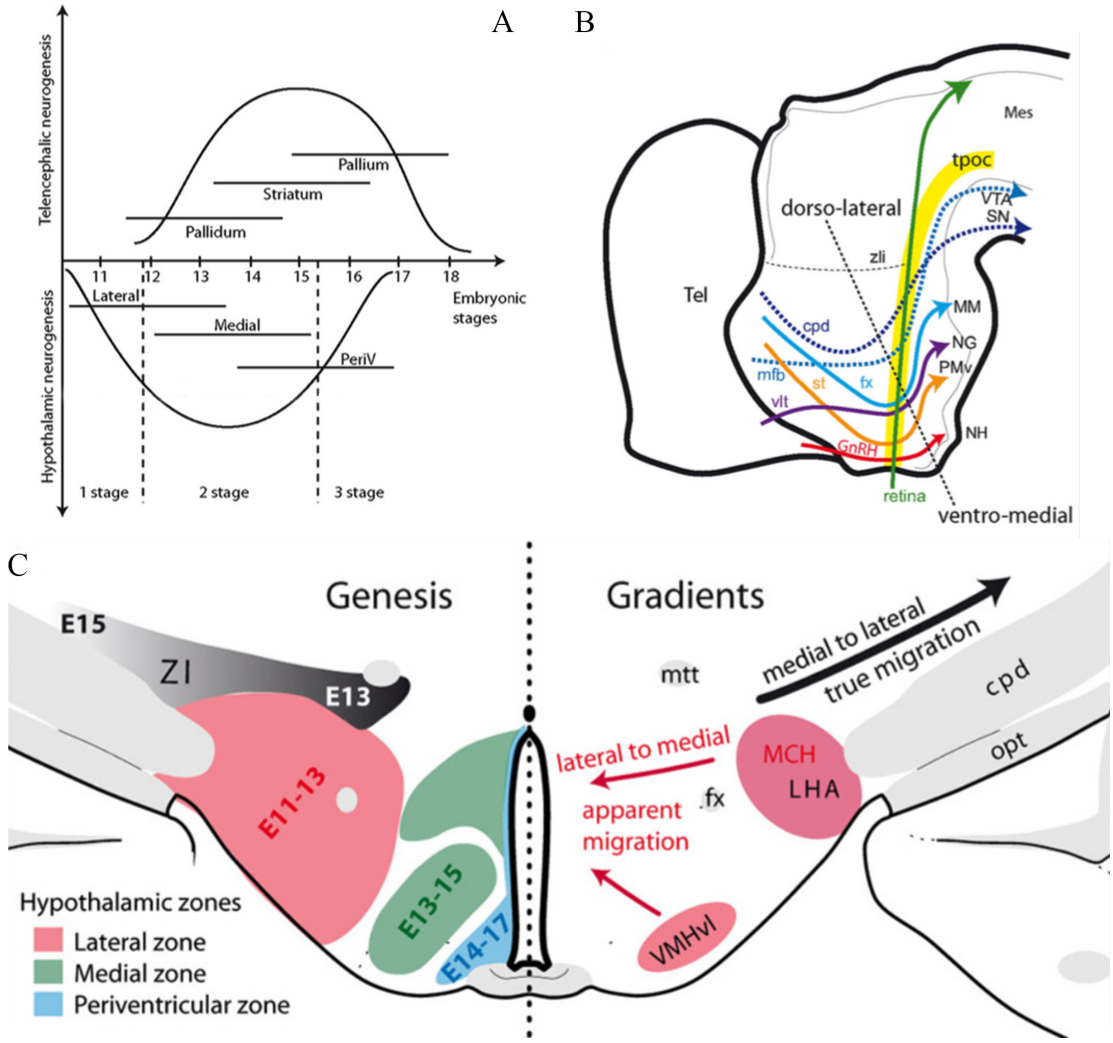

Figure 5. Schematics of hypothalamic embryogenesis in mice.

(A) Timeline of hypothalamic and telencephalic neurogenesis. Three temporal windows of neurogenesis have been identified, progressing from lateral to medial. (B) Schematic representation of the primary neuronal tracts in the ventral prosencephalon in a sagittal view of the embryonic brain (C) Left side: timing of formation of several key hypothalamic nuclei. Right side: gradients of neurogenesis in the ventral diencephalon. Abbreviations: cpd: cerebral peduncle; fx: fornix; GnRH: gonadotropin-releasing hormone; MCH: melano-concentrating hormone; mes: mesencephalon; mfb: medial forebrain bundle; MM: mammillary body; NG: nucleus Gemini; NH: neurohypophysis; periV: periventricular; PMv: ventral premmamillary nucleus; SN: substantia nigra; st: stria terminalis; tel: telencephalon; tpoc: tractus postopticus; vlt: ventrolateral hypothalamic tract; VTA: ventral tegmental area; zli: zona limitans intrathalamica. Adapted from Crozier et al., *Frontiers in Neuroanatomy*. 2015, (8)161

1.3 Anatomy of the adult hypothalamus

> "*Here in this well-concealed spot, almost to be covered with a thumbnail, lies the very main spring of primitive existence – vegetative, emotional, reproductive – on which with more or less success, man has come to impose a cortex of inhibitions*"
>
> –Harvey Cushing, 1932

Cushing's eloquent description of the hypothalamus which is approximately 4g in weight (equivalent to 1% of the total brain volume), came at a time when serious study of its function was in its infancy. Although the infundibulum and its surroundings had held an anatomical significance since the time of Galen, an appreciation of the hypothalamus and its functions had escaped generations of anatomists and medical scientists – to the point where it would often remain unlabelled in anatomical drawings. Due to a lack of obvious physical boundaries, the exact delimitations of the hypothalamus continue to be a cause of research and redefinition to this day (Morales-Delgado et al., 2014). Although its exact boundaries remain 'under review', it is universally accepted that the hypothalamus is the major integrative centre of vegetative, homeostatic and endocrine signals in the brain (Elmquist et al., 2005).

Homeostasis is the process by which a steady state of equilibrium in an organism, with respect to physiological functions and chemical compositions of fluids and tissues is maintained. A process that has been essential to maintaining life from the first single celled organisms, to the largest animal to ever live, the blue whale *balaenoptera musculus*. Physiological set points refer to a baseline level at which biological functions are maintained, and in bilaterians these set points are represented in neural networks by the firing rates of specific neuronal populations, each dedicated to the maintenance of a physiological process. This occurs by integrating internal and external sensory signals, processing them, then exerting regulatory autonomic signals and neuroendocrine releasing peptides to maintain homeostasis (Pearson and Placzek, 2013). The hypothalamus possesses the highest concentration of nuclei which encode set points and is therefore considered the key brain region for homeostatic and allostatic control (**Figure 6**).

As previously mentioned, the hypothalamus resides just superior to the hypophysis, with the two regions connected by the infundibulum. The infundibulum contains both neural projections from the hypothalamus that target the neurohypophysis and a network of specialised portal blood vessels derived from the anterior hypophyseal artery, that act as a conduit for releasing hormones of the hypothalamus to target the adenohypophysis. This portal vasculature is composed of fenestrated capillaries that form a primary plexus within the median eminence of the hypothalamus, and a secondary plexus within the adenohypophysis. It is here at the primary plexus, where neurosecretory releasing hormone neurons (such as GnRH neurons) form neuro-haemal junctions and exocytose their cargo. Interestingly, although a proportion of GnRH fibres can be found projecting into the infundibulum in most species, it has uniquely been shown that in humans some projections reach all the way into the adenohypophysis itself (King & Anthony, 1984).

The median eminence is a specialised region of the brain that has as its superior aspect the ventral portion of the third ventricle and the portal capillaries and infundibulum at its bottom. This privileged location outside of the blood-brain-barrier (BBB), whilst also containing modified ependymal glial cells that contact the wall of the third ventricle, is consistent with its specialised role in communicating peripheral signals to hypothalamic regions to regulate homeostasis (Balland et al., 2014; Langlet et al., 2013).

The hypothalamus, as previously described in the prosomeric model above, is a rostral forebrain entity, ventral to the telencephalon and rostral to the diencephalon proper, with no clear demarcations outlining its boundaries in adulthood. In addition to a lack of clear physical boundaries, the hypothalamus is not a homogeneous territory. Puelles et al. (2012b) mapped molecularly 33 discrete hypothalamic progenitor areas, and suggested that these areas produce a minimum of 150 derived nuclei or distinct cell populations that have been categorised, named and renamed in several different ways over the years. In the 1930's and 1940's it was proposed and since widely accepted, that the hypothalamic region should be extended to include the pre-optic region, based on its histologically similar appearance and its anatomical location (relative to unifying the anterior aspect of the third ventricle). Recent molecular fate mapping studies

have indicated, however, that this was unsound (Bulfone et al., 1993; Gelman et al., 2011; Puelles et al., 2004, 2012a).

Historically our anatomical knowledge of the complex nuclear composition of the hypothalamus is still redolent of the frustrating "potatoes- in-a-potatosack approach" as referred to by Puelles and Rubenstein (2015). It has traditionally been proposed to anatomically divide the human hypothalamus into three regions based on the arterial blood supply each receives:

- chiasmatic (anterior) region, extending between the lamina terminalis and the anterior infundibular recess which is supplied by branches of the anterior cerebral and anterior communicating arteries
- tuberal (median) region, the largest hypothalamic region proceeds to the anterior column of the fornix and contains the median eminence, the basal surface of the hypothalamus which is continuous with the infundibulum providing the physical communication to the adeno and neurohypophysis. The tuberal region is supplied by the posterior communicating artery
- posterior (mammillary) region, stretching to the caudal mammillary bodies supplied by the posterior communicating, posterior cerebral and basilar arteries

these regions can be further morphologically subdivided based on their laterality; the medial and periventricular regions contain the majority of nuclei, while the lateral region is largely composed of bidirectional fibre tracts, the medial forebrain bundle – connecting the hypothalamus to the limbic system and autonomic centres of the brainstem. The locations and main functions of the various hypothalamic nuclei are detailed in **Figure 6.**

The structural organisation and connectivity of the hypothalamus underscores this function as almost every major component of the neuraxis both communicates with, and is subjected to its influence. Thus, the anatomical, connectional and physiological complexity of this region matches the importance and intricacy of its functions.

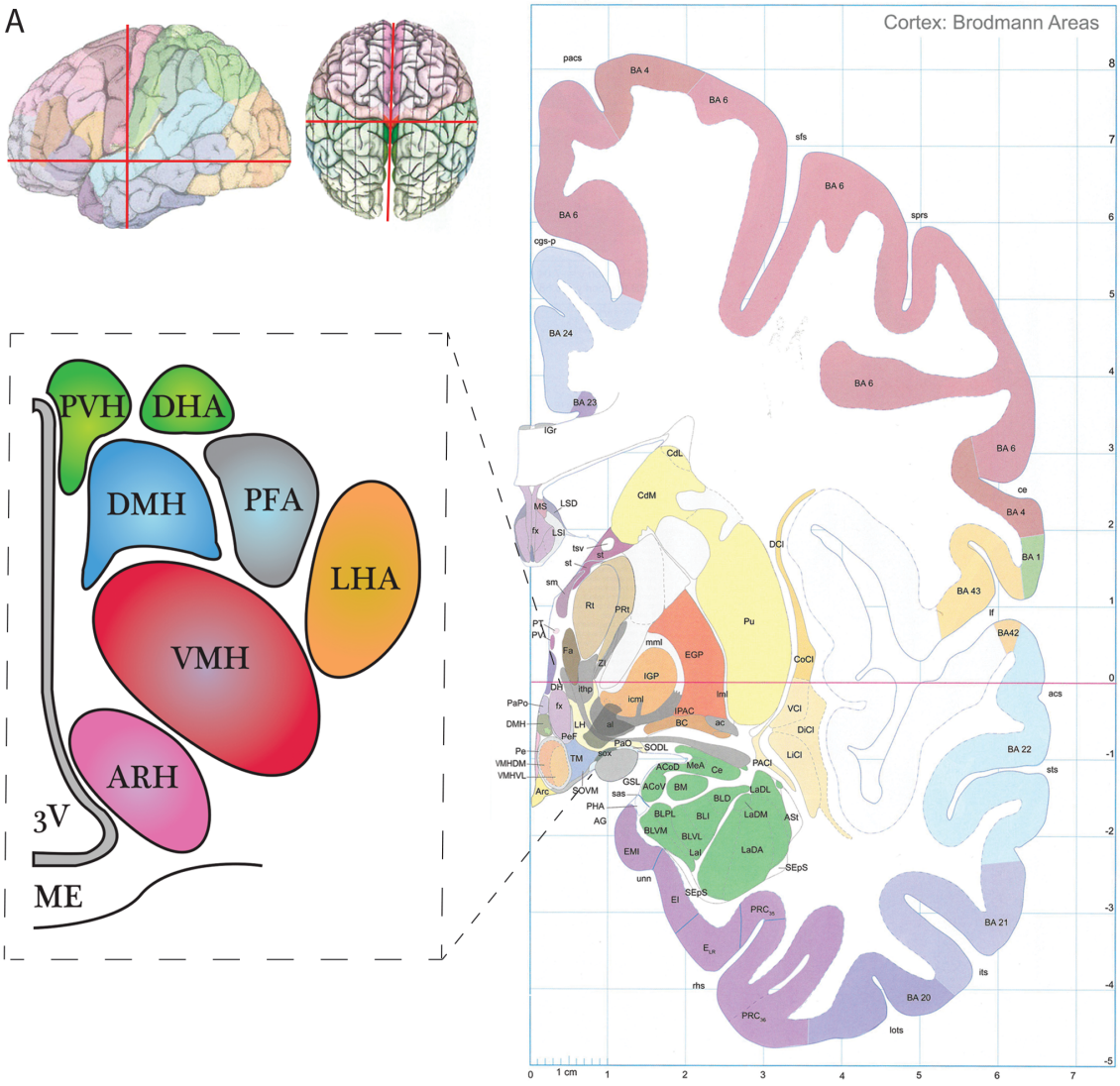

B

PVH & SON
- regulate water balance
- VP and oxytocin secretion
- projects to brainstem & SC

DMH
- satiety & aggression

PoN
- thermal regulation
- stimulates sympathetic NS

AHA
- thermoregulation
- stimulates parasympathetic nervous system

LHA
- stimulation induces eating
- destruction causes starvation

POA
- regulates GnRH release
- sexually dimorphic

Mammilary bodies
- receives hippocampal tracts
- projects to the thalamus

SCH
- receives input from retina
- controls circadian rhythms

VMH
- satiety & aggression

ARH
- hypothalamic releasing factors
- kisspeptin population regulates GnRH
- regulation of energy homeostasis

Figure 6. The anatomy of the adult human hypothalamus.
(A) Schematic representations showing the anatomical planes of the hypothalamus in man and a coronal hemisphere taken from Mai et al., Atlas of the Human Brain, 4th Edition. The bounded box indicates the positioning of several hypothalamic nuclei in relation to the 3rd ventricle and median eminence. (B) A sagittal representation of hypothalamic nuclei and their major functions. (B) modified from https://www.thinglink.com/scene/578173245958651906. Abbreviations: 3V: 3rd Ventricle; AHA: anterior hypothalamic area; ARH: Arcuate (infundibular) nucleus; CN III: oculomotor nerve; DHA: dorsal hypothalamic area; DMH: dorsomedial nucleus; LHA: lateral hypothalamic area; ME: median eminence; PFA: peri-fornical area; POA: pre-optic area; PVH: paraventricular nucleus; SCH: suprachiasmatic nucleus; SON: supraoptic nucleus; VMH: ventromedial hypothalamus

1.4 The Role of the Hypothalamo-Hypophyseal-Gonadal Axis in Reproduction

Located at the border of the diencephalon and telencephalon, the hypothalamus is a very ancient region of the brain, necessary for regulating key homeostatic processes and lesion of the canine hypothalamus results in death in under 24 hours. Accordingly, it controls diverse processes, such as water and electrolyte balance, cardiovascular function, sleep, metabolism, stress, thermoregulation, and reproduction (Elmquist et al., 2005). This is coordinated through both neuronal pathways (Lemaire et al., 2010) as well as sensing of hormonal and nutrient levels due to its privileged location – containing the most inferior aspect of the 3rd Ventricle forming the median eminence – a circumventricular organ outside of the blood brain barrier (Langlet et al., 2013). By bringing the control of endocrine systems under the hypothalamus it permits it access to both external and internal stimuli, learned behaviour and the cortical processes needed for normal physiological functions to be sensitively and optimally adapted to an ever-changing environment (reviewed in Raisman, 1997).

This myriad of signals converging on the hypothalamus provide the feedback necessary to coordinate precise and timely firing of neurons in order to trigger sexual maturation (pubertal onset) and eventually reproductive competence. Collectively the tissues that regulate reproductive function are known as the HPG axis, with it therefore playing a crucial role in ensuring the survival of the species, preserving the integrity of an organism and its offspring (**Figure 7**). This was initially discovered through a combination of works demonstrating that the ovulation and maintenance of corpora lutea (indicating pseudo pregnancy) of rabbits is dependent on the secretory activity of the adenohypophysis (Smith 1927), electrical stimulation of the hypophysis had no ability to trigger these effects (Markee et al., 1946; Harris 1948) but electrical stimulation of the hypothalamus is sufficient to elicit both effects in rabbit and rat does in oestrus (Harris 1936, Harris 1937).

It is not hard to imagine how diverse the inputs are that regulate reproductive function in different species dependent on their evolutionary niche and requirements. These range from the developmental clock, internal cues (e.g. leptin being necessary but not causative of puberty in humans), external cues (e.g. day length in seasonal breeders, pheromones), behaviour (e.g. copulation in solitary species such as camels and rabbits) and sex steroid feedback (e.g. oestradiol, progesterone, testosterone) (reviewed by Sisk & Foster, 2004). In all vertebrate species, these inputs eventually converge on a singular common neuronal population – the gonadotropin–releasing hormone neurons.

These neurons primarily send projections to exert their reproductive effects by secreting the neuro–hormone into the portal capillary system (the *rete mirabile* of Galen) connecting the hypothalamus to the adenohypophysis at the level of the median eminence. The peptide then traverses the fenestrated capillaries through the infundibulum and exits the rete, where it targets the G–Protein coupled receptor (GnRHR) expressing cells of the adenohypophysis. These cells regulate the synthesis and secretion of LH and follicle stimulating hormone (FSH) in response to GnRH signalling, with these hormones in turn regulating gonadal gametogenesis, production of sex steroids and secondary sex characteristics (**Figure 7**). Accordingly, disruption to the firing rate of GnRH neurons, their ability to secrete the peptide or disruption to endocrine feedback

results in either sub fertility or complete infertility. This was elegantly demonstrated using the Hpg mouse, an infertile hypogonadal mouse which harbours inactivating mutations in exons 3 and 4 the *GNRH1* gene (Mason et al., 1986a), with its fertility able to be rescued by transplantation of immortalised GnRH cells (Silverman et al., 1992), introduction of an intact *GNRH1* gene into the genome (Mason et al., 1986b), or transplantation of embryonic POAs into the third ventricle (reviewed by Charlton 2004).

That a hypothalamic releasing factor controls the hypophyseal release of the gonadotropin hormone Luteinising hormone (LH), which was already known to regulate gonadal function, was first described by McCann in 1960. At this time, there was great interest in the molecular identification of hypothalamic releasing factors, resulting in a race in the 1970's between several labs to classify them. The identification of this LRF (Luteinising hormone Releasing Factor, which in time would be renamed GnRH), as well as corticotrophin (CRH) and thyrotropin (TRH) releasing factors became like a quest for the grail, and in living up to this moniker it entailed a prolonged purgatory for all those involved to complete. In order to purify a useful amount of extract, several hundred thousand hypothalami of domesticated animals were dissected, lysed and fractionated by the laboratories of Shally and Guillemin, eventually leading them to simultaneously discover the tripeptide TRH in 1969. The identification of the decapeptide GnRH came a few years later by Shally (Amoss et al., 1971; Matsuo et al., 1971), and finally CRH, the hormone that had initially triggered the race, remained unidentified until 1981 – several years after Shally and Guillemin received the Nobel Prize in Physiology and Medicine in 1977. Shally later remarked upon the scepticism and ridicule he had endured during those long years, likening the peptides to both the abominable snowman and the Loch Ness monster.

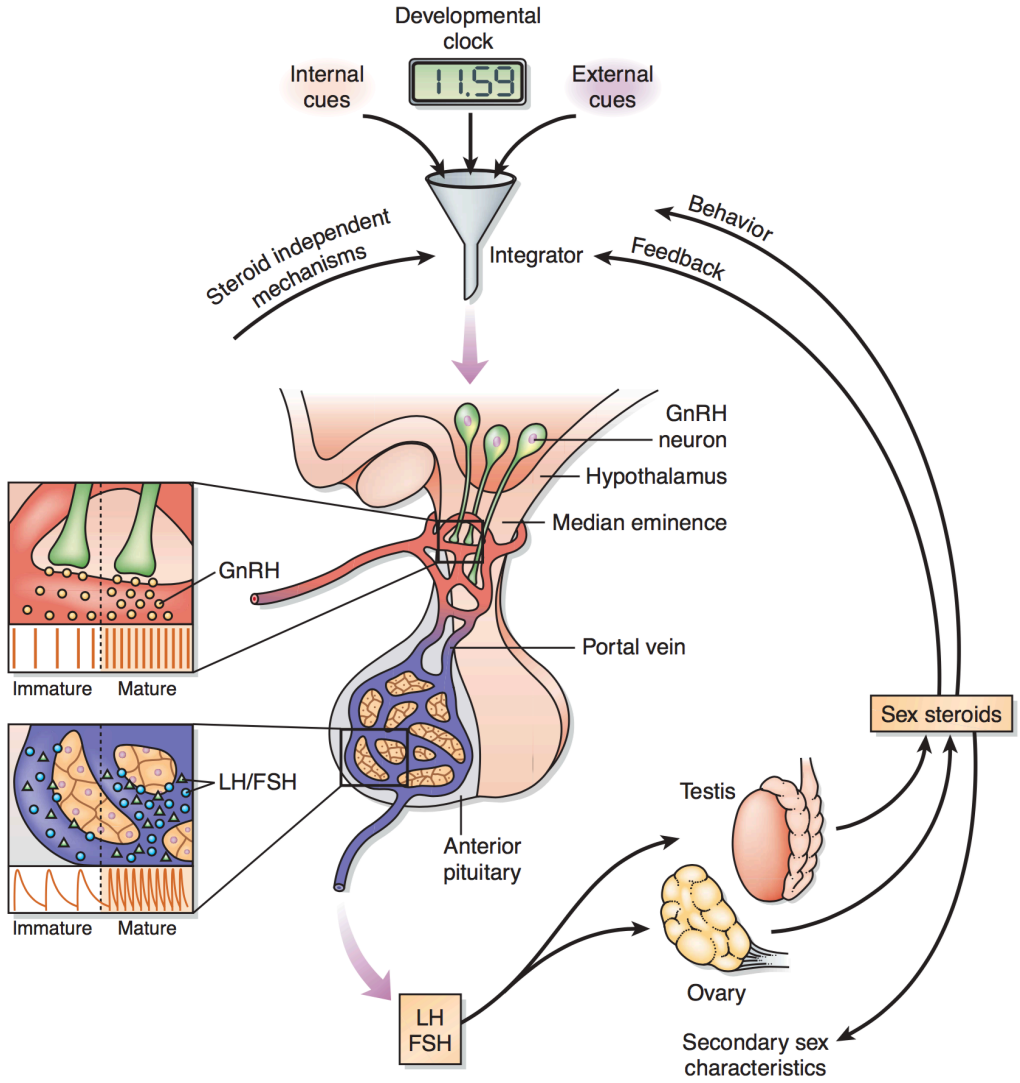

Figure 7. The hypothalamo–adenohypophyseal–gonadal (HPG) axis

Schematic representing the three principle regions governing the control of fertility in vertebrates. Hypothalamic GnRH neurons form the final common neural pathway, with the pulsatile release of GnRH a summation of multiple input and feedback mechanisms that can regulate the fertility of the organism. GnRH release from neurovascular synapses travels in the portal circulation to regulate the release of LH and FSH from adenohypophyseal gonadotroph cells. These hormones are released into the systemic circulation where they regulate gonadal function and stimulate the secretion of sex steroid hormones that are essential to fertility. The sex steroids in turn target the hypothalamus and pituitary, forming a feedback loop to regulate both GnRH and gonadotropin release. Figure taken from Sisk & Foster, *Nature Neuroscience* 2004

CHAPTER 2

Gonadotropin-Releasing Hormone Neurons: Development and Regulation

2.1 The GnRH System

The neurons that secrete gonadotropin-releasing hormone (GnRH, also known as LRF, LHRH) have been quantitatively assessed by many laboratories and the number of GnRH neurons in the brains of mammalian species is estimated at ranging from 800 cells in the entire brain in adult rodents to 2,000 neurons in the hypothalamus of adult human and non-human primates (Crowley et al., 2008; King and Anthony, 1984; Latimer et al., 2000; Silverman et al., 1982; Tobet et al., 2001). It is worth noting that the number of GnRH neurons in mice is higher during embryonic development (1,000-1,200 neurons) and is fewer in adulthood (Messina et al., 2011; Parkash et al., 2012) although the reason for this postnatal reduction is currently unknown. GnRH cell bodies are predominantly found scattered in a bilateral continuum throughout the diagonal band of Broca, where they can be found in the septum, organum vasculosum laminae terminalis (OVLT), pre-optic region (POA) and mediobasal hypothalamus (Figure 8). In the sheep, rat and mouse, the vast majority of GnRH somata are located in and around the rostral pre-optic area (rPOA). In contrast, a more homogeneous distribution of GnRH cell bodies is found in guinea pigs, primates and humans (Barry 1979; Goldsmith et al., 1990; King & Anthony, 1984; Krey & Silverman, 1978; Silverman et al., 1982). In primates there also exists a distinct population of GnRH neurons that reside in the infundibular nucleus (known as the arcuate nucleus in other species). These scattered neurons by definition are heterogeneous, with only a proportion believed to form a diffuse neural network that functions co-ordinately as a GnRH pulse generator (Knobil, 2015).

Although originally named for its role in regulating the HPG axis, two related GnRH genes have been identified in vertebrates, first from chickens (Miyamoto et al., 1984) and then from salmon (Sherwood et al., 1983). Each form of GnRH is a decapeptide, showing conservation at protein residues 1, 4, 9 and 10. Although the genes and amino acid sequences of these multiple GnRH peptides is homologous (Fernald & White, 1999), they are encoded by different genes and each GnRH peptide has its own distinct promotor sequence (Fernald & White, 1999). These additional forms of GnRH are classically localised to the *nervus terminalis* (TN) of the forebrain

(GnRH3) and to the midbrain (GnRH2). GnRH3 neurons of the TN have been shown to possess a neuromodulatory role in the forebrain and olfactory epithelium (Abe and Oka, 2002; Eisthen et al., 2000), and also act as modulators of olfactory mediated behaviours (Wirsig-Wiechmann et al., 2002). Similarly, the GnRH2 cells of the midbrain also appear to modulate sexual behaviours (Temple et al., 2003). All tetrapods examined possess at least two forms of GnRH, with GnRH1 playing an endocrine role in most species and other forms regulating reproductive behaviours; as although both GnRH1 and GnRH2 (human chromosome 20) have been found in the pituitary, only GnRH1 is thought to elicit the secretion of gonadotropins (Kobayashi et al., 1994; Montaner et al., 2001). From this point, references to GnRH will refer solely to GnRH1 unless otherwise stated.

Figure 8. Distribution of GnRH neurons in the adult mouse brain.

Representative images of GnRH immunostaining in the adult mouse, acquired with light sheet imaging. GnRH neurons are stained in white, with surface modelling of the ventricular system (VII: lateral ventricle) in grey. Bottom panel: GnRH neurons (black dots) in the sagittal (top) and coronal (bottom) planes. Neurons are found scattered in a bilateral continuum from the olfactory bulb to the hypothalamus forming an 'inverted Y' shape when viewed coronally. The site of GnRH projections, the median eminence is indicated in red. Abbreviations: 3V: 3rd ventricle; AC: anterior commissure; AHA: anterior hypothalamic area; MS: medial septum; OB: olfactory bulb; CB: cerebellum; OC: optic chiasm; CN II: optic nerve; OVLT: organum vasculosum of the lamina terminalis; rPOA: rostral pre-optic area; VDBB: ventral diagonal band of Broca. Immunostaining by Malone S. Bottom schematic taken from Herbison A, chapter 11, Knobil's physiology of reproduction 2014.

Whole Mount Immunostaining of GnRH in the Adult Mouse

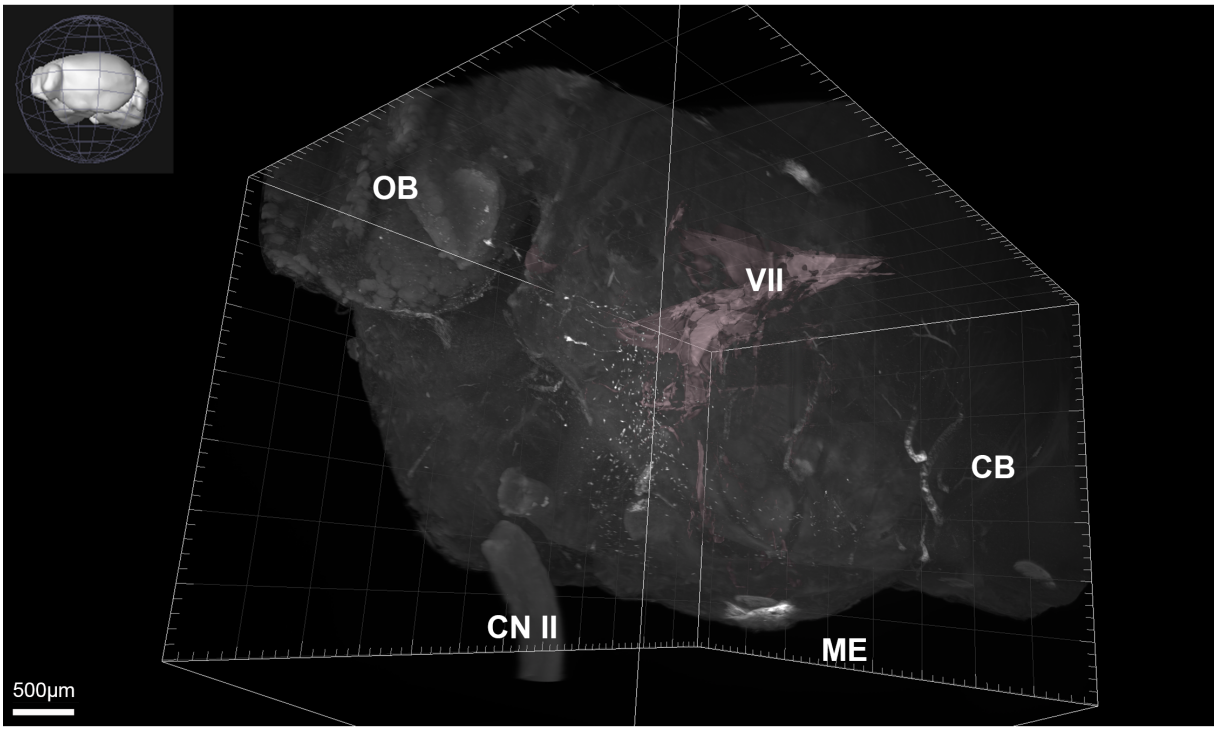

Oblique Hemisphere

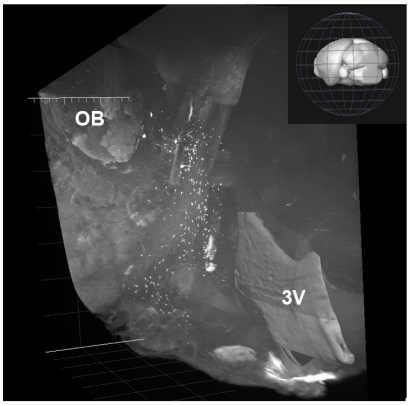

Superior-Posterior

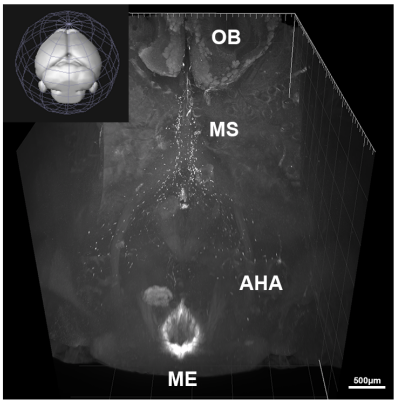

Posterior

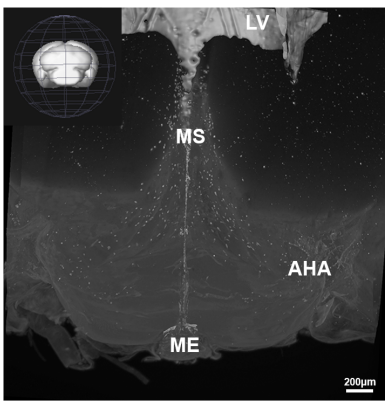

Schematic Representation of GnRH distribution

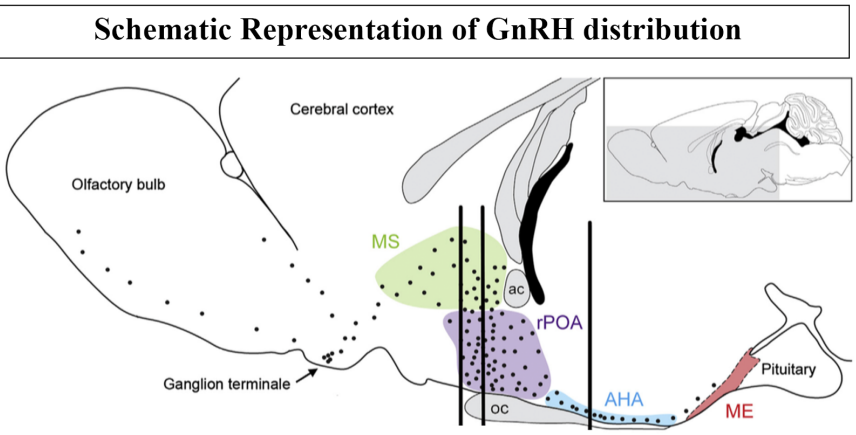

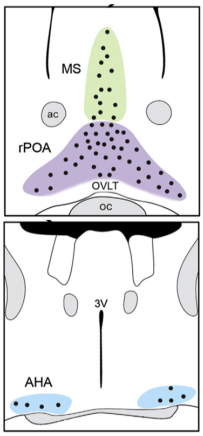

2.2 GnRH hypothalamic network

Although there exist species differences in the anatomical locations of GnRH neurons, all mammals thus far studied generate pulses of LH secretion, which correlate with pulsatile GnRH release at the median eminence. The transplantation of GnRH neurons into the ventricular system of the aforementioned Hpg mouse indicate that as few as 20 GnRH neurons are capable of generating pulsatile LH secretion (Kokoris et al., 1988). Similarly, the males of a mouse line that possesses only 80 GnRH neurons, were able to father offspring (Herbison et al., 2008) – underscoring the fundamental importance of GnRH release while also lending insight to the heterogeneous nature of the GnRH population.

During reproductive life, ovarian (oestrous) cycling depends on the maintenance of GnRH release within a narrow range of pulse frequency and amplitude (Ebling, 2005). The intervals between GnRH pulses *in vivo* range from 40–60 minutes in the gonadectomised monkey (Terasawa 1985), sheep (Caraty et al., 1989) and rat (Levine & Duffy, 1988), with longer intervals reported in intact animals (Evans et al., 1995; Park & Ramirez, 1989). Additionally, changes in hypothalamic GnRH expression and secretion have been implicated in the transition through menopause (Wise et al., 1996; Yin et al., 2006), further highlighting the importance of the tight regulation of its expression.

The regulation of pulsatile GnRH secretion has been widely studied, as how such a diffusely spread population could coordinate their firing to generate a synchronous pulse is not immediately evident. However, classical tracing studies have shown that in both the rodent and primate brain only 50–70% of GnRH neurons are hypophysiotropic; suggesting not all GnRH neurons are involved in pulsatile release and only a subset should be required to coordinately fire (Goldsmith et al., 1990; Silverman et al., 1987). The idea of an 'internal' pulse generator (that is, a property intrinsic to GnRH neurons that would allow them to fire in synchrony), is currently falling out of favour, recently being supplanted with an 'extrinsic model' of pulse generation (reviewed by Herbison 2016).

GnRH neuron morphology is seemingly unique amongst all the neurons in the mammalian CNS and may help to explain how such a pulse generator could be effected. They appear to possess two long dendrites, with either one or both projecting to the median eminence (Herde et al., 2013; Herde & Herbison, 2015); with both projections receiving synaptic inputs and able to propagate action potentials towards their neurosecretory terminals (Campbell et al., 2005; Herde & Herbison, 2015). These projections also form a network, becoming interwoven and even sharing synaptic inputs (Campbell et al., 2009). Administration of neurotransmitter receptor antagonists is capable of abolishing GnRH secretion (Kordon et al., 1994), suggesting that an external pulse generator may only need to act on GnRH dendritic/axonal projections as they converge together to innervate the median eminence. Indeed, it now appears likely that the arcuate population of Kisspeptin, neurokininB and dynorphin expressing neurons (KNDy neurons) is likely to play a fundamental role in generating pulses of GnRH release (Navarro et al., 2009).

Of course, whilst the regulation of GnRH pulsatility is important to ensuring continued reproductive competence, the physiological regulation of GnRH secretion is far more complex than being regulated by kisspeptin alone. For instance, the network first becomes active during mid gestation in humans (Clements et al., 1976; Kaplan et al., 1976) and there exists an abrupt, 1–12 hour surge in LH secretion shortly following birth in both male rodents and primates (Corbier et al., 1978; Corbier et al., 1990; de Zegher et al., 1992). A further transient activation occurs amongst human infants beginning at 1–2 postnatal weeks, and persists for several months in males and around 2 years in females (Schmidt & Schwarz, 2000; Winter et al., 1975) only for the axis to enter a state of quiescence until reactivation at puberty. Additionally, in spontaneously ovulating species, a surge of LH and GnRH (several times greater in magnitude than typical pulsatile release) at the end of the follicular phase of the oestrous cycle initiates ovulation. The mechanisms that regulate the GnRH network are complex, with first order connections proposed to number in the millions (Herbison, 2015) and species-specific requirements resulting in differing hierarchical importance of their inputs.

One core component regulating the hypothalamic network that impinges on GnRH neurons is

the various internal homeostatic factors, such as gonadal steroid and metabolic hormones that act indirectly to modulate the afferent inputs to GnRH neurons. This arrangement likely ensures feedback to multiple hypothalamic networks simultaneously (e.g. testosterone being able to regulate the growth and reproductive axes). Outside of the core homeostatic feedback and arcuate nucleus control of pulsatile release, there is a growing realisation of the key importance of glial and neuronal inputs that control GnRH neurons (Prevot et al., 2010; Sharif et al., 2013). These assemblies of neurons and glial cells can be represented as modular functional units that interconnect in a species-specific manner to endow relevant function on the GnRH neuron, summarised in Figure 9.

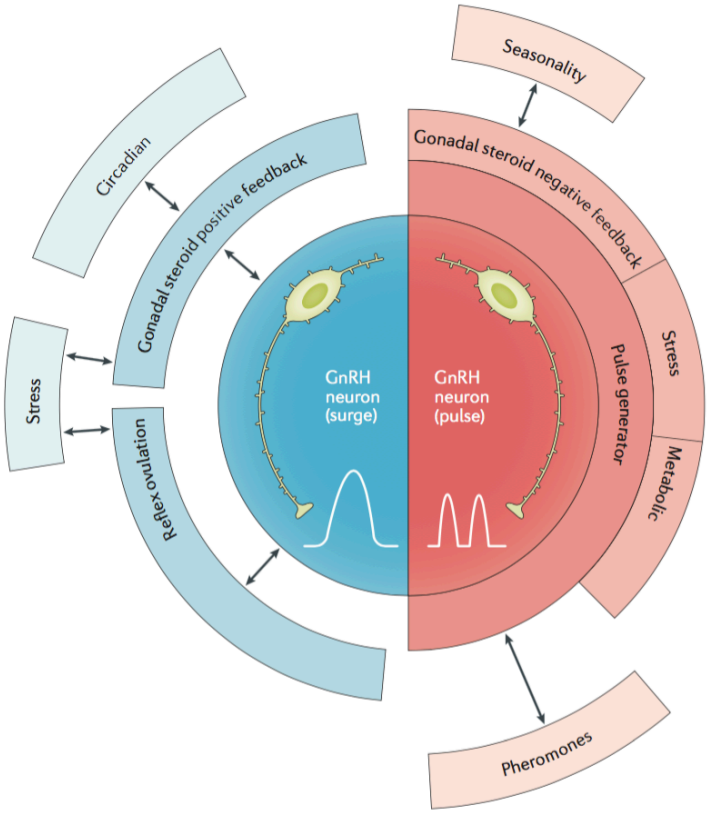

Figure 9. Modular assembly of the GnRH neuronal network.

The model proposes that there are two populations of GnRH neurons. One population is involved in generating pulses (red), whereas the other generates the surge (blue). Modules present in all mammals are shown directly connected to the population that they influence. Species-variable modules may be added when required (shown with bidirectional arrows). Figure taken from Herbison A, Nature reviews endocrinology 2016

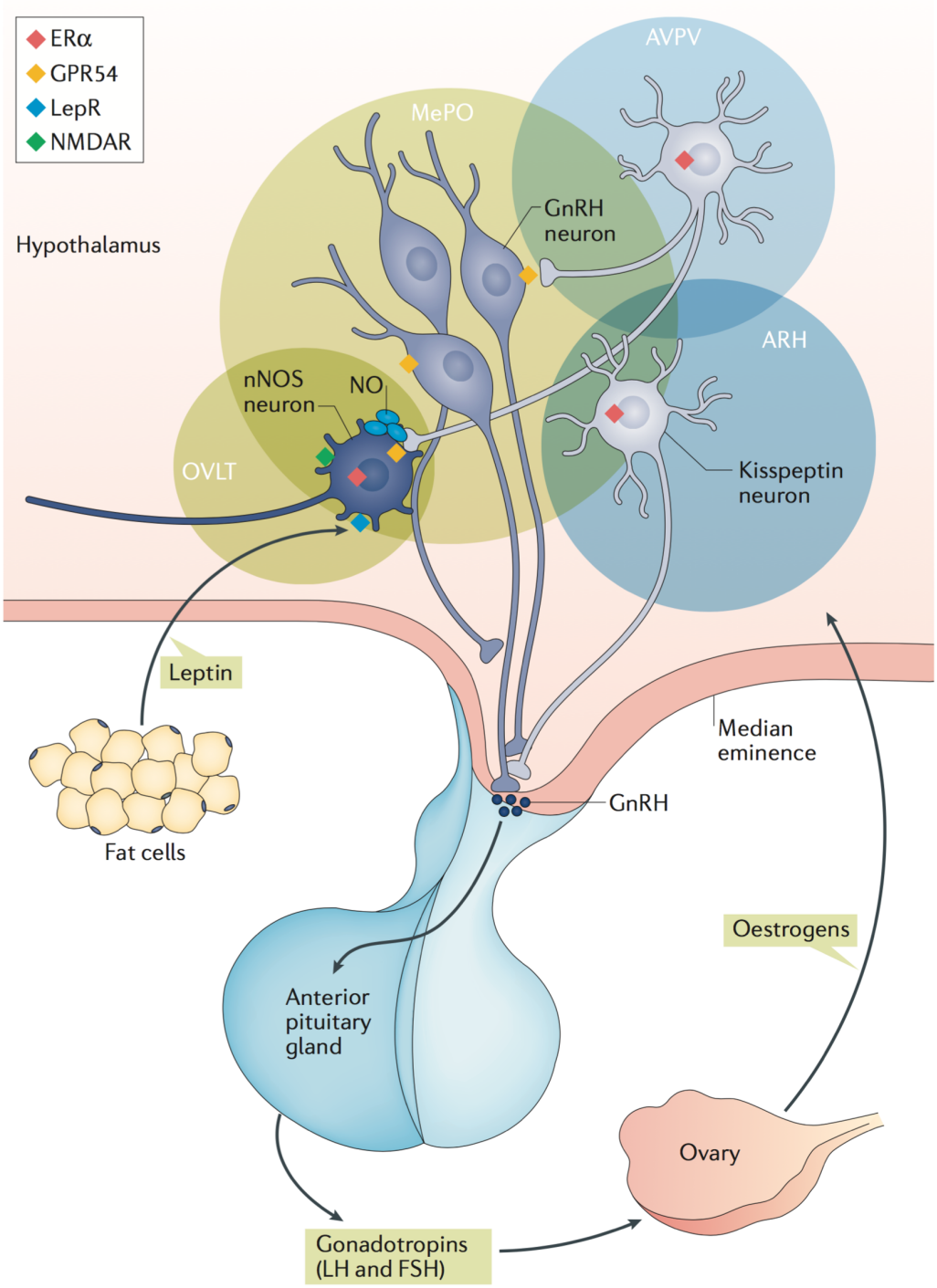

Figure 10. Proposed mechanism of GnRH synchronisation.

Oestrogen receptor expressing arcuate kisspeptin neurons are believed to act directly on GnRH dendrites within the median eminence to synchronise GnRH firing. Leptin, a circulating metabolic hormone, is believed to indirectly regulate GnRH pulsatility through the population of neuronal nitric oxide synthase (nNOS)–expressing cells residing in the organum vasculosum laminae terminalis (OVLT) and median preoptic nucleus (MePO), 'fine tuning' its release. Figure taken from Chachlaki & Prevot, *Nature reviews neuroendocrinology* 2017.

2.3 GnRH – From gene to protein

The *GnRH1* gene is located on human chromosome 8p21.2 and chromosome 14 in mice. The GnRH RNA primary transcript comprises four exons and three introns. Exon 2 encodes the GnRH decapeptide, the enzymatic amidation and precursor processing site and the first 11 amino acids of GAP1 (see below). Exons 3 and 4 encode the remaining amino acids of GAP1 and the 3' untranslated region (Selmanoff et al., 1991). Processing, and removal of introns was found to be largely conserved between species and is largely outside of the scope of this thesis (reviewed by Gore & Roberts, 1997).

GnRH1 is synthesised as part of a precursor protein (prepro-GnRH) of 92 amino acids. This includes the N-terminus composed of 23 amino acids, which contains the pro-GnRH, followed by a C-terminus of 69 amino acids that will give rise to GAP1 (GnRH1 associated peptide), a 56-amino acid peptide that has been suggested to participate in the regulation of both prolactin and gonadotropin secretion (Adelman et al., 1986; Seeburg & Adelman, 1984). Human and rat GAP1 share approximately 70% sequence homology (Adelman et al., 1986), with the majority of variation occurring in the N-terminal region of the peptide. Immunocytochemical staining showed that GAP1 co-localises with GnRH cell bodies and fibres in the mature rat (Phillips et al., 1985), foetal rhesus macaque (Song et al., 1987), juvenile baboons (Song et al., 1987) and human hypothalamus (Skrapits et al., 2015). Its presence in dense-core vesicles of terminal varicosities within the median eminence (Phillips et al., 1985), eventually led to its detection in the portal circulation in ovariectomised ewes, with its levels highly correlated with GnRH levels (Clarke et al., 1987) supporting this notion. Recently a GAP1 antibody that specifically recognises the human form of GAP1 (hGAP1) has been developed (Skrapits et al., 2015), allowing the strict identification of GnRH1 expressing neurons in humans.

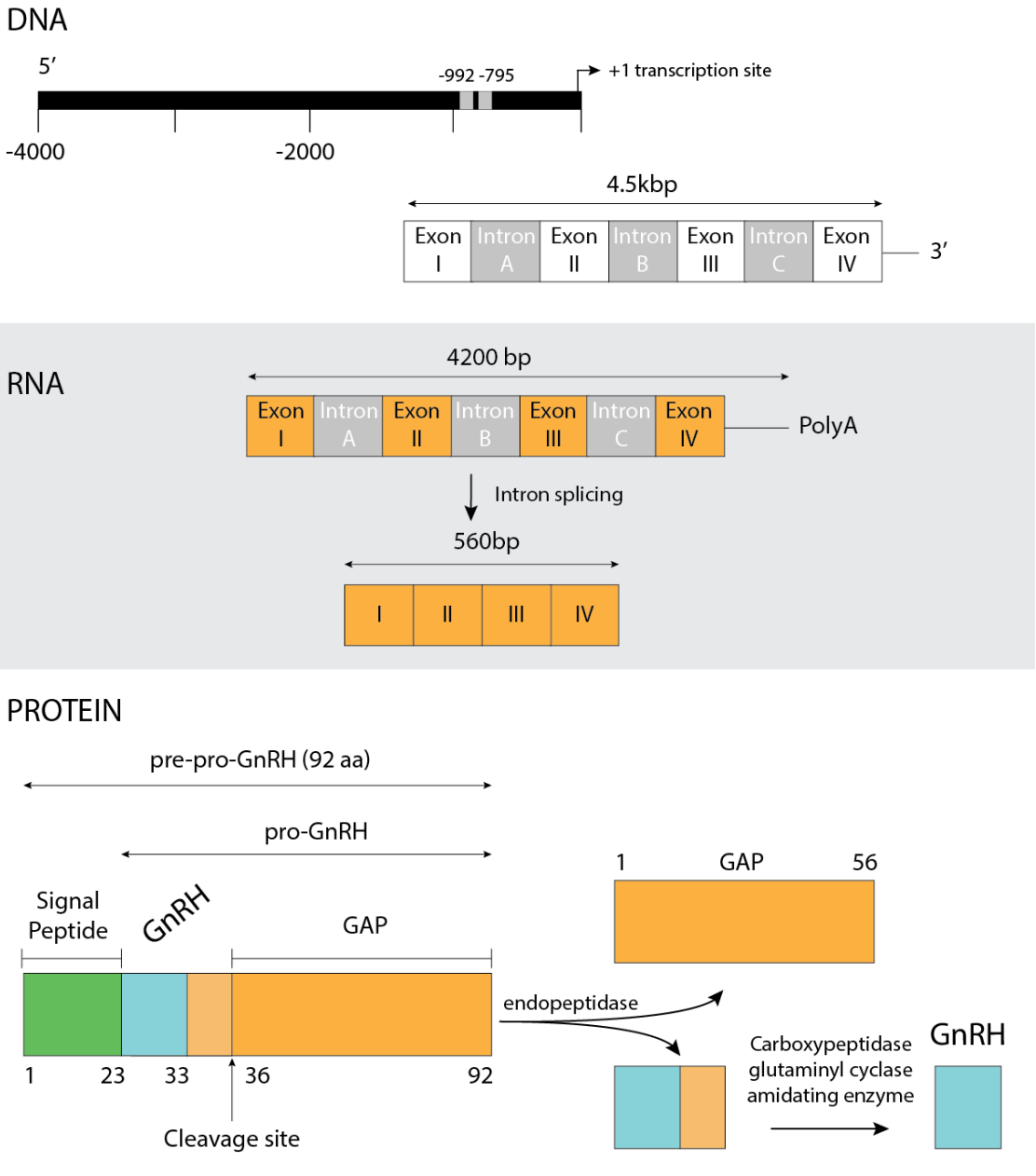

Figure 11. Biosynthesis of GnRH and GAP.

(DNA) The structure of the human, rat and mouse GnRH gene with the 5' regulatory sequence and specific regions of known function highlighted. (RNA) GnRH RNA and various splicing and processing intermediates. (Protein) translation and posttranslational modifications that result in the final GnRH decapeptide. Figure made by Malone SA

The regulation of biologically available GnRH is controlled at a multitude of bio-synthetic levels. *GnRH* gene expression is determined by the rate of transcription of pro-GnRH, polyadenylation and capping of the RNA, processing of the GnRH primary transcript to form the mature mRNA and transport of the mRNA from the nucleus to the cytosol. Next, mRNA levels are determined by the turnover of the mRNA, while the rate of the translation of the mRNA into the pro-GnRH peptide determines the amount available to be processed into the mature form of GnRH that will be packaged into large dense core vesicles to be secreted (King & Anthony, 1983; Rangaraju et al., 1991). Thus, GnRH biosynthesis is regulated at many levels (reviewed by Gore & Roberts, 1997). Studies have shown that in rodents, GnRH neurons possess a large, steady state pool of GnRH mRNA that appears to function as a cytoplasmic reserve. This accumulation due to lack of immediate processing is compounded as GnRH mRNA half-life ($t_{1/2}$) is 22-30h under basal conditions (Bruder & Weirman, 1994; Yeo et al., 1996). This reserve may be important for rapid generation of the peptide in order to replenish peptide levels in anticipation of the pre-ovulatory surge (Wang et al., 1995), although this evidence is far from conclusive. Indeed, it has been repeatedly suggested that GnRH biosynthesis and secretion are not tightly linked. For instance, *in vitro* treatment of immortalised GnRH cell lines with the glutamate analogue *N*-methyl-D,L-aspartate (NMDA), causes rapid increases in GnRH mRNA levels in the absence of changes in the GnRH primary transcript levels – supporting a largely post-transcriptional regulation of GnRH expression (Gore & Roberts, 1994).

The mature form of GnRH1 is a decapeptide, where the N-terminal residue consists of a pyroglutamate and the C-terminus possesses a glycine-amide. These two modifications have long been thought to stabilise its structure and slow its degradation in the blood (Chertow, 1981), where it has a native $t_{1/2}$ of 2-4 minutes due to rapid peptidase degradation and glomerular filtration. The amino acid sequence of GnRH1 is extremely conserved, with near identical sequences being identified in all mammals, with the exception of two amino acid substitutions in the guinea pig (Jimenenz-Linan et al., 1997).

2.4 Embryonic Origin of GnRH Neurons

Postnatally, GnRH neurons possess several characteristics that liken them to the other parvocellular releasing neurons of the hypothalamus (TRH, CRH, GHRH expressing neurons) in that they all secrete a neuropeptide into the portal capillary system and form the apex of a tripartite feedback axis, fulfilling the criteria of Harris described in chapter I. The embryonic origin of the TRH, GHRH and CRH expressing neurons has been determined by *in situ* hybridisation (ISH) studies and been determined to be primarily in the peduncular paraventricular domain of the developing hypothalamus, with expression first detectable around embryonic day E10.5 in mice (Morales-Delgado et al., 2014). GnRH neurons however, are unique amongst the population of releasing hormone neurons in that they do not arise from the embryonic hypothalamus, as was first demonstrated in 1989 (Schwanzel-Fukuda & Pfaff, 1989; Wray et al., 1989a; Wray et al., 1989b), but instead arise in an extra-encephalic region, namely the olfactory placodes.

2.4.1 Formation of the olfactory placodes

The olfactory placodes are derived from the primitive placodal thickening that arises concurrently with the formation of the neural plate (Brunjes & Frazier, 1986; **Figure 12**). The primitive placodes become separated from the neural crest (NC) and developing CNS as the neural plate begins folding to form the neural groove, resulting in a thinning of the ectoderm along the border of the plate. In mice, by E9 the olfactory placodes are visible and already possess a pseudostratified appearance; and as the placodes grow, they invaginate to form the nasal pits. The central region of the nasal pit gives rise to olfactory epithelium – the chemosensory olfactory system (responsible for the detection of volatile odorants), while the medial wall develops into the vomeronasal organ (VNO) – the pheromone receptive system of rodents (Halpern, 1987). The presence of a functional VNO in adult humans is debatable, although its existence in a substantial portion of adult humans was recently demonstrated (Frasnelli et al., 2011) and it is easily distinguishable until birth (Bhatnagar & Smith, 2001; Smith & Bhatnagar, 2000).

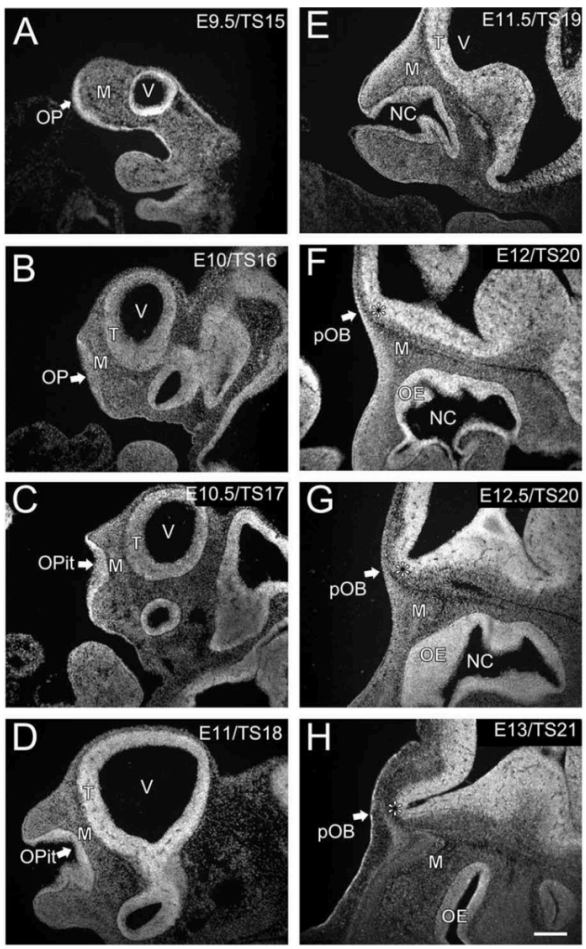

Figure 12. Development of the olfactory placodes and olfactory bulbs.

Sagittal sections of the development of the nasal region of the mouse between embryonic day 9.5 (E9.5) to E13.

Abbreviations: OPit: olfactory pit; pVNO: presumptive vomeronasal organ; M: mesenchyme; pOB: presumptive olfactory bulb; NC: nasal cavity; T: telencephalon. Scale bar = 200 μm

Figure taken from Miller et al., *Journal of Comparative Neurology* 2010

As they both arise in the developing nose, the development of the GnRH and olfactory systems are inextricably linked; however, identifying the embryonic precursor lineage that gives rise to GnRH expressing cells has remained elusive despite their importance to the field of reproductive physiology. One limitation has been the lack of markers found to distinguish GnRH populations, with GnRH being the sole marker capable of labelling the entire population. No other transcription factor or gene product has been demonstrated to label all GnRH neurons during development. Studies utilising the GnRH::GFP mouse lineage (where expression of the green fluorescence protein is driven by the GnRH promoter) have failed to resolve the problem, as GFP expression is weak during early development. There also exist discrepancies between GFP expression and total immunostained GnRH, suggesting only a portion of the population is being labelled (Spergel et al., 1999; Suter et al, 2000). What is clear, however, is that fate specification occurs before migration begins (Wray et al., 1989b). Studies on different animal models have provided contrasting, yet compelling evidence for neural crest (NC), placodal and non-placodal ectodermal origins for GnRH cells.

2.4.2 Evidence for the olfactory placode

In humans, as in other vertebrates, the nasal placodes develop as thickenings of the ectoderm on the ventrolateral sides of the head around the fifth week of gestation (Muller and O'Rahilly, 2004). The nasal placodes in mice develop from the anterior neural ridge as ventrolateral ectodermal thickenings and are detectable at embryonic day 9.5 (E9.5). At E10, the placode invaginates to form the olfactory pit and neuronal differentiation commences with GnRH expression first detected 6 hours later. An exact 'birth date' of GnRH neurons in humans is difficult to accurately determine due to the scarcity of available tissue, but has been thought to occur around 42 days of gestation (Kim et al., 1999; Schwanzel-Fukuda et al., 1989). The placodes give rise to multiple cell types including olfactory sensory neurons (OSNs) that will project to the brain (Wray et al., 1989b) and olfactory ensheathing cells (OECs) that will act as guidance for migrating olfactory sensory neurons (OSN) axons.

One of the first papers to document the nasal origin of GnRH neurons isolated their differentiation to the OP (olfactory placode) with 70-80% of GnRH neuron progenitors undergoing fate specification between E9.5 and E10.5 (Wray et al., 1998b) and ablation of the OP in both mice and chicken results in reduced GnRH cell numbers in adulthood (Daikoku et al., 1993). Indirect evidence supporting an OP origin comes from studying a human reproductive disorder called Kallmann's syndrome (KS). This disorder results in infertility due to a lack of GnRH in the brain, coupled to a lack of smell (anosmia) – a function that is dependent on correct OP formation and development (Cariboni & Maggi, 2006).

2.4.3 Evidence for the neural crest origin of GnRH neurons

Fate mapping studies in zebrafish and chicken that focused on pre-placodal stages demonstrated that the OP arises from a mix of different lineages, including the NC. The NC arises at the junction between the neural tube and epidermis, and derivatives of the NC form neurons and glia of the peripheral nervous system as well as cranial cartilage and bone (Bronner-Fraser, 1995). In fish, the cranial neural crest (CNC) develops in close association

with the developing olfactory placode and it has been shown that a large proportion of GnRH3 neurons that stay attached to the terminal nerve are derived from the CNC (Whitlock et al., 2003). This was determined using a fate mapping technique, significant because the targeting of the CNC occurred before OP differentiation suggesting that the GnRH cells migrated into the OP from the CNC and GnRH1 and GnRH3 are hypothesised to have arisen from a gene duplication.

Diseases caused by lack of GnRH in the brain (see **2.11**) can be associated with additional syndromic disorders such as CHARGE syndrome (Ogata et al., 2006; reviewed by Boehm et al., 2015). CHARGE (coloboma of the eye, heart defect, choanal atresia, retarded growth and development, genital hypoplasia, external ear anomalies and deafness) syndrome also presents with NC-associated defects including cleft palate, dental agenesis and craniofacial dysmorphisms, suggesting a potentially shared developmental origin for these syndromes. That GnRH neurons do not express common markers of the olfactory system, while being nestin positive (a marker of NC progenitors as well as the CNS in general) (Kramer & Wray, 2000) is suggestive of sharing a lineage with neural crest derived cell types.

Using complementary Cre-lox fate mapping of specific NC and ectodermal derivatives in mice, Forni et al. (2011) were able to demonstrate significant intermingling of CNC and ectodermal cells in the OP. These NC cells eventually gave rise to both a population of GnRH cells as well as 100% of OECs. This study found approximately 30% of the total number of GnRH neurons were derived exclusively from the NC (with good correlation between both *in vivo* and in *ex vivo* nasal explants), while 70% originated from the ectoderm (as of yet unidentified OP precursors). A number of studies have identified and validated mutations that consistently affect 30% of the GnRH population (Kramer et al., 2000; Kruger et al., 2004; Givens et al., 2005; Tsai et al., 2005; Cogliati et al., 2007; Giacobini et al., 2007; Miller et al., 2009), while Dlx5 expression was constrained to 70% of migrating GnRH neurons (Merlo et al., 2007), further lending credence to a dual site of origin.

2.5 Migration of GnRH Neurons

The migration of GnRH neurons from the nasal placode to their resting place in the ventral forebrain necessitates a long, ever expanding migratory pathway traversing distinct molecular environments. This process is extremely conserved through evolution, occurring in all vertebrates thus far studied – indicating an ancient origin for this fundamental process. Although the reason necessitating this developmental journey remains largely a mystery, intriguingly a GnRH-expressing neuron mediating both chemosensory and reproductive functions exists in the placode of ancestral chordates (Abitua et al., 2015). It is hypothesised that these functions became anatomically segregated during evolution, with the chemosensory neuron remaining in the olfactory epithelium and the neurosecretory neuron migrating to the hypothalamus to regulate hypophyseal function. Nevertheless, continuing in the absence of understanding why evolution progressed in such a manner, much work has been done to characterise the migratory pathway GnRH neurons take and the factors that regulate this process. While many species have been analysed, perhaps an underutilised model is marsupials as early steps in development of the olfactory and GnRH system occur during the first month after birth while the pup is suckling (Brunjes et al., 1992), instead of *in utero* as in eutherian mammals. One such marsupial, the Brazilian short-tailed opossum *Monodelphis domestica* possesses the added advantages that it can be bred in laboratory environments (Kraus & Fadem, 1987) and that its CNS can survive intact in culture (Nicholls et al., 1990). Unfortunately, few studies have been conducted using this model (Tarozzo et al., 1995) but it should remain of interest to future researchers. What follows is a summation of the key results that have informed our understanding of the GnRH migratory process from studying mice, humans and non-human primates.

2.6 GnRH Migration in Mice

As discussed above, the expression of GnRH occurs while the cells still reside in the OP and therefore before migration has commenced, suggesting that fate specification occurs before migration begins; with that caveat, four distinct steps of migration have been characterised in mice (Tobet & Schwarting, 2006; Wray 2010).

i) GnRH neurons begin migrating together with axons of olfactory [vomeronasal nerve (VNN)] and/or the TN through the nasal mesenchyme to the nasal/forebrain junction (cribriform plate).

ii) at the cribriform plate the vomeronasal nerve divides, with GnRH neurons following one branch towards the ventral forebrain.

iii) long processes form that guide the GnRH neurons that migrate towards the hypothalamus.

iv) finally the neurons detach from their axonal guides and disperse further in the hypothalamus, ready to send projections to the external zone of the median eminence.

This entire process is completed by birth and although some species-specific characteristics are present, a similar set of mechanistic steps are critically required to ensure GnRH is correctly targeted to be delivered to the adenohypophysis and regulate reproductive competence.

Beginning at E10.5 in mouse, the nasal placodes invaginate and give rise to multiple cell types including GnRH neurons, OSNs that project to the olfactory bulb (Wray et al., 1989), and other cell types including OECs that provide essential growth and guidance for OSN axons (Su and He, 2010). The coalition of GnRH neurons, placode-derived migratory cells [GnRH immunonegative, olfactory marker protein (OMP)+ve] and OSN axons within the mesenchyme is collectively termed the "migratory mass" (MM). The MM is first detected at E10 and is mainly cellular, with the first OSN fascicles present at E10.5. The first OSNs penetrate the developing forebrain to reach the presumptive olfactory bulb (OB) at E11 (reviewed by Miller et al., 2010), termed 'pioneer neurons' as they ensure the migratory scaffold used by GnRH is in place.

In mice, GnRH neurons migrate across the nasal region on axons originating from cells in the olfactory pit/VNO (Wray et al., 2001). A number of molecules expressed by olfactory and VNNs are able to label these pathways, however, no one marker has been found to be exclusively expressed by the cells that guide GnRH neurons. At E11.5, the presumptive VNO begins to bud (Garrosa et al., 1992) and olfactory axons emerge from the VNO to form the VNN. At E12.5 the VNN splits to form a branch orientated dorsally that projects to the accessory olfactory bulb, and a caudal branch (cVNN) that extends to the basal forebrain (Yoshida et al., 1995). GnRH neurons begin migrating and leave the nasal placode at E11.5, migrating in close association with the proximal VNN in what is considered to be axonophilic migration. The outgrowth of the VNN targeting the base of the developing telencephalon precedes GnRH migration, providing them with a pathway to reach the nasal forebrain junction (N/FbJ). This initial step of migration requires both the movement of GnRH neurons and the specific factors that promote the adherence of the neurons to axons of the VNN (discussed in greater detail below).

At E12.5, more than 50% of the GnRH population have reached the nasal septum (Tobet et al., 1996b) and here at the N/FbJ they momentarily pause, before entering the forebrain between E13.5 and E14.5. There is no consensus for why there exists a temporary halt to the migration as at first thought it seems illogical – the size of the embryo is expanding rapidly and with every day that passes the migratory pathway to the hypothalamus extends. It has been proposed that GnRH neurons pause at the N/FbJ in order to undergo a 'maturation' process (Wray 2001), where they, or their axonal guides could alter their expression of factors related to cell guidance. This is because it is here that GnRH cells express a strong preference for targeting the cVNN and turn ventrally in a characteristic arch, changing trajectory to target the septal and POA (**Figure 13**). The first GnRH neurons reach the POA at E14.5 and begin detaching from their axonal guides, and by E16.5 they have sent axons and dendrites along a ventral path to innervate the median eminence of the hypothalamus.

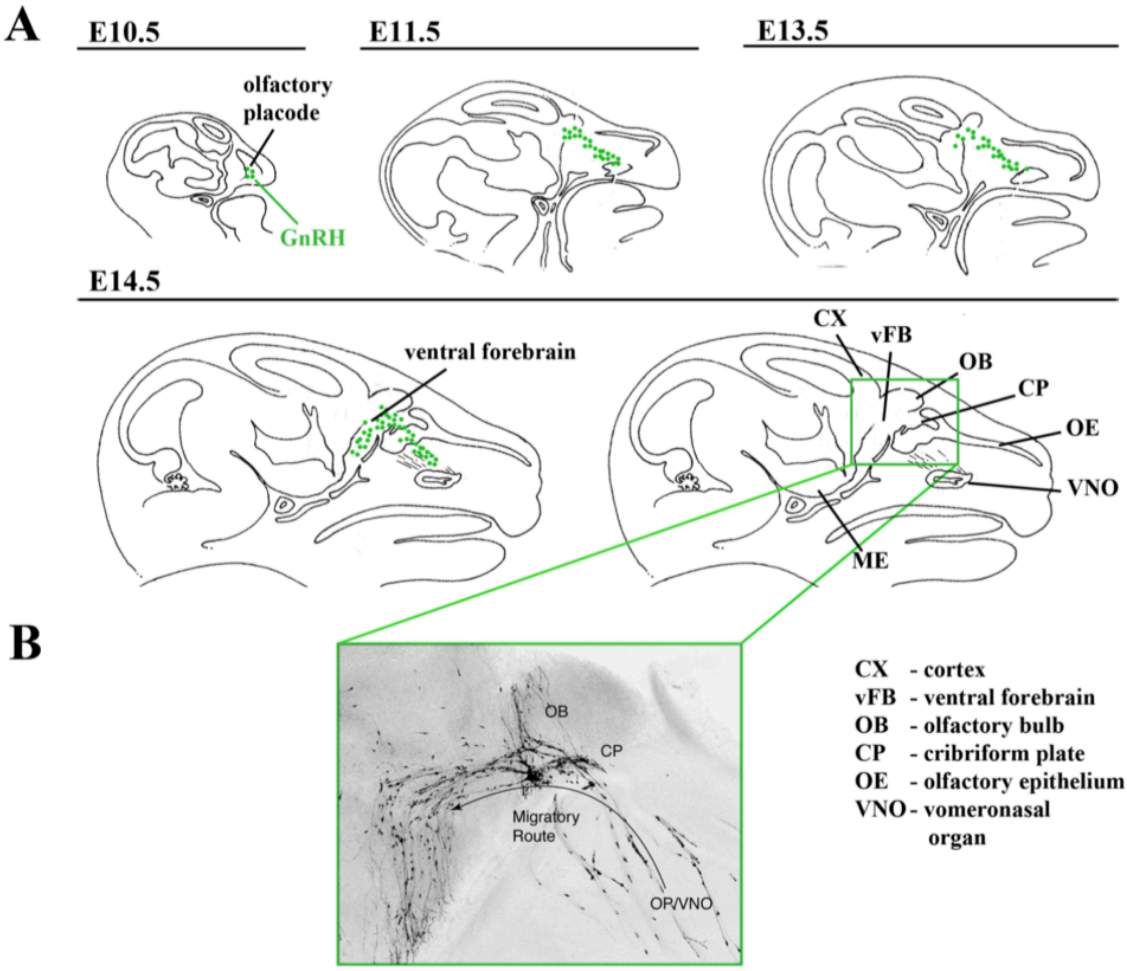

Figure 13. GnRH distribution through embryonic development.

(A) schematic representation of the location of GnRH neurons that can be found between embryonic day 10.5 (E10.5) and E14.5. At E10.5 GnRH expression is confined to the olfactory placode and at E14.5 GnRH cell bodies are found distributed approximately half in the ventral forebrain and half in the nasal region. (B) Immunohistochemistry on a sagittal section of an E14.5 mouse embryo for GnRH. Note the dense expression at the cribriform plate where the cells halt their migration and accumulate before progressing and turning ventrally into the forebrain. Figure taken from Tobet et al., Molecular and Cellular Endocrinology 185 (2001) 173–184

2.6.1 Differential timing of migration

In the mouse, GnRH expression is first detectable at E10.5 in the VNO, and the first cells to leave the nasal placode do so at E11.5. This is notable as the migration of GnRH neurons is described as occurring in 'waves', indicating a heterogeneity in the population initiated from fate specification. This is important to keep in mind, firstly because of the wide topological distribution of the population found during adulthood, but also because these different populations have been shown to exhibit different phenotypes and physiological roles (Simonian & Herbison, 2001). Further, the timing of GnRH migration, neuroanatomical location and function are correlated (Jasoni et al., 2009).

Splitting the population of GnRH neurons into 'early' and 'late' cells, Jasoni and colleagues (2009) assessed whether time of fate specification was correlated to their final neuroanatomical position. Injection of 5'-bromo-2-deoxyuridine (BrDU), a thymidine analogue, permits labelling of dividing cells as it is intercalated into the DNA during cell division, while an *in vivo* clearance time of under 24 hours allows for timely identification of mitotic division (Cameron & Mckay, 2001). BrDU injections between E9.5 and E12.5, indicated that 45% of GnRH neurons undergo fate specification (a final mitotic division) at E9.5 and this fell to >5% of neurons being born at E12.5. The total number of immunoreactive GnRH neurons that had incorporated BrDU when summed across the different injection days was 97%, indicating almost all GnRH neurons are born during this time window. Early born neurons represented an increased percentage of GnRH neurons that occupied the medial septum and pre-optic region, whilst late born neurons preferentially migrated to all regions; however, as a percentage, they form the largest contributor to anterior hypothalamic populations.

2.6.2 Molecules regulating early GnRH migration

The axonophilic migration of GnRH has been shown to rely on oscillating calcium currents that promote remodelling of the actin cytoskeleton (Hutchins et al., 2013). Calcium release was found to stimulate leading process actin flow away from the cell body; in contrast, actin contractions at the cell rear were unaffected by calcium signalling. Several classes of molecules

have been shown to be involved in the initiation of GnRH migration and their adherence to the axons of the VNN (the contribution of FGFs and semaphorins are discussed in section 2.12.2 and 2.12.3 respectively).

2.6.3 Adhesion molecules

Adhesion molecules are essential to the initial stage of migration as it requires both the movement of GnRH neurons and the specific factors that promote the adherence of the neurons to their axonal guides.

2.6.3.1 PSA–NCAM (polysialic acid form of neural cell adhesion molecule)

NCAM is a glycoprotein of the immunoglobulin (Ig) superfamily, and along with its long α 2,8–linked sialic acid polymer (PSA), has been shown to act as a negative regulator of cell–cell interactions (Brennaman & Maness, 2010). PSA–NCAM is highly expressed in the nose during embryological development and plays a key role in axonal tract formation (Fryer & Hockfield, 1996), where it can be used as a surface marker of developing olfactory axons. Indeed, GnRH neurons appearing to preferentially migrate along axons expressing PSA–NCAM in mice. NCAM has previously been associated with roles in promoting both cell–cell adhesion and neurite outgrowth, acting via the fibroblast growth factor receptor (FGFR), supporting a potential role in GnRH migration (see Chapter 2.12.3). This was suggested as sialylation with the enzyme endoneuroaminidase–N interfered with GnRH cell migration *in vivo* (Yoshida et al., 1995). The majority of studies, however, suggest no clear role for PSA–NCAM in regulating GnRH migration. While NCAM is expressed along the length of the terminal nerve, GnRH neurons only remain associated with the terminal nerve along its medial portion in Macaques (Quanbeck et al., 1997). Further, evaluation of NCAM and NCAM–180 null mice revealed no significant disruption of GnRH neuron migration. These discrepant results may have been due to the redundancy of the NCAM subtype system.

2.6.3.2 Glycoconjugates including cell surface glycoproteins

Little is known about how glycoconjugates may influence early GnRH migration, however, it has been reported that a cell surface glycoconjugate, carrying a lactosamine moiety, influences GnRH neuron migration (Bless et al., 2001). The glycosyltransferase ß1,3-N acetylglucosaminyltransferase-1 (ß3GnT1) aided lactosamine addition to a sub-population of GnRH cells and an expression pattern with a peak at E13 followed by a subsequent downregulation was consistent with a role in regulating GnRH migration. Mice null for ß3GnT1 displayed an accumulation of GnRH neurons in the nasal compartment at E15, and a tendency for the neurons that did enter the brain to be mistargeted away from the ventral forebrain.

2.6.4 Guidance factors

2.6.4.1 Ephrins

Ephrins are a group of cell surface molecules that are well known to play a role in axon guidance in many areas of brain development (Gamble et al., 2005). Ephrins signal through the membrane tyrosine kinase receptors EphA and EphB, and were initially implicated in GnRH migration due to a mutation that resulted in a 67 kb deletion within the Ephrin receptor EphA5. As a consequence of the mutation, the GnRH neurons of these mice overexpressed EphA5, resulting in an abnormal accumulation of GnRH neurons in the nasal compartment. Due to the 'clumped' nature of GnRH cells that remained attached to olfactory axons, it was hypothesised that overexpression of EphA5 caused increased adhesion to the axons and prevented their migration. Phenotypic analysis of the adult GnRH population found that only 12% of the neurons were found in the hypothalamus (Gamble et al., 2005). As Ephrins and their receptors are both membrane-bound proteins, signalling can only occur through direct cell-cell contacts, suggesting that Ephrins should be expressed by VNN axons.

2.6.4.2 NELF (Nasal embryonic LHRH factor)

NELF was initially isolated from expression profiling of migrating and non-migrating primary rodent GnRH neurons, with its expression localised to the membranes of migrating GnRH and olfactory neurons (Kramer & Wray, 2000). The expression pattern of NELF is highly supportive of a role in regulating migration of these neurons as its expression is downregulated when the cells enter the forebrain. Knockdown of NELF in embryonic *ex vivo* nasal explant cultures resulted in decreased complexity of migrating olfactory axons and a reduction of the GnRH cell population by 33% (Kramer & Wray, 2000).

2.6.5 Neurotransmitters

2.6.5.1 GABA (γ-aminobutyric acid)

GABA is the chief inhibitory neurotransmitter found in the mammalian CNS, classically functioning to reduce neuronal excitability (although it is excitatory to mature GnRH neurons (Chen & Moenter, 2009; Watanabe et al., 2009). GABA is synthesised from glutamate by the enzymatic activity of glutamate decarboxylase (GAD) and its co-factor pyridoxal phosphate. The 67 kDa isoform of GAD (GAD67) accounts for 90% of GABA synthesis in the murine brain (El Mestikawy et al., 2011), and consistent with the heterogeneity of the GnRH neuronal population around 30% are GABAergic during development (Tobet et al., 1996a). Overexpression of a GAD67 transgene targeted to GnRH neurons results in increased dispersion of GnRH neurons in the forebrain (Heger et al., 2003), which resulted in sub-fertility of the female progeny. *Gad1*$^{-/-}$ (the gene encoding GAD67) mice display advanced GnRH migration from the nasal placode at E14.5, however, the neonatal lethality of these mice precluded reproductive analysis from being conducted (Lee et al., 2008). In *ex vivo* nasal explants, GABA has also been shown to inhibit the migration of embryonic GnRH neurons (Fueshko et al., 1998), confirming GABAs actions in regulating GnRH migration.

2.6.5.2 Glutamate

Glutamate is the principle excitatory neurotransmitter in the vertebrate nervous system, accounting for over 90% of synaptic connections in the human brain (reviewed by Meldrum 2000). It has also been widely shown that glutamate plays an important role in regulating radial migration within the cerebellum (Komuro & Rakic, 1993) and neocortex (Behar et al., 1999), acting through NMDA (N-methyl-D-aspartate) receptors to regulate intracellular calcium levels (Komuro & Rakic, 1998). Although only a small proportion of migrating GnRH neurons (~5%) appear to express NMDA receptors, its expression can be found all along the migratory pathway during embryogenesis, and treatment of *ex vivo* brain slices after E12.5 with an NMDA receptor antagonist resulted in an increase in GnRH cells found in the DBB (dorsal band of Broca) and POA (Simonian & Herbison, 2001). This is suggestive of Glutamate signalling through NMDA receptors to inhibit the final step of GnRH migration from the medial septum to target hypothalamic areas.

In contrast to this inhibitory role of NMDA receptor activation on GnRH migration, AMPA (α-amino-3-hydroxy-5-methyl-4-isoxazolepropionic acid) receptor signalling appears to promote GnRH migration from nasal regions, as a treatment with an AMPA antagonist resulted in an accumulation of GnRH neurons in the nose (Simonian & Herbison, 2001).

2.6.5.3 CCK (Cholecystokinin)

CCK is a peptide hormone initially characterised for its role in causing the release of bile and digestive enzymes from the gallbladder and pancreas. It signals via GPCRs, and knockout mice for the CCK-1R possessed an increased number of migrating GnRH neurons had entered the brain at E14.5 (Giacobini et al., 2004). The actions of CCK are expected to be direct as the CCK-1R expression was colocalised with embryonic GnRH cells (Giacobini et al., 2007).

2.6.6 Guidance molecules

2.6.6.1 Hepatocyte Growth Factor (HGF)

HGF is a member of the plasminogen regulated growth factor family that, via its membrane tyrosine kinase receptor Met, exhibits mitogenic, motogenic and chemoattractant properties in neuronal cells (Caton et al., 2000; Gutierrez et al., 2004; Segarra et al., 2006). HGF-induced signalling requires cleavage by plasminogens such as tissue plasminogen, (tPA) and uroplasminogen (uPA) or coagulation factors (Naldini et al., 1992; Mars et al., 1993). While both HGF and Met are widely distributed in the embryonic brain, HGF is expressed in the embryonic nasal mesenchyme, with an increasing gradient of expression towards the forebrain (Sonnenberg et al., 1993; Thewke & Seeds, 1996), while c-met and tPA expression is localised to the olfactory epithelium at E11 (Sonnenberg et al., 1993; Thewke & Seeds, 1996). Met expression co-localised with NCAM expression in developing olfactory fibres, while the majority of migrating GnRH neurons express Met *in vivo* (Giacobini et al., 2007). HGF has been shown to exhibit motogenic and chemotactic effects on immortalised GnRH cells *in vitro* (Giacobini et al., 2002) and treatment of embryonic nasal explants *ex vivo* with HGF increased GnRH migration, a phenomenon that was reversed by the inhibition of HGF (Giacobini et al., 2007). It is also interesting to note that no effect on olfactory axon outgrowth was found with HGF treatment, however, blocking of HGF function caused significant reduction in their outgrowth, suggesting that HGF effects on GnRH migration may be both cell autonomous and indirect. Primary, migrating GnRH neurons express tPA, while tPA expression is downregulated in post-migratory neurons consistent with a role in HGF promoting GnRH migration (Giacobini et al., 2007). Finally, mice that carry combined deficiencies for tPA and uPA ($tPA^{-/-}$:$uPA^{-/-}$), are subfertile (Carmeliet et al., 1994), most likely as a result of the 35% decrease in total GnRH cell population found postnatally (Giacobini et al., 2007). Met signalling exhibits a large degree of 'cross talk' with other tyrosine kinases, GPCRs and multiple docking proteins – suggesting a potential interaction of this pathway with several other factors known to regulate GnRH migration.

2.6.6.2 Netrin/DCC (Deleted in colorectal cancer)

Netrins are a genetically well conserved class of laminin-related proteins that can function as either chemoattractants or chemorepellants in multiple regions of the developing CNS (Killeen & Sybingco, 2008), with their importance to neuronal guidance underscored by the observations in the netrin deficient mice that fail to form the hippocampal commissure or the corpus callosum. Both DCC and UNC-5 (unco-ordinated-5) receptors have been shown to transduce netrin signalling, with UNC5 principally implicated in repulsive signalling, and DCC in attractive signalling (reviewed by Moore, 2007; Sun et al., 2011). Additionally, DSCAM (Down syndrome cell adhesion molecule) has been previously confirmed as a netrin receptor that evokes chemoattractant responses to netrins independently of DCC (Ly et al., 2008).

Transiently high expression of DCC in the rat olfactory system is found from E14-E18 (Deiner & Sretavan, 1999), while DCC expression is found in within the VNO, VNN and in a sub-population of migrating GnRH cells in mice (Schwarting et al., 2001; Schwarting et al., 2004). The expression of DCC was found to be downregulated beginning at E12, suggesting that DCC may be important in the initial stages of GnRH migration. Using IHC it was discovered that $DCC^{-/-}$ mice have disrupted axonal targeting of the VNN and hence GnRH migration, with the caudal branch of the VNN failing to turn ventrally into the forebrain and resulting in a pathway that instead progressed into the cerebral cortex (Schwarting et al., 2001).

This result was phenocopied in the netrin-1 mutant mice ($Ntn1^{-/-}$) in contrast to UNC-5 mutants ($Unc5h3rcm^{-/-}$) – who instead displayed typical development of the GnRH system (Schwarting et al., 2004). These results are consistent with the idea tha the chemoattraction of DCC positive vomeronasal axons by a gradient of netrin-1 guides the caudal branch of the VNN, in turn regulating the direction of GnRH migration to the ventral forebrain.

In the chick embryo, failure of ventrally directed migration of GnRH neurons and their misrouting to the dorsomedial forebrain was induced by misexpression of netrin-1 in a dorsocaudal septal region near the top of the commissural plate (Murakami et al., 2010), highlighting the evolutionarily conserved nature of netrin signalling on GnRH migration.

2.6.6.3 Slit–Robo

Slits are secreted proteins, best known as repulsive axon guidance cues that signal through the transmembrane receptor Robo. Indeed, Robo expression is required for repulsion of axons from the midline in both ipsilateral axons that never cross the midline and commissural axons that have already crossed (Kidd et al., 1998). In vertebrates, four different Robos and three slits have been identified, with all Robos shown to interact with netrin–1, a receptor of DCC (Stein & Tessier–Lavigne, 2001). Slits act as repellents of developing olfactory axons (Li et al., 1999; Wu et al., 1999) and VNNs (Cloutier et al., 2004; Prince et al., 2009) guiding their expression to the olfactory bulb. *Slit2* $^{-/-}$ mutants display a delayed migration of GnRH neurons at every time point analysed prenatally, resulting in decreased GnRH innervation of the median eminence (Cariboni et al., 2012). Importantly, no effect of removal of Slit2 on the total number of GnRH neurons was observed. Fluorescence–activated cell sorting (FACS) of GnRH::GFP neurons at E14.5 revealed expression of *Slit2, Robo1* and *Robo2* in migrating GnRH cells (Cariboni et al., 2012). Knockout mice for Robo1 and Robo2 showed no significant alterations to the development of the GnRH system, however, *Robo3* $^{-/-}$ mutants were a phenocopy of *Slit2* $^{-/-}$ mice. *In vitro* chemotactic experiments confirmed the specificity of Slit2 signalling through Robo3 alone to regulate GnRH migration.

2.7 GnRH Migration in Humans and non-human primates

The extant literature detailing GnRH migration in humans is understandably sparse. While the genetic manipulations and experiments described above and below could never be performed on humans for ethical reasons, the difficulty surrounding working with prenatal human tissue has precluded even simple anatomical observations from animal models being confirmed in humans. For instance, do GnRH neurons migrate in a migratory mass as is described in other species? Do they follow TN or VNN axons?

In spite of this, several papers have documented GnRH migration in small samples of prenatal humans and non-human primates.

2.7.1 Terminal nerve anatomy

The standardised nomenclature of the cranial nerves (CN) I-XII derives from the work of Samuel Thomas von Sömmerring (1775-1830), with each nerve named according to the anterior-posterior (rostro-caudal) location of their cranial foramina (Moore et al., 2006; Drake et al., 2010). Outside of the textbooks that teach anatomy to medical students, however, it has long been known that there exists a 13th CN, sometimes referred to as CN-0 or CN-N (N preserving the Latin derived nomenclature: *nulla* [none], as no true Arabic concept of 0 was known to the Romans) due to its positioning rostral to the olfactory nerve (CN-I). It is now commonly referred to as the terminal nerve *nervus terminalis* (TN) due to the morphological observations of Loci (1905) identifying that it branches in the region of the laminae terminalis.

The anatomy of the TN appears similar in many species and it is readily visible, attached to the pia mater between the olfactory stalk and the rostral section of the optic chiasm (**Figure 14**). It passes through the medial region of the stria olfactoria and courses via the orbital surface of the frontal lobe, where it passes through the cribriform plate of the ethmoid bone just caudal and lateral to the crista galli and as noted by Loci, proceeds to the lamina terminalis. The terminal ganglion, located on the terminal nerve below the forebrain, divides the terminal nerve into two

segments: an extracranial segment, composed of processes originating from cells in the vomeronasal organ and extending into the terminal ganglion; and an intracranial segment, composed of processes originating from the terminal ganglion as well as vomeronasal cells and extending into the forebrain.

The function of the TN may be species specific with both reproductive and olfactory functions postulated, however, GnRH immunoreactivity has been found in TN fibres and its ganglion in multiple vertebrates including humans (reviewed by Vilensky 2012). This is especially true during embryonic development, when GnRH cells outnumber non-immunoreactive GnRH cells within the TN, with the ratio reversing to approximately 1:15 by birth.

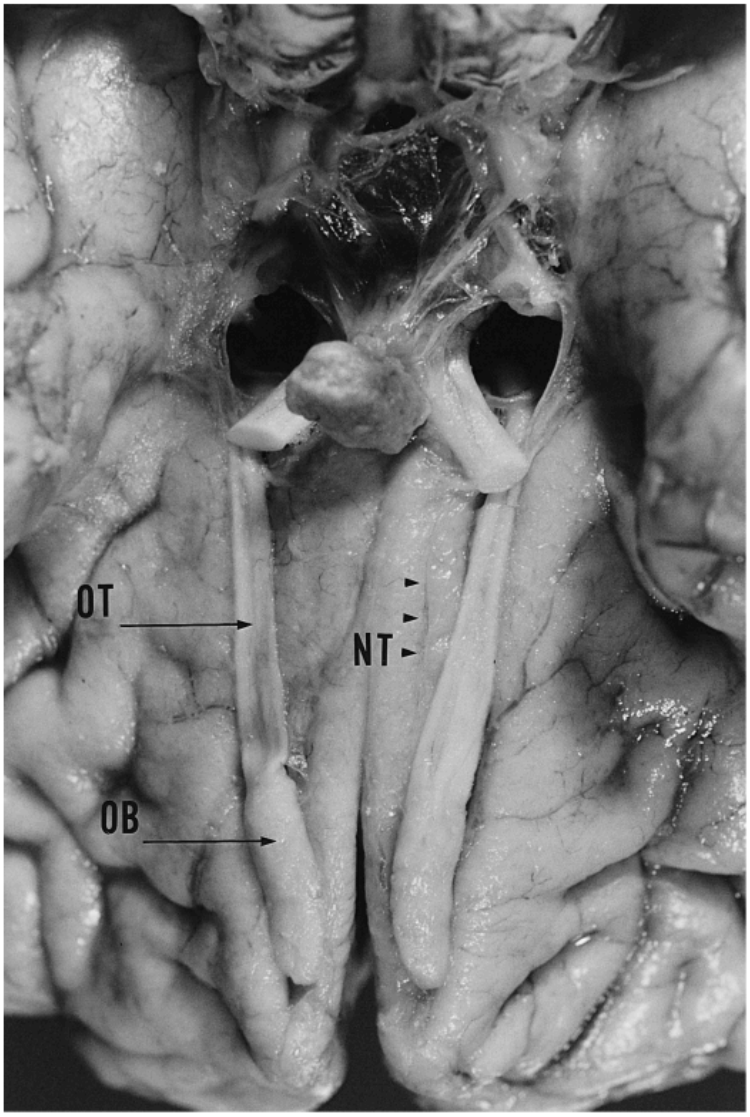

Figure 14. Anatomy of the adult human terminal nerve (TN).
Inferior surface of the adult human brain illustrating the components of the olfactory system. The tract of the TN lies medial to the tract of the olfactory nerve (OT) coursing along the surface of the gyri recti. Anteriorly, it is intimately associated with the olfactory bulb (OB). Figure taken from Kim et al., *Brain Research* 1999.

Debate continues as to the embryonic origin of the TN, with data supporting both NC (Whitlock et al., 2003) and nasal placodal origins (Schwanzel-Fukuda & Pfaff, 1989; Wray et al., 1989) in different species. Nethertheless, initial reports on the development of the TN in humans (Pearson 1941) found that its branches in the nasal compartment are more medial and profound than those of the olfactory nerve bundles, coursing through the nasal septum with branches in the septal mucosa **(Figure 15)**, as it migrates from nose to brain (Quanbeck et al., 1997). While the VNN ends in the AOB (accessory olfactory bulb), the TN progresses deeper into the telencephalon and can be distinguished from the VNN by the presence of ganglia along its course. To the authors knowledge, no molecular factor has been shown to specifically label and distinguish the TN and VNN and it is very likely that in humans, non-human primates and perhaps all vertebrates that the axonal scaffold GnRH neurons use to migrate are actually branches of the TN.

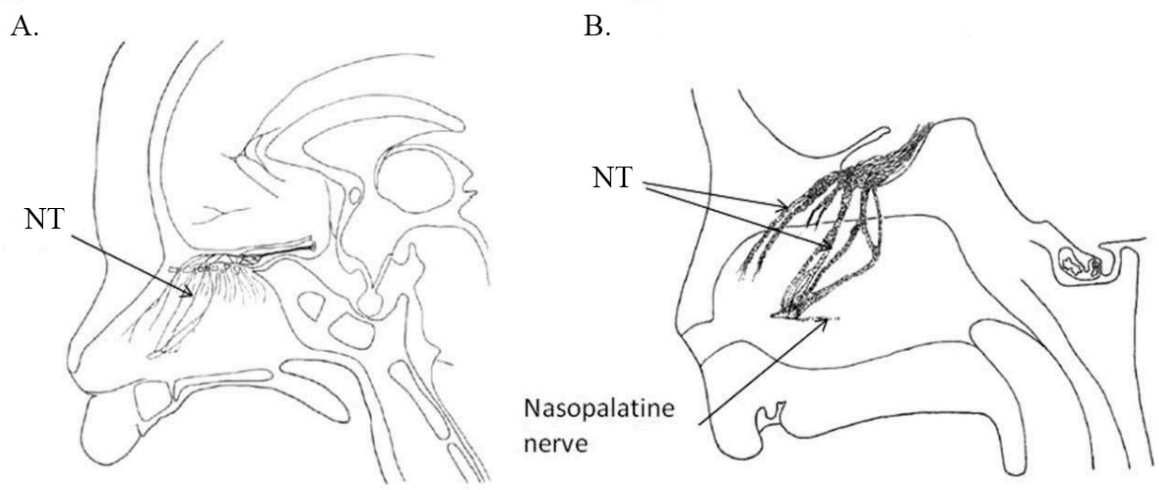

Figure 15. Anatomy of the embryonic human terminal nerve.

(A) A schematic representation showing a septal view of the terminal nerve (TN) in a six-month old human foetus. Modified from McCotter 1915. (B) Septal view of the TN in a 45mm human foetus. Modified from Pearson 1941

2.8 Primates

Several studies have performed characterisations of GnRH migration in foetal non-human primates, the Rhesus Macaques *Macaca mulatta*. Macaques have a gestation length of approximately 166 days (as opposed to 280 days in humans). In foetal macaques, GnRH-immunoreactive cells were first detected at 30 days gestation (Quanbeck et al., 1997) localised to the dorsal olfactory placode and at 36 days gestation (Ronnekleiv & Resko, 1990) localised to the nasal epithelium and nerve bundles along the path of the TN within the nasal region. GnRH neurons were first observed within the brain at 30 (Quanbeck et al., 1997) and 38 days gestation (Ronnekleiv & Resko, 1990), migrating into the brain along the dorsal surface of the olfactory bulbs, and first reached the anterior hypothalamus at 40 days gestation (Ronnekleiv & Resko, 1990). By day 47 the majority of cells had reached the POA, coinciding with the first appearance of GnRH cell bodies in the MBH (Ronnekleiv & Resko, 1990).

The differences in timings observed may be due to the antisera employed by the two groups, with Quanbeck and colleagues utilising two primary antisera (LR-1 and GF-6). LR-1, whose antigenic determinant is directed to amino acids 2-4 and 7-10 of GnRH1 (Silverman et al., 1990) and GF-6 that shows an increased affinity for hydroxyl-pro-GnRH1 with a 94% cross reactivity with sea bream GnRH (Quanbeck et al., 1997). They found that there was a population of cells that were positively labelled by both antisera, and a population that was exclusively labelled with GF-6. It was this GF-6(+)/LR-1(-) population that was detected at 30 days gestation and hence were described as "early cells", whilst double positive cells were described as "late cells". These early cells underwent huge proliferation from 1000-3000 cells between 30-32 gestational days, increasing to approximately 10,000 cells at 34 days. Quanbeck and colleagues also detailed a second, dorsal migratory pathway that was evident from 38 days gestation, which led to a large population of extra-hypothalamic GnRH neurons. These neurons were found scattered throughout the internal capsule, caudate, putamen, globus pallidus, and claustrum, while a large number were also found concentrated in the amygdala.

These neurons were invariably unipolar and possessed a different pattern of staining from hypothalamic GnRH neurons,

The authors noted by comparing coronally sectioned foetuses that the migration appeared to initially occur rostral–caudally, and after 50 days gestation progress in a lateral–medial direction. This is supported by a study that examined neurogenesis in the POA of rats using tritiated thymidine autoradiography (Bayer & Altman, 1987). They found that lateral neurons develop several days before medial neurons; that Crozier and colleagues (2011) also found a wave of migration in the lateral–medial aspect for the LHA suggests that this is likely an evolutionarily conserved mechanism of hypothalamic development, even if it is yet to be identified in better known models such as mice.

In the E135 foetus, the largest number of late GnRH neurons were seen rostrally in pericommissural areas, the diagonal band of Broca, medial preoptic area, medial septal nucleus, regions around the lamina terminalis, and the organum vasculosum of the lamina terminalis. Caudally, late GnRH neurons were seen in the arcuate nucleus and the median eminence (Quanbeck et al 1997). This was in accordance with the earlier work, with no difference in GnRH distribution found between 135 days gestation and birth and with the highest concentration of GnRH cell bodies located in the lateral arcuate nucleus, caudal to the median eminence. Of note, the VNO was undetectable past 50 days gestation (hypothesised by the authors to be the site of origin of GnRH neurons in the macaque).

These two works indicate many similarities between the migration pattern between mice and macaques, with the major exception being in the clear identification of a dorsal migratory pathway, resulting in seemingly ectopic populations of GnRH.

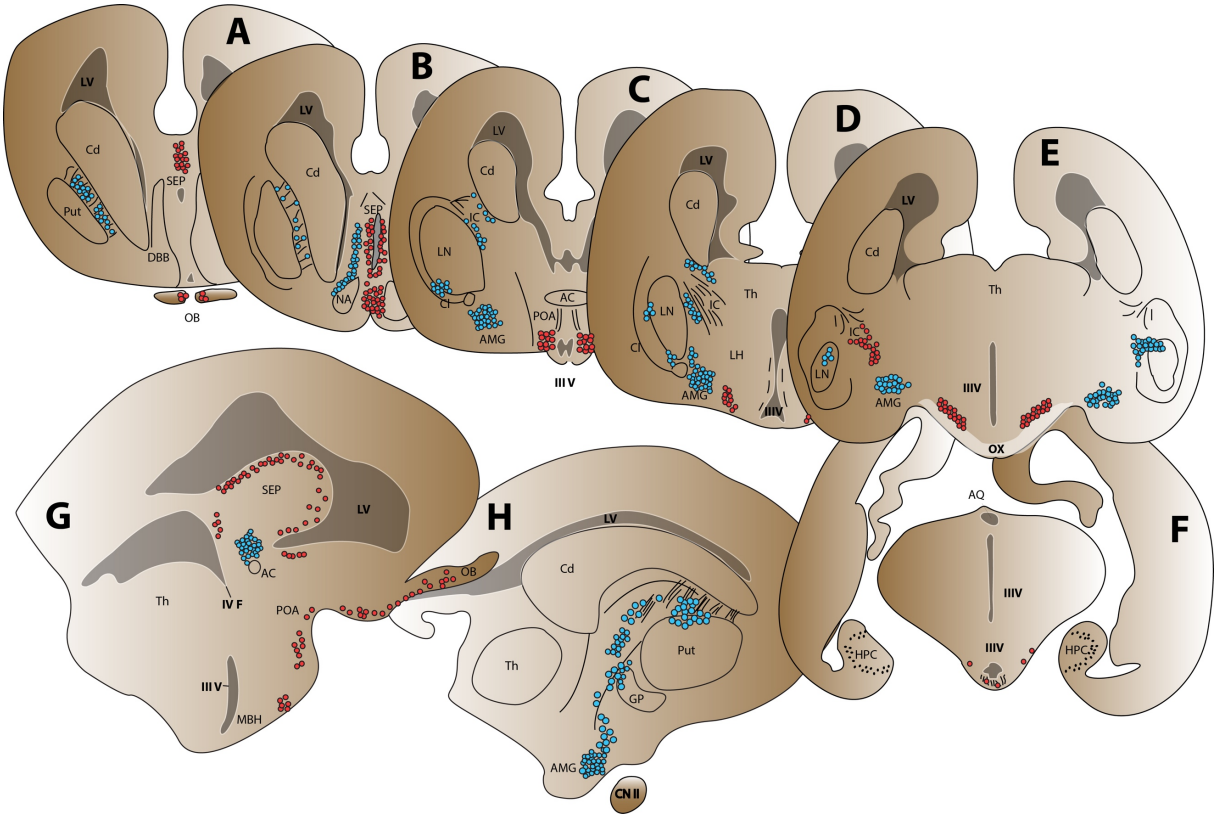

Figure 16. Distribution of early and late migrating cells in macaque foetuses.
(A–F) Camera lucida drawings representing coronal sections separated by 250 µm of foetal macaques at embryonic day 62. (G–H) Parasagittal sections separated by 1000 µm from E62 foetuses. Early GnRH cells (blue) were found in the POA, septum, striatum, amygdala, stria terminalis, internal capsule and claustrum. Late GnRH cells (red) were found in the olfactory bulbs, POA, hypothalamus and periventricular regions of the lateral ventricle and interventricular foramen.
Abbreviations: LV: lateral ventricle; Cd: caudate; Put: putamen; Sep: septum; DBB: dorsal band of Broca; OB: olfactory bulb; NA: nucleus accumbens; AC: anterior commissure; AMG: amygdala; POA: preoptic area; III V: 3rd ventricle; Th: thalamus; LH: lateral hypothalamus; OX: optic chiasm; IV F: interventricular foramen; MBH: mediobasal hypothalamus; CN II: optic nerve; GP: globus pallidus; AQ: cerebral aqueduct; HPC: hippocampus
Figure adapted from Quanbeck et al., 1997

2.9 Humans

The migration of GnRH neurons in humans has been documented in several papers in both physiological and pathophysiological conditions, here is summarised the findings from physiologically normal foetuses, while pathological conditions will be considered in **Chapter 2.12.2.** It has long been known that the approximate age of the formation of the primary plexus of the hypothalamohypophyseal portal vasculature is 14 GW, but that the continuity of the primary and secondary plexus has not been demonstrated to occur before 18–21 GW (Espinasse 1933; Niemineva 1949). Accordingly, a mid-gestation activation in GnRH activity (Clements et al., 1976; Kaplan et al., 1976) necessitates that the architecture of GnRH neurons sending projections contacting the median eminence should be in place at this time. Indeed, the first studies that examined GnRH expression during early embryonic life occurred before the discovery that the cells arose in an extra-encephalic region and while these studies identified GnRH expression prenatally, they only report expression in the hypothalamus. For instance, Paulin and colleagues (1977) analysed 22 foetuses from 6–24 GW, with the earliest age of GnRH immunoreactivity detected in the hypothalamus at 9 GW, however, no expression was detailed in extrahypothalamic regions.

Schwanzel-Fukuda and colleagues (1996) found that at 42 (but not at 28–32) days of gestation, GnRH immunopositive cells were found in the epithelium of the medial olfactory pit. At this stage GnRH was also found along NCAM positive fibres which appeared to bud from the epithelium of the medial olfactory pit along with the ganglia of the TN and with branches of the TN caudal to the olfactory bulb. At 46 days gestation (6.5 GW) GnRH cells were seen entering the forebrain with axons of the terminal nerve, while some cells could already be detected in the medial basal forebrain. The authors noted that the VNN and TN could be distinguished not only by their differential entrance points into the developing brain, but also by the presence of a blood vessel that separated the lateral, olfactory nerve derived portion of the scaffold from the medial, VNN-TN segment.

The development of the NCAM positive scaffold was seen to begin as early as 28–32 days post ovulation, with fine fibres and fascicles forming a network in the nasal mesenchyme, preceding the ontogenesis of GnRH neurons. By 42 days gestation, NCAM positive fibres were found through the entire migratory route, from the epithelium of the olfactory pit to the ventral forebrain.

Quinton and colleagues (1997) examined two foetuses of 14–16 GW, confirming the previous reports that at this time, GnRH immunoreactivity is present from the cribriform plate to the hypothalamus, although they failed to find any GnRH expressing cells still in the nasal compartment at 16 GW.

2.9.1 Perspectives

The limited work studying GnRH migration in primates and human foetuses has allowed seemingly good correlation with the hundreds of papers completed in mice. In all species, it is clear that GnRH neurons originate from a similar region and migrate along an axonal scaffold of VNN/TNs to reach the brain. Unreconciled differences also appear to exist however, for instance in the targeting of GnRH neurons to extrahypothalamic areas in the primate. Although this pathway has never been demonstrated in humans, it is likely that it exists as GnRH1 mRNA expressing cells are found in large numbers outside of the hypothalamus in adult human brains (Rance et al., 1994).

2.10 Hypogonadotropic Hypogonadism

Due to its fundamental role in initiating pubertal onset and hence gonadal function via gonadotropin secretion, aberrations in the development of the GnRH system fundamentally result in infertility syndromes. In humans, the failure of acquiring sexual competence due to a lack of central GnRH, form a range of clinical disorders that are broadly termed hypogonadotropic hypogonadism (HH) (Seminara et al., 1998). The prevalence of HH is difficult to accurately determine due to the phenotypic heterogeneity [congenital (CHH) or acquired] and severity (complete or partial).

As the GnRH axis is activated shortly after birth [a phenomenon recognised in both mice and humans, called mini-puberty (Kuiri-Hanninen et al., 2011a; 2011b)] this can provide the first opportunity to identify a dysregulation of the endocrine system. In males, micropenis and/or cryptorchidism can be suggestive of HH and hormonal profiling of LH, FSH, testosterone (Main et al., 2000) and inhibin B (Andersson et al., 1997) between the 4^{th} and 8^{th} weeks of life can form an effective diagnostic tool (Baetans et al., 2014). With no such virilisation of female genitalia so early in post-natal development, diagnosis is much more challenging, with mini-puberty levels of circulating FSH found to be the only empirically measurable factor able to predict HH. Cases diagnosed this early are exceptionally rare and instead the majority of diagnoses occur around or after puberty, when activation of the reproductive axis begins in full.

The absence of classical external changes observed during puberty such as development of the breasts and/or amenorrhea in females and development of the testes/sexual function in males are common complaints from adolescents with CHH. Unsurprisingly patients often present with impaired psychosexual development, distorted self-body image, low self-esteem and in rare cases gender dysmorphia (Dwyer et al., 2014). Diagnosis of true HH necessitates otherwise normal hypophyseal function, determining that GnRH deficiency is the root cause of infertility.

Clinical treatment of HH depends on the age of diagnosis and hence its expected goals. Early diagnosis in boys often results in first trying to induce male sexual characteristics by reversing

any anatomical features that may impact long term fertility (such as cryptorchidism) with surgery advocated between 6–12 months (Ritzen et al., 2007; Chan et al., 2014). Low dose testosterone or gonadotropin replacement therapy may also be employed to induce penile growth in the case of micropenis with the additional benefit of FSH stimulating gonadal development (Dwyer et al., 2013). One caveat is that these treatment protocols although seemingly sound, are still in their relative infancy and no long-term outcomes can yet be determined.

During adolescence, treatment aims to induce virilisation and normal sexual function, and provide psychological support to those suffering from dysmorphias. Sex steroid replacement therapies (testosterone in boys, oestradiol followed by combined oestradiol and progesterone in girls) are used to initiate puberty. It should also be taken into account that without treatment, HH patients who do not initiate puberty in a timely manner fail to experience a growth spout and instead body size increases in a linear fashion, leading to the eunuchoid proportions of the Castrati as noted earlier. As the pubertal window (the time when pubertal development can occur) is narrow, a timely diagnosis and initiation of treatment is essential. Testosterone treatment that occurs after the pubertal window has shut, typically fails to induce gonadal maturation and hence fertility, even when targeted to the high end of normal range (Young et al., 2012). Alternative approaches have been conducted using pulsatile GnRH replacement, or gonadotropin replacement of human chorionic gonadotropin (HCG) in combination with FSH, both with the intention of stimulating gonadal function.

Another important consideration for treatment is continued bone health, as is the case in all disorders with a reduction in gonadal steroids. Indeed, several reports of HH diagnosis have arisen from adult patients presenting to the clinic with osteoporotic tendencies.

It is important to note that although disruption to the embryonic migration of GnRH neurons can result in infertility, the cause of disruption may be complex and not simply explained by factors that are intrinsic to regulating this process. Several human infertility syndromes are

instead thought to arise from disruption of processes involved in guiding the axons that guide the migrating cells, called Kallman Syndrome (KS).

2.11 Congenital Hypogonadotropic Hypogonadism (CHH)

Congenital forms of HH (CHH) have a male prevalence of 3–5 to 1 (Seminara et al., 1998; Mitchell et al., 2011) and are known to exhibit a large degree of heterogeneity upon clinical diagnosis. Complex syndromes that include either CHH or KS include but are not limited to: combined pituitary hormone deficiency, septo–optic dysplasia, CHARGE syndrome, adrenal hypoplasia congenita with HH, Waardenburg syndrome, Bardet–Biel syndrome and Gordon Holmes syndrome (see Boehm et al., 2015). CHH is now commonly accepted to be an oligogenic disorder with variable penetrance and surprisingly, between 10–20% of CHH patients undergo spontaneous recovery of fertility – including patients with known mutations in CHH associated genes. This suggests a surprising amount of functional plasticity can occur in regulating the HPG axis, with no known correlating or prediction factors. Recent advances in our understanding of the factors contributing to CHH have largely been due to the advent of next generation sequencing (NGS) technologies, confirming its prismatic nature and resulted in the formation of a European consortium of researchers and clinicians in 28 countries studying GnRH biology (consensus statement: Boehm et al., 2015).

Several known CHH mutations including FGF8, FGFR1 and SEMA3A are also known to directly regulate bone mass (Miraoui et al., 2011; Hayashi et al., 2012) which should be taken into account by clinicians assessing long term treatment options with their patients harbouring these mutations. When diagnosed in a timely manner, CHH is actually one of the few male infertility disorders that is treatable with good predictive outcomes.

A full list of all CHH associated genes identified is summarised in **Table 1.**

2.12 Kallmann Syndrome

Kallmann syndrome (KS) is defined as CHH associated with anosmia due to a combination of abnormal migration of GnRH neurons and targeting of olfactory axons to the presumptive olfactory bulbs during development (Schwanzel-Fukuda & Pfaff, 1989; Seminara et al., 1998). It typically occurs in around 50% of clinically reported CHH cases. KS can be difficult to distinguish clinically from CHH or CDGP (constitutional delay of growth and/or puberty). Anosmia as detected by clinical olfaction tests, as well as olfactory bulb hypoplasia/aplasia as determined by MRI can be useful diagnostic tools. The condition was initially described by Dr Maestre de San Juan (1856) who observed the absence of olfactory nerves in a hypogonadic individual upon post-mortem examination. The syndrome is named however, after Franz Kallmann who identified a hereditary hypogonadic syndrome associated with anosmia (Kallmann et al., 1944), while Schwanzel-Fukuda & Pfaff (1989) were the first to prove that hypogonadism arises due to a failure of GnRH migration. KS is currently estimated to have a prevalence of 1 in 8,000 in men and 1 in 40,000 in women, again displaying a sex bias as seen in CHH (Cariboni & Maggi, 2006).

The traditional Mendelian view of monogenic inheritance of KS has recently been overturned, to become categorised as an oligogenic disorder having a complex aetiology (Sykiotis et al., 2010). This revision has come as mutations in more than one gene have been reported in several KS case reports involving different combinations of genes, with oligogenic inheritance currently thought to account for 10-20% of clinical cases. Several genes have more frequently been associated to digenic inheritance patterns. In several cases the segregation pattern of these digenic/oligogenic mutations within the family pedigree can account for the phenotypic variability between family members (Sykiotis et al., 2010). In addition, the olfactory and reproductive defects may be combined with other disorders or satellite symptoms, including: renal agenisis, synkinesis (mirror movement), syndactyly, craniofacial abnormalities, colomba and sensorineural deafness. Many of these associated disorders can be traced to embryonic anatomy, for instance, improper development of the olfactory and otic placodes. What follows

is a key summation of several important gene families that have been definitively proven to cause KS in humans.

2.12.1 Anos1

The first KS associated gene to be discovered was named after the syndrome itself, becoming known as *Kal1* (Bose & Sarma, 1975). Kal1, now referred to as Anos1 (de Castro et al., 2016), was first detected due to a genetic lesion at Xp22.3 and was definitively located to the X chromosome (Guioli et al., 1991; Hardelin et al., 1991). This positioning forms an X-linked mode of inheritance with high penetrance, partially explaining the increased prevalence of KS in men compared to women.

Anos1 encodes Anosmin-1, a 680-amino acid secreted extracellular matrix glycoprotein. Biochemically Anosmin-1 acts as a cell adhesion protein that plays an important role during development of the entire CNS, with its absence resulting in altered axonal pathfinding, collateralisation and cellular migration. Recently Anos1 mutations have also been described in multiple sclerosis cases (de Castro et al., 2014), with a recent report of multiple sclerosis in a Kallmann patient (Mantero et al., 2016). Mutations in Anos1 in KS result in arrested GnRH migration at the level of the cribriform plate (Franco et al., 1991; Legouis et al., 1991; Schwanzel-Fukuda & Pfaff, 1989; Texeira et al., 2010). To date no homolog of Anos1 has been identified in rodents, preventing the genetic manipulations and functional *in vivo* testing that would usually be possible.

2.12.2 Arrested GnRH migration in human foetuses

In spite of the relative rarity of KS and syndromes of olfactory bulb hypoplasia (such as trisomy 13), two foetuses with known mutations in Anos1, one CHARGE foetus and one trisomy 13 foetus have had their GnRH migration pattern analysed. Approximately 2/3 of CHARGE syndrome cases are caused by neomutations in CHD7 (Vissers et al., 2004) and mutations in this gene have been identified in KS patients (Jongmans et al., 2009; Kim et al., 2008) suggesting overlapping developmental causes.

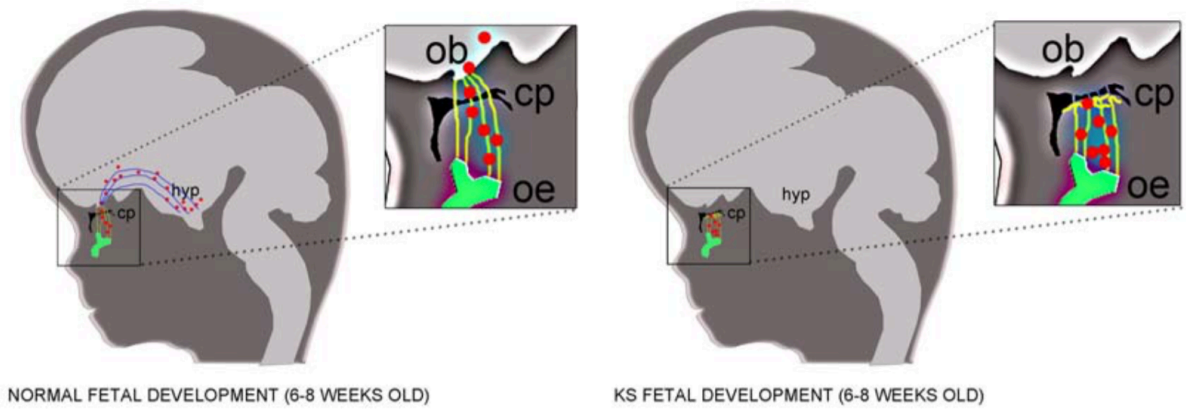

Figure 17. GnRH migratory process in normal and Kallmann's syndrome foetuses. Schematic Distribution of GnRH-1-immunoreactive cells (red dots) in the frontonasal region and forebrain of normal human foetuses (6-8 weeks old) and in foetuses with Kallmann's syndrome. Curved lines indicate the path of the olfactory (yellow lines) and vomeronasal/terminal nerve fibres (blue lines). In control foetuses at 6-8 weeks of gestation, GnRH expressing cells are distributed all along the migratory route from the frontonasal regions to the presumptive hypothalamus. In KS foetuses, GnRH cells accumulate along the discontinued path of olfactory and terminal nerve fibres that do not make contact with the forebrain. Figure taken from Giacobini P *Frontiers in Neuroendocrinology* 2015.

A recent study examined whether hypogonadism in CHARGE patients, as well as the absence of olfactory bulbs found in some individuals with trisomy 13 and trisomy 18 may result in defective migration of GnRH as in the Anos1 foetus (Texeira et al., 2010). This was achieved by examining a 25 GW male foetus carrying a nonsense mutation in Anos1, a 23 GW male carrying a frame-shift mutation in CHD7, an 18 GW female with trisomy 13 (47, XX+13 karyotype) and a 35 GW male with trisomy 18 (47, XY+18). In all arrhinencephalic foetuses, no GnRH cells were found in the POA or hypothalamus, while numerous GnRH cell bodies were found confined to the nasal region and the dorsal aspect of the cribriform plate, occasionally forming clusters in the ganglion of the TN. Importantly, in 2 control foetuses (22 and 24 GW), GnRH cells numerously populated the forebrain and no GnRH cells were found in the nasal region or in contact with the cribriform plate. Additionally, both the CHD7 and Anos1 foetuses possessed bilateral structures on the dorsal aspect of the cribriform plate

consistent with neuromas indicating an entanglement of nerve fibres, while similar bulges were observed next to the crista galli in an additional GW 13 arrhenencephalic foetus (**Figure 18**). These structures are reminiscent of the phenotype of *Prokr2*$^{-/-}$ mice (Pitteloud et al., 2007).

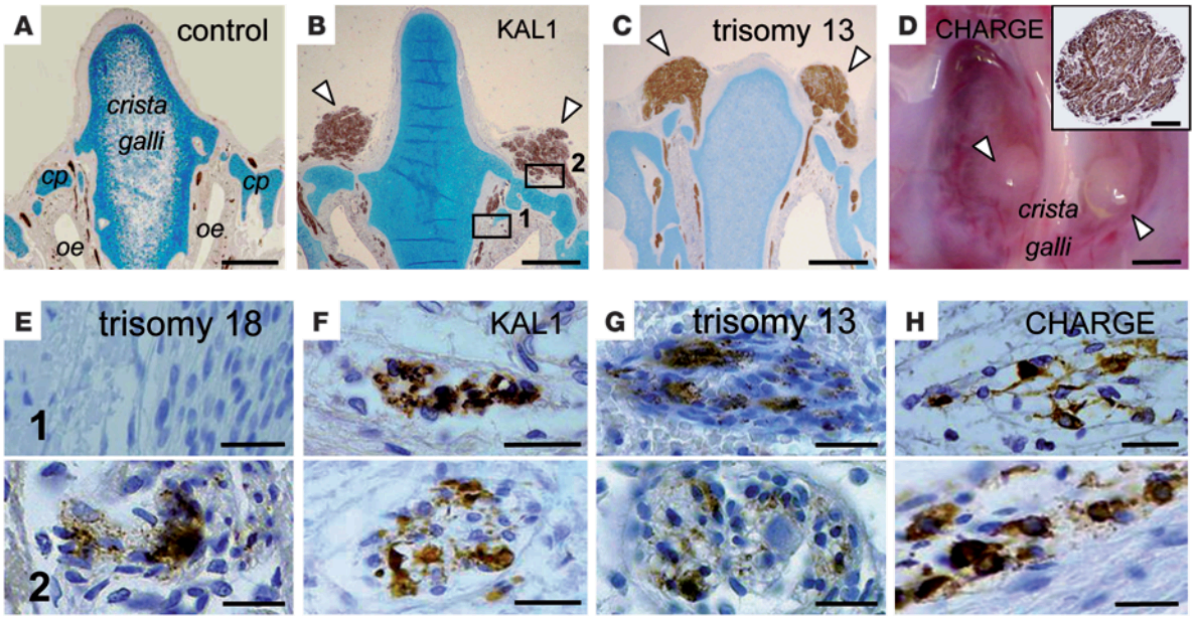

Figure 18. Arrested GnRH migration in human pathologies.

Coronal sections of the frontonasal region in the KAL1 foetus and 23-week-old trisomy 13 and control foetuses, immunostained for βIII-tubulin In the KAL1 and trisomy 13 foetuses, bilateral spherical structures corresponding to neuromas (arrowheads) are visible on the dorsal aspect of the cribriform plate (cp). (E-H) Coronal sections corresponding to the boxed regions in B. In all foetuses, GnRH1 cells were seen in the upper nasal region (region 1) and/or on the dorsal aspect of the cribriform plate (region 2). Note the presence of GnRH1 cells only on the dorsal aspect of the cribriform plate for the 35-week-old trisomy 18 foetus. Scale bars: 1 mm (A-D); 200 μm (D, inset); 30 μm (E-H). Schematic representations of the distribution of GnRH cells in normal and pathological development are also included. Abbreviations: oe: olfactory epithelium. Figure taken from Texeira et al., *JCI* 2010

2.12.3 Fibroblast Growth Factors (FGFs)

FGF family signalling is essential to multiple aspects of vertebrate and invertebrate embryonic development, angiogenesis, wound healing, and tissue homeostasis. FGFR1 is the principle receptor that mediates FGF signalling acting in conjunction with membrane associated heparin sulphate proteoglycans. FGFR1 expression has been identified in the nasal placode, developing olfactory bulbs and is expressed along the GnRH migratory pathway and by GnRH neurons themselves (Kim et al., 2008). FGF also plays an essential role in the morphogenesis of the telencephalon including the olfactory bulbs. FGFR1 has been shown to be essential for GnRH migration and mutations in FGFR1 are known to cause autosomal dominant forms of both KS and normosmic CHH (Kim et al., 2008; Xu et al., 2007). Although FGFR1 mutations are the second most common molecular cause of KS thus far identified, its mutations are known to have a wide phenotypic variability – suggestive of incomplete penetrance and oligogenicity (Bianco & Kaiser, 2009).

FGF8, one of the ligands of FGFR1, is also associated with KS and CHH (Falardeau et al., 2008). The mutations identified in FGF8 in patients were validated *in vitro* and *in silico* with both approaches suggesting deleterious effects on FGF8 signalling (Falardeau et al., 2008). Furthermore, mice homozygous for a hypomorphic Fgf8 allele lacked GnRH neurons in the hypothalamus, while heterozygous mice showed substantial decreases in the number of GnRH neurons and hypothalamic GnRH peptide concentration. Additionally, FGF17 which shares a strong sequence identity with FGF8 (Miraoui et al., 2013), has also been shown to be an important activator of FGFR1 signalling that may contribute to KS (Miraoui et al., 2013). Miraoui and colleagues also identified several mutations in IL17RD, a gene encoding a member of the interleukin-17 receptor protein family. This family forms part of a larger group known as SEF (similar expression to FGFs), with IL17RD shown to interact with FGFR1 in transfected human embryonic kidney cultures. The *in vivo* expression pattern of IL17RD is suggestive of a role in the early stages of GnRH fate specification.

Interestingly it has been shown that Anosmin-1 can act as a modulatory co-ligand with FGF8 to activate FGFR1, in a manner dependent on the presence of heparan sulphate (Tornberg et al., 2011). Seven mutations in the HS6ST1 (heparan sulphate 6-O-sulftransferase enzyme) gene have been identified in CHH patients with varying levels of olfactory function (Tornberg et al., 2011) further indicating the importance of FGF signalling in the ontogenesis of GnRH development.

2.12.4 Semaphorins

Semaphorins are secreted or membrane associated glycoproteins that contain a conserved 400 amino acid 'Sema' domain and are well characterised guidance molecules that are phylogenetically conserved across species from nematodes and insects to vertebrates, including humans. 4 classes of semaphorins have been identified in vertebrates, with class 3 semaphorins being secreted and classes 4-7 being membrane bound. The primary receptors mediating semaphorin signalling are neuropilins (Nrp1 and Nrp2) and plexins. Semaphorins were initially characterised for their role in mediating axon guidance during development but recent work has lead to the identification of semaphorins in a wide range of processes such as regulation of cell adhesion and motility, angiogenesis, immune responses and tumour progression (Casazza et al., 2007; Comoglio et al., 2004; Kruger et al., 2005; Mann et al., 2007; Mann and Rougon, 2007; Neufeld and Kessler, 2008; Pasterkamp and Giger, 2009).

The class-3 secreted semaphorins bind to neuropilins, which act as ligand-binding co-receptors. Neuropilin-2 null (*Nrp2*$^{-/-}$) mice have a 25% reduction in the total GnRH population during adulthood, while also having an increase in the number of neurons residing in the nasal septum (Cariboni et al., 2007) – suggesting a defect in migration. This was suggested to occur due to a defasiculation of the vomeronasal axons, disrupting the pathway along which GnRH neurons migrate. Cariboni and colleagues (2010) also identified roles for Sema3a using genetic mouse models. *Sema3a*$^{-/-}$ mice display severe defects in vomeronasal projections resulting in almost complete absence of GnRH immunoreactivity in the forebrain at E14.5 and E18.5. The validity of these findings in mice was confirmed in 2012 when two groups

identified lack of function mutations in Sema3a in KS syndrome patients (Hanchate et al., 2012; Young et al., 2012). Of note, several of the mutations identified by Hanchate and colleagues were also found in clinically unaffected individuals, suggesting that these mutations contribute to the oligogenic forms of KS.

Neuropilin1 (Nrp1) is an obligatory co-receptor of Sema3a and its expression delineates the GnRH migratory pathway, including the caudal branch of the VNN in both mice and humans (Hanchate et al., 2012). Mice lacking functional semaphorin signalling through Nrp1 (*Nrp1*$^{sema/sema}$) or *Nrp2*$^{-/-}$ only partially phenocopy the defects of *Sema3a*$^{-/-}$ mice, while the compound mutant *Nrp1*$^{sema/sema}$;*Nrp2*$^{-/-}$ mice display a comparable phenotype to Sema3a knockouts. The normal distribution and population size of GnRH neurons in adult conditional mutant mice lacking Nrp-1 only in GnRH neurons (*GnRH::Cre;Nrp1*$^{loxP/loxP}$ mice) (Hanchate et al., 2012) further confirms that the defective migration of GnRH neurons in these embryos is due to the abnormal routing of VNNs into the ventral forebrain. Taken together this suggests that Sema3a signalling involving both Nrp1 and Nrp2 controls vomeronasal axon targeting to the brain and that its disruption results in migratory deficits that are not cell autonomous (indirectly affecting GnRH migration). This was in contrast to *Sema3f*$^{-/-}$ mice that had normal GnRH development, suggesting that not all secreted Semaphorins are required for VNN targeting.

A shared point mutation in Sema3e has been identified in a familial case of KS (Cariboni et al., 2015). Interestingly, in contrast to the well characterised roles of secreted semaphorins in regulating axon guidance, Sema3e was shown to instead regulate survival of GnRH neurons through interactions with Plexin D1 (Cariboni et al., 2015). Of note, the fraternal Sema3e mutations co-segregated with a mutation in CHD7 and a *de novo* mutation in Sema3e was additinally identified in a cohort of CHARGE patients (Lalani et al.,2004), further supporting partially shared developmental aetiologies of these syndromes.

Sema4D is a transmembrane-bound semaphorin that is proteolytically cleaved to bind Plexin B1 and Met tyrosine kinase receptor (Conrotto et al., 2005). This interaction typically mediates

growth cone collapse of developing axons and induces chemotaxis (Derijck et al.; Deijck et al., 2010; Zhou et al., 2008). Sema4D expression forms a gradient in the embryonic nasal region, with a higher concentration at the level of the NFb/J, suggesting it acts s a chemoattractant for migrating GnRH cells, which was subsequently confirmed *in vitro* (Giacobini et al., 2008). Additionally, Sema4D null mice are subfertile (Dacquin et al., 2011). Sema4D, along with its high affinity receptors PlexinB1 and PlexinB2 are highly expressed in the developing olfactory system, with Plexin B1 expression found in the nasal placode and co-localising with NCAM positive fibres at E12.5. No expression of PlexinB1 was detected in either VNN or in GnRH neurons themselves at E14.5 or E17.5 – suggesting a highly localised effect early in GnRH migration (Giacobini et al., 2008). This idea was confirmed using an *ex vivo* nasal explant culture where PlexinB1 was detectable in early cell divisions, and ceased to be expressed in later divisions. PlexinB1 null mice exhibit a defect in the migration of GnRH neurons, that results in a decrease in the total population size in the adult brain.

Sema7A signals through PlexinC1 and β1-integrin with their expression patterns highly suggestive a role in regulating GnRH migration. Sema7A is highly expressed in the nasal pit and along the VNN during embryonic development, while the expression of its receptors is spatiotemporally regulated within migrating GnRH neurons (Messina et al., 2011). At early migratory stages, GnRH neurons specifically express β1-integrin, whereas they begin to express PlexinC1 once they reach the end of their migratory journey. This is consistent with *in vitro* experiments that demonstrated that Sema7a stimulates increased directional migration in immortalised GnRH cells dependent on β1-integrin signalling, whilst overexpression of PlexinC1 halted their migration (Messina et al., 2011). *In vivo* confirmation of Sema7A signalling in the regulation of GnRH migration came from analysis of mutant mice, with Sema7A deficient and conditional inactivation of β1-integrin in GnRH neurons resulting in a reduction in the adult GnRH population, as well as reduced gonadal size and subfertility (Messina et al., 2011; Parkash et al., 2012). Missense mutations in Sema7A have been identified in both CHH and KS patients (Känsäkoski et al., 2014), although as both patients with Sema7A mutations were already identified to possess mutations in known CHH/KS associated genes

(for example one patient possessed a mutation in Anos1), it was concluded that Sema7A mutations alone would be unlikely to be sufficient to generate a full KS phenotype.

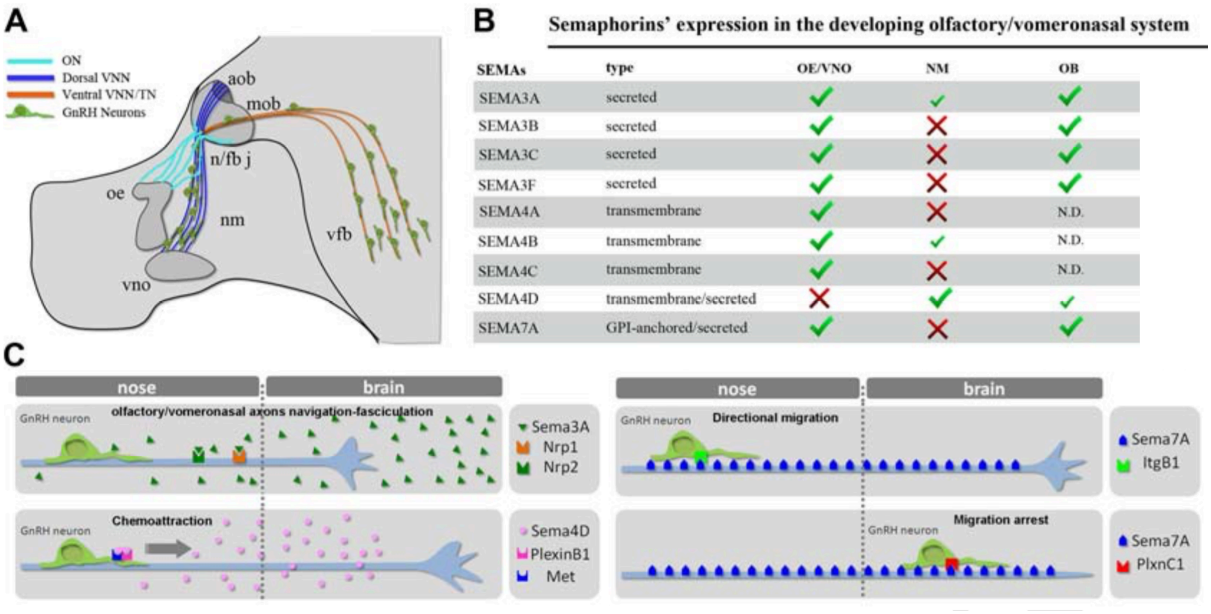

Figure 19. The role of Semaphorin signalling in regulating GnRH migration.
(A) Schematic representation of the head of a mouse embryo at E14.5 depicting the scaffold formed by the olfactory nerve (ON) and vomeronasal/terminal nerve (VNN/TN), along which GnRH cells migrate from the nose to the ventral forebrain. (B) Different semaphorins expressed in the developing nasal region. (C) Mechanisms of action of the semaphorins on GnRH neuron motility and/or navigation along VNN/TN. Abbreviations: oe: olfactory epithelium; vno: vomeronasal organ; nm: nasal mesenchyme; n/fb j: nasal/forebrain junction; aob: accessory olfactory bulb; mob: main olfactory bulb; vfb: ventral forebrain. Modified from Giacobini *Frontiers in Neuroendocrinology* 2015

2.12.4 Perspectives

The subsequent identification of mutations in KS patients, following characterisation of GnRH migratory disruption in mice models underlines the validity of this approach to identifying potential CHH/KS genes. An International consortium of physicians and scientists studying CHH and KS was formed in 2012, with the aim to rapidly advance our understanding of the many causes of these reproductive syndromes and translate these discoveries into improved patient care. This action culminated in the consensus statement (Boehm et al., 2015) that summarised the recent advances that had been made. A full list of all the known CHH and KS genes thus far identified is presented in **Table 1**, with their roles in regulating GnRH development and/or function summarised in **Figure 20**.

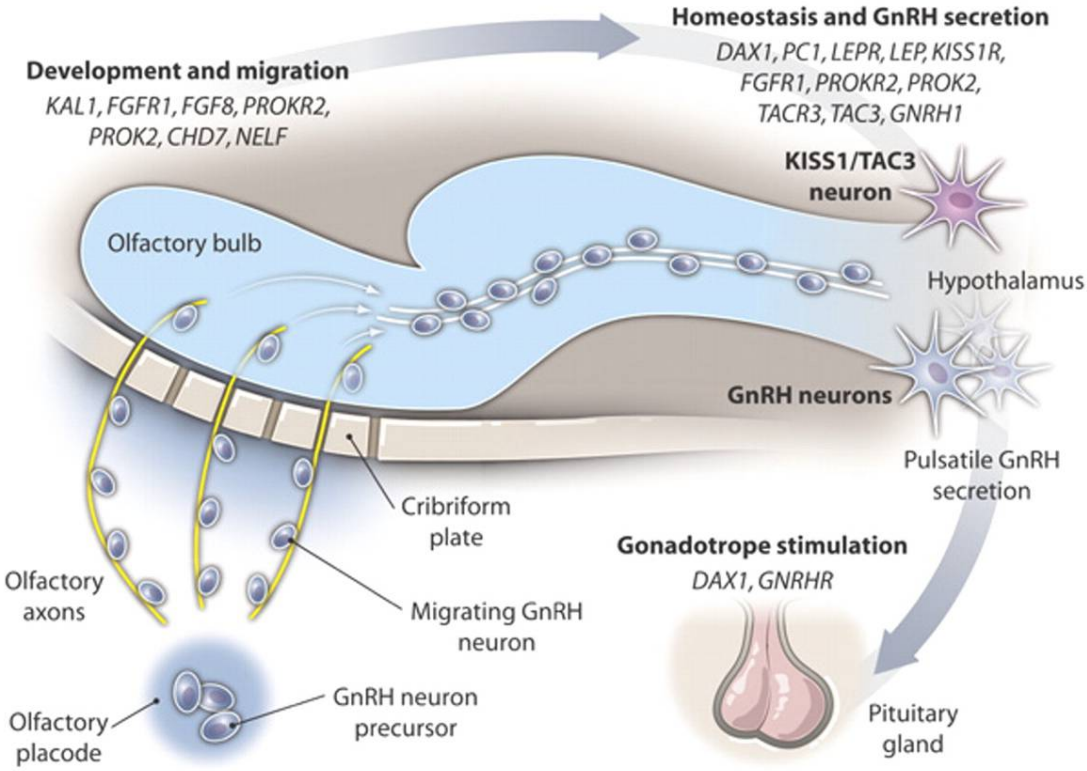

Figure 20. Schematic of known factors contributing to CHH (congenital hypogonadotropic hypogonadism)

CHH is a multifactorial, oligogenic disorder where disruption to GnRH signalling can occur due to developmental abnormalities or in rarer cases be acquired postnatally. This schematic represents many genes known to cause defective GnRH release in postnatal life, and also at what level they act to regulate part of GnRH physiology. Figure taken from https://kallmannsyndrome.wordpress.com/

Table 1. Genes known to contribute to CHH and KS

AD: Autosomal Dominant; AR: Autosomal Recessive; CHH: congenital hypogonadotropic hypogonadism; CHARGE: Colomba, heart defects, atresia of choanae, retardation of growth, genital and or urinary defects, ear anomalies or deafness; CPHD: combined pituitary hormone deficiency; GHS: Gordon Holmes Syndrome; HS; Hartsfield syndrome; MGS: morning glory syndrome; OMIM: online Mendelian inheritance in man; PEPNS: polyendocrine deficiencies and polyneuropathies; SHFM: split-hand/foot malformation; SOD: septo-optic dysplasia; WS: Waardenburg syndrome

Gene	OMIM	Location	KS	CHH	Inheritance	Estimated Prevalence	Overlapping Syndromes
ANOS1 (KAL1)	300836	Xp22.31	x		X-linked	5	
AXL	109135	19q13.2	x	x	AD (?)	?	
CCDC141	616031	2q31.2	x		AR (?)	rare	
CHD7	612370	8q12.2	x	x	AD (?)	6	CHARGE
DMXL2	616113	15q21.2		x	AR	rare	PEPNS
DUSP6	602748	12q21.33	x	x	AD	rare	
FEZF1	613301	7q31.32		x	AR	rare	
FGF17	603725	8p21.3	x	x	AD (?)	rare	DWS
FGF8	612702	10q24.32	x	x	AD	>2	CPHD
FGFR1	147950	8p11.23	x	x	AD	10	CPHD, CPHD+SOD, HS, SHFM
FLRT3	604808	20p12.1	x		AD	rare	
GNRH1	614841	8p21.2		x	AR	rare	
GNRHR	146110	4q13.2		x	AR	6-16	
HESX1	182230	3p14.3	x		AD (?)	rare	CPHD, CPHD+SOD
HS6ST1	614880	2q14.3	x	x	AD (?)	rare	
IGSF10	617351	3q25.1	x	x	AD (?)	rare	
IL17RD	606807	3p14.3	x		AR	3	
KISS1	614842	1q32.1		x	AR	2	
KISS1R	614837	19p13.3		x	AR	2	
LEP	614962	7q32.1		x	AR	>2	
LEPR	614963	1p31.3		x	AR	>2	
(DAX1)	300200	Xp21.2		x	X-linked	rare	
NSMF	614838	9q34.3	x	x	AD (?)	rare	
OTUD4	611744	4q31.21		x	AR	rare	GHS
PCSK1	162150	5q15		x	AR	>2	
POLR3B	614366	12q23.3		x	AR	rare	
PNPLA6	603197	19p13.2		x	AR	rare	GHS
PROK2	610628	3p13	x	x	AR	3-6	
PROKR2	147950	20p12.3	x	x	AR	3-6	CPHD, MGS
RNF216	609948	7p22.1		x	AR	rare	GHS
SEMA3A	614897	7q21.11	x		AD	rare	
SEMA7A	607961	15q24.1	x	x	AD	rare	
SOX10	602229	22q13.1	x		heterozygous	2	WS
SPRY4	607984	5q31.3	x	x	AD	rare	
TAC3	614839	12q3		x	AR	rare	
TAC3R	614840	4q24		x	AR	rare	
WDR11	614858	10q26.12	x	x	AD	rare	CPHD

CHAPTER 3

Anti-Müllerian Hormone

3.1 Sexual Development & Differentiation

Sexual differentiation is a process that begins during the foetal period and continues in the neonate and through puberty, leading to the establishment of sexual dimorphism. The genetic sex of mammals is determined at fertilisation and depends on the nature of the sex chromosomes possessed by the individual. In mammals, the default programming of our genes charts a course for female development, with the presence of the Y chromosome in men being the key signal to cause divergence in the paths. Regardless, however, of its chromosomal heritage, each individual will go through a sexually undifferentiated phenotype during early foetal life. The establishment of sex is a complex phenomenon, determined by the differential expression of critical genes during a brief window in both males and females. The major developmental stages leading to male or female sexual differentiation are very similar across mammals, even in *Tokudaia osimensis,* the Ryuku spiny rat, that has lost its Y chromosome and *SRY* (sex-determining region Y) gene (Otake & Kuroiwa, 2016).

The idea of a testicular factor regulating the sexual differentiation of the gonads was proposed following observations made by Alfred Jost in 1947. He found that the Müllerian ducts of the rabbit would independently differentiate into the female reproductive system (namely the uterus, fallopian tubes and upper two-thirds of the vagina) in the absence of testicular secretions (Jost, 1947). Following gonadectomy of sexually undifferentiated rabbits, Jost grafted either ovarian or testicular tissue inside the rabbits and witnessed the correct development of either the female or male genitalia respectively. The paradigm shifting experiment came when, following gonadectomy, he implanted a testosterone proprionate crystal alone, noting that whilst the Wolffian ducts were stimulated to develop, there was no regression of the Müllerian ducts – highlighting that a testicular factor other than testosterone was responsible for gonadal differentiation. Jost called this factor "hormone inhibitrice" or "inhibiteur müllerian" (Jost 1953), and today it is better known as anti-Müllerian hormone or Müllerian inhibiting substance (AMH, MIS).

AMH was first purified in 1984 by immunochromatography (Picard & Josso, 1984) and sequencing of both human and bovine forms followed shortly thereafter (Cate et al., 1986; Picard et al., 1986). The presence of an *AMH* gene is extremely well conserved through evolution, being present in almost all mammals (Munsterberg & Lovell-Badge, 1991; Haqq et al., 1992; Lahbib-Mansais et al., 1997; Pask et al., 2004), chicken (Oreal et al.,), reptiles (Western et al., 1999), marsupials (Pask et al., 2004), zebrafish (Schulz et al., 2007) and amphibians (Al-Asaad et al., 2013). All are formed of five exons, with the highest degree of homogeneity being observed between exons 2-5 between all species thus far studied.

AMH is a glycoprotein (detailed discussion of its structure in **Section 3.5**) found in the blood, suggesting it has a hormonal function. The primary sources of production, identified so far, are the Sertoli cells of the testes and the granulosa cells of the ovaries. However, AMH expression has also been detected in the brain and prostate, as well as in other peripheral tissues, such as lungs (La Marca et al., 2005; Long et al., 2000; Gustafson et al., 1993).

Serum AMH levels are extremely high during male prenatal development; however, significant levels in females are not present until puberty where they rise to approximately the same level seen in males ~20pM (**Figure 21**). As with all hormones that are expressed in a sexually dimorphic fashion, interest has focused on characterising the temporal patterns of its expression, thereby allowing inferences to be made as to possible physiological functions (detailed discussion in reproductive roles of AMH section)

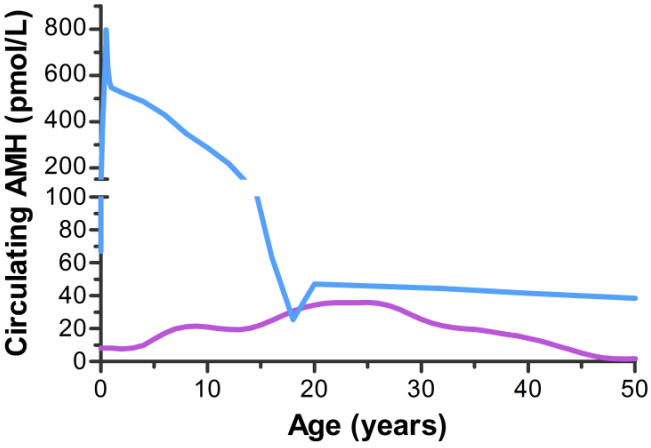

Figure 21. Circulating AMH levels in humans.
The general levels of detectable AMH in serum throughout male and female life. AMH levels are almost 20x higher in prenatal boys compared to any postnatal age in either males or females. In AMH levels are generally higher in males than females with similar levels found only from the mid-teens to the end of the third decade. The expression level in females is consistent with a reproductive role as levels increase through pubertal years and then begin decreasing as menopause approaches. Note the Y axis has been split. Adapted from Adams N 2012

3.2 Reproductive roles of AMH

3.2.1 Development of the embryonic gonad

In vertebrates, the development of the urogenital apparatus (including the kidneys, gonads, bladder and urinary and reproductive ducts) begins shortly after gastrulation by the differentiation of the intermediate mesoderm. This structure will initially proliferate and some cells undergo a transition from mesenchymal cells to epithelial cells to form the future male and female reproductive structures (Kobayashi and Behringer 2003). Such it is, that during part of embryonic development, every individual possesses both male and female reproductive ducts and thus has the potential to develop a male or female reproductive system. In order for normal male or female development to occur, one of the two pairs of ducts must regress and the other must develop.

The undifferentiated internal genital tract includes the Wolffian and the Müllerian ducts. Both form part of the mesonephros and extend along their caudal end to join the urogenital sinus leading to the genital tubercle (the origin of the genital tract). The Wolffian (mesonephric) ducts are first found along the embryonic kidney and can differentiate to form a duct, epididymis and seminal vesicles. In mice, the Wolffian ducts are fully formed at E10.5. The Müllerian (paramesonephric) ducts develop antero–posteriorly along the Wolffian ducts between E11.5 and E13.5 in mice and have the potential to develop into oviduct, uterus and upper vagina.

3.2.2 Sexual differentiation of the male gonad

The differentiation of the gonad is determined by the genetic sex in most mammals, with the presence of a Y chromosome containing the *SRY* gene being the critical requirement in most eutherian mammals (Gubbay et al., 1990; Sinclair et al., 1990). Indeed, the presence of *SRY* and *Eif2s3y* genes have been shown to be sufficient to replace the Y chromosome, resulting in the production of fertile male mice in adulthood (Yamauchi et al., 2014).

The presence of the *SRY* gene leads to morphological differentiation of the primary testicular gonad at E12 in mice, with the differentiation of Sertoli cells from the foetal testes marking the first step in testicular organogenesis (Magre & Jost 1991). These cells associate with each other by interdigitations and membrane junctions, progressively encompassing the germ cells and thus giving rise to seminiferous cords delimited by a basal membrane. AMH is the first endocrine factor secreted by Sertoli cells (Tran et al., 1977), and is first detectable at E10.5 and levels rise until birth (Kashimada & Koopman, 2010). In rats this process begins at E13 (Tsuji et al., 1992) and in humans AMH is first detectable at 7 weeks of gestation.

The timing of AMH expression and secretion by the Sertoli cells is tightly regulated (regulation of AMH expression discussed in Chapter 3.4), as the Müllerian duct only remains hormonally sensitive for a short period of time (known as the critical window), outside of which the Müllerian ducts will fail to regress (Taguchi et al., 1984; Tsuji et al., 1992). This window is around E13/E14 in mice and appears to be determined by the expression of receptors able to bind AMH – AMHR2, with levels sharply decreased outside of the critical window (Josso et al., 2001). The regression of the Müllerian duct once initiated by AMH, occurs in a cranio-caudal direction (Arango et al., 2008) and is irreversible, continuing even if AMH is no longer present (Taguchi et al., 1984). This is consistent with a paracrine action, with the tissues closest to the source regressing before distal structures, and is supported by rare cases of unilateral Müllerian duct derivatives being present in males after birth, (e.g. presence of a single testis) such as in mixed gonadal dysgenesis. Evidence for a hormonal rather than paracrine action on the Müllerian ducts arise from the freemartin cow. Freemartinism occurs when anastomoses of the blood supply to twin male and female calves form, where the AMH produced by the testes of the bull calf causes regression of the Müllerian ducts in the female calf (reviewed by Esteves et al., 2012).

The regression of the Müllerian ducts occurs through first regulating apoptosis then regulating epithelio-mesenchymal transformation of the mesenchymal cells surrounding the Müllerian ducts via AMH signalling (di Clemente et al., 1994; Teixeira et al., 1996). In rats the critical

window during which the Müllerian ducts are sensitive to AMH is E14–E15, with regression progressing from E14–E16 (Picon, 1969; Tsuji et al., 1992). In humans, the regression has been reported to be completed by gestational week 9 (Taguchi et al., 1984), even though our group recently reported that it might actually terminate later, around GW12 (Belle et al., 2017). In females where gonadal AMH levels are not detectable prenatally, the Wolffian ducts instead regress, allowing the development of the female reproductive tract.

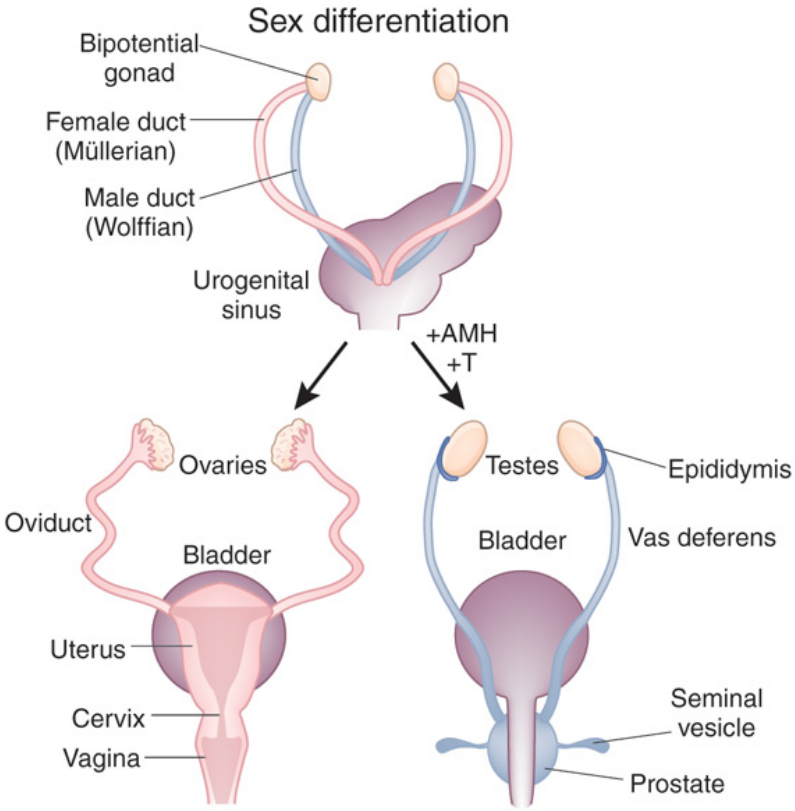

Figure 22. Mammalian sex differentiation.

All mammals develop a bilateral pair of Müllerian and Wolffian ducts during embryonic development. These structures are the anlagen of the female and male reproductive tracts respectively and true sexual differentiation requires the regression of one pair and the development of the other. The presence of a Y chromosome in males stimulates the release of AMH and testosterone from the primitive testis, which act to cause regression of the Müllerian duct during a narrow, critical window of embryonic development. In the absence of a Y chromosome and hence a testis to secrete AMH and testosterone, female gonadal development occurs passively with the automatic degeneration of the Wolffian ducts allowing the Müllerian ducts to differentiate and develop into the female reproductive tract. Reference: Matzuk & Lamb, *Nature Medicine* 2008

3.2.3 Persistent Müllerian Duct Syndrome (PMDS)

The significance of AMH signalling to the development of correct male genitalia is shown by mutations affecting the function of AMH or AMH receptors, which are known to cause a rare form of internal pseudo-hermaphroditism called Persistent Müllerian Duct Syndrome (PMDS). This syndrome is characterised by the persistence of Müllerian duct derivatives (i.e. uterus, cervix, fallopian tubes and upper two thirds of vagina) in a phenotypically and karyotypically male (46XY) patient. PMDS patients have normal development of the external genitalia and secondary sexual characteristics (Renu et al., 2010), with early detectable symptoms mainly confined to cryptorchidism and inguinal hernias. It is typically upon subsequent MRI or during surgery to treat the hernia, that remnants of the Müllerian structures are discovered, meaning that reporting frequencies for the condition are likely to be under-represented.

A meta-analysis of 262 case reports constructed a statistical model suggesting that malignancies of the Müllerian tissues would be experienced by 3.1-8.4% of PMDS patients without surgical intervention (Farikullah et al., 2012) and highly recommended their removal. Cryptorchidism is thought to occur in PMDS due to misdirection and anatomical obstruction by the abnormal presence and connection to the Müllerian structures, rather than a shortening of the internal spermatic vessels or vas deferens.

Approximately 45% of cases of persistent Müllerian duct syndrome are caused by mutations in the *AMH* gene [type 1 (OMIM: 600957)], while approximately 40% of cases are caused by mutations in the *AMHR2* gene [type 2 (OMIM: 600956)]. In the remaining 15% of cases, no mutations in the *AMH* and *AMHR2* genes have been identified; however, it is always inherited in an autosomal recessive manner.

Both $AMH^{-/-}$ and $AMHR2^{-/-}$ male mice present the same pseudohermaphroditic phenotype as seen in PMDS patients (Behringer et al., 1994; Mishina et al., 1996).

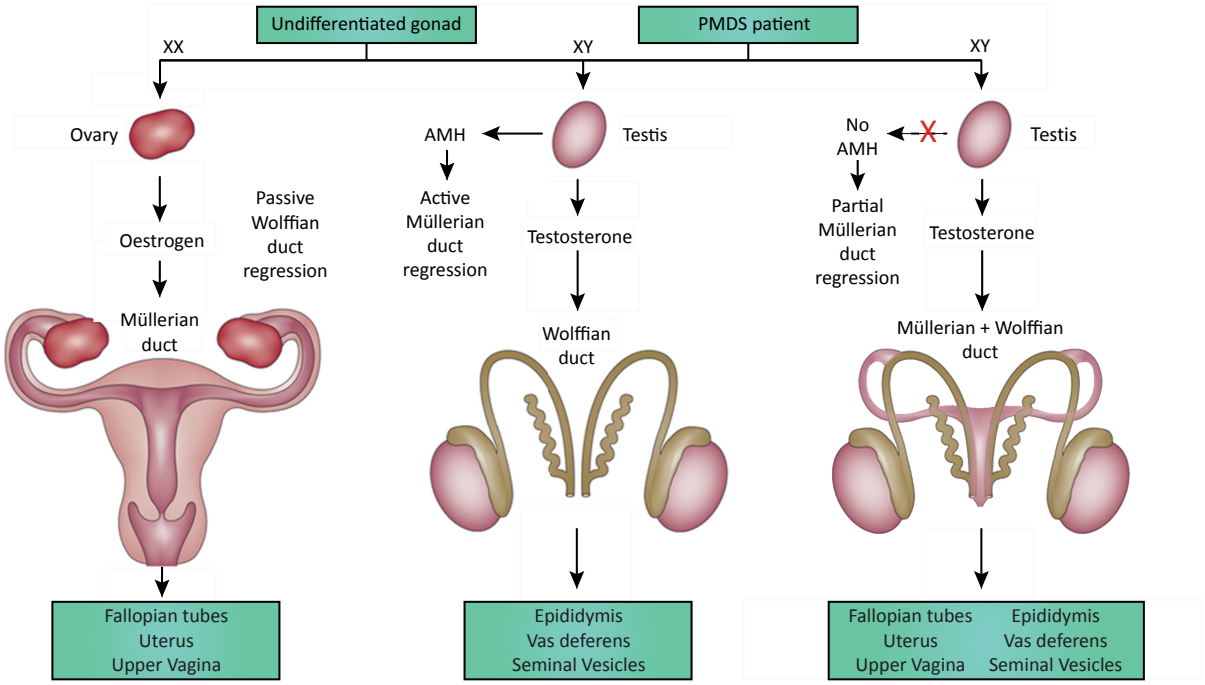

Figure 23. Insufficient AMH signalling results in persistent Müllerian ducts. Schematic depicting the physiological gonadal development during female (left) and male (middle) embryogenesis. In the case of inactivating mutations in the AMH or AMHR2 gene, AMH signalling fails to occur in male embryos during the critical window of sexual differentiation. In these cases, there is no initiation of the regression of the Müllerian ducts (MD) and while the Wolffian ducts develop normally, the MD fail to degenerate and persist into adulthood (right). This syndrome is known as persistent Müllerian duct syndrome (PMDS) a rare genetic infertility syndrome. Figure made by Malone SA.

Whilst PMDS is considered an infertility syndrome, the exact underlying cause may be complex. The human cases related to infertility may be explained by the long-term internalisation of the testes which may result in testicular dystrophy (Josso et al., 1997) whilst in $AMH^{-/-}$ and $AMHR2^{-/-}$ pseudohermaphroditic mice it is physical blockades that prevent correct ejaculatory patterning (Behringer et al., 1994). Mice with mutated SF-1 binding alleles had almost no detectable AMH levels and retained partial Müllerian derivatives – yet retained some fertility (Arango et al., 1999) and some mammals, for example the Male North American beaver *Castor Canadensis* typically retain residual uterine tissue throughout life (Meier et al., 1998). This raises the possibility that there may exist variable levels of PMDS within society, with most individuals retaining fertility (Meier et al., 1998).

3.3 Postnatal roles of AMH

3.3.1 AMH Actions in Female Reproductive Function

In females, the typical circulating AMH levels seen in **Figure 21** correlate well with the predictive power of AMH levels to ovarian reserve (Rooij et al., 2002) that has recently been widely adopted as the Gold Standard in primary health care systems (Grynnerup et al., 2012) and as a useful co-predictor of stimulated ovarian response (La Marca et al., 2010; Peñarrubia et al., 2005). Clinically observed correlations between enhanced basal levels of AMH and Polycystic Ovary Syndrome (PCOS) have led to a well-developed physiological role for AMH in follicular development (Reviewed by Catteau-Jonard & Dewailly, 2011; Visser, 2016). In this pathology enhanced numbers of primary follicles secrete abnormally high levels of AMH which results in a diminished suppression of androgen production and secretion coupled to arrested follicular maturation.

Mice that chronically overexpress AMH under the metallothionein-1 promotor possess fewer germ cells in the ovaries at birth, with the total number falling to zero within 2 weeks (Behringer et al., 1990). This is in contrast to *AMH*$^{-/-}$ mice, who have statistically increased levels of primary and secondary follicles at 25 days and 4 months of age versus heterozygous and wild type littermates. However, at 4 months and 13 months, decreased numbers of primordial follicles were observed in *AMH*$^{-/-}$ mice, suggesting a premature exhaustion of ovarian reserve (Durlinger et al., 1999). *AMH*$^{-/-}$ mice have unaltered oestrous cycle lengths however, indicating a subtle role in regulating ovarian fertility (Durlinger et al., 1999). The authors concluded that although the number of initial primordial follicles available immediately following birth was independent of the presence of AMH, it was an important factor in inhibiting follicular recruitment and thus AMH presence was essential for prolonging fecundity. AMH is first detectable in females at P4 in both rats and mice, coinciding with initiation of primary folliculogenesis (Durlinger et al., 2002).

In both rodent and human studies, it has been agreed that AMH secreted by primary and growing small antral follicles acts as a 'brake' inhibiting further follicular recruitment and development. Further, *in vitro* analysis of FSH dependent follicular maturation is halted by the addition of AMH, indicating that AMH is important in attenuating follicular sensitivity to cyclical FSH action (Durlinger et al., 2001). This is supported by a recent study that indicated that AMH levels parallel fluctuations in the antral follicle count through the menstrual cycle (Depmann et al., 2016).

In stitu hybridisation studies have characterised AMH and its cognate AMHR2 expression in granulosa cells of non-atretic, pre-antral and small antral follicles but not in larger follicles (Baarends et al., 1995). AMH & AMHR2 mRNA expression levels heterogeneously decrease at oestrus (in rats) but otherwise remain constant throughout the oestrous cycle (Baarends et al., 1995). *In vitro* experiments of cultured granulosa cells have indicated that exogenous AMH decreases aromatase activity and Luteinising Hormone Receptor (LHR) number (di Clemente et al., 1994) whilst inhibiting granulosa cell proliferation. In rats with chronically high LH, the ovarian pool of primordial follicles is depleted at an increased rate (Flaws et al., 1997).

Polymorphisms in both *AMH* and *AMHR2* have been associated with cases of unexplained idiopathic infertility in women (Rigon et al., 2010) and in a polycystic ovary syndrome (PCOS) cohort, a condition that is partly characterised by increased serum AMH levels (Georgopoulos et al., 2013). Several heterozygous mutations in *AMHR2* have also been identified in a cohort of Han Chinese women diagnosed with primary ovarian insufficiency (POI), with *in silico* analysis predicting the deleterious effects of three variants (Li et al., 2016).

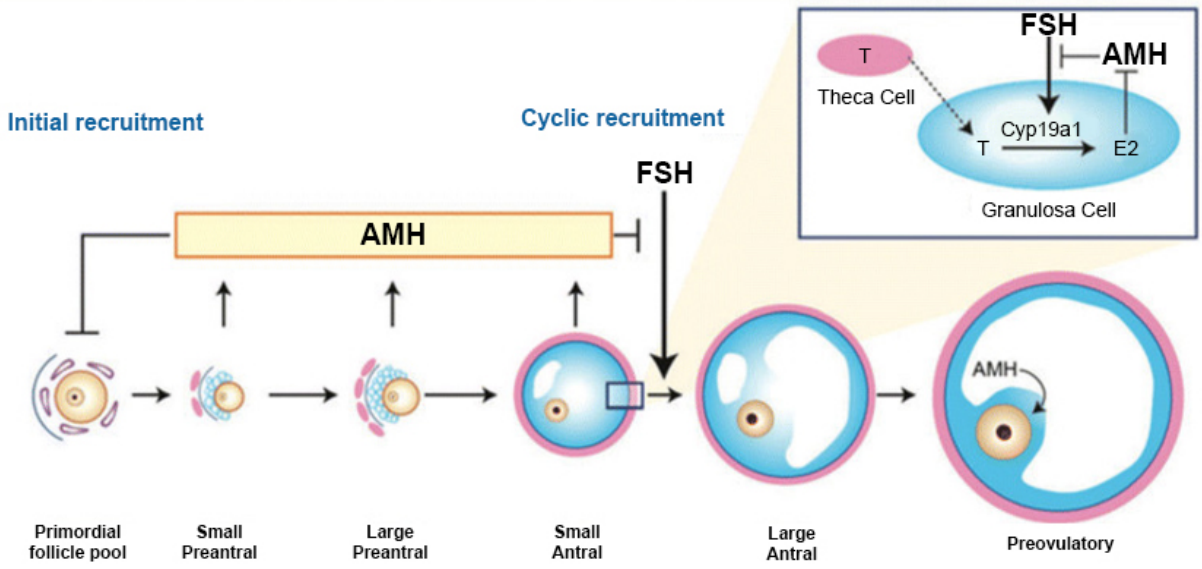

Figure 24. Effects of AMH during folliculogenesis.

AMH, produced by the granulosa cells of small growing follicles, inhibits initial follicle recruitment and FSH-dependent growth and selection of preantral and small antral follicles. In addition, AMH remains highly expressed in cumulus cells of mature follicles. The inset shows in more detail the inhibitory effect of AMH on FSH-induced CYP19a1 expression leading to reduced oestradiol (E2) levels, and the inhibitory effect of E2 itself on AMH expression. T, testosterone; Cyp19a1, aromatase. Figure modified from van Houten et al. (2010)

3.3.2 AMH Actions in Male Reproductive Function

Both Leydig and Sertoli cells of the testes express AMHR2 indicating a potential paracrine role in regulating male gonadal function (Arango et al., 2008). Indeed, high doses of AMH result in decreased aromatase expression and hence testosterone secretion *in vitro* (Racine et al., 1998) and *in vivo* (Laurich et al., 2001). Concomitantly, AMH also causes a decrease in LHR expression, which should further act to decrease testosterone secretion (Racine et al., 1998). This is confirmed as male mice that overexpressed AMH under the control of the metallothionein-1 promotor showed characteristic signs of low androgen levels, including vaginal opening, underdeveloped Wolffian ducts, undescended testes and nipples (Behringer et

al., 1990) – male mice normally do not have nipples. Physiologically, AMH levels fall in boys with the increase in testosterone and initiation of spermatogenesis (Rey et al., 2005); however, it should be noted that this this androgen mediated decrease in AMH levels is restricted to post-natal life, as immature Sertoli cells lack expression of the Androgen Receptor (AR) (Boukari et al., 2009; Chemes et al., 2008). Interestingly, AMH deficient mice have circulating levels of testosterone within the normal range, suggesting that compensatory mechanisms may act to replace the interconnected feedback between the two hormones. Meanwhile male mice with targeted mutations of *AMHR2* develop Leydig cell hyperplasia, suggesting an inhibitory role of AMH on Leydig cell proliferation (Behringer et al., 1994).

Whilst secreting AMH into the peripheral blood circulation, Sertoli cells also secrete AMH into the seminiferous tubules, where it exists at a much higher concentration compared to the plasma (Fallat et al., 1997; Fenichel et al., 1999). The role of AMH in semen is currently unclear. Reports of AMH levels correlating with sperm count (Tuttelmann et al., 2009), sperm not possessing AMHR2 (Baarends et al., 1994; Fallat et al., 1996) and improving sperm viability outside of the body (Siow et al., 1998) are seemingly contradictory.

3.3.3 AMH Actions on non-gonadal HPG tissues

In the adult brain, it has been shown that mature neurons express high levels of AMH receptors in both sexes (Lebeurrier et al., 2008; Wang et al., 2005; Wang et al., 2009). This raises the intriguing question as to their role in regulating neurological function. First it may be important to consider the circulating levels of AMH found in mature animals, being roughly similar between young adults, suggesting that the role of AMH has distinct and divergent roles between development and mature function.

Cimino and colleagues (2016) recently uncovered a direct action of AMH on GnRH neuronal activity. Demonstrating that AMHR2 is expressed in a significant subset of hypothalamic GnRH neurons both in mice and in humans and that exogenous AMH induces neuronal activation of approximately half of the GnRH population located in the POA in mice, independent of sex or

stage of the oestrous cycle. These electrophysiological data were supported by *in vivo* administration of AMH directly into the lateral ventricles that caused an increase in LH secretion equivalent to levels required to produce an ovulatory surge. It should also be noted that more than 80% of women with PCOS appear to have an increased LH pulse frequency (Taylor et al., 1997), suggesting that the pulse frequency of GnRH is persistently accelerated in this syndrome.

A majority of immature neurons in the mouse brain express AMHR2, suggesting that AMH signalling may be important in regulating some neurodevelopmental processes (Lebeurrier et al., 2008; Wang et al., 2009). Consistent with this, treatment of murine embryonic spinal motor and cortical neurons *in vitro* with AMH improved survival rates (Lebeurrier et al., 2008; Wang et al., 2005). The male increase in spinal and cerebellar motor neurons caused by AMH mediated survival has been hypothesised to contribute to the subtle sex-biased differences in some behaviour patterns such as increased exploratory behaviour (Wang et al., 2009). AMH signalling (through AMHR2 and BMPR1b, SMAD1/5/8) has been shown to regulate the neuronal serpin neuroserpin in adult neurons both *in vitro* and *in vivo* (Lebeurrier et al., 2008). Neuroserpin has been demonstrated to have several roles in the CNS, including the control of neuronal migration and neuronal death (Krystosek et al., 1981; Krueger et al., 1997; Yepes et al., 2002). Intriguingly Cimino and colleagues also demonstrated that migratory GnRH neurons expressed AMHR2 in both humans and mice, raising the possibility that AMH signalling may also play a role regulating GnRH prenatally.

In addition to regulating GnRH secretion postnatally, AMH has also been shown to preferentially stimulate secretion and adenohypophyseal gene expression of the gonadotropin FSH *in vivo* in rats (Garrel et al., 2016). This action of AMH was sex-dependent, being restricted to females and occurring only before puberty. *In vitro* analysis demonstrated the specificity of this response using cell lines derived from all pituitary cell types with only the LβT2 gonadotroph cell line responding to AMH. The increase in *Fshb* transcript levels was dependent on the SMAD 1/5/8 pathway, similar to what has been described to occur in the

ovary. Furthermore, AMH was shown to establish complex interrelations with canonical FSH regulators that are also part of the TGFβ family such as BMP2.

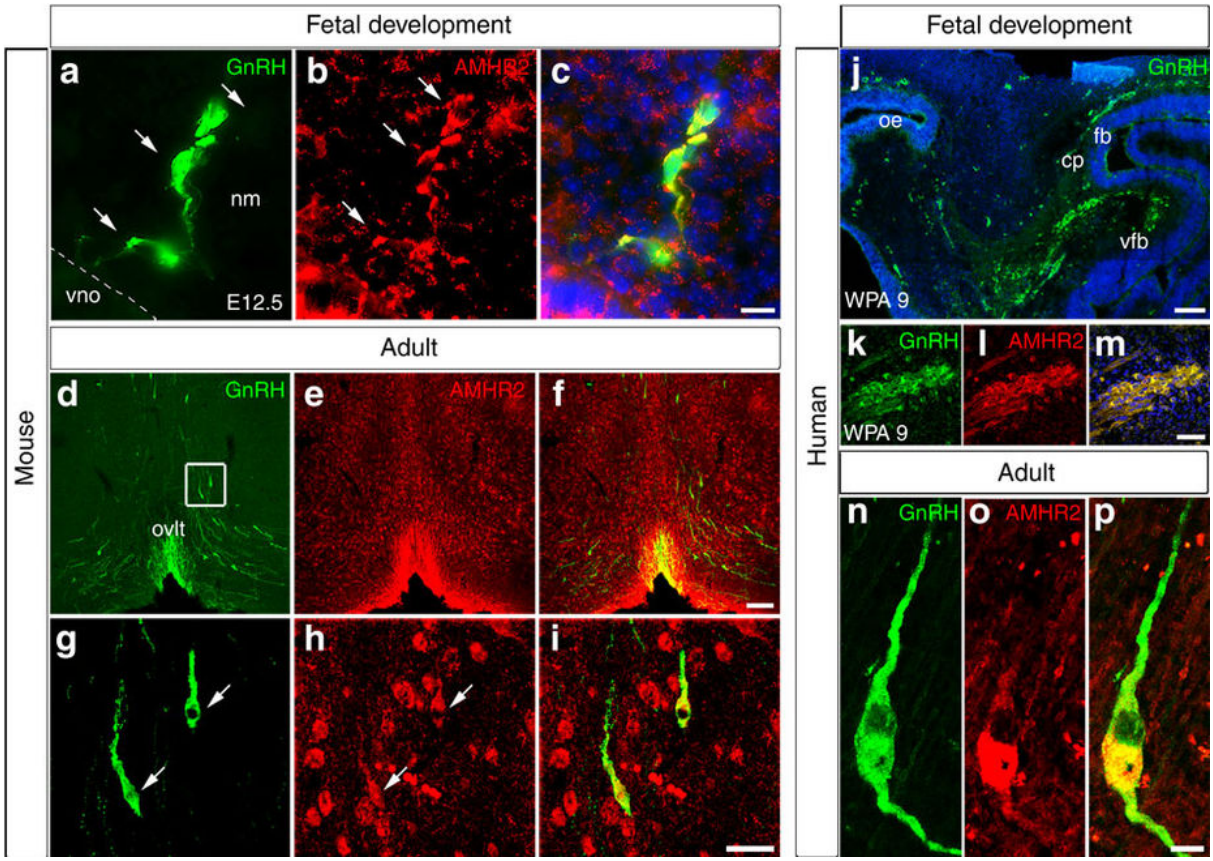

Figure 25 GnRH neurons express AMHR2 throughout life.

(A–C) Confocal images of murine GnRH neurons (green) at E12.5 that express AMHR2. (red) with Hoechst as a nuclear counterstain (blue). (D–I) Images from the adult OVLT showing GnRH and AMHR2 co-localisation. (J–M) Confocal images of a human foetus at 8 gestational weeks stained for GnRH and AMHR2. (N–P) Images from an adult human showing GnRH neurons also express AMHR2 postnatally. Figure taken from Cimino et al., *Nature Neuroscience* 2016

3.4 AMH: From Gene to Protein

The exact chromosome positioning of the *AMH* gene was identified one year after its initial sequencing (Cate et al., 1986) and cDNA cloning (Picard et al., 1986), localised human AMH to 19p13.3 (Cohen–Haguenauer et al., 1987) and the murine *AMH* on chromosome 10 (King et al., 1991). The *AMH* gene is small in size at 2.75 kbp, comprising 5 exons and is enriched with CG base pairs. The human *AMH* gene encodes a 1.8 kbp mRNA that contains a 5 'untranslated part of 10 nucleotides. The polyadenylation signal is present 90 nucleotides after the stop codon (Cate et al., 1986). In the rat, two distinct mRNAs have been described. They differ in the length of their polyA tails (Lee et al., 1992). A 2 kbp mRNA is predominantly present during foetal life at the time of testicular differentiation and decreases in the later stages of gestation, while a 1.8 kbp mRNA appears on day 18 after gestation (P18) and is the most abundantly detected form after this stage (Lee et al., 1992).

3.4.1 Regulation of the *AMH* promoter

As the expression of AMH exhibits a high degree of sexual dimorphism, and a strict temporal regulation of AMH expression is essential for the elaboration of the male and female phenotypes, the factors regulating its transcriptional activity have been studied in some detail. It should first be noted that the *AMH* promotor is located 434bp downstream of the stop codon of *Sap62*, a ubiquitously expressed spliceosome protein (Dresser et al., 1995). While it has been shown that for the initiation of *AMH* transcription, only a proximal region of 370bp is necessary (Beau et al., 2001), its positioning following Sap62 means it resides in a region where the chromatin is "open" and there exists the possibility that postnatal regulation may take place distally, within the *Sap62* gene.

Several direct regulators of the *AMH* promotor have been identified and validated using *in vivo* models. While generally the regulation of *AMH* remains similar between males and females, the absence or active repression of genes initiating male sexual differentiation prevents its prenatal expression in the developing female gonad. Therefore, the most important activators to consider

may be those responsible for initiating expression in the embryonic male gonad, whilst important repressors of *AMH* can be identified in the female embryonic gonad.

It has previously been reported that approximately 370 bp of the *AMH* 5' flanking region is essential for its expression from E12.5 until early postnatal stages in the male mouse (Beau et al., 2001). This region contains one SOX binding site (BS) (De Santa Barbara et al., 1998), two SF-1 BSs (Giuili et al., 1997; Shen et al., 1994), one GATA BS (Vigier et al., 1998) and one WT1 BS (Nachtigal et al.,1998), all of which are highly conserved in eutherian mammals and marsupials (reviewed by Pask et al., 2004).

3.4.1.1 Activators of the AMH Promotor

SRY (Sex determining region on Y) expression initiates the molecular cascades that will result in male differentiation under normal physiological conditions in mammals, and genes that become activated shortly after *SRY* and remain activated through the "critical window" form good candidates that may regulate *AMH* gene activity.

3.4.1.2 SRY (Sex determining region on Y)

In mice, AMH expression is first detected 20h after the initial expression of *SRY* making SRY itself a very logical candidate to regulate *AMH* expression. SRY has been shown to activate a 114bp *AMH* promotor *in vitro*, whilst a mutation in the SRY binding domain abolished AMH expression (Haqq et al., 1994). A mutation of the non-consensus SRY binding site, however, did not alter AMH expression, thereby indicating that the major role of SRY in inducing AMH expression occurs indirectly (Haqq et al., 1994), instead principally occurring through the activation of evolutionarily well conserved downstream activators.

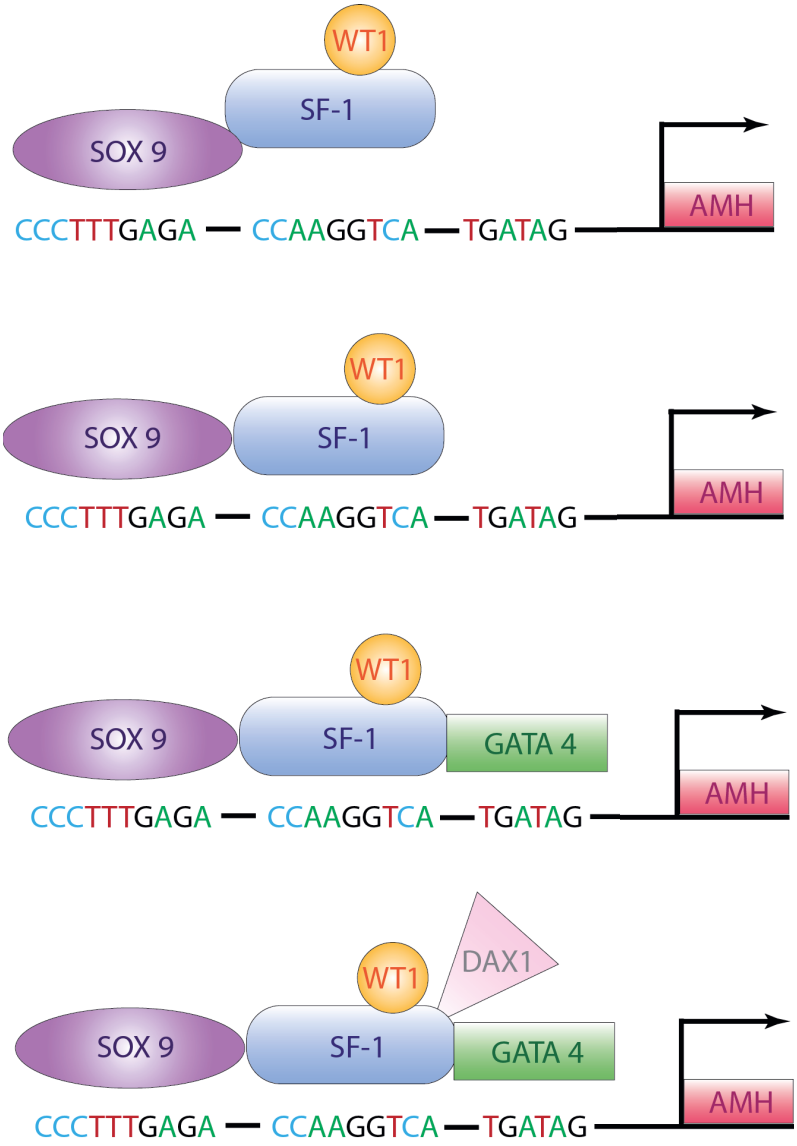

Figure 26. Differential transcriptional regulation of the AMH expression.
SOX9 is able to directly bind to a consensus sequence on the AMH promotor to induce its expression during embryogenesis. SF-1 can bind either directly to the promotor or act synergistically with SOX9. WT1 and DAX1 regulate transcriptional regulation through interactions with SF-1, while GATA4 can directly bind to the GATA sequence found within the promotor.

3.4.1.3 SOX9 (SRY-related homolog box protein 9)

SOX9 expression in the genital ridge occurs at E10.0 in both male and female embryos. Following SRY peak expression at E11.5, SOX9 is upregulated in the embryonic male gonad and falls to undetectable levels in the female gonad (Kent et al., 1996; Morais da Silva et al., 1996). It is this rise in SOX9 expression that induces AMH expression in Sertoli cells and initiate

male gonadal development. Humans with heterozygous null mutations for SOX9 develop campomelic dysplasia, a lethal bone malformation (Foster et al., 1994), although of note, approximately 75% of male SOX9 heterozygotes also showed sex reversal (Mansour et al., 1995). Arango and colleagues (1998) demonstrated that the SOX9 BS is the most critical region for determining AMH expression; intimating that SOX9 is therefore both necessary and sufficient for male sex determination in both mice and humans.

SOX9 has been shown to regulate *AMH* expression in prenatal Sertoli cells, whilst it is not expressed in adult granulosa cells (two well-known tissue types that secrete AMH). This is likely caused by the WNT / β-catenin pathway inhibiting the expression of SOX9 and hence AMH in the female gonad (Bernard et al., 2012). Indeed, β-catenin may prevent the binding of SF-1 to the *SOX9* enhancer region and thus the differentiation of Sertoli cells. Additionally, activation of this route in undifferentiated male gonads of mice (E11.5) induces sexual reversion. Rspo1 [R-spondin homolog (*xenopus laevis*)], Wnt4 (wingless-type MMTV integration site family member 4) and Foxl2 (forkhead box L2) pathways are all activated at E11.5-12.5 in the ovary and converge to repress the expression of SOX9 and subsequent male differentiation.

Of note, SOX9 belongs to the SOXE family of transcription factors, all of which are expressed by the testes during mammalian testes differentiation (Schepers et al., 2002; Schepers et al., 2003). *In vitro* studies have shown that other SOXE family members (SOX8 and SOX10) can activate the *AMH* promotor similarly to SOX9 – coupled to SF-1 and acting via TESCO [TES (testis-specific enhancer of SOX9) COre] (Polanco et al., 2009; Schepers et al., 2003). Additionally, overexpression of SOX10 causes sex reversal in female mice (Polanco et al., 2009), and its duplication on human chromosome 22q13 causes 46XX testicular disorders of sexual development (Aleck et al., 1999).

Taken together, these data suggest that SOXE family members can act to regulate male-female gonadal differentiation via AMH, and especially SOX9 activation results in AMH activation even in mammals where no Y chromosome is present (Otake et al., 2016).

3.4.1.4 SF-1 (Steroidogenic factor 1)

In mice, SF-1 expression is initiated in the genital ridges beginning at E9 (Luo et al., 1994); as sexual differentiation commences, SF-1 is upregulated in the foetal testes and downregulated in the ovaries, suggesting it may play a role in regulating *AMH* activity. The *AMH* promotor contains a conserved 20 bp motif (MIS-RE-1) that is capable of binding SF-1 *in vitro* (Arango et al., 1999), and SF-1 is required for the upregulation of *AMH* transcription but not essential for Müllerian duct regression (Arango et al., 1999). This was determined as mutations in the SF-1 binding site caused dramatic decreases in *AMH* transcript levels, yet the regression of the Müllerian duct system proceeded to completion. It was only when mutated and null alleles were combined, pushing AMH levels past a critical threshold, that Müllerian structures furthest from the testes were retained (Arango et al., 1999). That Müllerian duct regression occurred even when *AMH* transcript levels were so heavily reduced by mutation of SF-1 binding sites, which suggests that AMH levels during the sexual dimorphic window are significantly in excess of what is required for Müllerian ducts regression. SF-1 has been shown to act synergistically with other well-known activators of AMH to promote its expression including SOX9, WT1 and GATA4. SF-1 may therefore be important in regulating AMH levels in order to facilitate actions on non-Müllerian structures, or to regulate AMH levels postnatally.

3.4.1.5 GATA4

GATA4 is a member of the GATA nucleotide binding family of zinc finger transcription factors, named for the DNA consensus sequence it binds. GATA4 is expression has been characterised in both prenatal Sertoli cells and ovarian granulosa cells and has been shown to transactivate the AMH promotor in granulosa cells (Anttonen et al., 2003), a process that is negatively regulated by FOG2 (friend of GATA2). The presence of at least one GATA BS in the AMH promotor suggests that GATA4 may regulate AMH expression by direct DNA binding (Vigier et al., 1998) or in co-operation with SF-1 (Tremblay et al., 1999).

3.4.1.6 WT1 (Wilms' tumour suppressor-1)

WT1 is a transcription factor that contains four zinc finger motifs and a DNA binding domain that is essential for normal development of the urogenital system. In fact, synergistic actions of both SF-1 and WT1 are necessary for the formation of the gonads (Kreidberg et al., 1993; Luo et al., 1994). *In vitro*, a specific isoform of WT1 has been reported to physically interact with SF-1 to synergistically activate the *AMH* promotor through the SF-1 binding site (Nachtigal et al., 1998).

3.4.2 Repressors of the AMH Promotor

3.4.2.1 Dax1 (Dosage-sensitive sex reversal, adrenal hypoplasia critical region, on chromosome X, gene1)

DAX1 overexpression causes sex reversal of male mice with a weakened SRY allele, the *Poschiavinus* mouse (Swain et al., 1998), hence why it received the first part of its name. These results were unable to be replicated on other strains however, indicating its dose sensitivity. Genetic ablation of DAX1 was difficult to accomplish as it is important for embryonic stem cell pluripotency (Niakan et al, 2006). While DAX1 overexpression can cause sex reversal in males, Dax1 knockout results in normal ovarian development (Yu et al., 1998), intimating its actions are to repress male gonadal characteristics rather than promote female gonadal development.

DAX1 mRNA expression begins at E10.5 in the urogenital ridge (Swain et al., 1996). By E12.5 the expression is sexually dimorphic in the developing gonads, being present in the ovaries and extinguished in the testes where it acts as a dominant-negative regulator of SF-1 (Burris et al., 1995; Clipsham & McCabe, 2003). DAX1 has been shown to recruit the nuclear receptor co-repressor of SF-1 (Crawford et al., 1998), while also being shown to interact with SF-1 through its LXXLL motifs before translocating to the nucleus (Kawajiri et al., 2003). SF-1 stimulates the DAX1 promotor *in vitro* (Verrijn et al., 2007) indicating local feedback mechanisms regulate their expression.

Mutations in *DAX1* have been implicated both in X-linked congenital adrenal hypoplasia and CHH (Tabarin et al., 2000; Jadhav et al., 2012). The underlying cause of CHH in Dax1 mutated patients is seemingly complex, with DAX1 expression typically found at all levels of the HPG axis, and therefore unmasking the exact cause of the phenotype may be masked by abnormalities in multiple levels of the reproductive axis.

3.5 Synthesis of mature AMH

The *AMH* gene encodes a pre-proprotein of 560 amino acids in humans. It has a C-terminal domain carrying biological activity and an N-terminal domain that is purported to be devoid of intrinsic activity. The C-terminal portion of 149 amino acids is highly conserved between species and shares >30% homology with other growth factors of the TGFβ family. Following removal of the first 24 amino acids during synthesis, AMH is recognisable as a 140 kDa glycoprotein, composed of two monomers of 70 kDa, stabilised by disulfide bridges (Picard and Josso 1984). Like many molecules of the TGFβ superfamily, AMH must then be cleaved into two N and C terminal dimers to acquire its biological function. The cleavage of AMH gives rise to a 110 kDa N-terminal homodimer formed by two 57 kDa subunits and a 25 kDa active C homodimer composed of two identical 12.5 kDa subunits. The non-covalent complex and pro-hormone are the two forms predominantly found in the blood of humans (Pankhurst & McLennan, 2013).

It has been shown that the N-terminal portion of the protein, although having no intrinsic activity, has the role of amplifying the activity of the C-terminus (Wilson et al., 1993), with only the biologically active C-terminus region required to cause regression of the Müllerian ducts (Wilson et al., 1993).

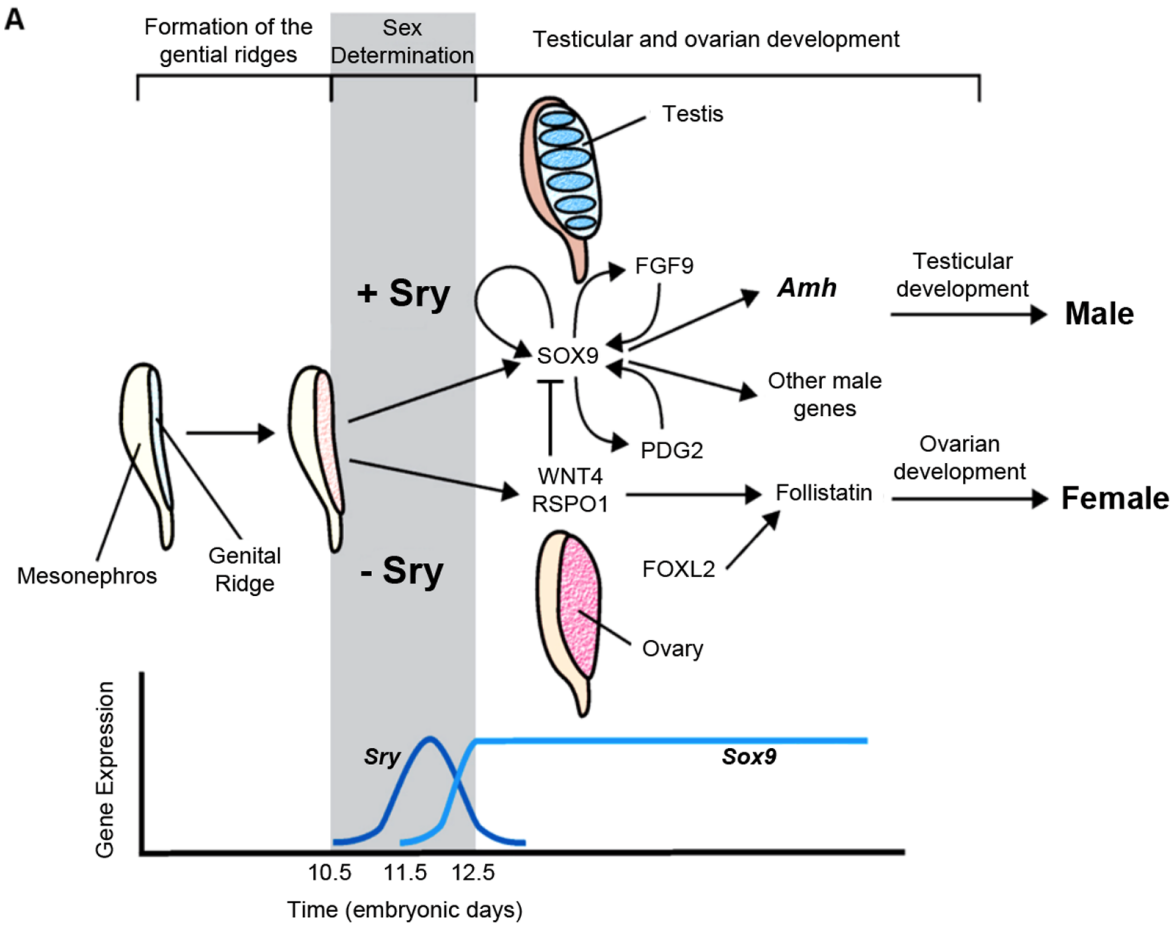

Figure 27. Molecular timing of the critical window of sexual determination in mice. Sexual differentiation of the gonads relies on the precise activation of a signalling cascade that involves numerous genes. Following the appearance of the bipotential gonad at E10.5, the expression of SRY (sex determining region on Y) reaches a peak at E11.5. A few hours later, SOX9 transcription becomes activated in the testis, reaching peak expression between E12 and E13.5. SOX9 is one of the key regulators of AMH expression that initiates the regression of the Müllerian duct. Outside of this critical window, the embryonic gonads become hormonally insensitive and regression of one pair of ducts cannot be initiated. Adapted from Kashimada & Koopman 2010

As determined experimentally *in vitro*, recombinant AMH can be cleaved by plasmin (Pepinsky et al., 1988). However, *in vivo*, the enzymes capable of cleaving AMH remain largely unknown. Although the site of cleavage to form the bio-active AMH is currently unknown, subtilisin/kexin-like proprotein convertases are thought to be responsible for AMH cleavage and studies have shown that furin and prohormone convertase (PC5), two such endoproteases,

were co-expressed with AMH in the embryonic rat testicle (Nachtigal and Ingraham 1996). Additionally, only PC5 is capable of cleaving this hormone after co-transfection into mammalian cells. It is also noteworthy that these convertases have been shown to be expressed by neurons (Cain et al., 2003).

These results primarily suggest that AMH is cleaved at its site of secretion. However, other experiments showed that only 5-15% cleaved AMH was present in the serum and incubation medium of the calf testes. This assumes a potential cleavage at the site of action of the hormone rather than at the level of the producing cells (Nachtigal and Ingraham 1996).

The circulating levels of several members of the TGFβ family are regulated by their interaction with binding proteins (e.g. activins and follistatins). A recent doctoral thesis sought to identify whether AMH levels were also regulated by binding proteins, and thereby also provide some clues as to its site of cleavage (Kawagishi, 2015; Kawagishi et al., 2017). The follistatins had the greatest effect on AMH signalling [detected by (BRE)2-Luc reporter assay in P19 cells], however, the effect was only found at low AMH concentrations, comparable to adult circulating levels (Kawagishi et al., 2017). Several binding proteins were shown to have a small effect on sub EC_{50} concentrations of the AMH C-terminal induced signalling, including brorin and decorin, indicating that AMH cleavage most likely occurs at its site of action.

In 2010, the team of di Clemente and Cate proposed that cleavage occurs following the interaction of AMH with its receptor AMHR2 (di Clemente et al., 2010). Following its pre-cleavage, the N and C-terminal portions of the AMH remain associated by non-covalent bonds and bind to AMHR2 in this form. Binding to the receptor induces dissociation of the N-terminal pro-region and makes it possible to generate the mature ligand capable of bioactive signalling.

AMH clearance from the blood has been determined in humans by ELISA of female patients before undergoing combined hysterectomy and bilateral salpingo-oophorectomy, and on consecutive days following the surgery (Griesinger et al., 2012). The half-life of AMH was

calculated as 27.6 ± 0.8 hours, with 95% clearance after 5 days and AMH levels were undetectable at 8 days post-surgery. As is current clinical convention, concentrations assumed a molecular weight of 140kDa for quantitating blood AMH.

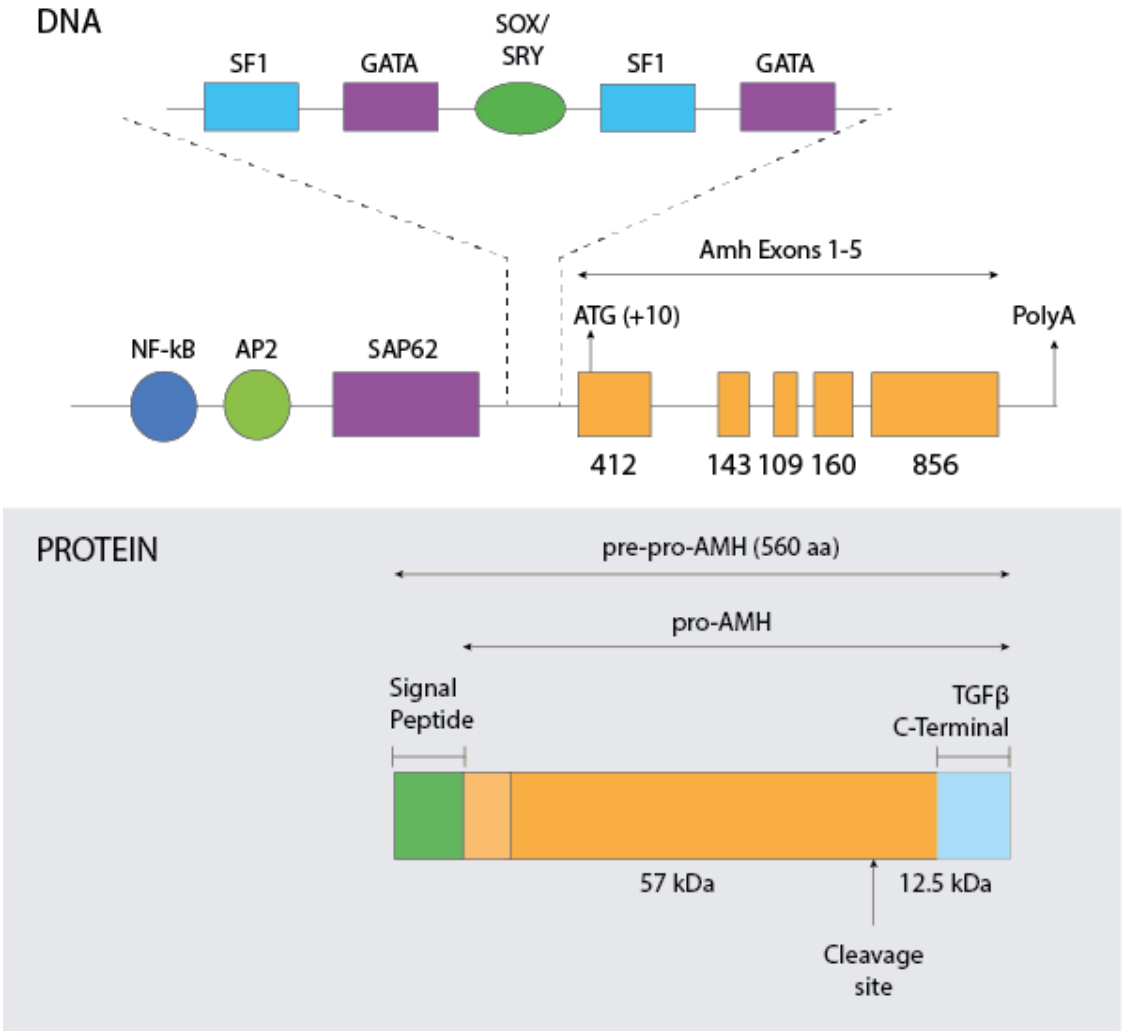

Figure 28. Synthesis of AMH precursors from the AMH gene.

Structure of the AMH gene indicating the positioning of exons and introns. The promotor sequence with the positioning of consensus sites for regulators of AMH expression are also shown in the expanded box. Structure of the AMH protein. Formation of mature AMH requires proteolytic cleavage from a pre-pro-hormone to form the mature form that is detectable within the blood. Figure made by Malone SA

3.6 AMH signalling

3.6.1 Transforming Growth Factor-β (TGFβ) Family

AMH is a divergent member of the TGFβ superfamily, a group consisting of over 30 protein signalling molecules. The biological importance of the TGFβ family extends to a wide variety of physiological processes including: development (e.g. cytoskeletal organisation and migration), proliferation and cellular differentiation (Watabe & Miyazono, 2009; reviewed by Weiss & Attisano, 2013) and includes activins, TGFβs, nodals, bone morphogenic proteins (BMPs) or growth and differentiation factors (GDFs). TGFβ family members signal through a heteromeric complex of transmembrane serine-threonine kinase receptors that requires the association of two different types of receptor class. In vertebrates, there exist ligand binding receptors (type II) that typically recruit type I receptors that possess the ability to confer signal transduction (Moustakas & Heldin, 2009). More specifically, it has been shown that TGFβs signal through a dimerised ligand and an activated complex comprised of two type II receptors and two type I receptors, although there exist diverse molecular mechanisms through which this may be brought about (reviewed by Schmierer & Hill, 2007). Once the active complex is brought about, the type II receptor kinase, which is constitutively active, phosphorylates the intracellular GlySer domain of the type I receptor, thus activating its kinase activity and resulting in the phosphorylation of SMAD proteins that are associated with type I receptors.

In vertebrates, all members of the TGFβ family share the use of just 7 type I receptors, whilst the 5 type II receptors may either be specific for several or just one single ligand. Therefore, understanding the molecular basis for the diverse activities of these multifunctional factors is complex, as in addition to the promiscuity of the receptor complexes, the intracellular responses are both developmental, and cell-context dependent.

AMH has been shown to bind exclusively to one type II receptor, AMHR2, whilst no other ligand has been shown to have effective binding to it (Mishina et al., 1996). AMHR2 has been

shown to interact with three type I receptors of the Activin like kinase (ALK) family – AcvR1 (Activin receptor 1: ALK2), BMPR1a (Bone morphogenic protein receptor 1A: ALK3) and BMPR1b (Bone morphogenic protein receptor 1B: ALK6). All three type I receptors activate the canonical SMAD 1/5/8(9) pathway (See **Figure 31**)

Type I Receptor	Alternative names	Ligands	Examples of regulatory roles
TsR1	ALK1	TGFβ1, 2, 3 Activins BMP-9, 10	Proliferation and differentiation of endothelial cells Activation of angiogenesis
AcvR1	ALK2, SkR1, ACTR1A	**AMH** Actvins BMP-6, 7, 9 TGFβ	Müllerian duct regression Heart morphology Promotes chondrocyte differentiation Embryonic patterning
BMPR1a	ALK3, Brk1	**AMH** BMP-2, 4, 5, 6, 7, 10 GDF5, 6, 9	Müllerian duct regression Embryonic patterning Osteoblast differentiation Heart morphology Chondrocyte differentiation
AcvR1b	ALK4, SkR2, ActR1b	Activins Nodal Myostatin	Embryonic patterning Hear morphology Inhibits adenohypophyseal proliferation Inflammatory response
TβR1	ALK5	TGFβs GDF9 Myostatin	Regulates extracellular matrix Thyroid function Cellular apoptosis Cellular migration and invasion
BMPR1b	ALK6	**AMH** BMP-2, 4-7, 10, 15 GDF5, 6, 9	Folliculogenesis and ovulation Appendicular skeletal development Diffeerentiation of osteoblasts Postnatal bone formation
AcvR1c	ALK7	Activins Nodal	Embryonic patterning Decreases cell proliferation Increases cell apoptosis

Table 2. Type I TGFβ receptor ligands and known functions
adapted from Sedes L, 2014

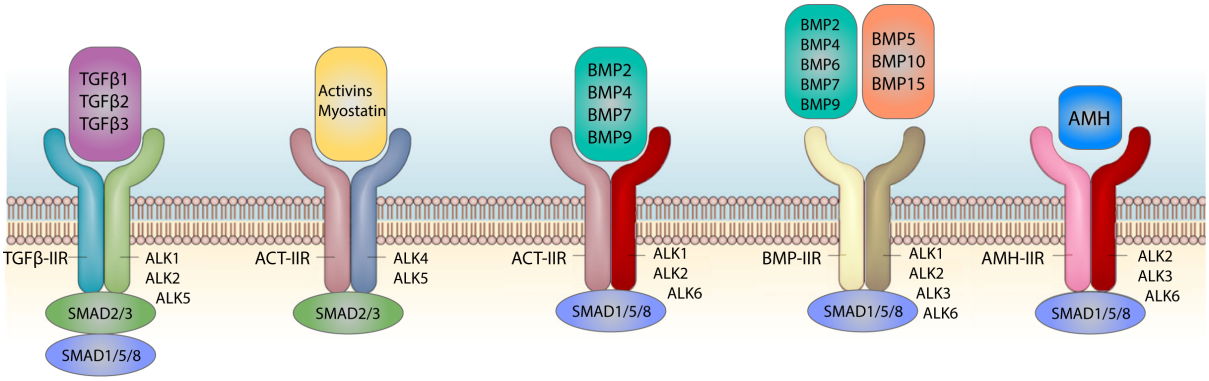

Figure 29. TGFβ family members and their cognate receptors.

A schematic illustrating the complex overlapping of ligand–receptor combinations that can occur in TGFβ family signalling. Each type II ligand binding receptor can dimerise with multiple shared type I receptors in order to induce intracellular signalling pathways. AMH is the only known ligand of AMHR2 and its signalling requires dimerisation with one of three type I receptors, each of these type I receptors is shared with every member of the superfamily with the exception of the true TGFβs. Figure made by Malone SA.

3.7 AMH Receptors

AMH is suspected to only have one ligand binding receptor (Visser, 2003) as $AMH^{-/-}$ mice are a phenocopy of $AMHR2^{-/-}$ mice (Mishina et al., 1996). As AMH is essential to the regression of the Müllerian ducts,

As indicated in **Figure 29**, AMH is not the only member of the TGFβ family that signals through a combination of AcvR1, BMPR1a and BMPR1b. BMP7 shares all three co–receptors and is already known to share several similar roles with AMH, including as neuronal survival factors (Yabe et al., 2002; Wang et al., 2005) and regulators of bone development (Adams, 2012). While the already known actions of the type I receptors can provide clues about potential roles of AMH signalling, the widespread expression of type I receptors and the cell type dependent context of type II receptor expression mean some caution should be urged when proposing novel roles for AMH. AMH is, however, the only known ligand for AMHR2 and therefore AMHR2 expression in tissues necessitates a specific role for AMH signalling within the tissue.

3.7.1 AMHR2

AMHR2 was cloned in 1994 by two independent groups (di Clemente et al 1994; Baarends et al., 1994) using both a rabbit ovarian and rat testis library. The specificity of the target was confirmed by its expression pattern *in vivo* and its ability to bind iodinated AMH when expressed in COS cells (di Clemente et al., 1994). Finally, its biological relevance was confirmed by the detection of a mutation in a patient affected by persistent Müllerian duct syndrome (PMDS – discussed in greater detail in Section 3.2.3) (Imbeaud et al., 1995).

The *AMHR2* gene is located on human chromosome 12 and chromosome 15 in mice, with the *AMHR2* mRNA encoding an 82 kDa protein totalling 573 amino acids. The genetic sequence encodes 11 exons, exons 1–3 encode the extracellular domain, exon 4 the transmembrane domain and exons 5–11 encode the intracellular domain.

Little is currently known about the regulation of the *AMHR2* promotor, although SP1, SOX, SF-1 and GATA sites have all been identified on the promoter of *AMHR2*, suggesting similar regulatory mechanisms to those of AMH itself (Josso and di Clemente 2003). One study noted overlapping expression of WT1 and AMHR2 during Müllerian duct regression, and demonstrated that WT1 binds the *AMHR2* promotor *in vitro* (Klattig et al., 2007). This notion is supported by the absence of AMHR2 expression in the urogenital ridge of $Wt1^{-/-}$ mice.

The K_D (dissociation constant) of AMHR2 for AMH is 2–3 nM (Imbeaud et al., 1995; Salhi et al., 2004), which is within the physiological range of AMH found in the gonads ~ 7nM (Anderson et al., 2010). Circulating AMH levels in adults are much lower; however (in the range of low Picomolar concentrations), suggesting that circulating AMH should only produce trace or minimal receptor activation although this is clearly not the case (Wang et al., 2005; Wang et al., 2009). Alternative splicing of the *AMHR2* gene has been described in rabbit (di Clemente et al., 1994) with the resulting isoform lacking exon 2, although this isoform was originally described as non-functional (di Clemente et al., 1994; Imbeaud et al 1995). More recently the idea of this isoform contributing as a dominant-negative alternative splice variant has been proposed, along with an isoform lacking exon 8 or 9 (Imhoff et al., 2013). The splice

variants were found in both mice and rats, with the proportion of total *AMHR2* mRNA represented by these two isoforms estimated at under 5%. Further work is required to better elucidate their physiological roles.

The mechanism through which AMH interacts with AMHR2 is likely distinct from other members of the TGFβ family (di Clemente et al., 2010). It has been proposed that cleavage of full-length AMH results in a conformational change in the C-terminal domain which facilitates receptor binding (**Figure 30**). Binding of AMHR2 induces the dissociation of the pro-region via a negative allosteric interaction between the receptor- and pro-region-binding sites on the C-terminal dimer. It is currently unknown whether pro-region dissociation occurs before engagement with AMHR2 but it is unlikely that free C-terminal AMH exists as it tends to aggregate at neutral pH. This mechanism is also supported by previous reports that the purified C-terminal dimer is less biologically active by a factor of 10 compared to cleaved AMH, with full activity restored by re-addition of the pro-region which forms a complex with the C-terminal dimer (Wilson et al., 1993).

Prenatally, AMHR2 expression has been well characterised in the mesoepithelial cells of the Müllerian ducts, foetal lungs (Catlin et al., 1990; Catlin et al., 1997) and embryonic motor neurons (Wang et al., 2005). Additionally, the utilisation of the $AMHR2^{+/Cre}LacZ^{+}$ mouse at E18 identified widespread β-gal staining, in the: lungs, spinal cord, peripheral ganglia, brain, testes and all epithelial tissues, amongst others (Adams, 2012). One caveat that is important to consider when interpreting these results, is, in this model the endogenous activity of the *AMHR2* gene promotor drives the expression of the Cre recombinase enzyme (excising the stop codon that interrupts the expression of LacZ), and once activation has occurred, the LacZ gene cannot be inactivated. Therefore, the staining that is seen at any given point in time may not be a true reflection of the expression of the AMHR2 protein, rather indicating that the cells (or their mothers) once had an activated *AMHR2* promotor.

Postnatal expression of AMHR2 has been shown in the endometrium (Wang et al., 2009), breast (Segev et al., 2001), prostate (Hoshiya et al., 2003), cervix (Barbie et al., 2003), neurons (Lebeurrier et al., 2009) and the gonads of both sexes (reviewed by Texeira et al., 2001).

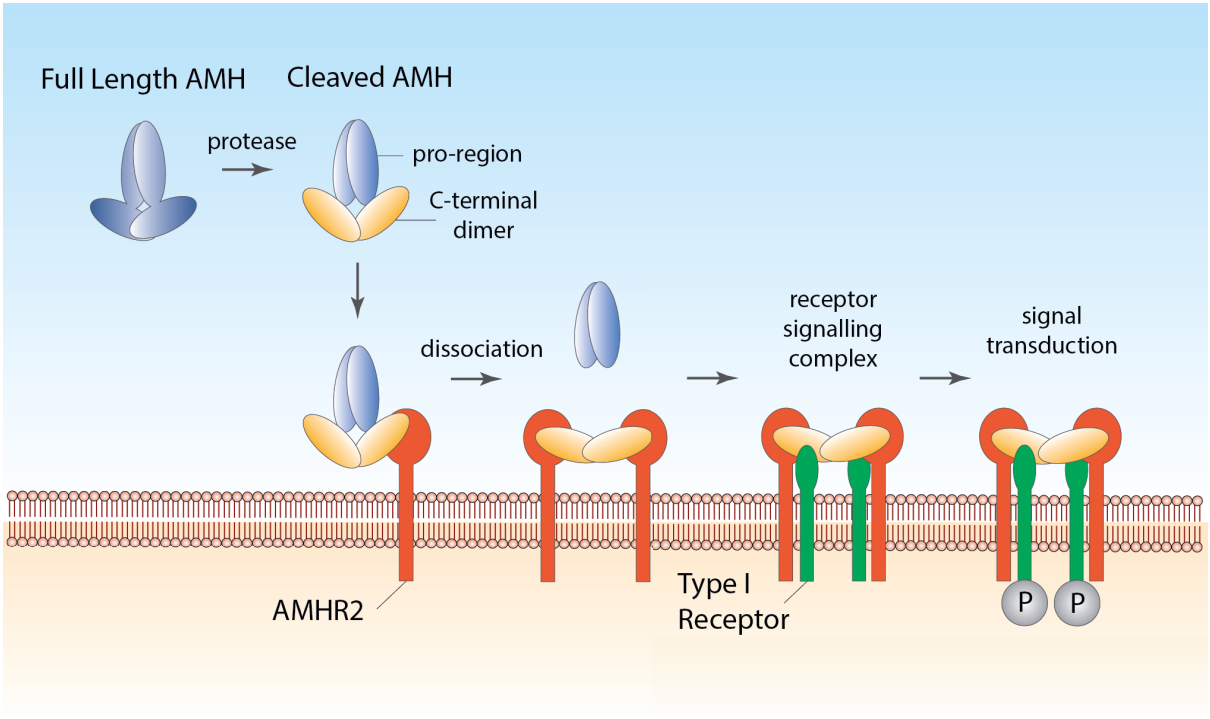

Figure 30. Proposed model of AMH–AMHR2 signalling.

The exact mechanism of AMH interaction with its cognate receptor is currently unknown. As circulating AMH requires cleavage to liberate the biologically active C–terminal and the N,C–terminal complex has been shown to more effectively bind AMHR2 compared to the C–terminal alone, the lab of Nathalie de Clemente have proposed this model of ligand–receptor interaction. Local cleavage of AMH from the circulating homodimer to an N,C–terminal complex occurs before the complex binds to AMHR2. Once bound, the receptor can dimerise with a further AMHR2 molecule and dissociate the N and C terminals of AMH. This causes recruitment of one pair of type I receptors, with the interaction of the tetrameric receptor complex activating intracellular signalling pathways. Figure adapted from di Clemente et al., 2010.

3.7.2 Activin Receptor 1 (AcvR1/ALK2)

AcvR1 has been shown to be the only TGFβ type I receptor that interacts with AMHR2 in P19 cells (an embryonic carcinoma derived cell line), and transduces its signal through SMAD1 (Clarke et al., 2001). In overexpression systems, AcvR1 has been shown to activate SMAD1, SMAD5 and SMAD8 (Chen et al., 1997).

AcvR1 expression is observed in male rat embryos at E15.5 in the mesenchyme of the Müllerian duct, overlapping the expression pattern of AMHR2 (Clarke et al., 2001; Tsuji et al., 1992). The same expression pattern was also confirmed embryonically in mouse, with expression of AcvR1 also found in the mature gonads of both sexes (Visser et al., 2001). Whole body knockout of AcvR1 results in embryonic lethality before E9.5 (Mishina et al., 1999), however, conditional removal of AcvR1 in the Müllerian duct mesenchyme using the *AMHR2::Cre* mouse have been generated. Male *AMHR2::Cre; AcvR1*$^{-/-}$ mice showed proper regression of the Müllerian duct in 100% of cases studied (Orvis et al., 2008). In order to achieve Müllerian duct regression in 100% of conditional mutants, inactivation of both AcvR1 and BMPR1a was required suggesting that there may be functional redundancy in the use of type I receptors in this process (Orvis et al., 2008).

Dominant negative or kinase-inactive AcvR1 transfections into P19 cells severely reduced the activation of the Tlx-2 promotor reporter gene in response to bioactive AMH (Visser et al., 2001). This increased activation was only observed with bioactive AMH and was not observed with either conditioned medium or inactive, noncleaveable AMH (AMH-RAGA) confirming the specificity of AMHR2 interaction with AcvR1.

Ex vivo studies of Müllerian duct regression have shown that pre-treatment with an antisense AcvR1 morpholino oligomer partially or fully blocked AMH-induced regression of the Müllerian ducts (Visser et al., 2001).

3.7.3 Bone Morphogenetic Protein Receptor 1a (BMPR1a/ALK3)

BMPR1a is expressed in the Müllerian duct mesenchyme along with AMHR2 and AcvR1, but dominant-negative forms do not block the AMH-stimulated SMAD1/5/8 pathway (Clarke et al., 2001; Gouedard et al., 2000). However, *in vivo* conditional inactivation of BMPR1a using an *AMHR2::Cre* allele resulted in the retention of the Müllerian duct in ~50% of the male mice (Jamin et al., 2002), whilst overexpression of a human *AMH* transgene in BMPR1a conditional mutants, resulted in complete regression of the Müllerian ducts (Jamin et al., 2003).

Another group who employed conditional deletion of BMPR1a using an *AMHR2::Cre* allele specifically removed expression of BMPR1a from the mesenchyme of the Müllerian duct and resulted in ~55% of the mutant males retaining Müllerian ducts, suggesting that BMPR1a is the primary type I receptor involved in mediating Müllerian duct regression *in vivo* (Orvis et al., 2008).

BMPR1a has been shown to transduce AMH signalling by activating the SMAD1 pathway in the SMAT-1 Sertoli cell line (Belville et al., 2005). *Cyp17c*$^{++}$ mice were crossed with *BMPR1a*$^{loxp/loxp}$ mice to obtain conditional knockout mice where the *BMPR1a* gene was specifically invalidated in Leydig cells. This deletion altered the synthesis of androgens as well as the maturation and differentiation of Leydig cells (Wu et al., 2012). Since the authors had previously observed phenotypically comparable Leydig cells in *AMH*$^{-/-}$ mice (Wu et al., 2005), they concluded that AMHR2/BMPR1a interactions mediated AMH signalling in Leydig cells.

3.7.4 Bone Morphogenetic Protein Receptor 1b (BMPR1b/ALK6)

Co-immunoprecipitation studies have shown that BMPR1b interacts in a ligand-dependent manner with AMHR2 (Gouédard et al., 2000; reviewed by Josso et al., 2001). AMHR2/BMPR1b interaction has been shown to activate the SMAD1 pathway in both SMAT-1 (derived from immature Sertoli cells by targeted oncogenesis) and MA-10 (derived from a mouse Leydig cell tumour) cell lines (Josso et al., 2001), although it has also been shown to act as a negative regulator of intracellular signalling (Belville et al., 2005).

BMPR1b expression has been shown in both male and female rat embryos at E15.5 in the epithelium of the Müllerian and Wolffian ducts, but not in the mesenchyme surrounding the ducts (Clarke et al., 2001). As AMHR2 expression is predominantly in the mesenchyme surrounding the ducts, this supports data from the male *BMPR1b*$^{-/-}$ mice, that do not exhibit any evidence of Müllerian duct retention (Clarke et al., 2001). The female null mice undergo normal gonadal development, indicating that BMPR1b signalling is not essential for Müllerian duct formation or regression. This is supported by *ex vivo* studies of Müllerian duct regression that have shown that pre-treatment with an antisense BMPR1b morpholino oligomers had no effect on AMH-induced regression of the Müllerian ducts (Visser et al., 2001).

Whilst BMPR1b is undetectable in the embryonic gonads of both sexes, it is readily detectable in the postnatal ovary where it is expressed by oocytes of small antral follicles and granulosa cells of large antral follicles (Yi et al., 2001). In one of the few studies to examine AMH signalling in neurons, Lebeurrier and colleagues (2008) demonstrated that the pro-survival effects of AMH were mediated via BMPR1b by regulating the survival factor neuroserpin.

BMPR1b has also shown to mediate the migration of mesenchymal cell aggregates in chick embryos *in vitro*, possibly by promoting the expression of extracellular matrix proteins (Inai et al., 2007). During *xenopus* embryogenesis BMPR1b is strongly expressed in the brain, and migrating neural crest cells (Schille et al., 2016).

3.8. Intracellular Signalling Pathways

3.8.1 RSMADs

The classical intracellular signalling pathway of the TGFβ family is the SMAD pathway and is a common feature of this superfamily. This is because the type I receptors are able to directly transduce extracellular cues by phosphorylating receptor associated SMAD molecules that subsequently dissociate from the receptor and translocate to the nucleus. Within the SMAD family there are eight distinct SMAD proteins, comprising three functional classes: receptor

regulated SMADs (R-SMAD), co-mediator SMADs (Co-SMAD/ SMAD4) and the inhibitory SMADs (I-SMAD/ SMAD6, 7) (Heldin et al., 1997). R-SMADs (SMAD1, 2, 3, 5 and 8/9) remain directly associated with type I TGFβ receptors and are directly phosphorylated by the kinase activity of the receptor once activated. These R-SMADs can be further subdivided into the BMP activated SMADs (SMAD1, 5, 8) or TGF-activated SMADs (SMAD2, 3) based on their type I receptor preference.

Once phosphorylated, the SMADs can form a heterotrimeric complex with the Co-SMAD (SMAD4) and translocate to the nucleus. The I-SMADs act as competitive inhibitors of SMAD signalling by binding to and sequestering activated type I receptors or R-SMADs, thus preventing signal transduction. I-SMADs are often upregulated by the specific pathways that they inhibit, thus providing a negative feedback mechanism – ensuring that the magnitude and duration of the response correlates with the continuing presence of the extracellular ligand (Nakao et al., 1997). This is also the case with AMH, as 2 hours treatment of Leydig derived immortalised cell lines caused an increase in SMAD6 and SMAD7 activity, with activity peaking at 6 hours (earliest activation detected by Northern analysis was at 90 minutes following AMH treatment) (Clarke et al., 2001).

Accumulation of SMAD complexes within the nucleus results in transcriptional responses to alter gene expression. The simplest of which is direct DNA binding, where SMADs function as transcription activators (Wrana, 2000). This typically occurs via a SMAD binding element (SBE) 5'-GTCT-3 'and its 5'-AGAC-3' complementary sequence within the promotor region. The SBE displays some degree of tolerance however, with substitutions of the second nucleotide of the 5'-GTCT-3' sequence shown not to interfere with SMAD binding (Shi et al., 1998).

Several other mechanisms have been described, however, including binding to other transcription factors through protein-protein interactions, recruitment of transcriptional co-activators or co-repressors, blocking or competing with other transcription factors and finally, increasing the degradation rate of other transcriptional repressors (reviewed by Wrana, 2000).

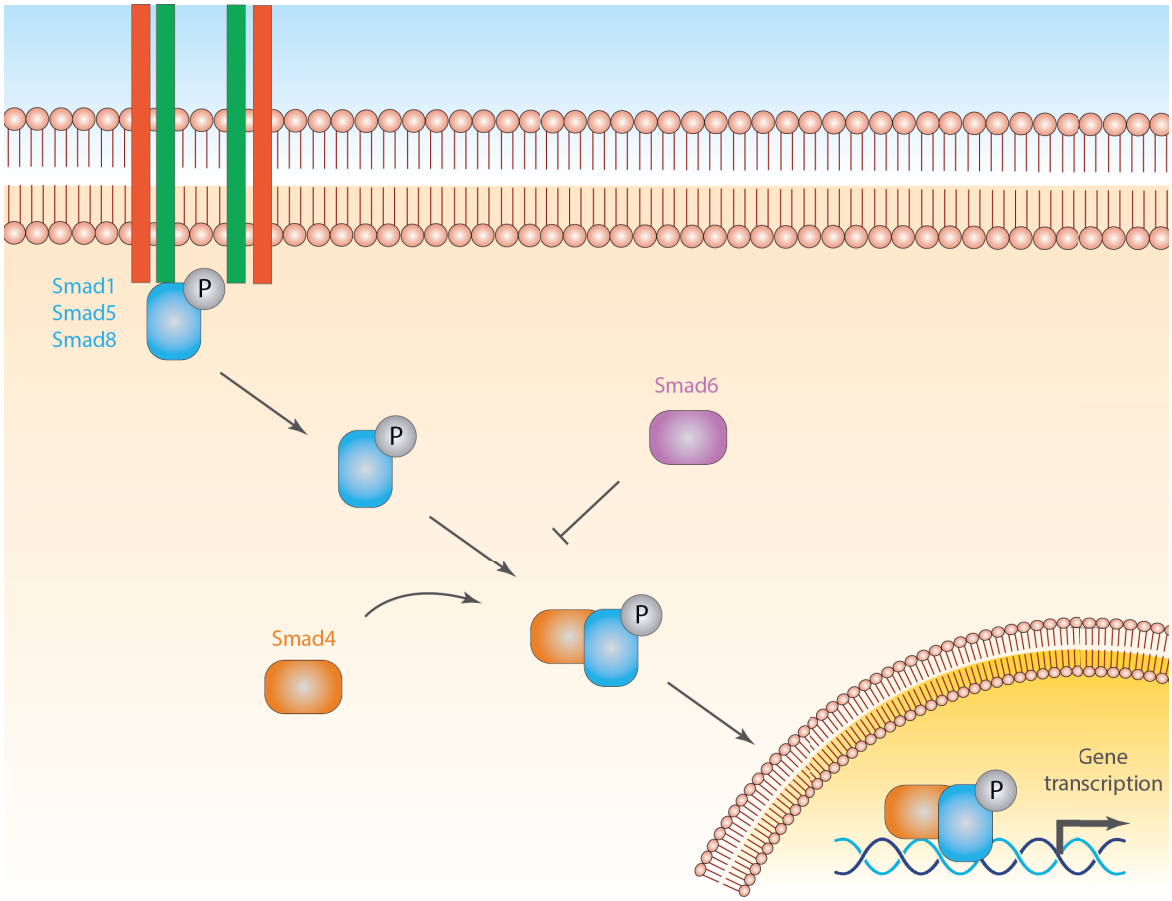

Figure 31. Canonical RSMAD intracellular signalling pathway.
Receptor associated SMADs (SMAD1,5 and 8) are phosphorylated and able to detach from type I TGFβ receptors following recruitment by AMHR2 in response to AMH binding to its receptor. The RSMADs then form heteromeric complexes with SMAD4 and translocate to the nucleus where they primarily function to regulate gene transcription. Figure made by Malone SA.

All three AMH type I receptors share an affinity for the BMP activated SMADs (1/5/8). Knockout studies show embryonic lethality for SMAD1 and SMAD5 but SMAD8 knockout mice are viable and fertile (Chang et al., 1999; Lechleider et al., 2001).

Multiple studies have shown that AMH can activate the traditional SMAD1 pathway using the Tlx-2 (T-cell leukaemia homeobox 2) promotor reporter gene (TLX2-LUX) (Clarke et al., 2001; Visser et al., 2001); a response that is abolished when a kinase inactive AMHR2 was co-transfected or replaced WT AMHR2 (Visser et al., 2001). Overexpression of SMAD5 or

SMAD8 increased the reporter activity in response to AMH stimulation, whilst overexpression of SMAD2 had no effect (Visser et al., 2001). Müllerian duct retention analysis has been performed on conditional inactivation mouse models that inactivated either SMAD1, SMAD5 and SMAD8 alone or in combinations in *AMHR2::Cre* expressing cells (Orvis et al., 2008). The authors showed that each SMAD can activate Müllerian duct regression but to differing degrees. Loss of SMAD1 or SMAD1/SMAD8 had no effect on Müllerian duct regression. Loss of SMAD5 in any combination resulted in a partial retention of Müllerian structures, while only a triple knockdown (SMAD1/5/8) was able to cause complete retention of the Müllerian ducts (Orvis et al., 2008). These results suggest that there exist functional redundancy between the SMADs in regulating AMH mediated effects on the Müllerian ducts.

3.8.2 Non-Canonical Signalling Pathways

While the SMAD intracellular signalling pathway is a ubiquitous feature of TGFβ family signalling, a number of SMAD independent cascades that operate in a context-dependent manner are responsible for number of cell-specific responses. This has been hypothesised to occur as TGFβ receptor complexes have been reported to exhibit dual specificity, phosphorylating tyrosine residues (reviewed by Zhang, 2009). For instance, in epithelial cells, TGFβ has been shown to activate the mitogen-activated protein kinase (MAPK) pathway by inducing the activation of MAPK kinase kinase (MAP3K7) via TRAF6 (Sorrentino et al., 2008; Yamashita et al., 2008). The kinetics of Extracellular signal-regulated kinase (ERK) phosphorylation in response to TGFβ can vary, with peak activation occurring from minutes, to hours after stimulation (Olsson et al., 2001).

The canonical pathway of WNT signalling induces an accumulation of β-catenin in the cytoplasm and its translocation in the nucleus. β-catenin acts as a co-activator of the transcription factors of the TCF / LEF family. In the absence of stimulation by WNT proteins, the majority of the cytoplasmic β-catenin pool is kept inactive by a destruction complex that constitutively phosphorylates the β-catenin which will be targeted by ubiquitin ligase E3 (βTrCP) and earmarked for proteasome degradation (reviewed by Clevers & Nusse, 2012).

In order to study the effect of the absence of WNT4 on the adult ovary, conditional knockout mice were generated. In *AMHR2::cre;Wnt4*$^{loxp/loxp}$ mice, expression of Wnt4 is abolished only in granulosa cells (Boyer et al., 2010). Consistent with WNT4 being a potential signalling target of AMH, the mice were hypofertile with reduced ovarian volume. At 42 days postpartum (P42), mice possessed only few healthy antral follicles, most likely attributed to an increase in follicular atresia and consistent with the early follicular exhaustion of AMH mutant mice lines. Additionally, another WNT, WNT7a is expressed in the Müllerian epithelium and the Wnt7a null male mice exhibit retention of the Müllerian ducts (Parr & McMahon, 1998). This overlap in expression and phenotype suggest a common pathway mediates their effects.

E14 rat urogenital ridges cultured with AMH for 24 hours *ex vivo* showed a cytoplasmic accumulation of β-catenin in peri-Müllerian mesenchymal cells, which was absent in untreated samples (Allard et al., 2000). Subsequent experiments determined the nuclear translocation of β-catenin to be caused by LEF1, and involved in the apoptosis of the mesenchymal layer preceding the epitheliomesenchymal transition that is essential for the regression of the Müllerian duct.

Nuclear factor κ-light-chain-enhancer of activated B cells (NF-κB) is a protein that is part of the superfamily of transcription factors. It has been previously implicated in a wide range of cellular processes including: the immune response, the response to stress, and apoptosis. NF-kB is a cytoplasmic protein composed of two subunits: p50 and p65 (RelA) and is held in an inactive state by binding to the IkB protein. The IKK kinase phosphorylates IkB in response to extracellular signals, permitting the release of NF-kB into the cytoplasm. Liberated NF-kB translocates to the nucleus where it regulates target genes (Gilmore 2006) (**Figure 32**). The Nf-kB pathway can be activated by a variety of extracellular cues, with AMH being just one.

Administration of AMH to mice induces activation of the NF-kB pathway and expression of the Iex1 gene in the mammary gland (Segev et al., 2001) and the prostate (Segev et al. 2001). Similarly, stimulation with AMH has shown that synergistic activation of NF-kB and SMAD1 had anti-proliferative effects in breast cancer cells (Gupta et al., 2007).

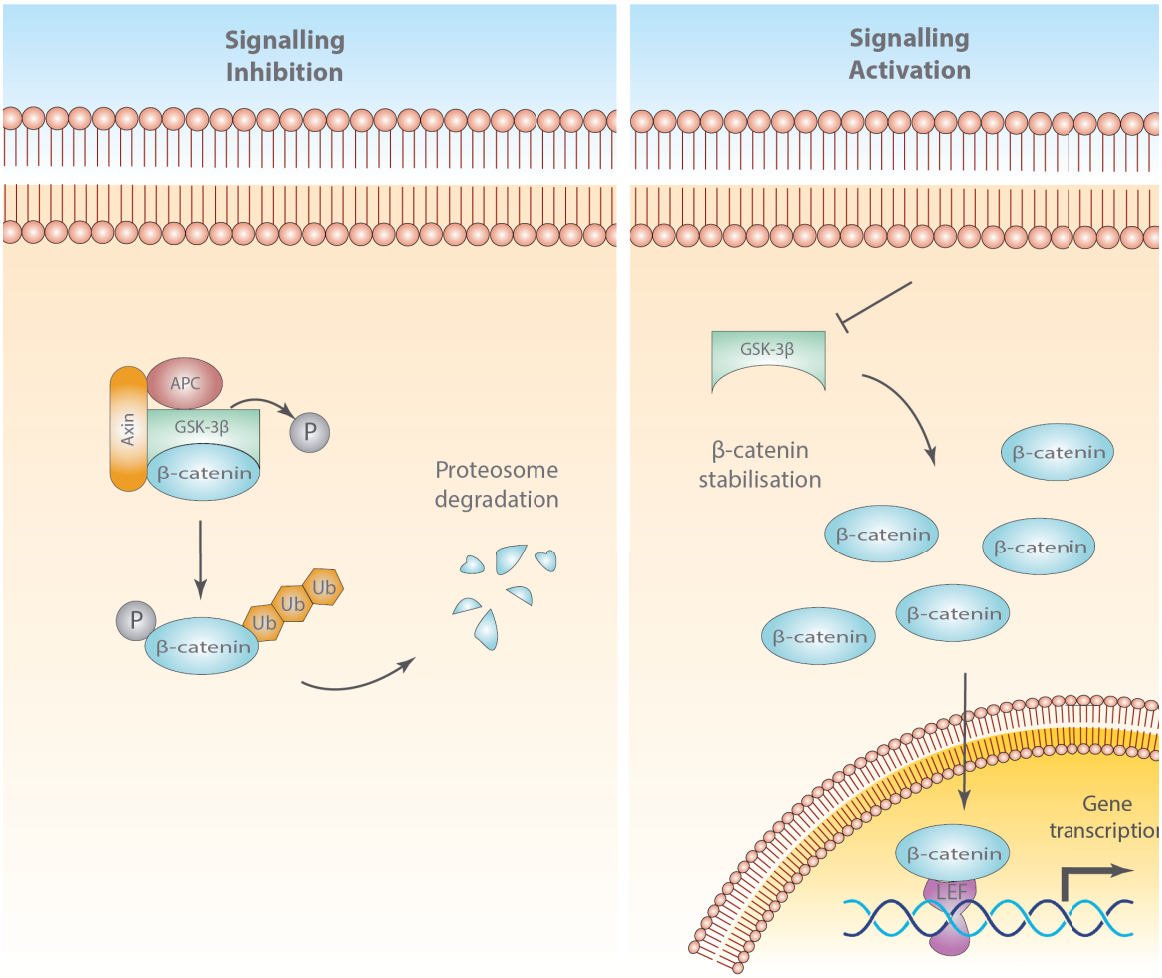

Figure 32. β-catenin intracellular signalling pathway.

β-catenin signalling has been implicated in AMH mediated regression of the Müllerian ducts. β-catenin is constitutively ubiquinated and degraded by the proteasome, however, upon activation of the signalling pathway, ubiquitination is halted and β-catenin can undergo nuclear translocation to regulate gene transcription. Figure made by Malone SA, Figure adapted from Baron & Kneissel, *Nature Medicine* 19, 179-192 (2013)

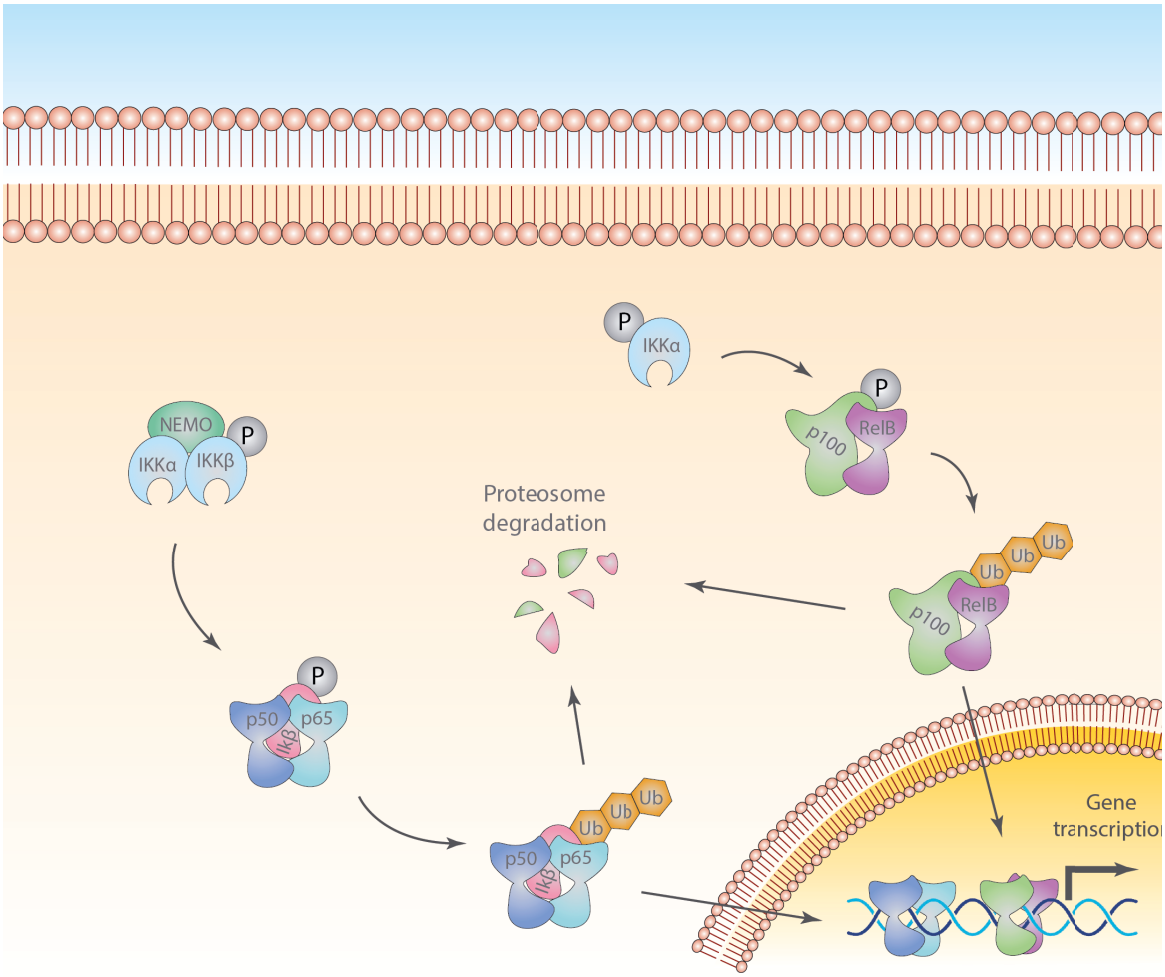

Figure 33. NF−kB intracellular signalling pathway.

NF−kB signalling traditionally mediates cell−survival related functions including apoptosis, immunological and stress responses. The two active forms of NF−kB are held in an inactive complex by the IkB protein and upon activation of the pathway, phosphorylation of IkB results in its dissociation from p50 and p65 which, when liberated, can translocate to the nucleus to regulate gene transcription. Figure adapted by Malone SA from Oeckinghaus et al., *Nature Immunology* 12, 695 – 708 (2011)

CHAPTER 4

Aims & Objectives

4.1 Aims & Objectives

Throughout history, the desire of scientists to understand physiology and disease by thoroughly studying anatomical features, has always faced an intractable limitation: they cannot simply see through the tissue. Dissection has therefore been the modus operandi of anatomists: from Galen's pioneering studies, to modern day biologists who routinely section tissues to label structures for microscopic analysis.

Whilst these methods have informed a wealth of knowledge linking anatomical form to function, they are inherently flawed due to a 3-Dimensional appreciation of structures being lost. This has been especially problematic for the study of developmental processes, where structures are continually evolving, and therefore a precise visualisation has been impossible to achieve through traditional methods and anatomical atlases. Further to this, a majority of our knowledge of developmental systems arises from studies in chicken and zebrafish; which, although excellent models in which to study these processes, may possess significant differences from humans. Coupled with the difficulties in tissue access, our understanding of human development has progressed perhaps the slowest of any biological process since the 1930's; whilst in some cases observations from lower vertebrates have been erroneously applied to humans resulting in stark contradictions in the extant literature.

Without a good understanding of physiological development, we lack the fundamental knowledge required for clinicians and researchers to tackle developmental syndromes that inflict a severe healthcare and emotional burden upon society. Recent advances in non-invasive, *in vivo* imaging techniques, have shown great promise in detecting congenital abnormalities as well as providing information on gross topological features of foetal development; however, they lack sufficient resolution in order to inform developmental biologists of currently unknown features of organogenesis. This has recently been most strikingly highlighted by the surge in Zika virus infections and reports of its detrimental effects on cephalic development.

Another developmental disorder, the infertility syndrome congenital hypogonadotropic hypogonadism, can be caused by a disruption of correct migratory behaviour of GnRH neurons. Although this migratory behaviour was initially described almost 30 years ago, a comprehensive description and anatomical mapping of these cells in human embryology, whether due to sociocultural, religious or moral reasons, remains lacking. Currently, approximately only 50% of clinical CHH cases have explained genetic causes, with the remaining proportion attributed to unknown genetic mutations.

The key aims of this work are therefore to:

- apply recent advances in the field of tissue clearing and whole mount immunostaining to characterise the development of human urogenital and peripheral nervous systems during the first trimester of gestation
- use these techniques in combination with traditional histological methods to provide the first detailed description of GnRH migration in human development and to create a 3D atlas of their spatial distribution during early development
- characterise a potential role of Anti-Müllerian hormone signalling in the development of the GnRH system and its potential contribution to CHH

CHAPTER 5

Materials & Methods

5.1 Human Experiments

5.1.1 Tissue collection and processing

The human gestational period spans the embryonic (first 8 weeks) and foetal stages of development. The 23 Carnegie stages cover mostly the embryonic period (~60 days) and provide a standardised system to characterise developmental age based on the internal and external morphology of the human embryo.

The ages of the embryos in our study were estimated based on the following criteria: 1) the attending physicians' information about the 'menstrual weeks' age of the embryos, generally a fortnight greater than the 'postovulatory age', 2) external morphology of the embryo, 3) embryonic (crown-rump) length. The last two criteria were evaluated using O'Rahilly and Muller's atlas of developmental stages of human embryos (O'Rahilly and Muller, 1999, The Embryonic Human Brain: An Atlas of Developmental Stages. Second edition; New York: Wiley-Liss, John Wiley & Sons, Inc.) and Bossy's study on the development of olfactory structures in human embryos (Bossy, 1980). Human embryos/foetuses were obtained from voluntarily terminated pregnancies with the parent's written informed consent (Gynaecology Hospital Jeanne de Flandre, Lille, France). Tissues were made available in accordance with French bylaw (Good practice concerning the conservation, transformation and transportation of human tissue to be used therapeutically, published on December 29, 1998). Permission to utilise human brain tissues was obtained from the French agency for biomedical research (Agence de la Biomédecine, Saint-Denis la Plaine, France).

Sex determination was obtained by isolating DNA from extracted tissues using lysis buffer containing 0.1mg/ml proteinase K, 5M Sodium Chloride, 20% Sodium dodecyl sulfate, 1M Tris pH 8.0, solution in water and stored at 54° C overnight. DNA was precipitated with isopropanol (1:1) and re-suspended in RNase/DNase-free water for 3h at 65° C. A PCR was performed in a thermocycler (Biorad) using the following steps: 94° C for 3mins and 35 cycles of 94° C for 1min; 56° C for 30s; 72° C for 30s and 72° C for 5min. For genotyping the

following primers were used (Table 3). Only 20 embryos could be assessed, as prior tissue processing prevented DNA extraction for other cases.

Table 3. Human sex determination PCR primers

Sex determination PCR primers	
5'-AGCGATGATTACAGTCCAGC-3'	SRY sense
5'-CCTACAGCTTTGTCCAGTGG-3'	SRY antisense
5'- CGGGAGGGATACAGGACTAAAC-3'	FGF16 sense
5'- CTGTAGGTAGCATCTGTGGC-3'	FGF16 antisense
5'-CAGGCCATGCACAGAGAGAA-3'	SRY2 sense
5'-GGTAAGTGGCCTAGCTGGTG-3'	SRY2 antisense
5'-ACGCATTCATCGTGTGGTCT-3'	SRY3 sense
5'-AACTGCAATTCTTCGGCAGC-3'	SRY3 antisense

Embryos and foetuses were fixed by immersion in 4% PFA at 4° C overnight or for 3-5 days depending on sample size. The tissues were cryoprotected in 30% sucrose/PBS at 4° C overnight, embedded in Tissue-Tek OCT compound (Sakura Finetek, USA), frozen in dry ice and stored at -80° C until sectioning. Frozen samples were cut serially using a Leica CM 3050S cryostat (Leica Biosystems Nussloch GmbH, Germany). The sections were thaw-mounted onto glass slides and then, stored at -80° C until processing. Four series of sections were generated for CS16, five for CS17, CS18 and CS19, and six for older embryos and foetuses. The thickness of the section was 20μm for each sample.

For whole-mount staining and 3DISCO clearing, samples were washed in ice-cold PBS at least 2 times for 20 min. Next, they were fixed by immersion in 4% paraformaldehyde (PFA) at 4° C for 24h for GW 6-8 embryos, 3 days for 9 GW foetuses, and 5 days for GW 10-12 foetuses. After fixation samples were stored at 4° C in 1xPBS containing 0.01% sodium azide until use. The number of embryos/foetuses analysed, the Crown-Rump length referred to these specimens and the type of processing are listed in Table 4.

Table 4. Human samples

Stage (CS or GW)	Number of specimens analysed	Crown rump length (mm)	Experiment
CS 16 (GW 5.5)	1	8	IHC/GnRH cell quantification
CS 17 (GW 6)	2	11–13	IHC/GnRH cell quantification
CS 18 (GW 6)	1	15	IHC/GnRH cell quantification
CS 19 (GW 7)	1	17	IHC/ISH/GnRH cell quantification
CS 23 (GW 8)	2	25–28	IHC/GnRH cell quantification
GW 9	3	29–32	IHC/GnRH cell quantification
GW 10	2	38–40	IHC/GnRH cell quantification
GW 11	2	45–47	IHC/GnRH cell quantification
GW 12	1	50	IHC/GnRH cell quantification
CS 19 (GW 7)	1	18	IHC/3DISCO/LSM
CS 21 (GW 7.5)	1	22	IHC/3DISCO/LSM
GW 9	1	29	IHC/3DISCO/LSM
GW 9	1	31	IHC/iDISCO/LSM
GW 9	2	30	3D Reconstruction
GW 12	2	50–55	3D Reconstruction
Total number	23		

5.1.2 Bleaching

To remove pigmentation and reduce signal-to-noise ratio related to hematomas, the tissue bleaching was carried out (Renier et al., 2014). The samples were dehydrated for 1hr at RT in ascending concentrations of methanol in 1xPBS (50%, 80%, 100%). The samples were then treated overnight at 4° C with a 6% hydrogen peroxide solution in 100% methanol. The

following day, samples were re-hydrated for 1hr at RT in descending concentrations of methanol (100% twice, 80%, 50%) and washed in 1xPBS for 1hr. Samples were kept at 4° C for further processing.

5.1.3 Whole-mount immunostaining

Samples were permeabilised and blocked by rotation at 70 rpm in 1XPBS containing 0.2% gelatin (Prolabo), and 0.5% Triton X-100 (Sigma-Aldrich) (PBSGT) at RT (Belle et al., 2014). For immunostaining, samples were transferred to a solution containing 0.1% saponin (10mg/mL) in PBSGT together with the primary antibodies (**Table 7**) and placed at 37° C (Benchmark, Incu-Shaker Mini), with rotation at 70 rpm, for 7 to 14 days depending on tissue size and density. This was followed by six washes of 30 min in PBSGT at RT. Next, secondary antibodies (**Table 8**) were diluted 1:500 in a solution containing 0.1% saponin (10mg/ml) in PBSGT and passed through a 0.22µm filter. Samples were incubated at 37° C (Benchmark, Incu-Shaker Mini) in the secondary antibody solution overnight or for 2 days depending on sample size and density. After six washes of 30 mins in PBSGT at RT, samples were stored in the dark at 4° C in until tissue clearing. The protocol was similar for single and multiple labelling.

5.1.4 3DISCO

For all tissue clearing, a modified 3DISCO clearing protocol was used. All incubation steps were performed in dark conditions at RT in a fume hood, on a tube rotator (SB3, Stuart) at 14 rpm, using a 15 ml centrifuge tube (TPP, Dutscher). Samples were first dehydrated in ascending concentrations (50%, 80%, and 100%) of tetrahydroflurane (THF; anhydrous, containing 250 ppm butylated hydroxyl-butoluene inhibitor, Sigma-Aldrich) diluted in H_2O. The initial 50% THF wash was performed overnight while the 80% and 100% THF incubations were left for 1h30 each. Samples next underwent a delipidation step of 30 min in dichloromethane (DCM; Sigma-Aldrich) followed by an overnight clearing step in dibenzylether (DBE; Sigma-Aldrich). The next day, samples were stored in individual light-absorbing glass vials (Rotilabo, Roth) at

RT. In these conditions, samples could be stored and imaged for up to 9 months without any significant fluorescence loss.

5.1.5 Methanol clearing

For large tissues, methanol clearing was used to achieve higher transparency using a modification from the iDISCO+ protocol (Renier et al., 2016). Whole embryos (<GW8) and tissues (>GW8) were dehydrated in methanol/1xPBS series (n = 7): 20%, 40%, 60%, 80%, 100% x2 for 1h each at RT on a tube rotator (SB3, Stuart) at 14rpm, using a 15ml centrifuge tube (TPP, Dutscher) covered with aluminium foil to avoid contact with light. Then samples were incubated overnight in 2/3 DCM/ 1/3 Methanol. After 30min in 100% DCM, samples were transferred to DBE.

5.1.6 3D imaging

3D imaging was performed as previously described. Acquisitions were performed by using an ultramicroscope I (LaVision BioTec) with the ImspectorPro software (LaVision BioTec). The light sheet was generated by a laser (wavelength 488, 561 or 640nm, Coherent Sapphire Laser, LaVision BioTec) and focused using two cylindrical lenses. Two adjustable protective lenses were applied for small and large working distances. A binocular stereomicroscope (MXV10, Olympus) with a 2× objective (MVPLAPO, Olympus) was used at different magnifications (0.63x, 1x, 1.25x, 1.6×, 2x, 2.5x, 3.2x, 4×, 5×, and 6.3×). The corresponding zoom factors and numerical apertures are available at http://lavisionbiotec.com/ultramicroscope-ii-specifications.html.

Samples were placed in an imaging reservoir made of 100% quartz (LaVision BioTec) filled with DBE and illuminated from the side by the laser light. A PCO Edge SCMOS CCD camera (2,560 × 2,160 pixel size, LaVision BioTec) was used to acquire images. The step size between each image was fixed at 1 and 2µm. All tiff images were generated in 16-bit. For large samples, a platform was created using PDMS (SYLGARD) fixed to a sample holder from LaVision.

5.1.7 Image processing

Images, 3D volume, and movies were generated using Imaris x64 software (version 8.0.1, Bitplane). Stack images were first converted to Imaris file (.ims) using ImarisFileConverter and 3D reconstruction was performed using the "volume rendering" function. To facilitate image processing, images were converted to an 8-bit format. To obtain opaque visualizations, the normal shading view was applied. Optical slices were obtained using the "orthoslicer" tool. To isolate a specific region of the tissue, the surface tool was used and the mask option was selected. For isolation of smaller structures, i.e. nerve segmentation, the surface tool was manually applied and each nerve was subsequently pseudo-coloured. In order to visualize bone structures in 3D, skin is artificially removed by segmentation and the contrast is modified using normal shading. 3D pictures were generated using the "snapshot" tool.

5.1.8 Immunolabelling

Human tissues were cryosectioned (Leica cryostat) at 20µm. Immunohistochemistry was performed as previously reported (Cimino et al., 2015). Briefly, the sections were thawed at room temperature (RT) and washed in 1x PBS pH 7.4 several times to remove the OCT embedding medium. Sections were blocked in 1x PBS containing 10% normal donkey serum, 0.3% Triton X-100 for 1 hour at RT. They were then washed in 1 x PBS for 5 mins, three times before being incubated with primary antisera overnight at 4° C. After removal from primary antibody, tissues were washed (3 times, 15mins) in 1x PBS and incubated for 1h in secondary antibodies (1:500) at RT. Sections were then washed with 1x PBS several times and incubated with Hoechst (1:10,000) for 5 minutes to provide a nuclear counterstain. Sections were then washed once more in 1x PBS and mounted with Mowiol as an anti-fade agent. The primary and secondary antisera used are detailed in Table 7 and Table 8. The anti-GnRH LR5 was used for whole-body immunostaining of the E16.5 mouse embryo. The other two anti-GnRH antibodies were used for all immunostaining procedures performed on human tissues (sections or intact tissues).

5.1.9 Specificity tests

Two forms of GnRH are present in the human brain. Mammalian GnRH (GnRH-I) regulates the reproductive axis, whereas the function of GnRH-II, originally isolated from the chicken hypothalamus (cGnRH-II) 71, is largely unknown. In order to verify that the migratory GnRH neurons we observed indeed expressed GnRH-I, each antiserum was preadsorbed for 24 hours at 4° C with the mammalian GnRH-I (GeneCust, Luxemburg) at 5μg/ml before application, which completely eliminated GnRH immunoreactivity in the nasal region and brain of CS 18 embryos (**Figure 34**). However, high sequence homology between the GnRH-I and GnRH-II decapeptides (only 3 amino acid substitutions) could allow GnRH-I antibodies to cross-react with GnRH-II. We therefore performed fluorescent in situ hybridization (FISH) experiments using a cRNA probe directed against GnRH-I mRNA (described below), where lack of significant nucleotide sequence homology would rule out the cross-reaction of the GnRH-I probe with GnRH-II mRNA. These experiments confirmed that the migratory GnRH neurons in humans expressed GnRH-I (**Figure 34**).

5.1.10 GnRH cell counting

Serial coronal sections (20μm) from embryos and foetuses were cut and labelled for GnRH as described above. Four serial series were generated for CS16 (n = 1), five serial series were generated for CS17-CS19 (CS17-18, n = 3), six series for older embryos and foetuses were generated (CS19-23, n = 3; GW 9-10, n = 5; GW 11-12, n = 3). GnRH-immunostained sections were examined using an Axio Imager.Z1 ApoTome microscope (Zeiss, Germany), equipped with a motorised stage and an AxioCam Mrm camera (Zeiss, Germany). To visualise and count the cells a Zeiss 20x objective (NA 0.8) was used. GnRH neurons were counted every 80μm spanning the entire head of embryos and foetuses. Total numbers of GnRH cells were calculated in each sample and combined to give group means ± SEM All analyses were performed using Prism 5 (GraphPad Software) and assessed for normality (Shapiro-Wilk test) and variance, when appropriate. Sample sizes were chosen according to the standard practice in the field. Data for GnRH cell number between the four groups analysed (CS17-18, CS19-23,

GW 9–10, GW 11–12) were compared by one-way ANOVA followed by Bonferroni's *post hoc* analysis test.

Total numbers of GnRH cells were also calculated as a function of sex in foetuses aged 7–10 GW (n = 4 males; n = 4 females). Data were compared by a two-tailed unpaired Student's t test. In all statistical tests, the significance level was set at $p < 0.05$.

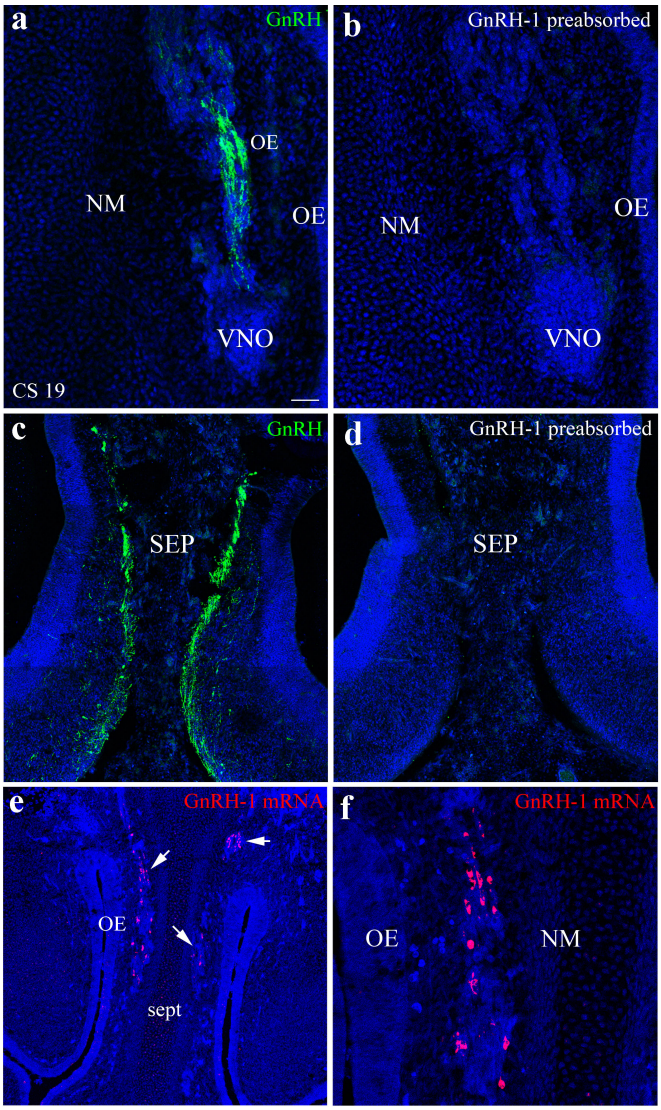

Figure 34. Validation of specificity of GnRH expression in human embryonic head sections.
Representative coronal sections of a CS 19 nose and forebrain. Migratory neurons expressing GnRH mRNA (a–b; fluorescent in situ hybridisation; arrows) or immunoreactive for GnRH (c, e) are shown. (d, f) are adjacent sections of c and e, respectively, incubated with anti-GnRH antibody preabsorbed with GnRH-I peptide. The lack of signal reveals that all GnRH neurons are GnRH-I and not GnRH-II cells. Scale bars: a–b, 50 μm; c–d, 100 μm; e, 80 μm; f, 20 μm.

5.1.11 Image analysis

Confocal images were taken on a confocal microscopy Leica LSM710 with EC Plan NeoFluor 10x/0.3 NA, 20x/0.5 NA and 40x/1.3 NA (Zeiss) objectives (Imaging Core Facility of IFR114 of the University of Lille 2, France).

ImageJ (National Institute of Health, Bethesda, USA) and Photoshop CS6 (Adobe Systems, San Jose, CA) were used to process, apply adjustments and merge the photomontages. For 3D reconstruction, 9 and 12-week-old embryos were serially sagittally sectioned (20µm thick) and immunolabelled with GnRH antibody and counterstained with Hoechst 33342 (1:10,000, Molecular Probes # H3570). To create a 3D reconstruction of the distribution of GnRH neurons in the head of the embryos, 1 in 5 (for 9GW) or 1 in 6 (for 12GW) series of sections were immunostained with GnRH antisera. A subset of these sections, representing an entire hemisphere of the head were manually traced with Neurolucida 7.0 (MBF Bioscience) and aligned using Reconstruct software version 1.1 (Copyright 2004, John C. Fiala, Boston University, Boston, MA; http://tech.groups.yahoo.com/group/reconstruct_users). The nasal region of the GW 9 foetus was sampled with a higher number of sections (mean distance between sections 140 micron) than the caudal part of the brain (mean distance between sections 430 µm). For the GW 12 foetus all sections were spaced 480 µm. 3D models were rendered in Blender 2.7 (www.blender.org).

5.1.12 Fluorescent *in situ* Hybridization (FISH)

Three CS19 whole embryos were fixed by immersion in 4% Paraformaldehyde (PFA), pH 7.4, at 4° C over night. The sections (16µm) were cut on a cryostat, mounted on Superfrost Plus slides (Fisher Scientific, Pittsburgh, PA), and stored at −80° C until processing for hybridization. We employed a fluorescence in situ hybridisation procedure using a digoxigenin-11-UTP (Dig)-labelled GnRH-I cRNA probe transcribed from a rat GnRH-I cDNA, previously published 72. The plasmid vector GST7 containing the 330-bp BamHI/HindIII insert of GnRH-I cDNA was linearised with HindIII for antisense and with BamHI for sense probes. The riboprobes were synthesised in vitro with 1µg linearised GnRH cDNA, 1X digoxigenin

RNA labelling mixture (Roche), RNA polymerase (T7 for antisense and SP6 for sense), and 1x transcription buffer. This mixture was incubated at 37° C (T7) or at 39° C (SP6) for 2h. Residual DNA was digested with deoxyribonuclease. The probes (1µg/µl) were diluted 1:200 with hybridisation buffer.

Following treatment with proteinase K (5µg/ml in Tris 0.1M, EDTA 0.05M, DEPC H_2O, pH 8) and acetic anhydride, the sections were incubated for 2h at room temperature (RT) in pre-hybridisation buffer (50% Formamide, sodium chloride-sodium citrate SSC 5X, Denhardt's solution 1 mg/ml, yeast tRNA 250µg/ml, herrings sperm DNA 500µg/ml, H_2O DEPC) before being hybridised overnight at 60 ° C with Dig-GnRH-I cRNA. The next day, the slides were washed at high stringency (final wash: 0.2X SSC at 60 ° C for 1 h). Thereafter, the sections were incubated for 1 h at RT in blocking buffer containing 0.1M Tris-HCl pH 7.5, 0.15M NaCl, 0.5% blocking reagent (Roche).

Following these blocking steps, the sections were incubated for 45 min at RT with anti-Dig-POD (Roche) diluted in TNT buffer (Tris-HCl 0.1M pH 7.5, NaCl 0.15 M, 0.5% Triton X-100). Then, the sections were washed in TNT buffer (three times, 10 min each) before a 15 min incubation at RT with tyramide signal amplification reagent (TSA)-biotin Stand Alone Tyramide Kit (PerkinElmer) diluted 1:50. Following three washes in TNT buffer (10 min each), the sections were incubated with Streptavidin 568 (Invitrogen/Molecular Probes) diluted 1:200 in TNT buffer for 45 min at RT. Thereafter, the sections were again washed in TNT buffer (3 times, 10 min each time), and finally incubated with Hoechst 33258 (Invitrogen) at 0.1 µg/ml for 1 min, washed in PBS and coverslipped with aqueous mounting medium before fluorescence microscopy examination.

5.2 Animals

C57BL/6J mice (Charles River, USA) were housed under specific pathogen-free conditions in a temperature-controlled room (21-22° C) with a 12h light/dark cycle and ad libitum access to food and water. *AMHR2-Cre* knock-in mice (*AMHR2::Cre*) have been previously characterised (Jamin et al., 2002). *GnRH::GFP* (Spergel et al., 1999) were a generous gift of Dr. Daniel J. Spergel (Section of Endocrinology, Department of Medicine, University of Chicago, IL). Animal studies were approved by the Institutional Ethics Committees of Care and Use of Experimental Animals of the University of Lille 2 (France). All experiments were performed in accordance with the guidelines for animal use specified by the European Union Council Directive of September 22, 2010 (2010/63/EU). Animals were genotyped using primers listed in table.

Table 5. *AMHR2* genotyping primers

AMHR2 PCR primers	
5'-ACGTGGGTCAGACCCAGAGCC -3'	AMHR2 WT sense
5'- CGATGACCTCCTTCCTGGATT -3'	AMHR2 WT antisense
5'-CCGCTTCCTCGTGCTTTACGGTAT-3'	AMHR2 MUT sense
5'-ACGTAGTAGAGAGGCTGCGTTGAGTGTG-3'	AMHR2 MUT antisense

5.2.1 Mouse tissue preparation

Embryonic day 16.5 (E16.5) mouse embryos were obtained after cervical dislocation from timed-pregnant C57BL/6J mice. Embryos were washed thoroughly in cold 0.1 M PBS, fixed in 4% PFA in 0.1 M PBS pH 7.4 overnight at 4° C and stored at 4° C in 1x PBS containing 0.01% sodium azide for whole-mount immunolabelling.

Adult mice (n = 2, 4 months old male mice; *n* = 2, 5 months old female mice) were anaesthetised with 100mg/kg of ketamine-HCl and 10 mg/kg xylazine-HCl and perfused transcardially with 20ml of saline, followed by 100 ml of 4% PFA, pH 7.4. Brains were collected, postfixed in the same fixative for 4h at 4° C, and the two hemispheres of each brain were stored at 4° C in 1x PBS containing 0.01% sodium azide until whole-mount immunolabelling.

Embryos were harvested at embryonic day E14.5 from black C57BL/6 mice. Heads from the embryos were washed thoroughly in cold 0.01M PBS, fixed in fixative solution [4% paraformaldehyde (PFA), 0.01M PBS, pH 7.4] for 6–8 h at 4° C and cryoprotected in 20% sucrose overnight at 4° C. The following day, heads were embedded in OCT embedding medium (Tissue-Tek, Torrence CA, USA), frozen on dry ice, and stored at -80° C until sectioning. The embryo heads were coronally cryosectioned (Leica Microsystems, Wetzlar Germany) at 16µm intervals directly onto slides and stored at -80° C until use. Adult mice were anaesthetised with 50-100mg/kg of ketamine-HCl and 5-10mg/kg xylazine-HCl and transcardially perfused with 40mL of saline, followed by 100mL of 4% PFA, pH 7.4. Brains were collected, postfixed in the same fixative for 2h at 4° C, cryoprotected in 20% sucrose overnight. Embedded in OCT embedding medium, frozen on dry ice and stored at -80° C until cryosectioning. Adult brains were sectioned at 35µm using the cryostat and stored in anti-freeze medium at -20° C until use.

5.2.3 Immunofluorescence

3DISCO was performed as described in Section 5.1.4-5.1.7. Immunolabelling was completed as follows: sections were thawed at RT before 3 x 5min washes in 0.01M PBS. Sections were then incubated with primary antibody in a solution containing 10% normal donkey serum and 0.3% Triton X100 for 3 days at 4° C. 3 x 5 min washes in 0.01M PBS were followed by incubation in appropriately conjugated secondary antibodies (Table 8) for 1h before incubation with Hoechst 1:10,000. After 3 x 5 min washes in 0.01M PBS sections were coverslipped using Mowiol as an anti-fade mounting medium.

5.2.4 Nasal explants

Embryos were obtained from timed-pregnant animals. Nasal pits of E11.5 WT C57BL/6J mice were isolated under aseptic conditions in Grey's Balanced Salt Solution (Invitrogen) enriched with glucose (Sigma-Aldrich) and maintained at 4° C until plating. Explants were placed onto glass coverslips coated with 10µl of chicken plasma (Cocalico Biologicals, Inc.). Thrombin (10µl; Sigma-Aldrich) was then added to adhere (thrombin/plasma clot) the explant to the

coverslip. Explants were maintained in defined serum-free medium (SFM) containing 2.5 mg/ml Fungizone (Sigma-Aldrich) at 37° C with 5% CO_2 for up to 30 days in vitro (div) (Fueshko & Wray, 1994). From culture day 3 to 6, fresh medium containing fluorodeoxyuridine ($8x10^{-5}$ M; Sigma-Aldrich) was provided to inhibit the proliferation of dividing olfactory neurons and non-neuronal explant tissue. The medium was replaced with fresh SFM twice a week.

5.2.5 *In Utero* injections

Timed-pregnant mice carrying E11.5 embryos were anaesthetised, and the uterine horns were gently placed outside the abdominal cavity and constantly hydrated with 35° C sterile saline. Using a Nanofil syringe and a 35 GA needle attachment (World Precision Instruments), 2µl containing 0.4µg of AMHR2 Neutralising Antibody (AMHR2-NA, Table 7 for reference) and Fluorogold™ tracer 1:1500 (Sigma Aldrich, #39286) diluted in saline was injected intra-utero in the olfactory placode of the embryos. The respective controls were injected either saline 1% DMSO. The uteri were gently returned and the mothers sutured and monitored for few days. Embryos were collected at embryonic day 14.5 (E14.5) for GnRH neuron quantification. Fluorogold™ was used in order to verify the specificity of the injection sites. The concentration of AMHR2-NA was determined based on the manufacturers recommendations. In order to validate whether the concentration was cytotoxic, overall morphology of the nasal structures was examined and GnRH cell numbers counted.

5.2.6 GnRH cell counting

Serial sagittal sections (16µm) from E14.5 WT embryos, (n = 4 per group) were prepared as described above. Quantitative analysis of GnRH neuronal number, as a function of location, was performed over four regions (the nasal compartment, the nasal/forebrain junction, ventral forebrain and cortex). Serial coronal sections (30µm) of *AMHR2* $^{+/+}$ (females, n = 4; males, n = 3), *AMHR2* $^{+/-}$ (females, n = 4; males, n = 3) and *AMHR2* $^{-/-}$ mouse brains were used to count the total number of GnRH cells throughout the entire brain and combined to give group means ± SEM.

5.2.7 Fluorescence Activated Cell Sorting (FACS)

Embryos were harvested at E12.5 from timed-pregnant GnRH::GFP mice, previously anesthetised with an intraperitoneal injection of 100mg/kg of Ketamine-HCl and sacrificed by cervical dislocation. Juvenile (P12) and adult female mice (3 months old) were anesthetised with 50-100 mg/kg of Ketamine-HCl and 5-10mg/kg Xylazine-HCl before being sacrificed by cervical dislocation. Microdissections from embryonic nasal region and post-natal/adult hypothalamic preoptic regions were enzymatically dissociated using a Papain Dissociation System (Worthington, Lakewood, NJ) to obtain single-cell suspensions as previously described (Messina et al., 2016). After dissociation, the cells were physically purified using a FACSAria III (Beckman Coulter) flow cytometer equipped with FACSDiva software (BD Biosciences). The sort decision was based on measurements of GFP fluorescence (excitation: 488nm, 50 mW; detection: GFP bandpass 530/30nm, autofluorescence bandpass 695/40nm) by comparing cell suspensions from GnRH-GFP and wild-type animals. For each animal, 500 GFP-positive cells were sorted directly into 8µl extraction buffer: 0.1% Triton® X-100 (Sigma-Aldrich) and 0.4 U/µL RNaseOUT (Life Technologies). Captured cells were used to synthesise first-strand cDNA using the protocol detailed below.

5.3 *In Vitro* Experiments

5.3.1 Culture of GN11 and GT1-7 cell lines

GN11 and GT1-7 cells were grown in monolayers at 37° C under 5% CO_2, in DMEM (Invitrogen, Carlsbad CA, USA) containing 1mM pyruvate, 2mM L-glutamine (Invitrogen, Carlsbad CA, USA), 100µg/ml streptomycin, 100 U/ml penicillin and 9mg/ml glucose (MP Biomedicals, Santa Ana CA, USA), supplemented with 10% foetal bovine serum (complete medium). Medium was changed every 2 days for GN11 cells and every 4 days for GT1-7 cells. Cells were maintained below full confluence by trypsination and seeding onto 10 cm^2 dishes. Cells used for experiments were between their third and eighth passage. Treatment of cells used recombinant human AMH (1737-MS. R&D systems, Minneapolis MN, USA) and recombinant human TNFα (210-TA. R&D systems, Minneapolis MN, USA), diluted to indicated concentrations in DEPC treated water.

5.3.2 RT-PCR

Medium was removed by aspiration and cells were washed twice in sterile 1xDPBS in the absence of Calcium and Magnesium before being immediately frozen in dry ice and stored at -80° C. RNA was then phenol-chloroform extracted and ethanol precipitated. Briefly, 1ml of Trizol (Life Scientific, Carlsbad CA, USA) was used to dissociate cells, before adding 100µl of chloroform (Merck, Darmstadt Germany) and centrifuging at 12,000 g for 15 mins at 4° C. The aqueous phase was carefully collected and added to isopropanol at 1:1 before centrifuging at 12,000 g for 10 mins at 4° C. The aqueous phase was then discarded and the pellet washed in 70% ethanol before being centrifuged at 12,000 g for 5 mins at 4° C. The purity and quantity of the RNA was determined by UV spectroscopy (Nanodrop 1000. Thermo Scientific, Waltham MA, USA). RT-PCR was completed using the Invitrogen SuperScript® III First-strand synthesis kit (#18080093, ThermoFisher Scientific). 500ng of RNA was combined with oligo(dT)20, dNTPs and the reaction volume completed to 10µl with DEPC-treated water. Tubes were incubated at 65° C for 5 mins and at 4° C for 1 min. 10 x RT buffer, $MgCl_2$, DTT,

RNaseOUT™ and SuperScript® III reverse transcriptase were then added before incubating for 50 mins at 50° C and terminating the reaction at 85° C for 5 mins. Finally, RNase H was added and tubes were incubated for 20 mins at 37° C. Concentrations used according to kit instructions. Controls without reverse transcriptase were performed to demonstrate the absence of contaminating genomic DNA Reaction products were stored at −20° C until use.

Figure 35. Origin of Gn11 & GT1−7 cell lines

Both Mellon et al. (1990) and Radovick et al. (1991) used the T−antigen hybrid−gene approach to produce immortalized LHRH cell lines.

Mellon et al. (1990) constructed a hybrid gene which contained a portion of the promoter region of the rat LHRH gene. This transgene was injected into one−cell embryos which were subsequently transplanted into the uteri of pseudopregnant mice. Cells from the tumor of one of these mice were dispersed and, through a series of differential plating procedures, were purified to a homogeneous population. These GT−1 cells were subcloned by serial dilution, to produce GT1−7 cells.

In contrast to Mellon, Radovick et al. (1991) constructed a hybrid gene containing the promoter from the human LHRH gene that was similarly fused to the T−antigen coding sequence. A tumor which immunostained for both T−antigen and LHRH was excised from one of the F1 progeny (male), the cells were dispersed and purified, and a cell line (GN) was developed. Figure from Wetsel et al., 1995.

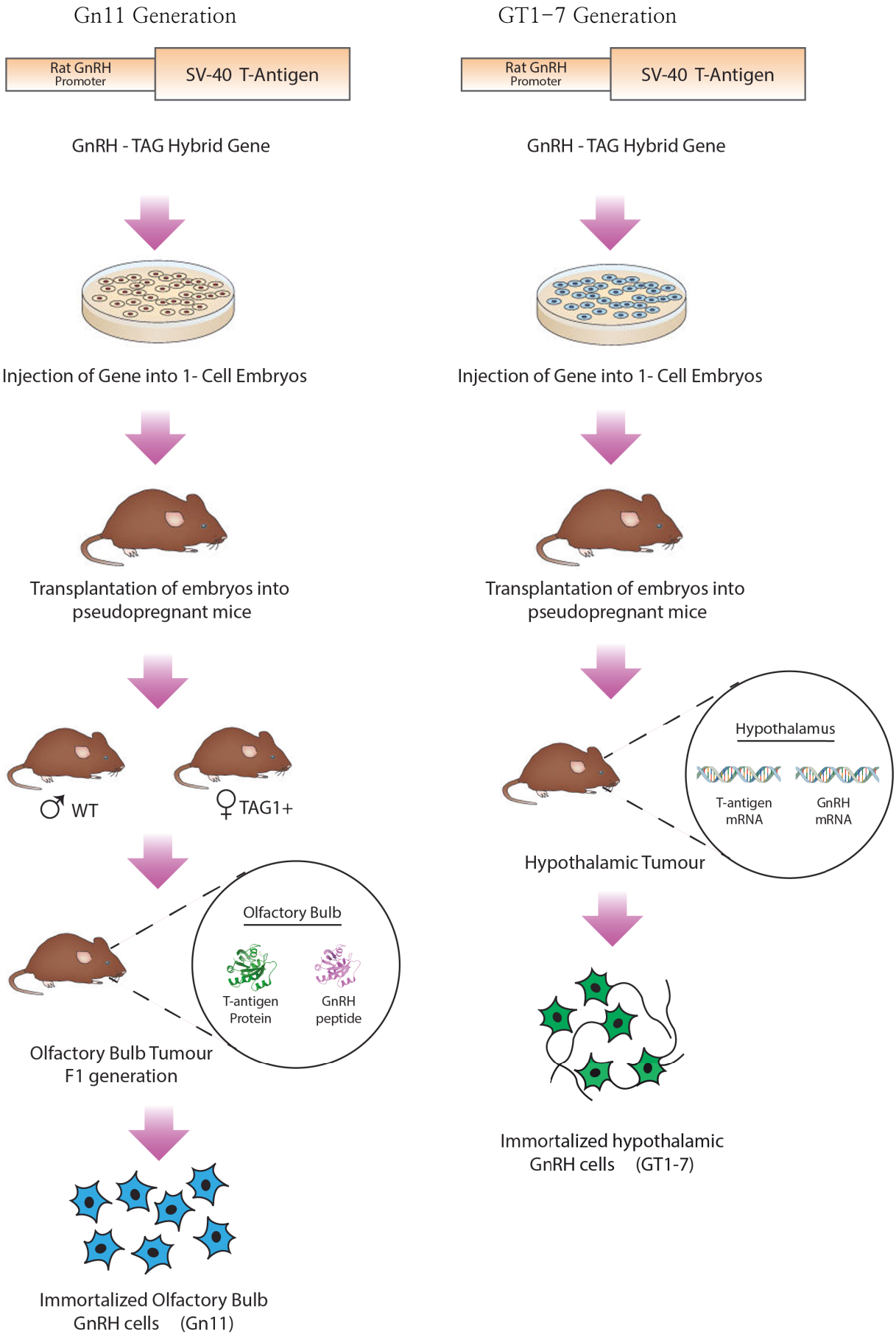
Gn11 Generation
Rat GnRH Promoter
SV-40 T-Antigen
GnRH - TAG Hybrid Gene
Injection of Gene into 1- Cell Embryos
Transplantation of embryos into pseudopregnant mice
♂ WT
♀ TAG1+
Olfactory Bulb
T-antigen Protein
GnRH peptide
Olfactory Bulb Tumour F1 generation
Immortalized Olfactory Bulb GnRH cells (Gn11)
GT1-7 Generation
Rat GnRH Promoter
SV-40 T-Antigen
GnRH - TAG Hybrid Gene
Injection of Gene into 1- Cell Embryos
Transplantation of embryos into pseudopregnant mice
Hypothalamus
T-antigen mRNA
GnRH mRNA
Hypothalamic Tumour
Immortalized hypothalamic GnRH cells (GT1-7)

5.3.3 Quantitative RT-PCR

For gene expression analyses, cDNA obtained from RT-PCR (as **5.3.2**) were reverse transcribed using SuperScript® III Reverse Transcriptase (Life Technologies, Carlsbad CA, USA). Real-time PCR was carried out on Applied Biosystems 7900HT Fast Real-Time PCR System using exon-span-specific TaqMan® Gene Expression Assays (Applied Biosystems, Carlsbad CA, USA). *AMHR2* (Mm00513847_m1); *AcvR1* (Mm01331069_m1); *BMPR1a* (Mm00477650_m1); *BMPR1b* (Mm03023971_m1). Control housekeeping genes: *Rn18s* (Hs99999901-s1) and *Actb* (Mm00607939). Amperase activation was achieved by heating to 50° C for 2mins, before dentaturing at 95° C for 20s, followed by 40 cycles of 1s 95° C with a 20 s extension time at 60° C. Gene expression data were analysed using SDS 2.4.1 and Data Assist 3.0.1 software (Applied Biosystems, Carlsbad CA, USA).

5.3.4 Qualitative PCR

Following qRT-PCR, primer products were run at a constant 120V on a 2% agarose gel with SYBR™ gold (ThermoFisher Scientific, USA) and bands visualised using an ultraviolet transilluminator.

5.3.5 Western Blot

Culture plates were frozen as described above, quickly thawed and protein immediately extracted with 500µl of freshly prepared lysis buffer [25mM Tris pH 7.4, 50mM β-glycerophosphate, 1% Triton x100, 1.5mM EGTA, 0.5mM EDTA, 1mM sodium orthovanadate, 10µg/ml Leupeptin and Pepstatin A, 10µg/ml aprotinin, 100µg/ml PMSF (reagents sourced from Sigma Aldrich, St. Louis MO, USA)]. Protein extracts were then homogenised using a 26 gauge needle before centrifuging at 12,000g for 15 mins at 4° C. The supernatant was recovered and protein quantified using the Bradford method (BioRad, Hercules, CA). 1x sample and 1x loading buffer (Invitrogen, Carlsbad CA, USA) was added to the samples, which were then boiled for 5 min before electrophoresis at 120V for 100 mins in 4-12% tris-acetate precast SDS-polyacrylamide gels according to the protocol supplied with the NuPAGE system (Invitrogen, Carlsbad CA, USA). After size fractionation, the proteins were

transferred onto a PVDF membrane (0.2μm pore size, LC2002; Invitrogen, Carlsbad CA, USA) in the blot module of the NuPAGE system (Invitrogen, Carlsbad CA, USA) maintained at 1A for 75 min at room temperature (RT). Blots were blocked for 1h in tris-buffered saline with 0.05% Tween 20 (TBST) and 5% non-fat milk at RT, incubated overnight at 4° C with their respective primary antibody, and washed four times with TBST before being exposed to horseradish peroxidase-conjugated secondary antibodies diluted in 5% non-fat milk TBST for 1h at RT. The immunoreactions were detected with enhanced chemiluminescence (NEL101; PerkinElmer, Boston, MA).

5.3.6 Flow Cytometry

The Annexin V Apoptosis Detection Kit (Invitrogen, Carlsbad CA, USA) with Annexin V conjugated to AlexaFluor®488 and Propidium Iodide (PI) used as a method to distinguish and quantify apoptotic and necrotic cells. Briefly, cells were treated with either a) SFM, b) TNFα (10ng/mL. Invitrogen, Carlsbad CA, USA), c) AMH (250ng/mL), d) AMH + TNFα, e) AMH (500ng/mL) or f) 10μM PS-1145 for 24 or 48h, trypsinised and re-suspended in Annexin binding buffer at a concentration of $1x10^6$ cells/mL. AlexaFluor®488 conjugated Annexin V at 1:20 and 1μM Propidium Iodide were added before ambient incubation for 15mins. 400 μL of binding buffer was then added before measuring fluorescence emission using an LSR Fortessa cytofluorometer (BD Biosciences, San Jose CA, USA). Emission was detected at 530 nm and 575 nm respectively using 488nm excitation (filters appropriate for FITC and TRITC/Texas Red© dye). Annexin V alone, PI alone and no staining were used as controls. n = 3 for all groups; data for 24h not shown but were comparable to results at 48 h.

5.3.7 Transwell Migration Assay

Boyden microchemotaxis chambers were used according to manufacturer's instructions (Neuro Probe, Gaithersburg MD, USA). In brief, the cells grown in complete medium until sub-confluence were harvested, and the suspension ($1x10^5$ cells/μL in serum-free DMEM) was placed in the open-bottom wells of the upper compartment. Each pair of wells was separated by a polyvinylpyrolidone-free polycarbonate porous membrane (8μm pore size). The lower

chamber of the Boyden's apparatus was filled with DMEM containing AMH at either a) 50, b) 100 or c) 250 ng/mL. Chemokinesis (stimulation of increased random cell motility) was distinguished from chemotaxis by placing the same concentration of the factor in both the upper and lower wells of the Boyden chamber, thereby eliminating the chemical gradient. After 4h of incubation, cells attached to the upper side of the filter were mechanically removed. Cells that migrated to the lower side were fixed using 4% PFA and stained with Hoechst (1:10,000) nuclear dye. The stained cells were photographed at 20X magnification and blind counted using an ImageJ plugin (National Institute of Health, Bethesda, USA).

5.3.8 siRNA Transfections

Cells were grown to 70% confluence in 10cm^2 dish without the presence of antibiotics in preparation for transfection. For each siRNA, oligomer–Lipofectamine® 2000 complexes were prepared as follows: siRNA oligomers were diluted in 500µl Opti-MEM® Reduced Serum Medium without serum and gently mixed, for a final concentration of 400nM). Lipofectamine™ 2000 was mixed gently before use, then diluted 10µl in 500µl OptiMEM®. Tubes were gently mixed and incubated for 5 minutes at RT. After the 5-minute incubation, the diluted oligomer was combined with the diluted Lipofectamine™ 2000 and incubated for 20 minutes at RT. During the incubation, cells were trypsinised and dissociated, then re-suspended in the lipofectamine containing siRNA mixture. Cells were then incubated at 37° C in a 5% CO_2 incubator for 48h, changing the medium to OptiMEM® supplemented with 5% foetal bovine serum after 6 hours. Gene knockdown was assessed by quantitative PCR. All siRNAs were purchased from Dharmacon (MA, USA). *AMHR2* duplex, OligoID: TMOSLR-00551; *BMPR1b* duplex, OligoID: TMOSLR-005553. Lincode (#E-042047-00), *AcvR1* (#E-042047-00) and *BMPR1a* (#E-040598-00) Accell siRNA pool.

5.3.9 Statistical Analysis

qRT-PCR gene expression data were analysed using SDS 2.4.1 and Data Assist 3.0.1 software (Applied Biosystems, Carlsbad CA, USA). All other analyses were performed using Prism 5 (GraphPad Software). Data sets were assessed for normality (Shapiro-Wilk test) and variance.

Where appropriate a 1way ANOVA followed by Bonferroni or Dunnets's post hoc testing was performed and for non-Gaussian distributions, a Kruskal-Wallis test followed by Dunn's multiple comparison test was used. α was set at 0.05 for all experiments excluding WES data.

5.3.10 Image manipulations

ImageJ (National Institute of Health, Bethesda, USA) and Photoshop CS6 (Adobe Systems, San Jose, CA, USA) were used to process, adjust and merge the photomontages. Figures were prepared using Adobe Photoshop and Abode Illustrator CS6.

Table 6. List of reagents

Reagents	Source	Identifier
Tetrahydrofuran Anhydrous >99.9%	Sigma-Aldrich	Cat# 186562 CAS Number 109-99-9
Dichloromethane	Sigma-Aldrich	Cat# 270997 CAS Number: 75-09-2
Benzyl ether	Sigma-Aldrich	Cat# 108014 CAS Number: 103-50-4
Methanol	VWR Chemicals	Cat# 20847.360 CAS Number: 67-56-1
Hydrogen peroxide solution	Sigma-Aldrich	Cat# 216763 CAS Number: 772-84-1
Triton X100	Sigma-Aldrich	Cat# X100-500ml CAS Number: 9002-93-1
Gelatin	VWR Chemicals	Cat# 24350.262 CAS Number: 9000-70-8
Thimerosal	Sigma-Aldrich	Cat# T8784-5g CAS Number: 54-64-8

Table 7. Primary antisera

Antigen	Host species	Source	Dilution
AMH	Mouse	Abcam, Ab24542	1:500
AMH	Rabbit	Abcam, ab103233	1:500
AMHR2 NA	Goat	R&D system, AF1618	1:200
AMHR2	Rabbit	CASLO, 56G	1:2000
GnRH	Rabbit	Prof. G. Tramu, University of Bordeaux, France	1:3000
GnRH	Rabbit	LR5, Dr. R. Benoit, Montréal General Hospital, Montréal, Québec, Canada	1:1000
GnRH	Guinea-Pig	Dr. Erik Hrabovszky, Institute of Experimental Medicine of the Hungarian Academy of Sciences, Budapest, Hungary	1:10000
Peripherin	Rabbit	Millipore, AB1530	1:1000
TAG-1	Goat	R&D system AF2215	1:500
Doublecortin (DCX)	Goat	Santa Cruz, SC-8066	1:500
β-III tubulin (TUJ1)	Mouse	Sigma, T8660	1:800
DNER	Goat	R&D system, AF2254	1:200
PAX6	Rabbit	Millipore, AB2237	1:400
HuCD	Mouse	Life Technologies A21271	1:200
Ki67	Rabbit	Abcam, ab15580	1:200
SOX2	Goat	Santa Cruz, sc-17320	1:300
SOX10	Goat	N-20; Santa Cruz; sc-17342	1:200
AP-2 alpha	Goat	3B5 supernatant 1:3; DSHB	1:200
Neuropilin-2 (Nrp-2)	Goat	R&D system AF2215	1:400
ChAT	Goat	Millipore; AB144P	1:500
Myosin Heavy Chain	Mouse	Millipore, 05-716	1:1000
PAX2	Goat	R&D system AF3364	1:1000
PLVAP	Mouse	Abcam ab81719	1:500
Actin	Mouse	Sigma Aldrich; A5316	1:1000
P-ERK1/2 (Thr202/Tyr204)	Rabbit	Cell Signalling; 9101L	1:1000
ERK1/2	Rabbit	Cell Signalling; 9102L	1:1000

Table 8. Secondary antisera

Antibody	Source	Identifier	Dilution
Donkey anti-Rabbit IgG (H+L) Alexa Fluor 488	Molecular Probes	Cat# A-21206	1:500
Donkey anti-Rabbit IgG (H+L) Alexa Fluor 555	Molecular Probes	Cat# A-31572	1:500
Donkey anti-Mouse IgG (H+L) Alexa Fluor 488	Molecular Probes	Cat# A-21202	1:500
Donkey anti-Mouse IgG (H+L) Alexa Fluor 555	Molecular Probes	Cat# A-31570	1:500
Donkey anti-Goat IgG (H+L) Alexa Fluor 488	Molecular Probes	Cat# A-11055	1:500
Donkey anti-Goat IgG (H+L) Alexa Fluor 555	Molecular Probes	Cat# A-21432	1:500
Donkey anti-Goat IgG (H+L) Alexa Fluor 647	Molecular Probes	Cat# A-21447	1:500
Donkey anti-Guinea Pig IgG (H+L) Alexa Fluor 488	Jackson ImmunoResearch	Cat# 706-545-148	1:500
Horse anti-Mouse IgG (H+L) peroxidase labelled	Vector	Cat# U0122	1:5000
Horse anti-Mouse IgG (H+L) peroxidase labelled	Vector	Cat# P1-2000	1:5000

CHAPTER 6

Clarifying human development using 3D imaging of transparent whole embryos


Cell
Volume 169
Number 1
March 23, 2017
www.cell.com

Tridimensional Visualisation and Analysis of Early Human Development

Morgane Belle, David Godefroy, Gérard Couly, Samuel A. Malone, Francis Collier, Paolo Giacobini and Alain Chédotal

Published in Cell

Volume 169, Issue 1, pp161–173.e12 (2017)

6.1 New tools to explore human development

Our understanding of the development of the central (CNS) and peripheral nervous systems (PNS) is largely derived from work on chick embryos (e.g. summarised by Whitlock, 2004), with more recent work occurring using tracing studies in mice (Serbedzija et al. 1992), with very few studies examining human tissue. In addition to the scarcity and difficulty involved in working with human embryonic tissue, a further limitation to our understanding has been the limitations inherent in the process of traditional histology and microscope analysis. Although these permit excellent cellular and subcellular resolution, the thin sectioning of tissue necessitates a loss of 3Dimensional appreciation of structures. This is especially problematic during embryogenesis, which is a dynamic process involving constantly changing morphologies as tissues expand and differentiate.

Currently some 3D appreciation of structure can come from traditional sectioning and microscope analysis by processing serial 2D sections of tissue to create a 3D rendering (Griffini et al., 1997). This methodology has drawbacks, however, as it is time prohibitive, requires careful alignment of serial sections and some information may be destroyed by the sectioning process or during the immunolabelling, as tissues become non-uniformly warped, torn or lost. Several advances in microscopy such as the development of the confocal (Minsky, 1988) and 2-photon microscopes (Denk et al., 1990) have permitted analysis of single planes of a volume by minimizing contributions from other parts of the volume such as autofluorescence and myoglobin, haemoglobin and melanin light absorption, these too, however, are limited by their ability to image deep within tissues, currently limited to >1mm.

This difficulty is caused by the inherent 'milky' appearance of large volumes of tissue caused by light scattering within the tissue, coming as a result of the differing absorption properties of the water, proteins and lipids that make up biological tissues. In order to achieve good clarity for imaging, light emitted from the tissue and entering the detector of the microscope should pass in a single uniform direction. In large volumes, this does not readily occur as electrons from

hydrophobic molecules more readily absorb light, compared to hydrophilic molecules and so propagation of light within the tissue is not homogenous. The interfaces between these regions, causing light to propagate at differing speeds and angles can be represented as the refractive index of each type of molecule (reviewed by Richardson & Lichtman, 2015). In order to overcome this problem and achieve good visualisation deep within a large volume, an equilibration of refractive indices to reduce inhomogeneity in light scatter throughout a sample is required.

The first method to address this by 'optically clearing' tissues was proposed and developed by the German anatomist Werner Spalteholtz; based on the dehydration of tissues in order to achieve refractive index matching (Spalteholtz 1911; 1914). More recently with the advances in light sheet fluorescence microscopy (LSFM), a variety of optical clearing techniques have been developed that all result in tissue clearing by similar principles, despite the underlying differences in their chemical approaches (**Figure 36**). The exact details, advantages and disadvantages of each have been recently reviewed and compared with focuses on tissue specific requirements (Azaripour et al., 2016), their chemistry (Tainaka et al., 2016) and their physical principles (Richardson & Lichtman, 2015).

One of these protocols, 3DISCO based on the ability of specific organic solvents to dehydrate, solvate the lipids and cause refractive index matching also causes up to 50% reduction in total volume of the tissue (Becker et al., 2012; Ertürk et al., 2012a, 2012b). These properties mean it is ideally suited to examine the development of several body systems during the first trimester of human development. This work provides high resolution 3D images of the developing peripheral nervous, muscular, vascular, cardiopulmonary and urogenital systems, however, only on the work directly relevant to this thesis is presented here (**see Appendix** for full paper).

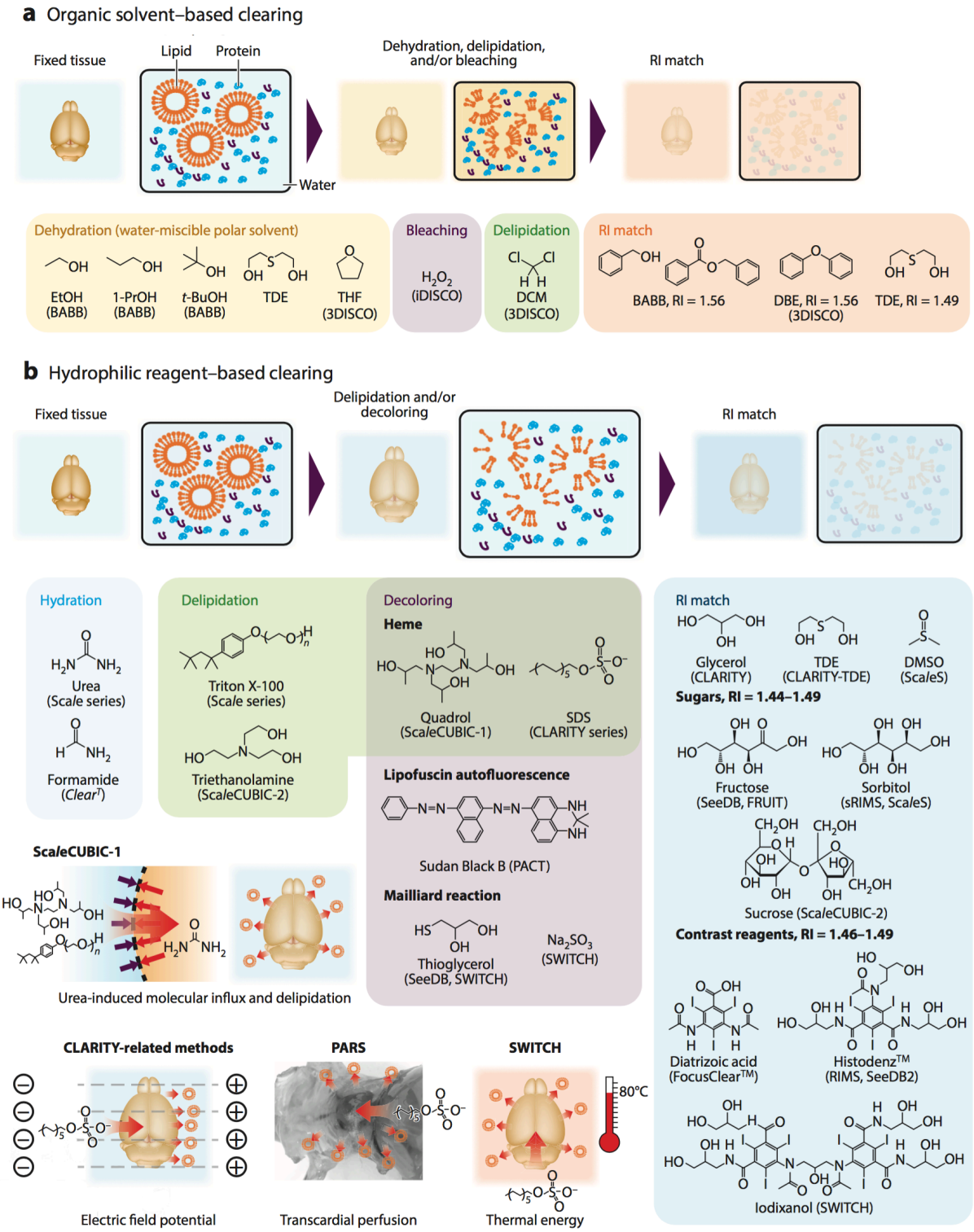

Figure 36. Comparison of optical clearing techniques

Optical clearing techniques can broadly be divided into organic solvent based (A) and hydrophilic based (B).

6.2 Development of the human peripheral nervous system

A protocol for whole-mount immunostaining and 3DISCO clearing was used to analyse the development of human embryos (first 8 weeks of gestation) and foetuses (from 8.5 to 14 weeks, see **Section 5.2** for stage determination and classifications). The development of sensory axons of the PNS was studied in human embryos at CS19 (n = 2), CS21 (n = 1) and CS23 (n = 3) using antibodies against the neuron-specific intermediate filament protein peripherin (Prph). In rodents, Prph is expressed by sensory and autonomic axons (Parysek et al., 1988) and in human foetuses, Prph has previously been shown to label auditory nerves (Locher et al., 2013).

As previously reported for mice (Belle et al., 2014; Renier et al., 2014), tissue-shrinkage was observed (20-40%) in all samples but remained homogeneous throughout the embryo. The size reduction after 3DISCO enabled imaging of whole embryos using LSFM and allowed visualisation of Prph+ peripheral nerves from the brainstem and spinal cord to their distal extremities (**Figure 37 A-C**). The imaging of entire embryos labelled for Prph (**Figure 37 A-B**) clearly show the increase in sensory innervation that occurs between 7-8 weeks of gestation.

6.3 Tracing the embryonic cranial nerves (CNI-CNXII)

The cranial nerves (CN) are thirteen pairs of nerves that emerge directly from the brain and primarily relay sensory and motor information to and from the head and neck regions (the vagus nerve, CNX being an exception). Cranial nerves are described as 'mixed' as they may carry sensory, motor or sensory and motor information (see appendix for a table of cranial nerve names and functions). Motoneuron cell bodies of the CNs are found within nuclei within the brainstem, while sensory neuron cell bodies form ganglia outside of the brain in a pattern homologous to spinal nerves. Examination of the inferior surface of an adult brain indicates CN0-II emerge from the forebrain, CNIII emerges from the midbrain and CNIV-XII all emerge from the hindbrain. (for a review on CN anatomy and function – Vilensky et al (2015). The Clinical Anatomy of the Cranial Nerves: The Nerves of "On Olympus Towering Top": ISBN 978-1-118-49201-7).

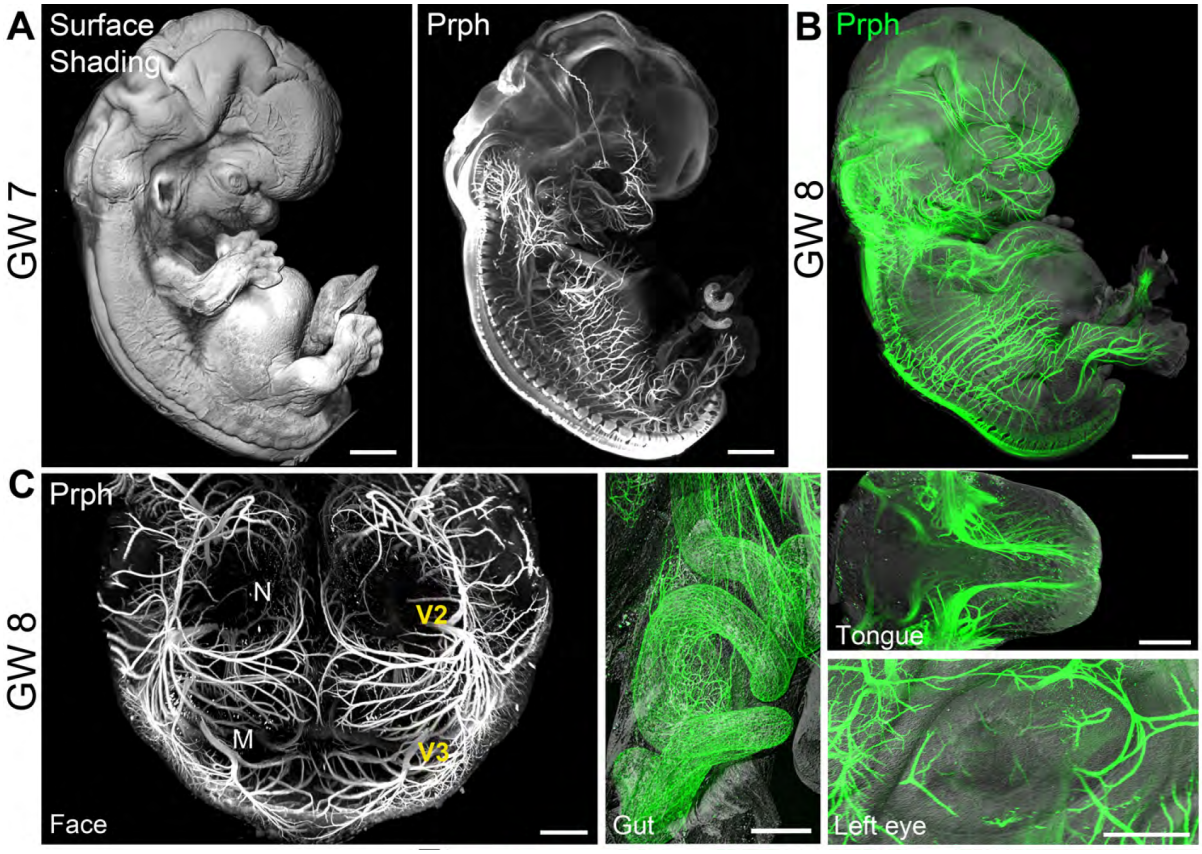

Figure 37. 3D analysis of peripheral nervous system development in human embryos.
All panels are LSFM images of solvent-cleared embryos.
(A) Surface shading image (left) and Prph labelling of peripheral nerves (right) at GW7. (B) Overlay of the surface shading image (grey) and Prph labelling (green) at GW8. (C) High magnification images of Prph+ innervation at GW8. The middle and right panels are overlays of the surface contrast image (grey) and Prph labelling (green). Abbreviations: N, nostrils; M, mouth; V_2 (maxillary) and V_3 (mandibular), second and third branches of the trigeminal nerve.
Scale bars: 1000 μm in A, 2000 μm in B, 500 μm in C

During early development of the hindbrain, regions of proliferating neuroepithelium establish distinct segments known as rhombomeres, which give rise to the motor nuclei of CNs IV–VII and VIII–XII. CN sensory ganglia originate from ectodermal placodes and NC cells, including the nasal and otic placodes as well as four epibranchial placodes of ectodermal thickening dorsal to the pharyngeal arches. The emergence of the NC derived ganglia of the largest of the cranial nerves (CNV) along with CNVII are first visible at CS10 (O'Rahilly & Muller, 2007), whilst the terminalis (CN0) is the final CN component to emerge, first detectable at CS13 (O'Rahilly & Müller, 2007).

Prph was again used as a marker of sensory CNs while choline acetyl transferase (ChAT) was used as a marker of embryonic motoneurons. ChAT is a transferase enzyme responsible for the synthesis of the neurotransmitter acetylcholine and is thus found in cholinergic motoneurons of both the PNS. Accordingly, in all experiments (n = 22) there was no overlap observed between ChAT+ and Prph+ immunoreactive axons, although that motor nerve roots were not immunoreactive for Prph (data not shown), suggests that in humans, Prph is differentially expressed between spinal cord and cranial motor axons. 3D virtual dissection of organ innervation with Imaris segmentation plugins was performed to trace, artificially colour and reconstruct individual nerve fascicles. This method was applied to GW7 (Carnegie stage 19, CS19; n = 2) and GW8 (n = 1; **Figure 38**) cranial nerves to provide the first realistic indication of their development at this time.

Figure 38. 3D analysis of cranial nerve development in human embryos.

All panels are LSFM images of solvent-cleared embryos.

(**A**) Right view of the head and cranial nerves at GW7 (Prph staining). On the right panel, cranial nerves are segmented and highlighted with specific pseudo-colours. (**B**) GW7 embryo stained for Prph. The left panel is a segmentation of the four nerves innervating the tongue (right side). The trigeminal nerve (V3, mandibular subdivision) and the chorda tympani of the facial nerve (VIIb or Wrisberg nerve) contribute to the lingual nerve. The two other nerves are the glossopharyngeal (IX) and hypoglossus (XII). The right panel is a ventral view of the tongue. (**B**) Dorsal views of the tongue in a GW9.5 foetus labeled for Prph (left) and ChAT (right). Scale bars:1000 μm in **A**, 500 μm in B (left panel), 300 μm in **B** (right panel) and **C**.

6.4 Development of the human urogenital system

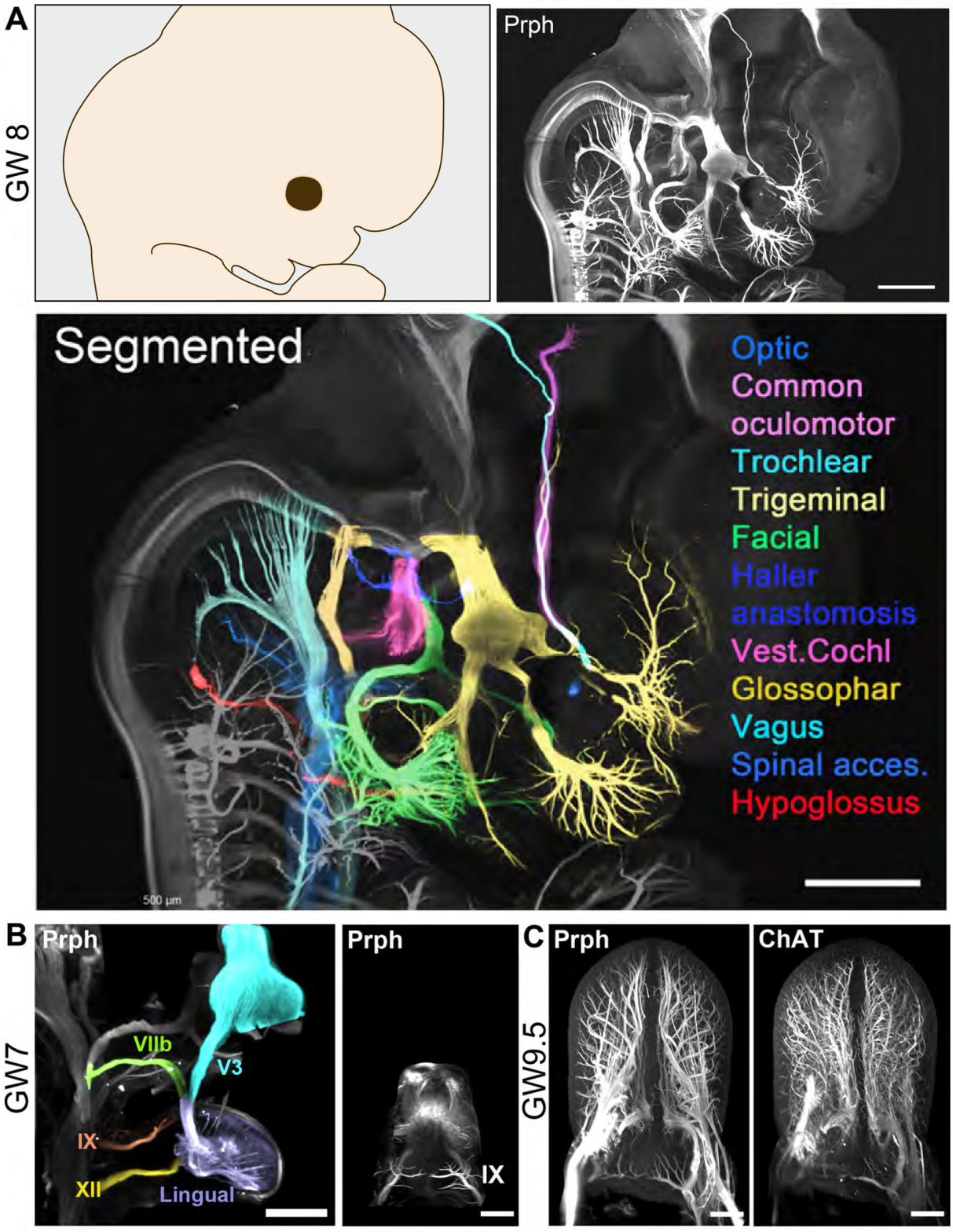

In adult mammals, the urogenital system is comprised of the kidneys, urinary tracts, gonads and reproductive ducts. Before GW7–GW8, the human gonadal ridges are undifferentiated, and the

genital ducts appear morphologically similar in both sexes with two paired structures: the Wolffian ducts (WD) which derive from the mesonephros and the Müllerian ducts (MD).

This knowledge is primarily based on histological and electron microscopy analysis (Fritsch et al., 2012; Hashimoto, 2003), and has not yet been studied at a cellular and molecular level in humans unlike in mice (Georgas et al., 2015; Little et al., 2007). Here the development of the human urogenital system was studied using antibodies against the Pax2 transcription factor as Pax2 mRNA was previously detected in the mesonephros and WD at 6-7 gestational weeks (Tellier et al., 2000). Embryos and foetuses of both sexes, including 11 males (GW8-GW14) and 9 females (GW7-GW14) were used to demonstrate the differences in sexual differentiation that occurs through this developmental window. All major components of the urogenital system could be visualised in 3D (**Figures 39-41**), and individually segmented. Foetuses older than GW8, too large for our LSFM microscope, were dissected prior to processing to image.

6.4.1 Development in Males

In the youngest male embryo (GW8), the caudal tip of the MD was in close contact with the WD but had not yet fully elongated (**Figure 39 A-B**) and mesonephric tubules stemming from the WD covered the testis primordium. The kidneys still occupied a ventral position adjacent to the genital ridges (**Figure 39A**). At GW9.5 (n = 1). At GW9.5, the MD further elongated along the WD, however, they still had not fused (**Figures 39 C-D**). In GW10 male foetuses (n = 2), the two MD have fused and extended medially between the two WD up to the urogenital sinus. In both cases, however, the MD started to fragment dorsally (**Figure 39 E-F and Figure 41A**). This remnant of the fused MD might give rise to the prostatic utricle. At older ages, such as GW14 (n = 1), the mesonephric nephrons of the WD have regressed while the epididymis ducts and vas deferens have emerged (**Figure 39G**). As previously reported (Jacob et al., 2012), an apical MD remnant is still present next to the rete testis by GW14 (**Figure 39 G-J**).

Sox9 is essential to testes differentiation in males and expression of its mRNA has first been detected around CS19-CS21 (Hanley et al., 2000). Using whole-mount immunostaining for

Sox9, on GW10, GW11, GW13.5 and GW14 foetuses (n = 1 for each) we could visualise the 3D organisation of the testis cords, containing Sox9+ Sertoli cells (**Figure 39 H–J**).

6.4.2 Development in Females

We also stained GW10.5–GW13 female foetuses with Pax2 (n = 6) and followed in 3D the reorganization of the urogenital tract (**Figures 40 and 41**). In our youngest female foetus (GW10.5) the MD have already fused to form the uterovaginal canal (**Figure 40**). The WD were still continuous but mesonephric tubules had begun to regress. At GW11.5, the disintegration of the mesonephros and WD was more pronounced and the length of the two MD increased (**Figure 40B**). At GW13, the distal part of the WD has dissolved whereas its cranial part transformed into the Fallopian tubes (**Figures 40C and 41B**).

The vascularisation of the developing gonads is thought to play a role in their maturation (Brennan et al., 2002; Coveney et al., 2008). We performed double staining for Pax2 and Plvap (plasmalemma vesicle–associated protein) to study the interaction between the vasculature and the genital tracts. Plvap; also known as PV–1 or PAL–E, is a transmembrane glycoprotein expressed by fenestrated microvascular endothelial cells (Elima et al., 2005). Interestingly, at GW8 and GW10, the developing testes and WD were embedded in a dense capillary meshwork but the MD was avascular (**Figure 40 D–E**). By contrast, in a GW10.5 female foetus, both the MD and the WD were vascularised (**Figures 40 E–F**) and a dense vascular network ensheathed the MD by GW13 (**Figure 40 F–G**). Although we could not study younger female embryos, these results suggest that MD associated angiogenesis may be sex dependent.

Information on the early development of human nephrons is scarce (Ludwig and Landmann, 2005). Staining of GW10–GW13.5 kidneys (n = 5) showed that Pax2 and Sox9 are both expressed in the epithelium of the ureteric tree. Pax2, together with another transcription factor, Six2, was also found in nephron precursors of the cap mesenchyme surrounding the ureteric tips in the nephrogenic zone of the developing kidney (O'Brien et al., 2016). Staining of the

endothelial cells with Plvap, could reveal the presence of developing glomeruli and their morphology (see Appendix).

Figure 39. 3D analysis of the urogenital system development in male embryos.

All panels are LSFM images of solvent-cleared embryos.

(A, B) GW8 embryo stained for Pax2. Raw LSFM image (left) and 3D rendering image (right). The middle panel shows the segmentation and pseudocolourisation of the kidney and ureters (yellow), Müllerian ducts (magenta, MD), and Wolffian ducts (blue, WD; the mesonephric tubules are indicated by an arrowhead). (B) High magnification of the MD/WD junction (arrow). (C, D) Segmented (left) and 3D (right) images of the GW9.5 urogenital system labelled with Pax2. (D) The apical tip has enlarged (arrow). The distal tips of the MD (arrowheads in C and D) have extended along the WD (compare with A) but have not yet fused. (E) Segmented (left) and 3D (right) images of the GW10 urogenital system labelled with Pax2. The MD have fused distally (arrow) and began to fragment (arrowheads). (F) More advanced stage of MD regression and fragmentation (arrowhead) in a second GW10 foetus. (G) 3D image of the GW14 urogenital system labelled with Pax2. A short fragment of the Müllerian duct persists (arrowhead) and the vas deferens (VD) appears more developed (arrow). (H) GW10 testis (Te) labelled with Pax2 (red) and Sox9 (green). Sox9+ Sertoli cells are seen in the developing testis cords (arrowheads). (I) Single optical section (2 μm z projection) through a GW10 foetus testis labelled for Pax2, Sox9 and Plvap (endothelial cells). The arrow indicates the rete testis. (J) GW14 testis labelled for Sox9 and Pax2 segmented. The Müllerian (magenta) and Wolffian (cyan) ducts (Pax2+) have been segmented and pseudocoloured.

Abbreviations: Kid, kidney; MD, Müllerian duct; PU, prostatic utricle; WD, Wolffian duct; ♂, male.

Scale bars: 400 μm in A, B, 500 μm in C and E, 100 μm in D and H (right panel), 300 μm in F, G, H (left and middle panels) and I, 350 μm in J.

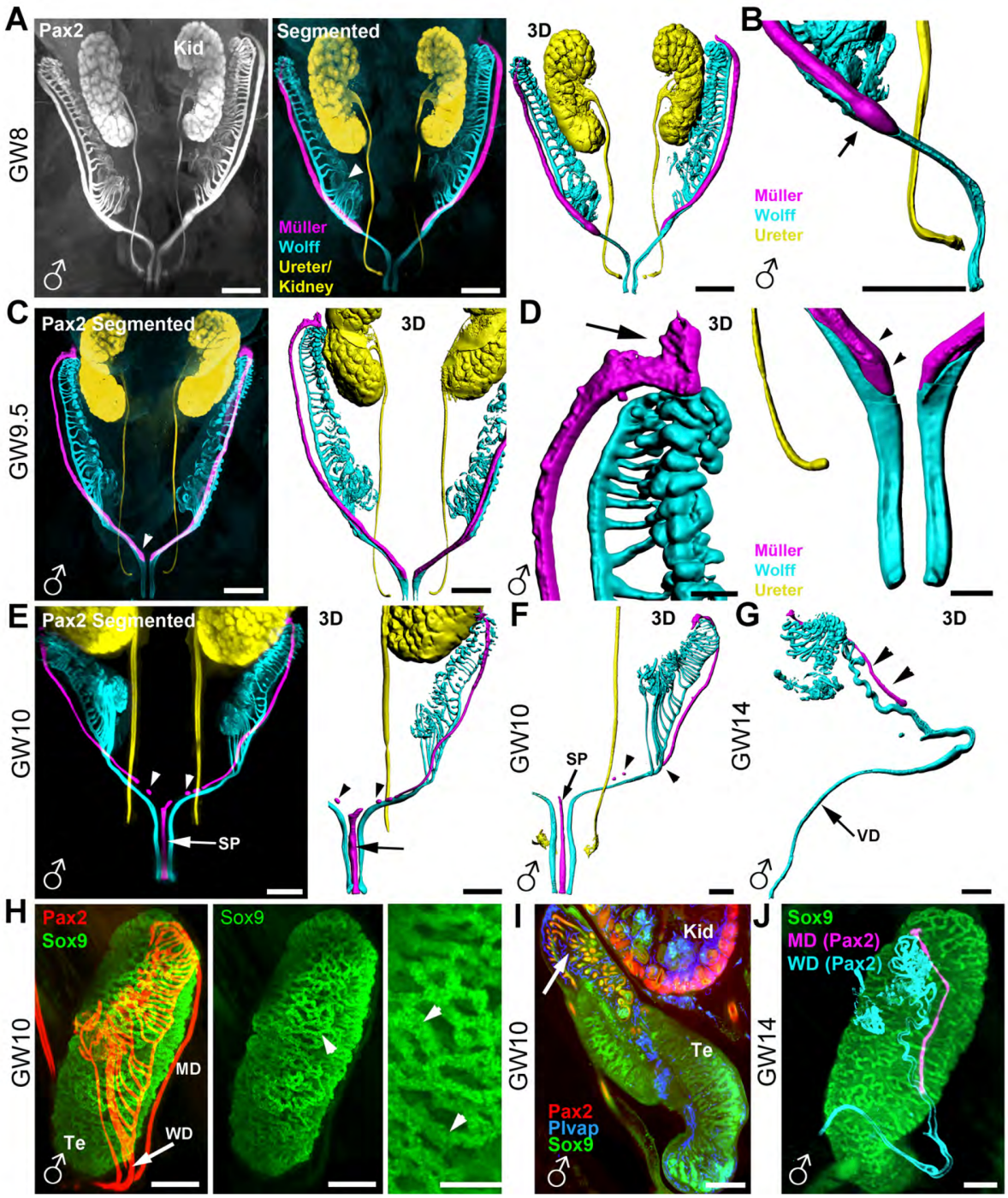
A
Pax2
Kid
Segmented
3D
B
GW8
Müller
Wolff
Ureter/
Kidney
Müller
Wolff
Ureter
C
Pax2 Segmented
3D
D
3D
GW9.5
Müller
Wolff
Ureter
E
Pax2 Segmented
3D
F
3D
G
3D
GW10
SP
GW10
SP
GW14
VD
H
Pax2
Sox9
Sox9
GW10
MD
Te
WD
I
Kid
Te
J
Sox9
MD (Pax2)
WD (Pax2)
GW10
Pax2
Plvap
Sox9
GW14

Figure 40. Comparative 3D analysis of the urogenital system development in female and male embryos.

All panels are LSFM images of solvent-cleared embryos.

(A) Original LSFM image (left), segmented/colorized (middle) and 3D (right) images of the urogenital system in a GW10.5 female foetus labelled with Pax2. The Wolffian ducts (cyan) are continuous and the Müllerian (magenta) ducts have fused. (B) Genital system of a GW11.5 female foetus stained with Pax2 after segmentation and 3D rendering. The arrow indicates the developing uterus and upper vagina. The Wolffian ducts start to regress (arrowheads). (C) Genital system of a GW13 female foetus stained with Pax2 after segmentation and 3D rendering. The size of the future uterus has increased and the Wolffian ducts have significantly regressed (arrowheads). The right panel is a high magnification at the level of the apical part of the Müllerian duct showing the developing fimbriae of the oviduct (arrow). (D-E) Vasculature of the developing gonads. (D) GW8 testis labelled for Pax2 and Plvap. A dense Plvap+ capillary network covers all the testis (arrow on the left) and the Wolffian duct (WD). By contrast, the Müllerian duct (MD) is not vascularized (arrowheads). The right panel is an optical section (1.2 μm) through the right testis and MD. (E) At GW10, the MD is still devoid of capillaries in male. (F-G) GW10.5 and GW13 ovaries labelled for Pax2 and Plvap. A dense vascular network covers the ovary (Ov). Unlike in males, both the Müllerian and Wolffian ducts are densely vascularised. Abbreviations, ♀, female; ♂, male; MD, Müllerian Ducts; WD, Wolffian Ducts; OV, Ovary.

Scale bars: 500 μm in A, B and C (left panel), 270 μm in C (right panel), 100 μm in D (middle and right panels), 160 μm in D (left panel), 200 μm in E-G

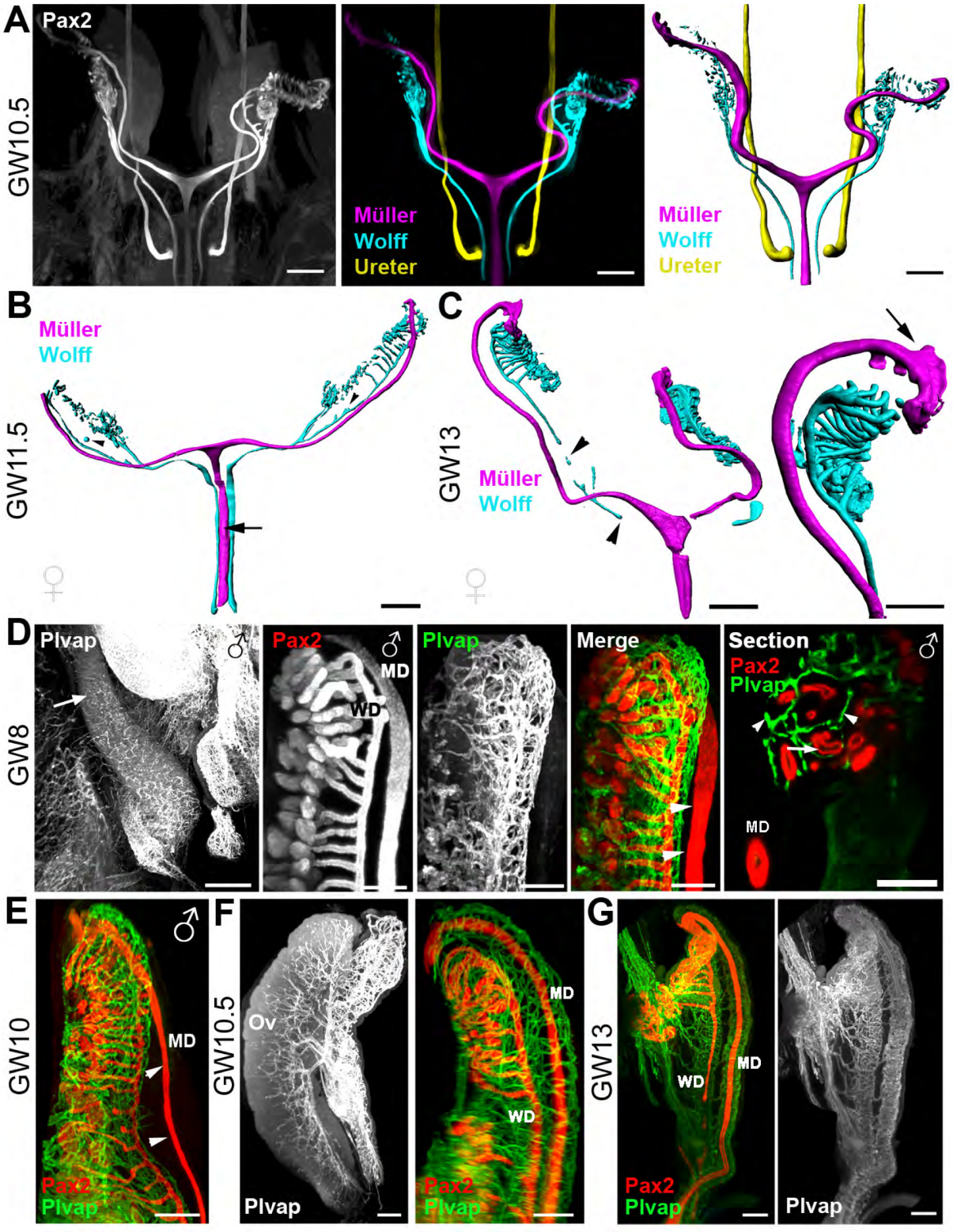
A
Pax2
GW10.5
Müller
Wolff
Ureter
Müller
Wolff
Ureter
B
Müller
Wolff
GW11.5
♀
C
GW13
Müller
Wolff
♀
D
Plvap
♂
GW8
Pax2
♂
MD
WD
Plvap
Merge
Section
♂
Pax2
Plvap
MD
E
♂
GW10
MD
Pax2
Plvap
F
GW10.5
Ov
Plvap
MD
WD
Pax2
Plvap
G
GW13
WD
MD
Pax2
Plvap
Plvap

Figure 41. Development of the Müllerian and Wolffian ducts in male and female human embryos.

All panels are LSFM images of the genital tracts of 3DISCO-cleared embryos and foetuses labelled with Pax2 antibody, segmented and pseudo-coloured. All images are at the same magnification. (A) In males, the Müllerian duct (MD) extends ventrally along the Wolffian duct (WD) and fuses with the opposite MD around GW9.5. The MDs then degenerate except the fused domain that will become the prostatic utricle. (B) In females, the MDs fuse to form the uterus and vagina and the WDs regress.
Scale bars: 400 μm in A and B.

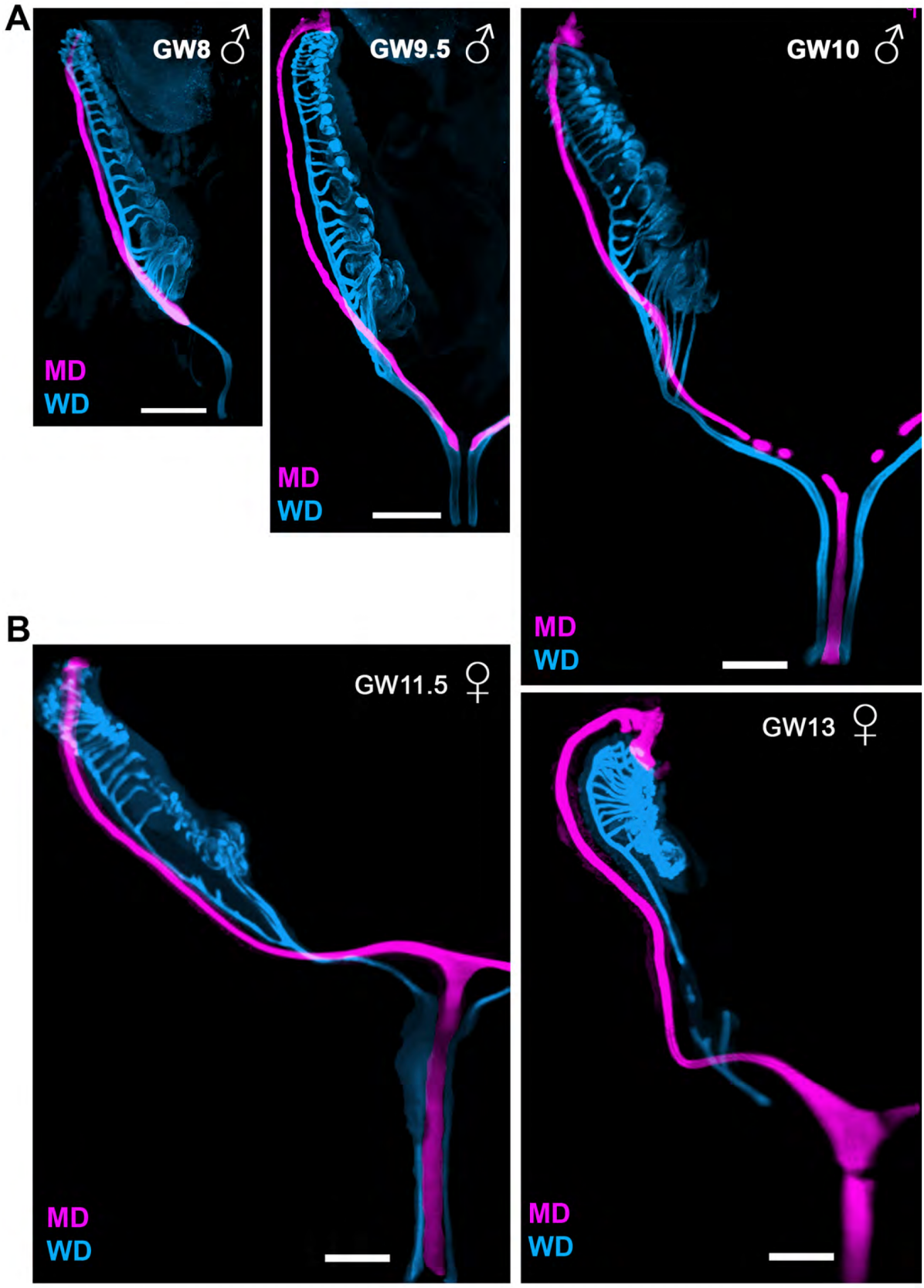
A
GW8 ♂
MD
WD
GW9.5 ♂
MD
WD
GW10 ♂
MD
WD
B
GW11.5 ♀
MD
WD
GW13 ♀
MD
WD

CHAPTER 7

Development of the GnRH system in Humans

Development of the Neurons Controlling Fertility in Humans: New Insights from 3D Imaging and Transparent Foetal Brains

Filippo Casoni*, Samuel A. Malone*, Morgane Belle, Federico Luzzati, Francis Collier, Cecile Allet, Erik Hrabovszky, Sowmyalakshmi Rasika, Vincent Prévot, Alain Chédotal and Paolo Giacobini

*Denotes co-first authorship

Published in Development
Volume 143, Issue 21, pp3969-3981 (2016)

7.1 Formation of the olfactory placode and VNO

Most vertebrates possess two anatomically distinct olfactory systems: the main olfactory system, responsible for the detection of volatile odorants, and the vomeronasal system, which mediates the detection of pheromones – primarily non-volatile signals related to social and reproductive behaviour (Dulac & Torello, 2003).

In all vertebrates studied so far, the differentiation of GnRH neurons (i.e the expression of GnRH transcript/protein and the acquisition of specific postmitotic features), occurs early during embryogenesis within the presumptive VNO (Forni & Wray, 2015; Schwanzel-Fukuda & Pfaff, 1989; Wray et al., 1989). Thus, we first studied the sequential morphogenetic steps leading to the formation of the human olfactory/vomeronasal systems, the appearance of the first GnRH-expressing neurons and the initiation of the GnRH neuronal migratory process.

In humans, the olfactory placodes develop as thickenings of the ectoderm on the ventrolateral sides of the head around the fifth week of gestation (Muller & O'Rahilly, 2004). While there is general agreement about the existence of a VNO in the human embryo (Smith & Bhatnagar, 2000), very little information is available about its development and molecular signature.

Here, we first observed that the placodes invaginate at CS 16 (approx. 39 day of gestation) to form simple olfactory pits (**Figure 42 a-b**). An invagination of the medial olfactory placode gives rise to the presumptive vomeronasal organ (pVNO; **Figure 42 c-d**).

We then analysed in a human embryo at CS 16 the expression of the transcription factors AP-2α and PAX6, whose graded expression define the site of the VNO anlage in rodents (Forni et al., 2011). AP-2α immunoreactivity could be detected in the epidermis, dorsal and ventral craniofacial mesenchyme, and a few ectodermal cells within the dorsal and ventral portions of the respiratory epithelium (**Figure 42 a-b**). In the nasal region, PAX6 expression was confined to the medial olfactory epithelium with a decreasing gradient towards AP-2α -positive

territories (**Figure 42 a–c**). We next analysed the development of the VNO at subsequent embryonic stages (CS 18–20, approx. 44 to 49 days of gestation). We were able to identify symmetrical bean–shaped VNOs, located at the base of the nasal septum, in all embryos (CS 16–23, n = 7; **Figures 43–44**) and foetuses (GW 9–12; n = 8) analysed. By CS 18, the VNO was closed and almost completely separated from the nasal cavity (**Figure 43 a–b**) except caudally, where it maintained contact with the olfactory epithelium throughout the first trimester of gestation (**Figure 43c; Figure 44g**).

Whether the VNO retains any proliferative capacity during embryogenesis in humans is unknown. At CS 20, numerous VNO cells expressed the proliferation marker Ki67 and high levels of the stem cell marker SOX2 (**Figure 43 m–n**). In contrast, they were negative for SOX10, a marker of olfactory ensheathing cells (a type of glial cell with myelinating capacity) and Hu–CD, a marker of immature neurons (Marusich & Weston, 1992) (**Figure 43 m–n**). These observations suggest that the embryonic VNO contains actively proliferating progenitors that could be the precursors of the neurons and olfactory ensheathing cells migrating into the telencephalon from the nasal region.

Figure 42. Ontogenesis and molecular signature of GnRH neurons at CS 16

(**a–b**) AP-2α and PAX6 expression in a sagittal section of a CS16 embryo head. AP-2α is expressed by dorsal and ventral craniofacial mesenchyme, and few ectodermal cells of the dorsal and ventral portion of the respiratory epithelium (RE). (**b**) Pax6 is expressed in an opposite gradient to AP-2α, defining the nasal neuroepithelium and the pVNO (arrow). (**c**) DAP staining showing that in the olfactory placode an invagination of the medial olfactory placode (MOP) forms the pVNO (arrow). (**d**) GnRH+ neurons differentiate outside the pVNO and express DCX as soon as they start migrating across the NM. (**e**), Early GnRH+ cells (arrows) are detected at the border between the NM and the epithelium of the pVNO. (**f**) Lateral sagittal section of a CS 16 human embryo head stained with DAPI. (**g**) High magnification of the boxed area in **f**. The neuronal migratory mass (MM, arrows) expresses the immature neuronal cell marker DCX. GnRH neurons coalescence with the MM (**h–j**), DNER and βIII-tub+ cells are detected in the medial NM forming the MM (**h**, arrow) and βIII-tub+ cells are present dorsally towards the developing olfactory bulb (**h**, arrowhead). βIII-tub+ neurons expressing DNER emerge from the OE (**i**, arrowheads) towards the coalescence of cells in the NM in a characteristic chain-like fashion. (**j**), High magnification of a βIII-tub+ cell expressing DNER moving from the OE to the NM.

Scale bars: **a** 200 μm; **b** 100 μm; **c**, **f** 200 μm; **d**, **i** 20 μm; **e**, **j** 10 μm; inset in **j** 5 μm; **g–h** 50 μm. Abbreviations: FB: Forebrain; NM: nasal mesenchyme; pVNO: presumptive vomeronasal organ; OE: olfactory epithelium; MM: migratory mass; MOP: medial olfactory placode.

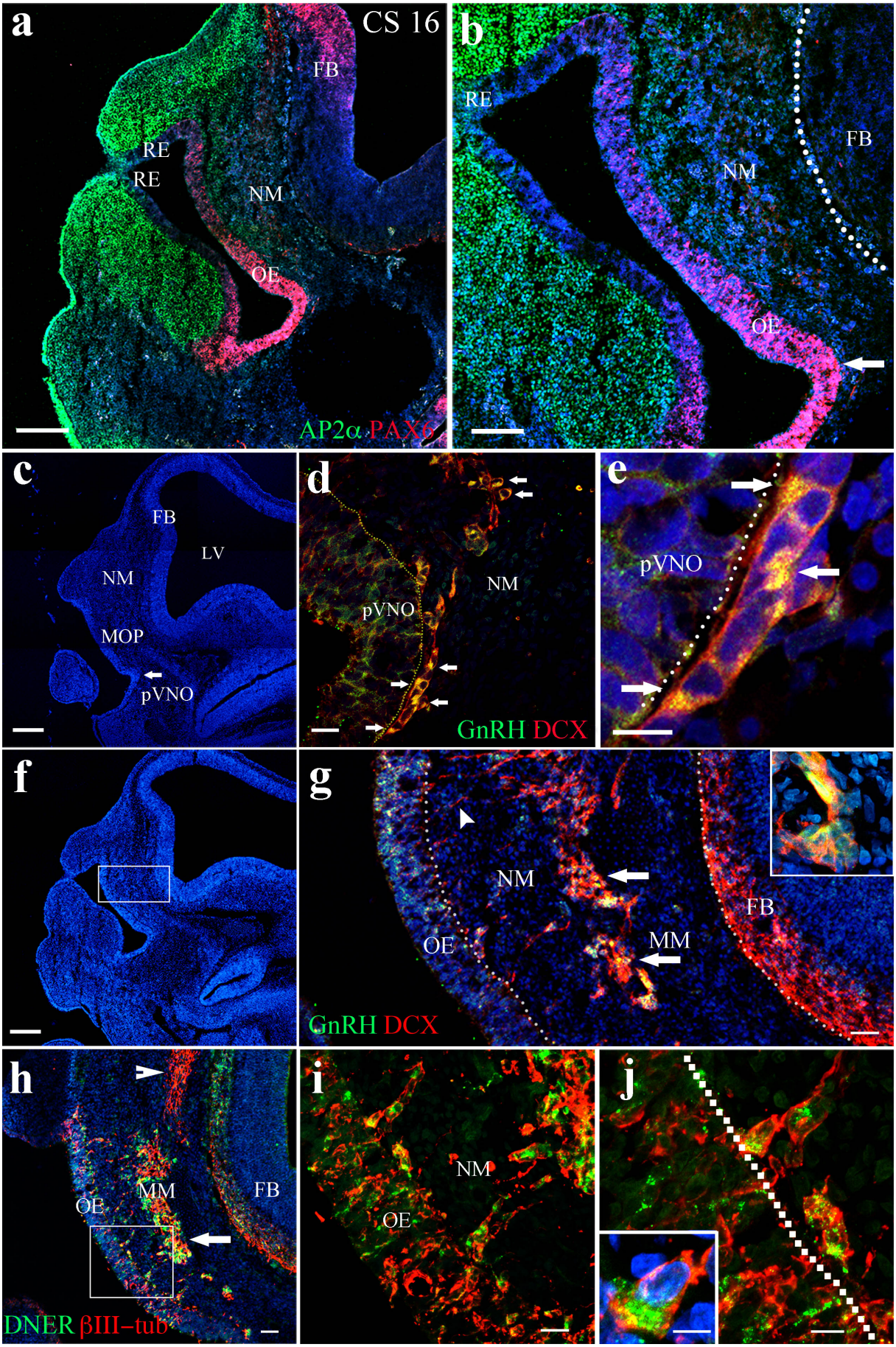
a
CS 16
FB
RE
RE
NM
OE
AP2α PAX6
b
RE
FB
NM
OE
c
FB
LV
NM
MOP
pVNO
d
NM
pVNO
GnRH DCX
e
pVNO
f
g
NM
OE
MM
FB
GnRH DCX
h
OE
MM
FB
DNER βIII-tub
i
NM
OE
j

7.2 Ontogenesis of GnRH neurons and the "migratory mass"

In rodents, early GnRH neurons migrate together with a heterogeneous coalescence of placode-derived and neural-crest-derived migratory cells (Forni et al., 2011) and olfactory axons, collectively called the "migratory mass" (Valverde et al., 1992; Miller et al., 2010). This cell migration precedes the targeting of olfactory sensory axons to the developing olfactory bulb (OB). The existence of a similar migratory mass in the human embryo has not yet been described. We thus immunolabelled consecutive sagittal sections of a CS 16 embryo for GnRH and Doublecortin (DCX; **Figure 42 d, e, g**), a marker of immature migratory neurons (Gleeson et al., 1999). We identified very few (50 in total) immature GnRH-expressing cells in the nasal mesenchyme, in the medial portion of the olfactory placode (**Figure 42 c-e**), adjacent to the basal lamina of the VNO, showing that the acquisition of cell identity occurs outside the vomeronasal epithelium, and several days earlier than previously thought (day 42 [Schwanzel-Fukuda et al., 1996]).

At this stage, we also observed a mixed mass of immature GnRH neurons expressing either DCX (**Figure 42 f-g**) or βIII-tubulin (**Figure 42 h-j**), migrating across the nasal mesenchyme towards the telencephalon. Furthermore, these pioneer neurons also expressed Delta/Notch-like EGF-related receptor (DNER, **Figure 42 h-j**), a transmembrane protein specifically localised in the dendrites and cell bodies of postmitotic neurons.

Our present data also suggest that the morphogenetic programs defining the development of the olfactory and vomeronasal systems and the molecular signature of the GnRH migratory route are at least partly conserved across evolution (Eiraku et al., 2002; Miller et al., 2010).

Figure 43. Development of the VNO and related cellular components

(**a–c**), GnRH and βIII-tubulin expression in a coronal section of a CS 18 embryo. (**a**), in the nasal placode GnRH+ cells (arrows) are apposed to the VNN (white square enlarged in **b**, arrows), in the OB, inside the brain at the level of the septum (white square). βIII-tub+ cells are detected in the olfactory placode at the level of VNN and the ON and inside the developing brain. (**b**), Magnification of the VNO and OE in (**a**). GnRH+ cells (arrows) are detected outside the VNO apposed to βIII-tub+ axons (arrowheads). (**c**), Caudally the VNO is fused with the developing OE. (**d**), GnRH+ cells migrate along Peripherin+ axons across the NM. (**e–g**) Expression of TAG-1 (**e**, arrows) and GnRH (**f**) in a CS 19 embryo shows that GnRH cells also use TAG-1 positive fibres as scaffold for migration (**g** merge). (**h–l**), Triple-immunostaining showing expression of GnRH, βIII-tubulin and SOX10 in a coronal section of a VNO at CS18. GnRH neurons (**i**) are intermingled in the NM with migratory neurons (βIII-tub+ **j**) and ensheathing SOX10+ cells (**k–l** merge). (**m–n**). Expression of Ki67, HuC-D (**m–n**) and SOX2 (**n**) inside the VNO at CS20.

Scale bars: **a** 500 μm; **b–c** 50 μm; **d**, **i–l** 10 μm; **e–f** 60 μm; **g**, **h**, **m**, **n** 20 μm.

Abbreviations: VNO: Vomeronasal Organ; OE: Olfactory epithelium; ON: Olfactory Nerve; OB: Olfactory Bulb; LV: lateral ventricle; VNN: Vomeronasal nerve; NEP: neuroepithelium.

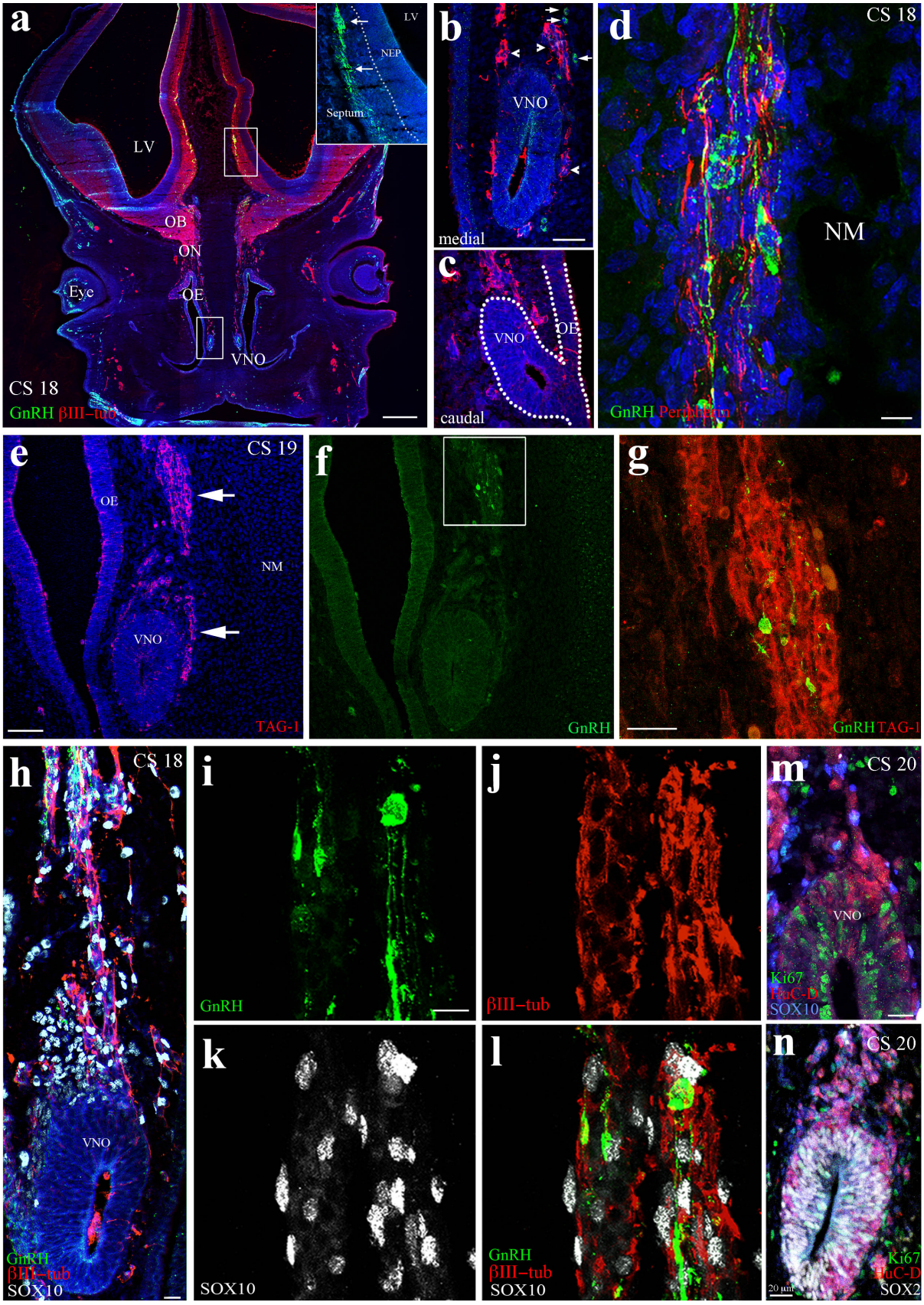
a
LV
NEP
Septum
OB
ON
Eye
OE
VNO
CS 18
GnRH βIII–tub
b
VNO
medial
c
VNO
OE
caudal
d
CS 18
NM
GnRH Peripherin
e
CS 19
OE
NM
VNO
TAG-1
f
GnRH
g
GnRH TAG-1
h
CS 18
VNO
GnRH
βIII–tub
SOX10
i
GnRH
j
βIII–tub
k
SOX10
l
GnRH
βIII–tub
SOX10
m
CS 20
VNO
Ki67
HuC-D
SOX10
n
CS 20
20 µm
Ki67
HuC-D
SOX2

7.3 Development of the vomeronasal and terminal nerves, and GnRH neuron migration

Neurons of the VNN and TN, which belong to the accessory olfactory system, develop simultaneously from the medial part of the nasal disc, together with GnRH neurons in mammals, including humans (Muller & O'Rahilly, 2004; Verney et al., 2002). The VNN and TN travel together across the nasal region (Brown, 1987), emerging from the vomeronasal epithelium and running medially from the olfactory epithelium towards the dorsal region of the OB. Their central entry, however, differs: it has been previously shown that the VNN reaches the dorsal region of the OB, namely the developing accessory olfactory bulb (AOB), responsible for coding pheromonal information after birth, whereas the TN projects both ventrally and dorsally within the forebrain, primarily to the septal, hypothalamic and limbic areas (Pearson, 1941a; Shwanzel-Fukuda & Silverman, 1980; Schwanzel-Fukuda & Pfaff, 1989; Verney, 1987; Wirsig-Wiechmann & Oka, 2002; Wray et al., 1989).

Our immunohistochemical studies of CS 18 embryos revealed a mixed population of VNN and TN axons emerging from the VNO, traveling across the nasal septum, crossing the cribriform plate and projecting into the telencephalon (**Figure 43a**). In other mammals, this axonal scaffold, which serves as a substrate for the migration of GnRH neurons, expresses the transient axonal glycoprotein 1 (TAG-1/Contactin-2) (Yoshida et al., 1995), the neuron-specific βIII-tubulin (Giacobini et al., 2008) as well as the neuronal type III intermediate filament protein peripherin (Wray et al., 1994). These markers are known to be expressed by a subset of developing olfactory, vomeronasal and terminal axons (Gorham et al., 1990; 1991) and to highlight the entire GnRH migratory scaffold from the olfactory pit to the medial septal area (Fueshko & Wray, 1994). Here, we provide evidence that peripherin (**Figure 43d**) and TAG-1 (**Figure 43e**) are also expressed along this scaffold of vomeronasal/terminal axons in CS 19 human embryos. At CS 18-20 (approx. 44 to 49 days of gestation), we observed GnRH-immunopositive neurons outside the VNO (**Figure 43a**). These cells were migrating across the nasal septum along βIII-tubulin- (**Figure 43a**) and TAG-1-positive (**Figure 43 f-g**) VNN/TN axon

bundles, which emerged from the VNO to project to the developing OB. Of note, only few days (approximately 5 days) after their initial appearance some GnRH neurons had already entered the telencephalon and could be seen in the OB, septum and ventral striatum (**Figure 43a**).

At CS 18, immunolabelling for the olfactory ensheathing cell marker SOX10 (Barraud et al., 2013; Forni et al., 2011; Miller et al., 2010) βIII-tubulin and GnRH revealed that olfactory ensheathing cells enwrapped VNN/TN axons (**Figure 43h**). GnRH neurons intermingled with SOX10-positive cells and immature migratory neurons (βIII-tubulin-positive) in the nasal mesenchyme, on their way from the VNO to the developing forebrain (**Figure 43 i-l**).

As mentioned above, in most terrestrial vertebrates, vomeronasal neurons project to the AOB. The presence of an accessory olfactory system has also been documented during foetal life in humans (Bossy, 1980; Chuah & Zheng, 1987). However, there is no evidence so far for a neuronal connection between the VNO and the AOB. We tested this possibility by performing immunohistochemistry for Neuropilin-2 (NRP-2) and GnRH on sagittal sections of GW 9 heads, which contained both the VNO and the AOB (**Figure 44 a-d**). NRP-2, the receptor for Semaphorin 3F, is highly expressed by a subset of vomeronasal sensory neurons in rodent embryos and along vomeronasal axons innervating the AOB (Cloutier et al., 2002). We also observed strong NRP-2 expression in developing neurons of the VNO at GW 9, as well as within the VNN as it crossed the nasal mesenchyme (**Figure 44 a-b**) and entered the brain through fenestrations of the cribriform plate (**Figure 44c**). GnRH neurons migrated in these regions in tight association with NRP-2-positive fibres (**Figure 44 a-c**). Moreover, analysis of the VNO target area revealed NRP-2-expressing fibres in the AOB but not the main OB (**Figure 44d**). These findings provide strong evidence for the anatomical connection between the human VNO and AOB.

7.4 High-resolution 3D imaging of the GnRH migratory pathway in human embryos

3D imaging of solvent-cleared organs (3DISCO) is a simple solvent-based clearing method used for transparentising the brain (Ertürk et al., 2012; Ertürk & Bradke, 2013). This method has been combined with immunolabelling followed by light-sheet laser-scanning microscopy (LSM) to study neuronal connectivity in mouse embryos and postnatal brains (Ertürk et al., 2012; Ertürk & Bradke, 2013; Belle et al., 2014). Here, we adapted this technique for the first time to a whole CS 19 human embryo (approx. 48 day of gestation, **Figure 45**). Whole-mount immunolabelling for GnRH and peripherin followed by 3DISCO optical clearing and LSM provided excellent clearing of the tissue and high-resolution imaging of immunofluorescent signals (**Figure 45 a-b**). The peripherin antibody allowed us to visualize motor and sensory fibres of the entire peripheral nervous system in human embryos, including cranial nerves and nerves innervating the limbs (**Figure 45 a-b**), in addition to the scaffold of olfactory, vomeronasal and terminal axons observed above by conventional 2D histology (**Figure 43d**).

High-resolution 3D imaging of the CS 19 head permitted us to visualize migratory GnRH neurons and the intracranial projections of the terminal nerve (**Figure 45 c-f**). The intracranial projections of the TN had already reached the medial septal area by this embryonic stage. Unexpectedly, a considerable subset of TN fibres sprouted dorsally and laterally to telencephalic regions corresponding to the neocortex and the developing hippocampus (**Figure 45 d-f**). We found that GnRH neurons were consistently juxtaposed to the peripherin-positive VNN/TN while migrating from the nose into these telencephalic areas (**Figure 45 d-f**).

We next optically sliced the immunolabelled head of the CS 19 embryo (**Figure 45g**) and analysed these digital coronal slices. The fact that GnRH neurons appear for the first time in the immediate vicinity of the VNO and nowhere else further establishes the VNO as their site of origin (**Figure 45g**). These studies also confirm that the VNO maintains continuity with the olfactory epithelium in more caudal positions (**Figure 45g**).

We next performed whole-mount GnRH immunolabelling of a CS 21 human embryo (approx. 53 day of gestation) and documented the 3D distribution of GnRH neurons (**Figure 46 a-b**). At this stage, GnRH cells migrated within the brain in chain-like structures and proceeded dorsally and laterally towards the septum, OB and cortex (**Figure 46 a-b**, arrowheads). Moreover, some GnRH-positive cells formed a loop and started turning ventrally towards the developing hypothalamus (**Figure 46 a-b**).

A few days later, at GW 9, many GnRH neurons were still found in the nasal compartment in close association with TAG-1-immunoreactive VNN/TN axons. In addition, some GnRH cells had assumed a peculiar ring-like distribution, forming two symmetric circles around the developing OB (**Figure 46 c-d**). Inside the brain, GnRH neurons were no longer organized in continuous chains but were rather more widely spaced and scattered across multiple areas (**Figure 46 e-f**).

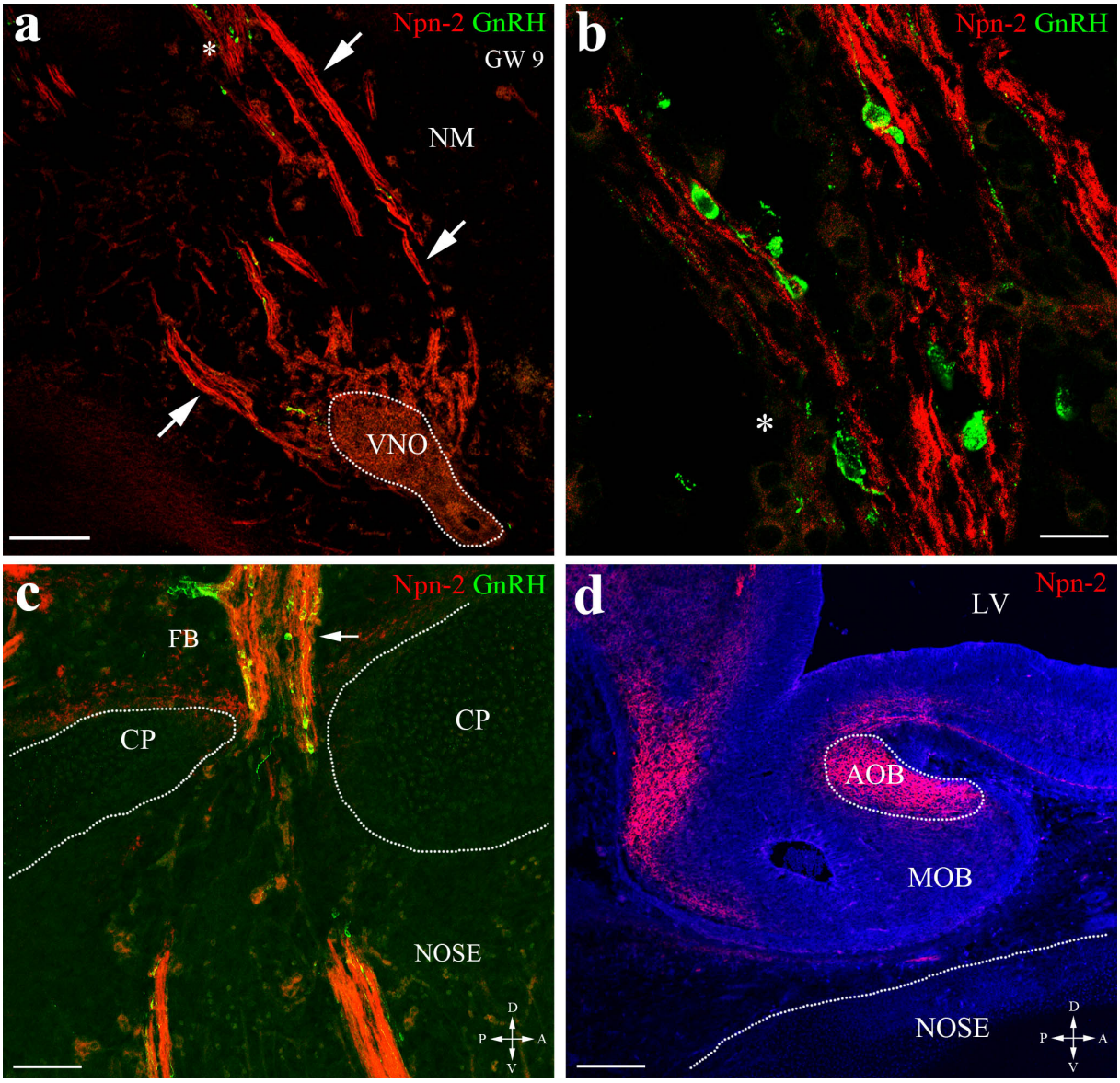

Figure 44. The AOB is anatomically connected with VNO

Sagittal (a, b, d) or coronal sections (c) through the nose of a GW 9 foetus immunostained for Npn-2 and GnRH. (a) Npn-2 is expressed by axons emerging from the VNO (arrows). (b) High magnification of the area indicated by the asterisk in a. GnRH neurons migrate toward the forebrain along Npn-2-immunoreactive VNO axons. (c) Npn-2 positive axons enter the forebrain through the fenestrations of the cribriform place (arrow). (d) Npn-2-immunoreactive fibres project to the AOB but not the MOB. Scale bars: a 100 μm; b 20 μm; c-d 80 μm. Abbreviations: CP: cribriform plate; FB: forebrain; NM: nasal mesenchyme; AOB: accessory olfactory bulb; MOB: main olfactory bulb; LV: lateral ventricle.

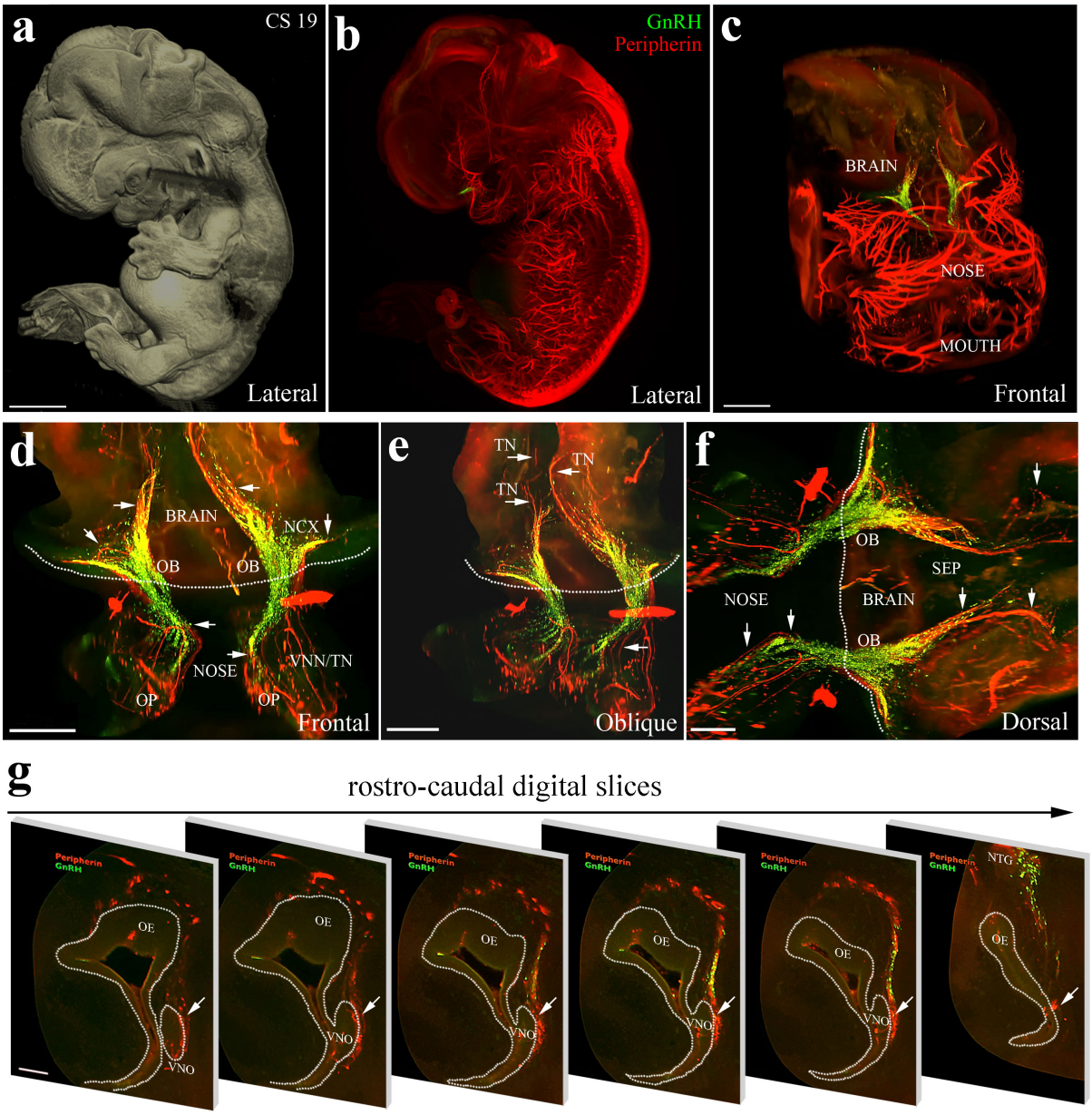

Figure 45. Whole-mount immunolabelling and optical clearing of a CS 19 embryo.
CS19 embryo labelled with anti-GnRH and anti-peripherin antibodies. (a) lateral view after digital surface contrast. (b) Lateral view of the entire transparent embryo depicting the peripheral nervous system (peripherin-immunofluorescence) and the GnRH migratory neurons (green). (c-d) frontal, (e) oblique, (f) dorsal view respectively. GnRH neurons migrate from the nose into the brain along the VNN/TN nerves. (g) Rostro-caudal optical sections of the nasal region of the same embryo. GnRH neurons emerge from VNO (arrows) and migrate along the VNN/TN. The VNO is separated from the OE rostrally but it is fused with the OE caudally.
Scale bars: a 1500 µm; c-f 300 µm; g 100µm. OP: olfactory placode; VNN: vomeronasal nerve; TN: terminal nerve; OB: olfactory bulb; PC: piriform cortex; SEP: septum.

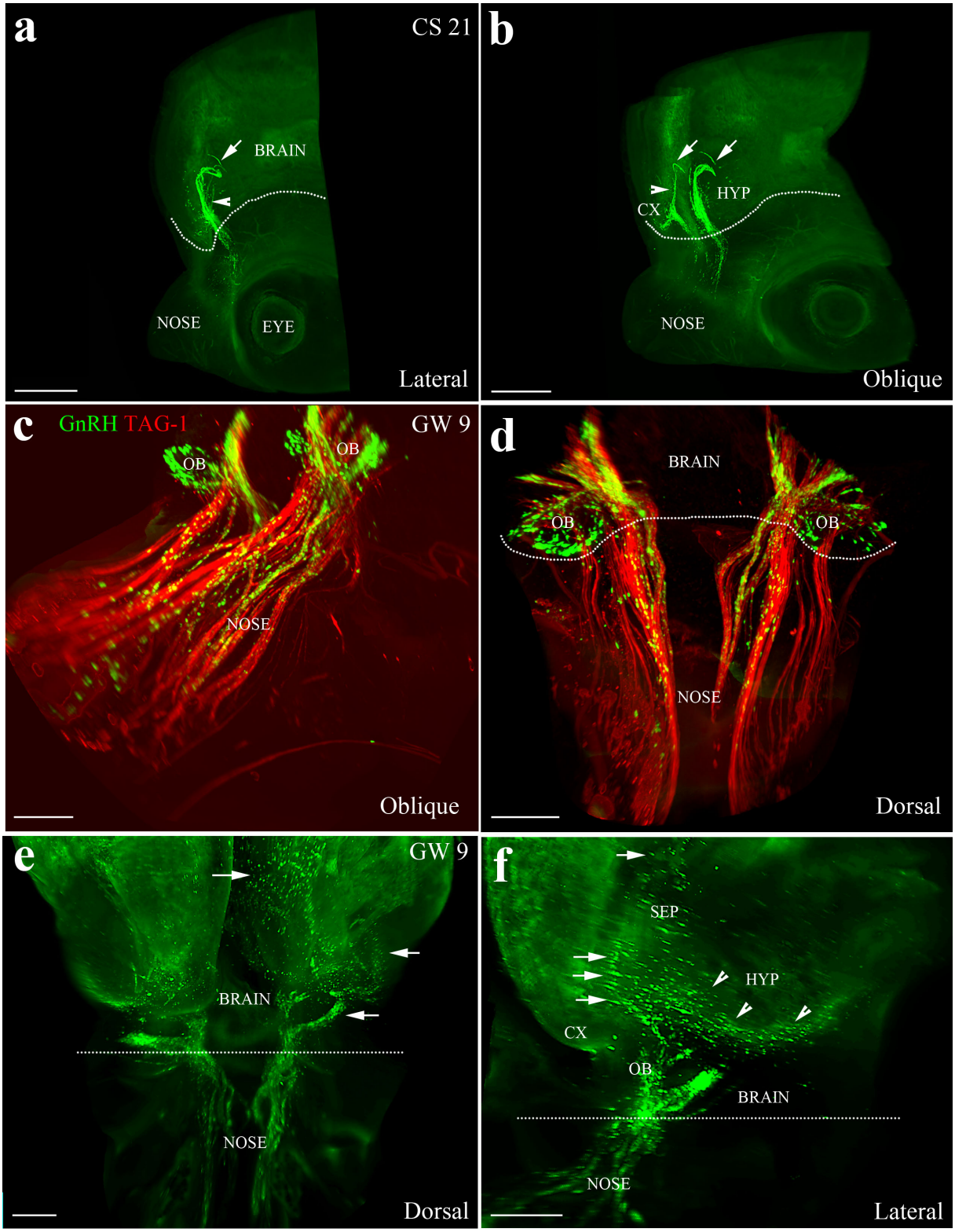
a
CS 21
BRAIN
NOSE
EYE
Lateral
b
HYP
CX
NOSE
Oblique
c
GnRH TAG-1
GW 9
OB
OB
NOSE
Oblique
d
BRAIN
OB
OB
NOSE
Dorsal
e
GW 9
BRAIN
NOSE
Dorsal
f
SEP
HYP
CX
OB
BRAIN
NOSE
Lateral

Figure 46. Whole-mount immunolabelling and 3DISCO clearing of a CS 21 embryo and two GW 9 foetuses.

(a-b) Lateral and oblique projections of the whole head of a CS 19 embryo immunostained for GnRH. Chains of GnRH neurons enter the brain and progress either dorsally (arrows) or ventrally (arrowheads) toward the developing hypothalamus. (c-d), whole-mount GnRH/TAG-1 immunolabelling of a GW 9 foetal nose. (e-f), dorsal and lateral projections of a GW 9 head immunostained for GnRH. At this stage, GnRH neurons are distributed in several brain areas, including the hypothalamus.

Scale bars: a-b 500 μm; c-d 200 μm; e 300 μm; f 400 μm. Abbreviations: CX: cortex; HYP: hypothalamus; OB: olfactory bulb; SEP: septum.

7.5 Distribution and number of GnRH neurons in the human foetal brain

In rodents, GnRH neurons migrate into the forebrain and appear to detach from the peripherin-positive terminals of VNN/TN fibres before entering the septal-preoptic area (Yoshida et al., 1995). In order to determine whether this was also the case in humans, coronal sections of a CS 23 foetus (approx. GW 8) were immunolabelled for peripherin and GnRH. Peripherin-positive fibres projected deeper than expected, to the mediobasal hypothalamus and developing median eminence (**Figure 47a**). GnRH neurons were detectable in these regions, but always in tight apposition to peripherin-positive fibres right up to their target sites (**Figure 47a**, inset), indicating that migrating GnRH neurons in humans never lose contact with the TN axonal scaffold right up to their target sites. This suggests a fundamental difference between rodents and humans in the mode of migration of GnRH neurons during the last phase of their journey. Alternatively, VNN/TN axonal terminals might also persist in these areas of rodents but they no longer express peripherin.

At GW 9, in keeping with the identification of a dorsal/lateral branch of the TN in CS 19 embryos, GnRH neurons were distributed along two different migratory streams. The first, a ventral migratory pathway directed towards the presumptive hypothalamic regions (**Figure 47b**, white arrow), has previously been documented in humans (Schwanzel-Fukuda & Pfaff, 1989; Schwanzel-Fukuda et al., 1996) and in other vertebrates (Forni & Wray, 2015). In addition,

here we provide evidence for an unexpected dorsal migratory pathway for GnRH neurons, directed towards pallial and subpallial telencephalic regions (**Figure 47b**, red arrow).

To understand in greater detail the anatomical distribution of GnRH neurons in human foetal brains, we performed 3D reconstruction analysis of serial sections at this foetal stage (GW 9, *n* = 2; **Figure 47c**). Our analysis confirmed that GnRH neurons migrated into the brain along two main migratory pathways, including the newly identified dorsal pathway. The latter pathway comprised two components:

- a medial one reaching the septum/diagonal band of Broca, indusium griseum/presumptive hippocampus and rostro-medial neocortex
- a lateral one reaching the ventral striatum, piriform cortex and amygdala (**Figure 47c**).

An anatomical atlas of the developing human GnRH cells is currently unavailable. To generate a detailed distribution map of GnRH neurons in GW 12 foetuses (the latest developmental stage available for these studies), we immunolabelled serial coronal sections of GW 12 heads and performed a 3D reconstruction of GnRH-immunoreactive cell bodies and fibres (*n* = 2; **Figure 48 a-b**). This experiment revealed a surprisingly wide/broad distribution of GnRH cell bodies and fibres in hypothalamic (**Figure 48 a-d**) as well as several extrahypothalamic areas, including the olfactory bulbs, cerebral cortex, hippocampus, piriform cortex, amygdala and habenula (**Figure 48 a, b, e**).

We next counted GnRH cells at different developmental stages between GW 5.5 (CS 16) and GW 12. At CS 16 (the earliest embryonic stage we had access to, n = 1), we observed 50 GnRH neurons, all of which were restricted to the nasal region, confirming that the birthdate of GnRH neurons in humans is around gestation day 39 (**Figure 49a**). Only a few days later (GW 6: CS 17-18, *n* = 3), the number of GnRH neurons had jumped to 7951 ± 2000, suggesting that most of these cells are already born by the 39th day of gestation, and that GnRH neuronal differentiation occurs between the 39th and 44th day (**Figure 49a**). On average, around 10000 GnRH neurons were detectable at 4 developmental stages: CS 17 and 18 and GW 11 and 12

(Figure 49a). We did not observe any sex difference in the number of GnRH cells in GW 7–10 foetuses (n = 4 males, mean GnRH cell number = 11123 ± 2815; n = 4 females, mean GnRH cell number = 10565 ± 1693; t–test P = 0.8706). At each stage, we also quantified the relative distribution of GnRH cell bodies in 3 different areas: the nose/OB, and the ventral and dorsal migratory streams (Figure 49b). At CS 16, GnRH–immunoreactivity was restricted to the nose. At CS 17–18, approximately 60% of the cells were migrating within the nose, 36% had entered the brain along the dorsal migratory stream and 4% had started to turn ventrally towards the basal forebrain. During subsequent stages (CS 19 to GW 12, n = 11; Figure 49c), the number of cells in the nose progressively decreased, with a concomitant increase in cells in the dorsal and ventral migratory pathways. At the latest time point analysed (GW 11–12, n = 3), only 23% of GnRH neurons were located in the more rostral regions (nose/OB).

Figure 47. GnRH neurons migrate following a dorsal and a ventral migratory pathway both in human and mouse foetuses

(a) Representative coronal section of a GW 9 foetal hypothalamus immunolabelled for GnRH (green) and peripherin (red). Peripherin-immunopositive fibres project to the basal hypothalamus and developing median eminence. Inset in (a) shows that GnRH neurons migrate to their final hypothalamic target areas in tight association with the peripherin-positive fibres. (b) Representative sagittal section of a CS 23 foetal brain immunolabelled for GnRH. GnRH neurons enter the brain following a dorsal (red arrow) and a ventral (white arrow) migratory pathway. Inset in b shows a high magnification of migratory GnRH cells in the dorsal pathway. (c) Front (left) and perspective (right) views of a 3D model of the GnRH neurons cell bodies distribution in a 9 GW embryo. Each cell is represented by a sphere (100 μm in diameter) coloured according to their location (legend on the left). Transparent contours of nasal mesenchyme (NS), olfactory bulb (OB) septum/diagonal band of Broca (SEP/DB) and induseum griseum/hippocampus are also shown for reference. In the inset, the position of these contours, together with the nasal turbinates (cyan) is shown. (d–e) Lateral, (f) frontal, (g) caudal and dorsal projections (h–i) of the whole head of an E16.5 mouse embryo immunostained for GnRH and cleared using 3DISCO. Arrowheads indicate chains of GnRH neurons entering the brain and progressing dorsally. GnRH neurons are found in the neocortex (NCX), septal/diagonal band of Broca (SEP/DB) and hypothalamus (HYP; arrows in e), around the olfactory bulbs (OB; arrow in f). NCX and piriform cortex (PCX; arrows in g and h) and in deep brain areas corresponding to fornix and developing hippocampus (arrow in i). NM: nasal mesenchyme. Scale bars: a, 100 μm; inset in a 20 μm; b 50 μm; inset in b 10μm; d 400 μm; e 200 μm; f 180 μm; g–i 600 μm.

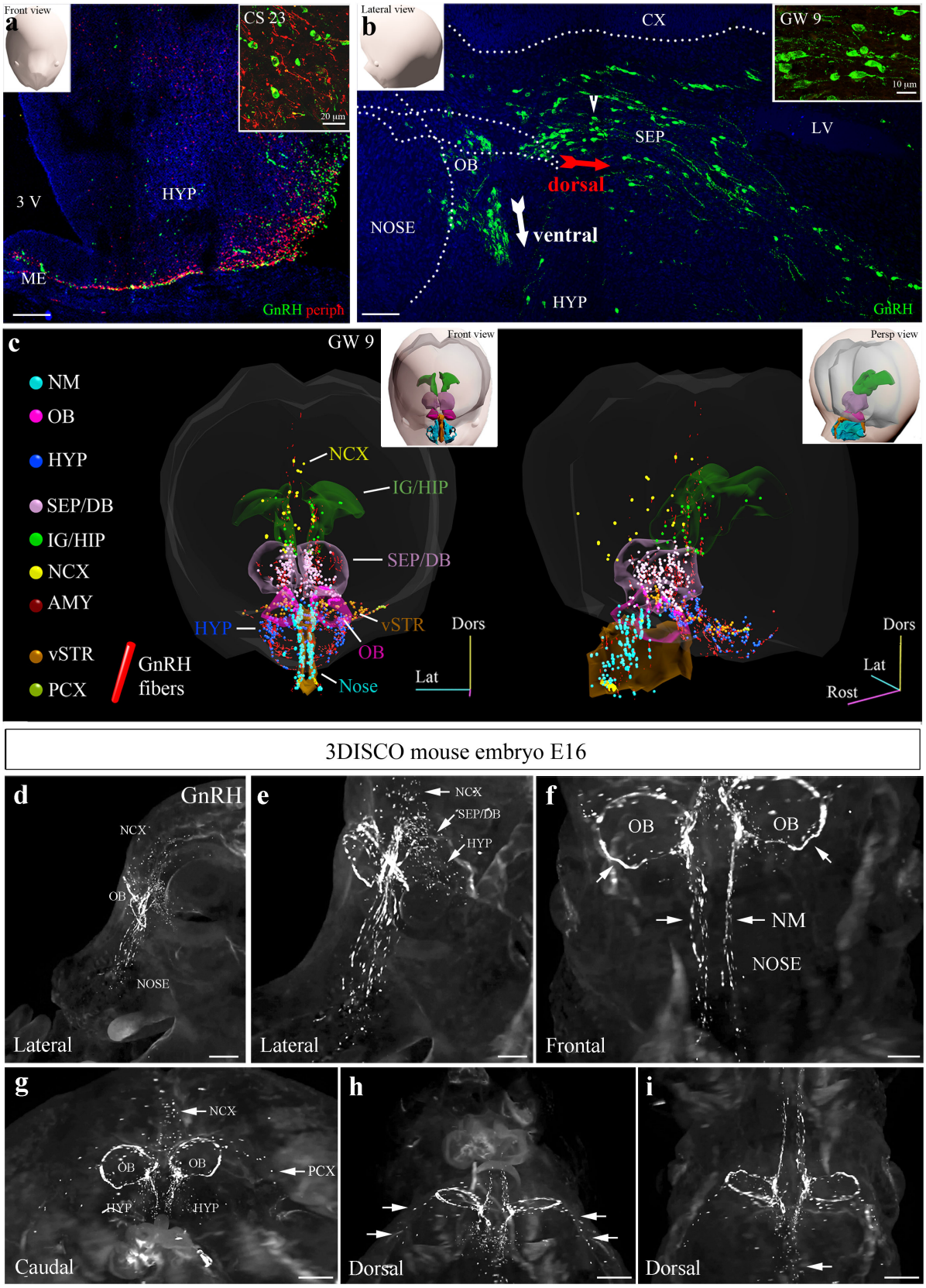
a
Front view
CS 23
20 µm
3 V
HYP
ME
GnRH periph
b
Lateral view
CX
GW 9
10 µm
SEP
LV
OB
dorsal
NOSE
ventral
HYP
GnRH
c
GW 9
Front view
Persp view
NM
OB
HYP
SEP/DB
IG/HIP
NCX
AMY
vSTR
PCX
GnRH fibers
NCX
IG/HIP
SEP/DB
HYP
vSTR
OB
Nose
Dors
Lat
Dors
Lat
Rost
3DISCO mouse embryo E16
d
GnRH
NCX
OB
NOSE
Lateral
e
NCX
SEP/DB
HYP
Lateral
f
OB
OB
NM
NOSE
Frontal
g
NCX
OB
OB
PCX
HYP
HYP
Caudal
h
Dorsal
i
Dorsal

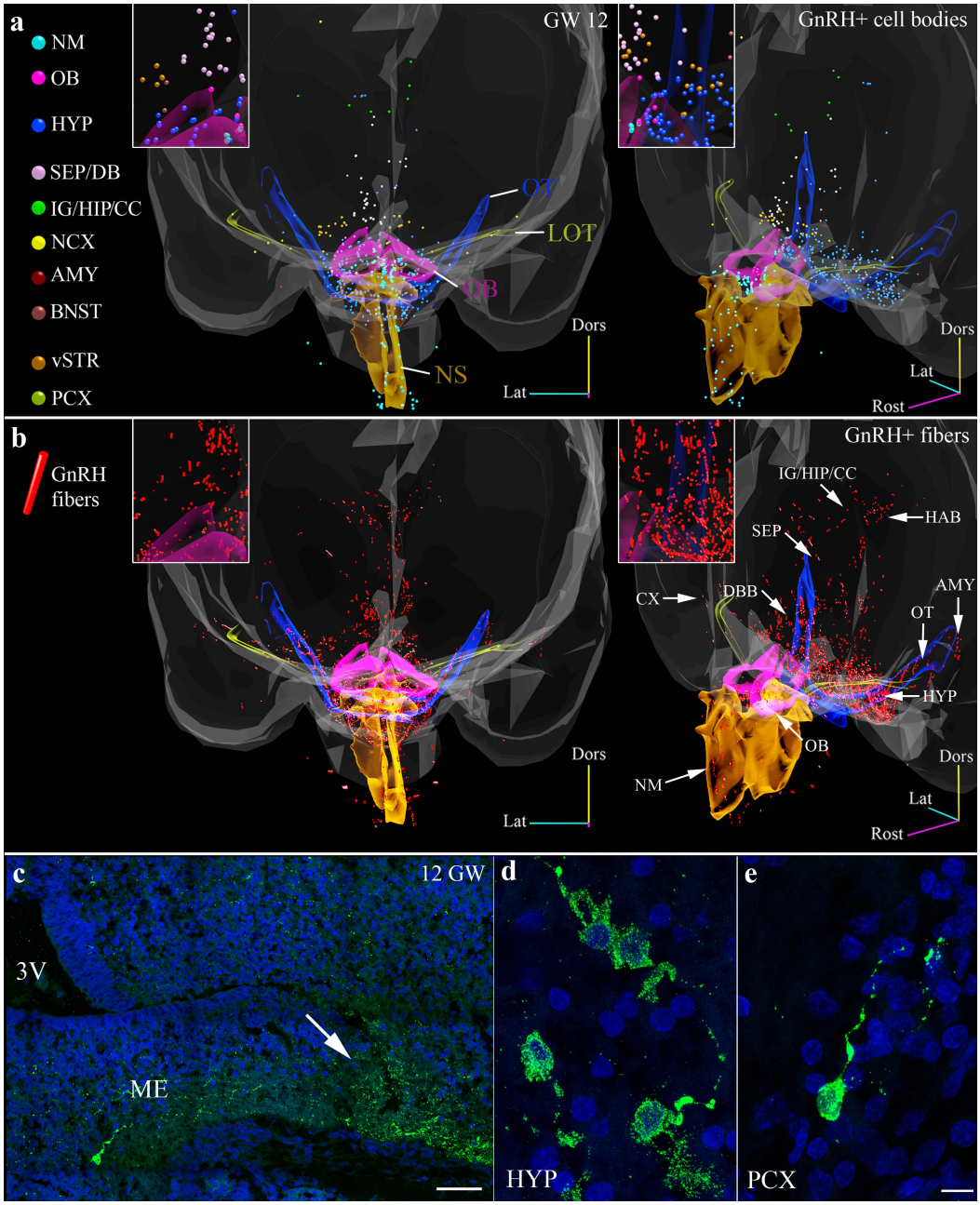

Figure 48. Distribution of GnRH cell bodies and neurites at GW 12.

(a) Front (left) and perspective (right) views of a 3D model of the GnRH neurons cell bodies distribution in a GW 12 embryo. Each cell is represented by a sphere (100 μm in diameter) coloured according to their location (see legend on the left). Transparent contours of nasal septum (NS), olfactory bulb (OB), lateral olfactory tract (LOT) and optic tract (OT) are also shown for reference. Higher magnification of a small detail of the 3D model is shown. (b) Same views of the 3D models in a) showing the distribution of GnRH fibres (red bars). (c–e) Representative sections of a GW 12 foetal brain immunolabelled for GnRH. GnRH terminals are already detectable in the median eminence (ME, arrows in c) and GnRH expressing cells are found in the hypothalamus (HYP, d) and piriform cortex (PCX, e). Scale bars: c 40 μm; d–e 10 μm.

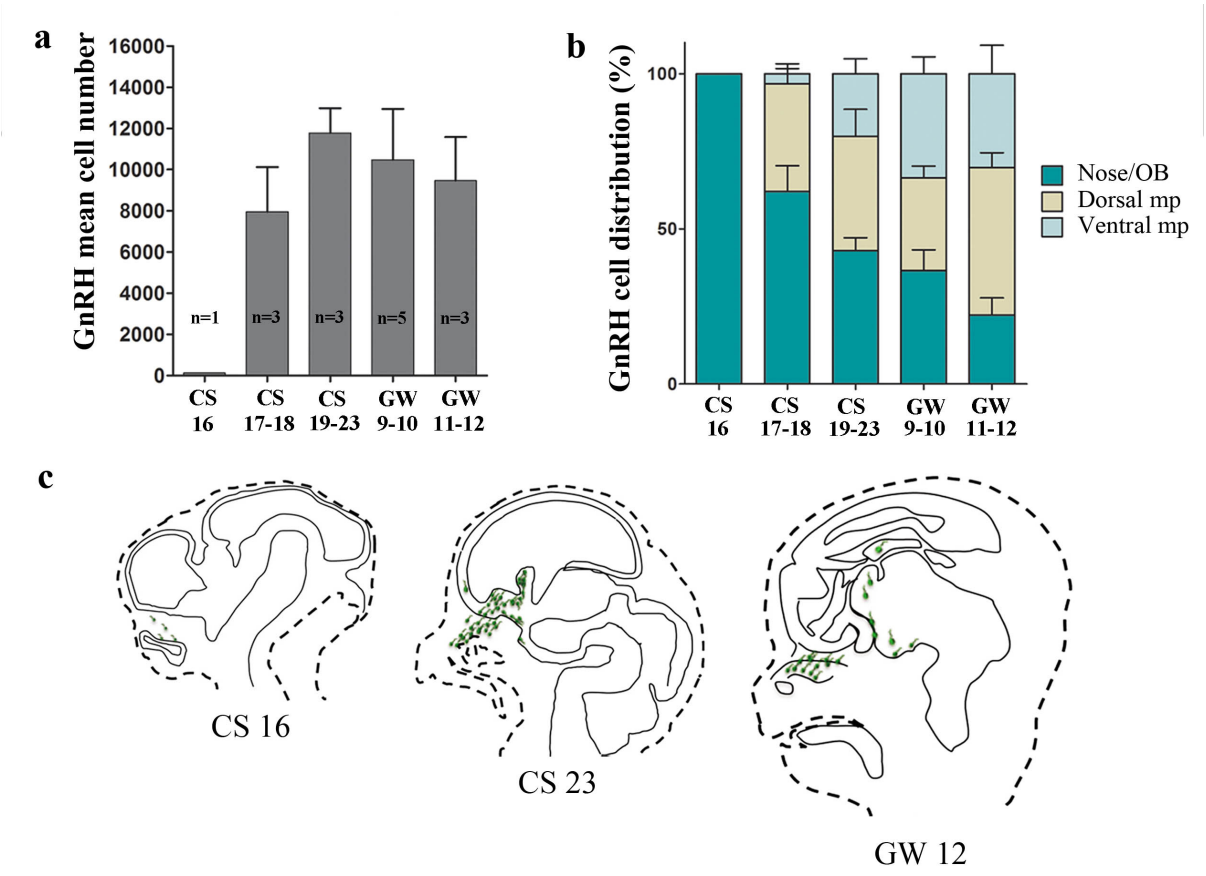

Figure 49. Quantification of GnRH neurons during the first trimester of gestation.
(a) Quantification of the total mean GnRH cell number during the first trimester of gestation in humans as function of the developmental stages. (b) Distribution of GnRH cells expressed as % of total cells calculated as function of the developmental stages in 3 anatomical compartments: nose, dorsal and ventral migratory pathway. (c) Schematic representation of GnRH migration during first trimester of gestation in humans. Values shown are means ± SEM.

7.6 Confirmation of novel human findings in the mouse embryo

In light of the various novel observations made above regarding GnRH neuronal migration and distribution in humans, we addressed the possibility that some of these features might have been previously overlooked in rodents due to their small (about 800 neurons) and scattered GnRH population and the limitations of conventional 2D histology. Using 3DISCO technology coupled with LSM, we performed a detailed topographical analysis of individual GnRH-immunoreactive neurons scattered over large brain areas of an E16 whole mouse embryo (**Figure 47 d-i**). This analysis confirmed the presence of a dorsal tract of migratory GnRH neurons, comprising two telencephalic cell populations oriented dorsally and laterally, respectively (**Figure 47 d-i**), in addition to the well-known ventral pathway. Our analysis also revealed a small GnRH neuronal population in pallial and subpallial regions (**Figure 47 e, h, i**).

Mimicking our observations on human foetuses (**Figure 46 c-d**), GnRH neurons of mouse embryos formed a peculiar ring of cells surrounding the trunk of the OB (**Figure 47f**). In postnatal day 1 mice, when GnRH neuronal migration is complete, 12-14 % of GnRH neurons are still known to reside within the nose (Hanchate et al., 2012). Using the same technique, therefore, we further investigated whether GnRH neurons were still present in the mouse OB postnatally or if they were lost during development (**Figure 50**). In whole-mount GnRH-immunolabelled adult mouse brain hemispheres (n = 2, 4 months old males; Fig. 6a-e), GnRH neurons and fibres were visible in the hypothalamic regions (**Figure 50b**), as expected. Moreover, we detected robust GnRH immunoreactivity at the caudal end of the OB (**Figure 50c**), at the border with the cortex. These GnRH neurons maintained their ring-like distribution around the trunk of the OB (**Figure 50d**). Within the OB, GnRH neurons were abundantly distributed inside the structure specialized in pheromone detection - the AOB (**Figure 50d**, dotted red circle, coronal view; **Figure 50e**, white dotted area, sagittal view). In adult mouse OBs (n = 2, 5 months old females; **Figure 50 f-g**) GnRH neurons were still detected in the glomerular layer of the main and accessory olfactory bulb (**Figure 50 f Figure 50**) as well as in the olfactory nerve layer (**Figure 50h**).

Figure 50. Whole-mount immunolabelling and 3DISCO clearing of adult mouse brain hemispheres.

Adult mouse brain hemisphere labelled with anti-GnRH antibody (4 months old, males, n = 2). (**a**) Lateral, frontal and ventral views after digital surface contrast masks. (**b-c**) Lateral views of the entire transparent hemi brain showing the GnRH-immunoreactive neurons respectively in the preoptic-hypothalamic regions (**b**) and in the OB (**c, arrows**). (**d-e**) Rostral and sagittal optical sections of the OB containing GnRH neurons. (**f-h**) GnRH immunoreactivity in a representative coronal section of an adult mouse OB (5 months old, females, *n* = 2). (**f**) Low magnification confocal picture of the OB depicting the distribution of GnRH cells and fibres in the glomerular layer (Gl) of the main olfactory bulb (MOB) and accessory olfactory bulb (AOB), and in the olfactory nerve layer (on). (**g-h**) High magnification picture of the AOB (**g**) and ON (**h**).

Other abbreviations, OB: olfactory bulb; CX: cortex; CC: corpus callosum; HYP: hypothalamus; POA: preoptic area; Grl: granular layer. Scale bars: **a** 1000 μm; **b** 400 μm; **c** 700 μm; **d** 500 μm; **e** 300 μm; **f** 120 μm; **g** 30 μm; **h** 20 μm, inset in **h** 10 μm.

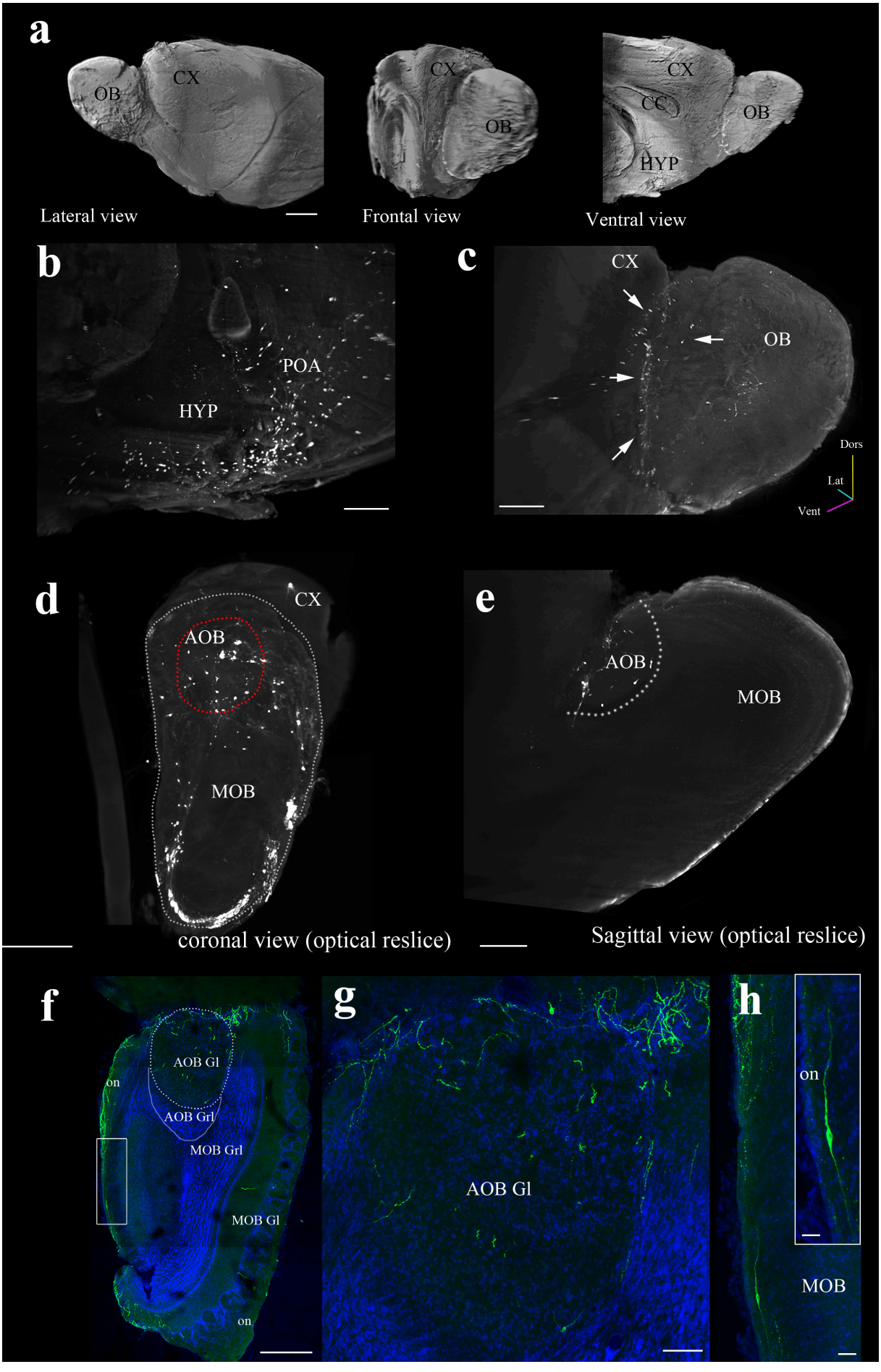
a
OB
CX
Lateral view
CX
OB
Frontal view
CX
CC
OB
HYP
Ventral view
b
POA
HYP
c
CX
OB
Dors
Lat
Vent
d
CX
AOB
MOB
coronal view (optical reslice)
e
AOB
MOB
Sagittal view (optical reslice)
f
AOB Gl
on
AOB Grl
MOB Grl
MOB Gl
on
g
AOB Gl
h
on
MOB

CHAPTER 8

Anti-Müllerian hormone & the regulation of the development of the GnRH system

Defective Anti-Müllerian Hormone Signalling Alters the Development of the GnRH/Olfactory Systems and Contributes to Congenital Hypogonadotropic Hypogonadism

Samuel A. Malone, Giorgos Papadakis, Daniele Cassatella, James Acierno, Andrea Messina, Cui Xu, Irene Cimino, Nour El Houda Mimouni, Pascal Pigny, Nelly Pitteloud and Paolo Giacobini

In preparation for submission

8.1 Introduction

Gonadotropin releasing hormone (GnRH) is essential for puberty onset and reproduction. GnRH is released into the pituitary portal blood vessels for delivery to the anterior pituitary where it controls the production and release of the gonadotropins LH (luteinizing hormone) and FSH (follicle stimulating hormone), which stimulate gametogenesis and sex steroid production in the gonads (Christian & Moenter, 2010). GnRH – secreting neurons are unusual neuroendocrine cells as they originate during embryonic development outside the central nervous system, in the nasal placode, and migrate to the hypothalamus apposed to vomeronasal and terminal nerves (VNN, TN) (Schwanzel-Fukuda & Pfaff, 1989; Wray et al., 1989). This process is evolutionarily conserved and follows a similar spatio-temporal pattern in all mammals (Schwanzel-Fukuda & Pfaff, 1989; Wray et al., 1989), including humans (Casoni et al., 2016; Schwanzel-Fukuda et al., 1996). Disruption of GnRH neuronal migration and/or defective GnRH synthesis and secretion lead to congenital hypogonadotropic hypogonadisms (CHH), a rare endocrine disorder (prevalence: 1 in 4,000) characterized by absent or incomplete puberty resulting in infertility (Boehm et al., 2015).

The association of CHH with a defective sense of smell (anosmia or hyposmia), which is found in approximately half of CHH patients, is termed Kallmann syndrome. CHH is clinically and genetically heterogeneous, with > 30 different causal genes identified to date (Boehm et al., 2015) and possesses various modes of transmission, including oligogenic inheritance (Sykiotis et al., 2010). However, the mutations thus far identified account for only half of clinically reported cases. This suggests that: 1) other causal genes remain to be discovered and 2) unravelling new genetic pathways involved in the regulation of the development of the GnRH system is relevant for understanding the basis of pathogeneses leading to human CHH disorders.

We have recently shown that GnRH neurons both in mice and humans express the AMH receptor (AMHR2) from early foetal development to adulthood (Cimino et al., 2016). AMH signals by binding to a specific type II receptor (AMHR2) (Baarends et al., 1994; di Clemente

et al., 1994), that heterodimerises with one of several type I TGF-β receptors (AcvR1 [ALK2], BMPR1a [ALK3] and BMPR1b [ALK6]), and recruits SMAD proteins that subsequently undergo nuclear translocation to regulate target gene expression (Josso et al., 2003). AMH is the only known ligand of AMHR2, suggesting that tissues expressing this receptor are likely to be targets of AMH. However, the sole source of AMH during embryonic development is considered to be the testis, which produces and secretes AMH, responsible for initiating regression of the Müllerian ducts, and thus controlling normal male sexual differentiation (Behringer et al., 1994).

Both in mice and humans, homozygous mutations of the AMH (OMIM: 600957) or AMH receptor (OMIM: 600956) genes lead to persistent Müllerian duct syndrome (PMDS), characterised by the retention of Müllerian duct derivatives: the uterus, Fallopian tubes, and upper part of the vagina, in otherwise normally virilised genetic males (46XY) (Behringer et al., 1994; Bellville et al., 2004; Josso & di Clemente, 2003; Mishina et al., 1999; Orvis et al., 2008).

Here, we report embryonic expression of AMH in extra-gonadal tissues, namely in olfactory and vomeronasal receptor neurons as well as on their axons, along which GnRH neurons migrate. We show that migratory GnRH cells and the olfactory/vomeronasal scaffold express both AMH and AMH receptors, while pharmacological perturbation of the AMH/AMHR2 signal transduction pathway *in vivo* alters GnRH migration. Furthermore, we employed tissue-clearing and whole-mount immunohistochemical techniques (Belle et al., 2014, 2017; Casoni et al., 2016; Ertürk et al., 2012) to meticulously study the 3D organization of the GnRH and olfactory systems in *AMHR2* wild-type and knock-out embryos. These experiments confirmed that AMH-defective signalling leads to abnormal development of the olfactory and terminal nerves and defective embryonic migration of the GnRH cells to the basal forebrain, leading to a reduced size of this neuronal population in adult brains and diminished ovulation. Using different experimental approaches, we demonstrated that AMH promotes the migratory activity of immortalized GnRH cells through AMHR2/BMPR1b signalling and activation of the MAPK pathway.

Finally, using an unbiased whole genome sequencing (WGS) approach, we identified significant evidence for association between functional mutations in the *AMH* gene and CHH. Collectively, our data reveal a novel functional role of AMH in the development of GnRH neurons, ensuring their appropriate entrance into the brain and they provide genetic evidence that AMH signalling insufficiency can contribute to a CHH phenotype in humans

8.2 AMH and its signalling pathway are expressed in and around the GnRH migratory pathway

We have recently shown that GnRH neurons both in mouse and human foetuses express AMHR2 during their migration (Cimino et al., 2016). We thus sought to understand whether there was a local source of AMH in the nasal compartment that may regulate GnRH migration. Qualitative PCR for *AMH*, *AMHR2*, its co-receptors and canonical intracellular signalling pathways revealed mRNAs expression of all genes (apart from *SMAD8*) in the embryonic nose at E11.5 (**Figure 51a**). We then performed qualitative and quantitative PCR analyses of FACS-isolated GFP-expressing GnRH neurons from *GnRH::GFP* mice (Spergel et al., 1999) and revealed expression of *AMH* transcript in GnRH neurons from early embryonic development (E12.5) to adulthood (PN90; **Figure 1b-d**).

Ex vivo cultures of E11.5 nasal explants have been used to study factors regulating GnRH migration by both our group (Giacobini et al., 2004, 2007) and others (Fueshko & Wray, 1994). At 4 days *in vitro* (DIV), olfactory axons, which express β-tubulin (TUJ1), emerge from the nasal explant tissue mass and GnRH neurons begin migrating out from the explant, tightly associated to those fibres (**Figure 51e**). We generated nasal explants from *GnRH::GFP* embryos and show that antisera against AMH labels migrating GnRH neurons at 4 days *in vitro* (**Figure 51 e-f**), confirming AMH protein expression in these cells.

We also verified that the AMH protein is expressed *in vivo* by immunolabelling of coronal sections of the nasal compartment at E13.5 (**Figure 51 g-k**). At this time, AMH expression is

found to be localised to the vomeronasal organ (VNO), olfactory epithelium (OE) and to presumptive VNN/TN fibres (as well as migrating GnRH neurons themselves), indicating that it is expressed all along the GnRH migratory route through the nose.

Figure 51. AMH and its signalling pathway is expressed in the embryonic nose

(a) Schematic of a mouse embryo indicating the plane of dissection to remove the nasal compartment. Representative qualitative PCR bands are shown for the expression of *AMH*, its obligatory receptor *AMHR2*, its known co-receptors *AcvR1*, *BMPR1a*, *BMPR1b* and its classical intracellular signalling pathways, *SMAD1/5/8* and *β-catenin*. All components of the AMH signalling pathway are present in adult brain lysate and expression of all components except *SMAD8* were found in the embryonic nose at E11.5 (b) schematic illustrating the FACS of GnRH::GFP mice to isolate a GnRH cell population. (c) Qualitative PCR demonstrating *AMH* is expressed by migrating GnRH cells at E12.5, and *AMH* expression is also found in the head at this time point. (d) qPCR showing the relative abundance of *AMH* mRNA expression in GnRH cells during embryogenesis and postnatal life. (e) Culture of a nasal explant after 4 days in vitro, at this point olfactory axons labelled with TUJ1 (red) can be seen migrating out of the explant, with GnRH cells (green) closely apposed. (f) Inset of e, these migrating GnRH cells express AMH ex vivo. (g) Coronal section of a mouse nose at E13.5 with both the OE and VNO positive for AMH immunoreactivity (red). (h-k) Inset of g, AMH is expressed by TAG-1 positive fibres (white), these fibres migrate from the VNO to the olfactory bulb, providing a migratory scaffold that GnRH neurons follow to reach the brain. (g-k) Hoechst (blue) used as a nuclear counterstain.

Abbreviations: AMH: anti-Müllerian hormone; AMHR2: AMH receptor2; AcvR1: Activin receptor1/ Activin like kinase 2 (ALK2); BMPR1a: Bone morphogenic protein receptor1a/ALK3; BMPR1B: Bone morphogenic protein receptor1b/ALK6; Div: days in vitro; NMC: nasal mesenchyme; OE: olfactory epithelium; TAG-1: transient axonal glycoprotein/contactin2; TUJ1: βIII-tubulin; VNO: vomeronasal organ.

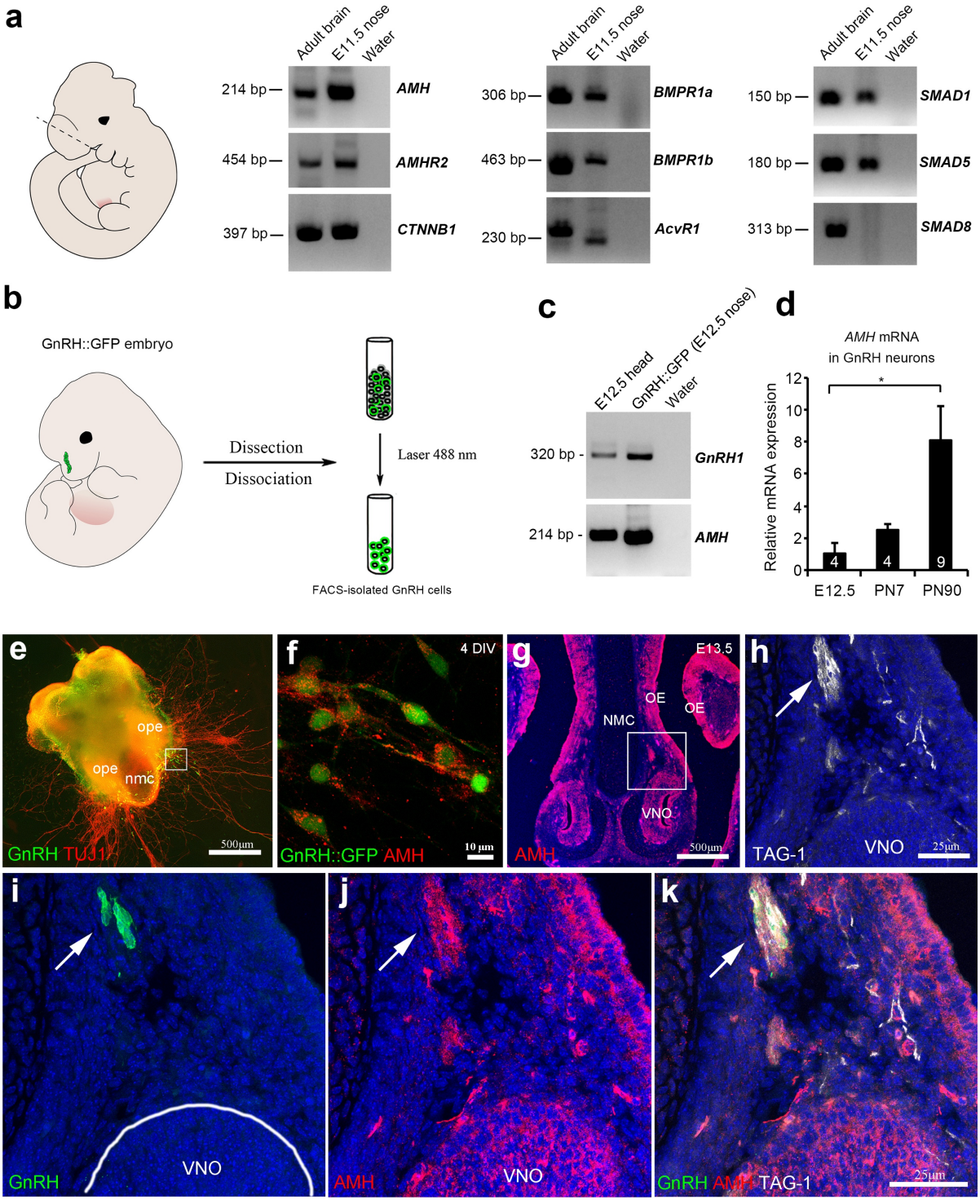
a
Adult brain
E11.5 nose
Water
214 bp
AMH
454 bp
AMHR2
397 bp
CTNNB1
306 bp
BMPR1a
463 bp
BMPR1b
230 bp
AcvR1
150 bp
SMAD1
180 bp
SMAD5
313 bp
SMAD8
b
GnRH::GFP embryo
Dissection
Dissociation
Laser 488 nm
FACS-isolated GnRH cells
c
E12.5 head
GnRH::GFP (E12.5 nose)
Water
320 bp
GnRH1
214 bp
AMH
d
AMH mRNA
in GnRH neurons
Relative mRNA expression
E12.5
PN7
PN90
e
ope
nmc
GnRH TUJ1
500µm
f
4 DIV
GnRH::GFP AMH
10 µm
g
E13.5
OE
NMC
VNO
AMH
500µm
h
TAG-1
VNO
25µm
i
GnRH
VNO
j
AMH
VNO
k
GnRH AMH TAG-1
25µm

8.3 Pharmacological and genetic invalidation of AMHR2 disrupts GnRH neuronal migration and the olfactory/terminal nerve targeting

As AMHR2 is the only receptor known to bind AMH, its expression is a necessary requirement for tissues to be responsive to the actions of AMH. We therefore investigated whether acute pharmacological blockage of the receptor with an AMHR2 neutralising antibody (AMHR2-NA) could affect GnRH migration and/or the olfactory system. This was achieved by *in utero* injection of AMHR2-NA targeted to the olfactory pit in E12.5 embryos and subsequent analysis of GnRH migration and its axonal scaffold 48 hours later (experiment schematic **Figure 52a**). Correct targeting of the injection site was ascertained by the use of the Fluorogold tracer. A representative image of Fluorogold uptake and GnRH-immunoreactivity is shown in **Figure 52b**.

Immunolabelling with Peripherin, a neuron-specific intermediate filament protein expressed by rodent sensory and autonomic axons (Parysek & Goldman, 1988), including the developing olfactory nerve (ON), VNN and TN (Casoni et al., 2016; Fueshko & Wray, 1994), was used to assess the development of the VNN/TN at E14.5 (**Figure 52c-f**). VNN/TN development progressed as has previously been reported (Yoshida et al., 1995) in saline injected groups; however, abnormal ON/TN targeting occurred in embryos injected with AMHR2-NA. In AMHR2-NA treated embryos, the axonal innervation of the olfactory bulb (OB) appeared incomplete as compared to controls (**Figure 52c, d**). This difference in axonal targeting was especially evident for the TN projecting to the ventral forebrain (vFB). In control animals, normal targeting of Peripherin positive fibres was seen as they turn ventrally to target the hypothalamus (**Figure 52e**), whereas in AMHR2-NA injected embryos, the fibres had a scattered appearance, suggesting that AMHR2 may be involved in the axonal guidance of the ON and TN during embryonic development.

Since this projection forms the axonal scaffold for the intracerebral migration of GnRH cells (Yoshida et al., 1995), we analysed the number and distribution of these cells in E14.5 embryos.

At E14.5, the total number of GnRH neurons was comparable between control and AMHR2-NA treated embryos (n = 4 for all groups; **Figure 52g**), indicating that AMHR2 neutralisation had no effect on GnRH neuron survival. However, a significant accumulation of GnRH cells in the nasal compartment, concomitant to decreased cell numbers within the brain, indicated abnormal cell migration in the AMHR2-NA injected embryos (**Figure 52h**). In addition, while GnRH cells normally turn ventrally towards the basal forebrain, in AMHR2-NA embryos, many GnRH cells were found to migrate dorsally towards the cortex (**Figure 52d**) and fewer neurons reached the vFB region (**Figure 52f**).

In light of these results, we sought to determine whether genetic invalidation of *AMHR2* would lead to similar defects in the GnRH migratory process and development of the ON and TN. We performed a detailed analysis of wild type and *AMHR2*$^{-/-}$ mice at E13.5 (n = 2 for both genotypes) using whole mount immunostaining for GnRH and Peripherin followed by 3DISCO clearing and light sheet microscopy (LSM) (**Figure 53**). In WT (*AMHR2*$^{+/+}$) embryos, Peripherin positive fibres were seen to innervate the OB forming a complete ring around its anterior surface (**Figure 53a, c, e**). In knockout mice (*AMHR2*$^{-/-}$), Peripherin positive axons had begun to innervate the OB, however, they had failed to form a ring around the bulb as seen in WT embryos (**Figure 53b, d, f**).

Figure 52. AMHR2 signalling is functionally required for GnRH migration.

(a) Schematic of a mouse embryo that was injected in the olfactory pit at E12.5 in utero to target the site of GnRH ontogenesis, with embryos recuperated 48 hours later at E12.5. (b) Coronal section of an embryo harvested at E14.5 showing that injection of a Fluorogold tracer at E12.5 in the olfactory pit successfully labels the olfactory epithelium (OE), GnRH labelled in green. (c–f) Embryos were injected with either saline or a neutralising antibody for AMHR2 and their GnRH (green) and olfactory/VNN migration (Peripherin, red) assessed at E14.5. Sagittal sections (c, d) show a clear difference in the development of the olfactory/VNN fibres which have delayed innervation of the olfactory bulb (OB) and a scattered appearance in the ventral forebrain (vFB) when AMHR2 signalling is neutralised (e, f). Quantification of the total number of GnRH immunoreactive neurons revealed no change to the total population size between groups (g). n = 4 for both groups, data shown are mean ± SEM. Ctrl 1499 ± 36.99, AMHR2 NA 1516 ± 21.55, P=0.3983 as determined by unpaired students t – test. (h) Analysing the distribution of cells revealed that blockage of AMHR2 results in an accumulation of GnRH cells in the nose $P < 0.01$, concomitant to a decrease in cells found in the forebrain at E14.5 $P < 0.01$. (h) data shown as mean ± SEM. n = 4, ** $P < 0.01$ by 2way ANOVA, Bonferroni post hoc test. Although not statistically significant, it was noted that there appeared to be an increased chance for GnRH neurons to migrate dorsally towards the cortex (cx) when AMHR2 was blocked (c, d, h).

Abbreviations: cx: cortex; FB: forebrain; N/FBJ: nasal/forebrain junction; oe: olfactory epithelium; NMC: nasal mesenchyme

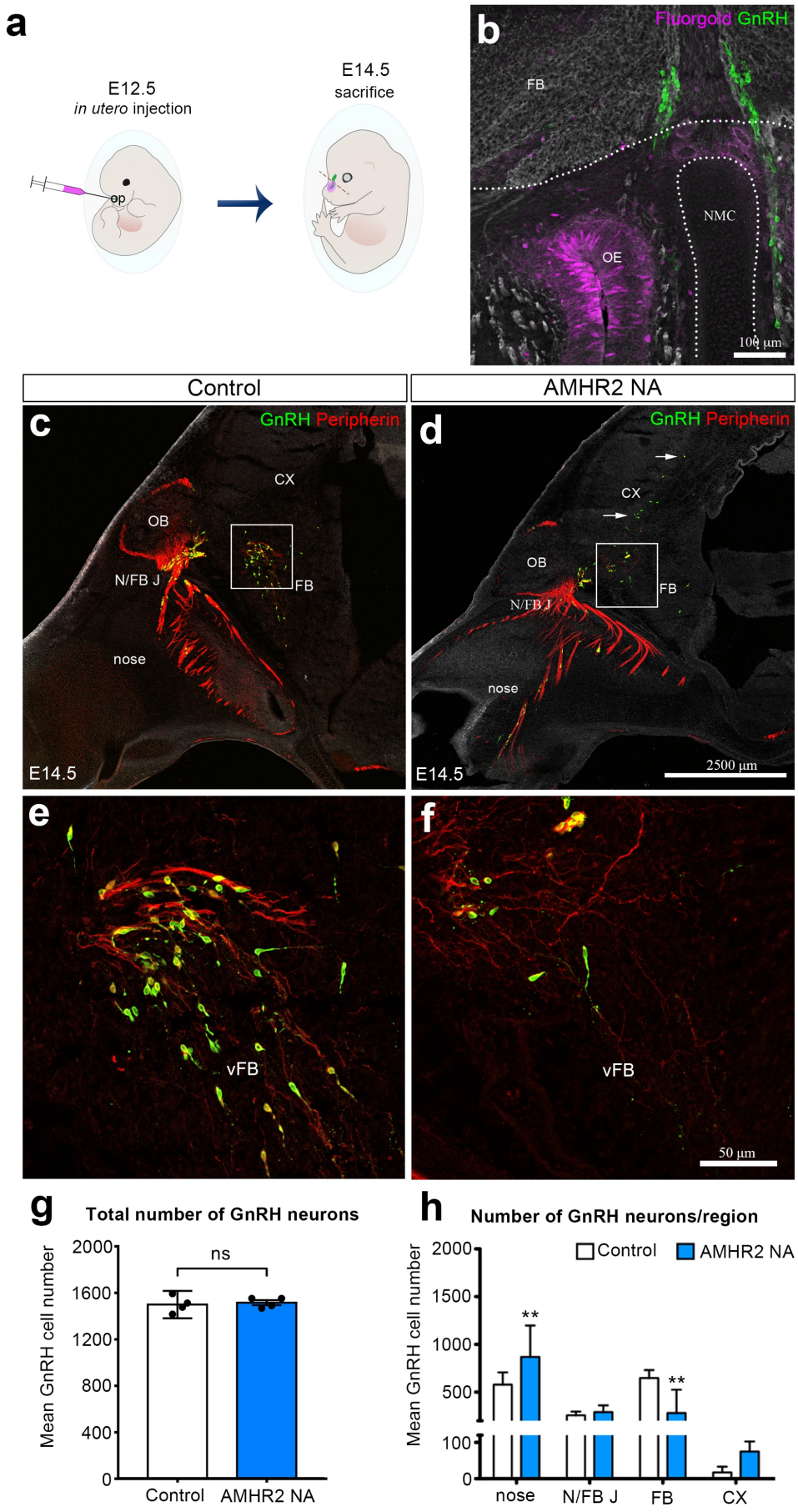
a
E12.5
in utero injection
op
E14.5
sacrifice
b
Fluorgold GnRH
FB
NMC
OE
100 µm
Control
AMHR2 NA
c
GnRH Peripherin
CX
OB
N/FB J
FB
nose
E14.5
d
GnRH Peripherin
CX
OB
N/FB J
FB
nose
E14.5
2500 µm
e
vFB
f
vFB
50 µm
g
Total number of GnRH neurons
Mean GnRH cell number
2000
1600
1200
800
400
0
ns
Control
AMHR2 NA
h
Number of GnRH neurons/region
Control
AMHR2 NA
Mean GnRH cell number
2000
1500
1000
500
100
0
**
**
nose
N/FB J
FB
CX

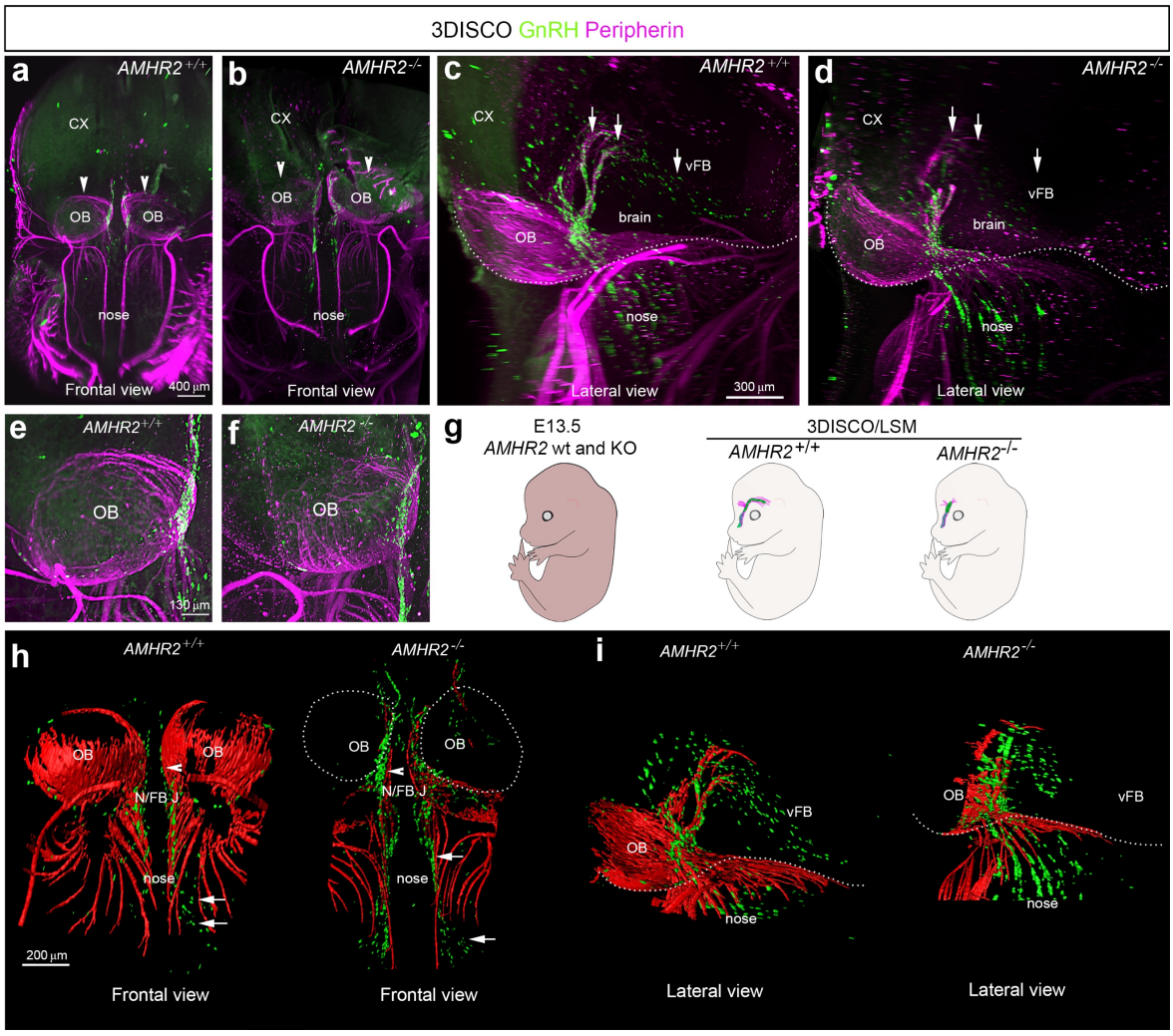

Figure 53. Olfactory fibre development and GnRH migration is perturbed in *AMHR2*$^{-/-}$ mice.

Entire E13.5 embryos were immunolabelled for Peripherin (purple) and GnRH (green), rendered transparent using 3DISCO and imaged using a light sheet microscope (**schematic g**). (**a–b, inset e–f**) Frontal views reveal a reduction in the innervation of the olfactory bulb (OB) by migrating olfactory axons (purple) in homozygous *AMHR2*$^{-/-}$ mice compared to wild types. Lateral views (**c, d**) clearly show *AMHR2*$^{-/-}$ mice have deficient migration of both olfactory fibres and GnRH neurons as the characteristic ventral curving of the migratory pathway is almost absent in the homozygous mice (**arrows in b and c**). Surfaces modelling in Imaris (**h, i**) of peripherin (red) and GnRH (green) further highlight the differences observed between *AMHR2*$^{-/-}$ and wild type mice. Abbreviations: cx: cortex; N/FBJ: nasal/forebrain junction; OB: olfactory bulb; oe: olfactory epithelium; NMC: nasal mesenchyme; vFB: ventral forebrain

The anatomical locations of the entire GnRH population could be assessed in both groups and representative images are presented in **Figure 53 a–f.** In *AMHR2*$^{-/-}$ embryos, GnRH neurons appeared more likely to cluster in the nasal compartment, with fewer immunoreactive neurons observed in the vFB (**Figure 53 c–d**; arrows), consistent with the results from the pharmacological blockage of AMHR2 reported above. A 3–Dimensional segmentation and rendering was also undertaken to better isolate Peripherin fibres and GnRH neurons (**Figure 53 h–i**). Using this technique, it was possible to better visualise the entire innervation of the OB in wild–type versus mutant embryos as well as the progression of the TN projections and distribution of GnRH neurons within the vFB.

Altogether, these experiments revealed that pharmacological or genetic invalidation of AMHR2 leads to abnormal development of the GnRH and olfactory system (**Figure 53g**), similar to what has been described in KS foetuses (Schwanzel–Fukuda et al., 1996; Texeira et al., 2010).

In order to determine whether the defect in GnRH cell migration found in *AMHR2*$^{-/-}$ mouse embryos was corrected later during development, we performed immunofluorescence experiments for GnRH in adult *AMHR2*$^{+/+}$ and *AMHR2*$^{-/-}$ mice (n = 7 for each group, **Figure 54**) and found decreased GnRH immunoreactivity at the level of the organum vasculosum laminae terminalis (OVLT; **Figure 54 a–d**), where the majority of GnRH neurons are normally located, and in the median eminence of the hypothalamus (**Figure 54 e–h**), which is the projection site of neuroendocrine GnRH cells. We next counted the number of GnRH–positive cells in *AMHR2*$^{+/+}$, *AMHR2*$^{+/-}$ and *AMHR2*$^{-/-}$ brains and found no difference between wild type and heterozygous mice, but a significant 40 % reduction in GnRH cell number in homozygous *AMHR2*$^{-/-}$ mice as opposed to wild–type and heterozygous animals (One–Way ANOVA, Bonferroni test, *P $<$0.05; ** P$<$0.01). The distribution of GnRH cells was also affected in *AMHR2*$^{-/-}$ mice, with a significant reduction in the number of cells found only from the level of the OVLT progressing caudally towards the hypothalamus (data not shown). This is suggestive of a defect in the migration of GnRH cells in *AMHR2*$^{-/-}$ mice, as it has been reported that the final anatomical positioning of GnRH cells is linked to the timing of the initiation of their migration (Jasoni et al., 2009).

Figure 54. AMHR2 deficiency reduces GnRH neuron number, projections to the ME and results in altered fertility

Immunolabelling of GnRH in adult wild type and *AMHR2*$^{-/-}$ mice (**a–h**). The majority of GnRH cell bodies are located at the level of the organum vasculosum laminae terminalis (OVLT) in both *AMHR2* $^{+/+}$ and *AMHR2*$^{-/-}$ mice, however the number of cell bodies found in *AMHR2* $^{-/-}$ animals is reduced (**arrows c, d**). (**i**) Quantitation of the total GnRH population revealed no difference between wild type (666.9 ± 34.30) and *AMHR2* $^{+/-}$ (613.1 ± 33.37) mice however *AMHR2* $^{-/-}$ mice have fewer (407.7 ± 27.25) GnRH neurons (*P<0.05, ** P<0.01, 1way ANOVA, Bonferroni post hoc test, n = 7 for all groups). GnRH cells project their nerve terminals to the median eminence (ME), where a reduction in the fibre density is observed in *AMHR2*$^{-/-}$ mice compared to wild types (**e–h**). As expected with a deficiency in GnRH innervation, the female *AMHR2* $^{-/-}$ mice have altered ovarian morphology, with a decrease in the number of corpora lutea (**j**). (**k, l**) In WT mice, TH expression is confined to the glomerular layer where immunopositive cells and fibres are widely found, however, this expression is markedly reduced in *AMHR2* $^{-/-}$ mice. (**i**) data shown as mean ± SEM. n = 7, * P <0.05, ** P <0.01 by One–way ANOVA followed by Bonferroni Post hoc test.

Abbreviations: OVLT, organum vasculosum of the lamina terminalis; ME, median eminence; 3V, third ventricle; GF, Grafian follicle; A, antral follicle; PA, preantral follicle; SA, small antral follicle; CL, corpus luteum; At, atretic follicle; MOB, main olfactory bulb; AOB, accessory olfactory bulb; gl, glomerular layer; opl, outer plexiform layer; gr, granular layer.

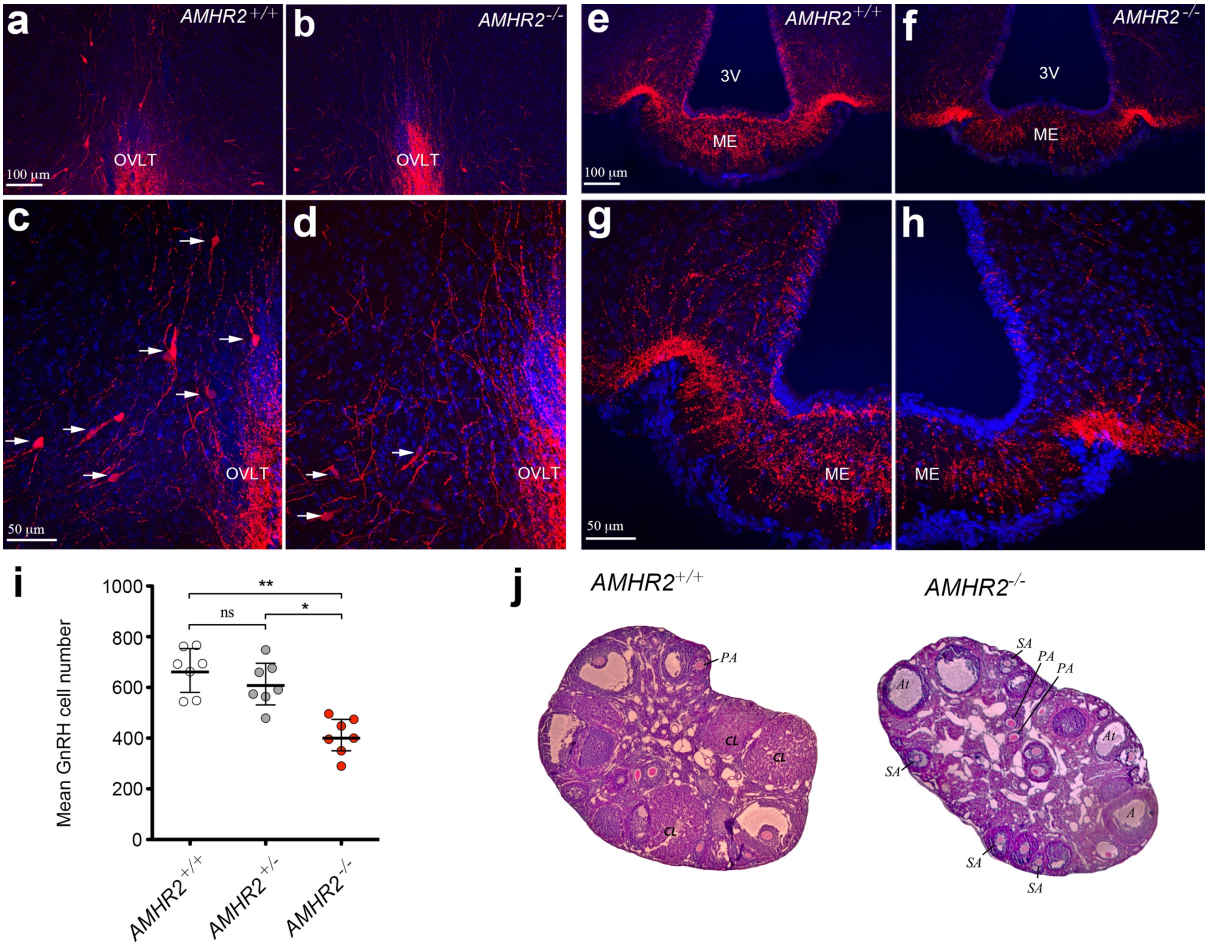
a
AMHR2+/+
OVLT
100 µm
b
AMHR2-/-
OVLT
e
AMHR2+/+
3V
ME
100 µm
f
AMHR2-/-
3V
ME
c
OVLT
50 µm
d
OVLT
g
ME
50 µm
h
ME
i
Mean GnRH cell number
1000
800
600
400
200
0
**
ns
*
AMHR2+/+
AMHR2+/-
AMHR2-/-
j
AMHR2+/+
AMHR2-/-
PA
cL
SA
At
A

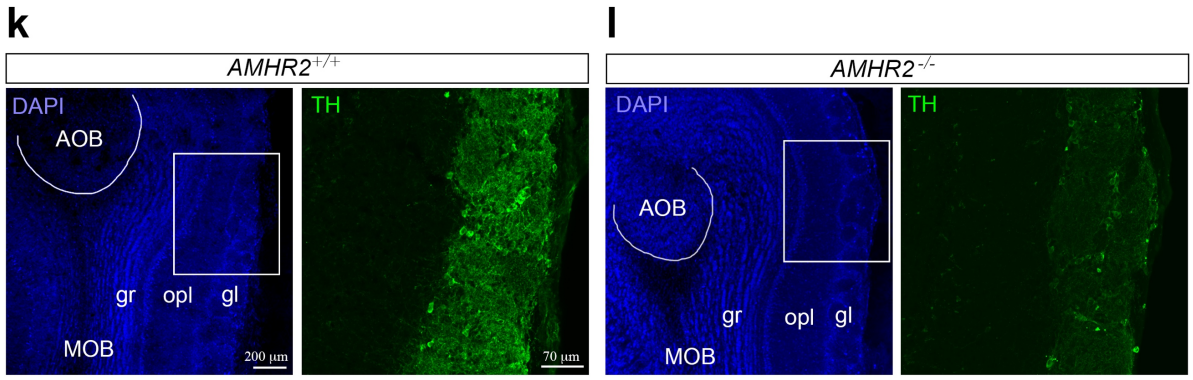
k
AMHR2+/+
DAPI
AOB
gr
opl
gl
MOB
200 µm
TH
70 µm
l
AMHR2-/-
DAPI
AOB
gr
opl
gl
MOB
TH

Ovarian histology of *AMHR2* deficient animals showed abnormalities suggestive of an anovulatory phenotype, with the presence of fewer post-ovulation corpora lutea, and accumulation of prentral and small antral follicles as compared to wild-type animals (PN 90, *n* = 3 per genotype; **Figure 54j**).

Currently, a constant 90-days mating protocol is ongoing to determine whether *AMHR2*$^{-/-}$ mice also have impaired fertility (indicated by a significant delay in their first litter, fewer litters and fewer pups per litter produced over a 3-month period).

We next wondered whether the developmental loss of afferent projection from olfactory sensory neurons (OSN) in *AMHR2*-null mice could result in the hypoplasia and/or disruption of the olfactory glomeruli. Previous studies have demonstrated that in the main olfactory bulb (MOB), only the glomerular layer (gl) expresses tyrosine hydroxylase (TH), the essential rate-limiting enzyme involved in the synthesis of dopamine from L-tyrosine (Halasz et al., 1981). Consistent with these reports, in the MOB of *AMHR2* WT mice, TH-immunopositive neurons were observed mainly in the gl (**Figure 54k**). TH-immunopositive neurons were also found surrounding the glomeruli, and strongly stained TH-immunopositive nerve fibres were widespread in the gl (**Figure 54k**). Few TH-immunopositive cells were observed in the MOB of *AMHR2*$^{-/-}$ compared with WT mice, while TH nerve fibres were markedly reduced in the glomeruli of *AMHR2*$^{-/-}$ (**Figure 54l**). These data suggest that the decrease in the number of TH-immunopositive neurons in gl could be caused by deficient afferent OSN projections. Previous studies have indeed demonstrated that deafferentation of OSN projections to the MOB lead to a marked decrease in the number of TH-expressing neurons in the gl (Baker et al., 1983; Nadi et al., 1981)

8.4 AMH increases GN11 cell migration via the AMHR2/BMPR1b signalling pathway

The manipulation of the GnRH migratory system and functional studies on these neurons have been challenging because of their limited number (800 in rodents) and anatomical dispersal along their migratory route. The generation of immortalised GnRH neurons (GN11 and GT1-7 cell lines: Mellon et al., 1990; Radovick et al., 1991) has permitted the study of respectively immature migratory and mature post-migratory GnRH neurons. In particular, GN11 cells display remarkable motility *in vitro*, and have been used to investigate the molecular mechanisms controlling the directional migration of GnRH neurons and to shed light on the biochemical pathways employed by GnRH cells (Cariboni et al., 2007; Giacobini et al., 2008; Messina et al., 2011).

To assess whether GN11 and GT1-7 cells expressed the molecular machinery to respond to AMH stimulation, RT-PCR analysis was carried out to verify the expression of AMH receptors (**Figure 55a**). Our data show that GN11 cells express *AMHR2*, *AcvR1*, *BMPR1a* and *BMPR1b*, whereas post-migratory GT1-7 cells express all receptors except *BMPR1b* (**Figure 55a**). These results indicate that AMHR2/BMPR1b signalling is a hallmark of migratory GnRH neurons and suggest that AMH could mediate a different biological response in migratory and post-migratory GnRH neurons depending on differential receptor complexes expressed throughout development.

Activation of the MAPK pathway has been previously associated with increased GN11 cell motility (Messina et al., 2011; Hanchate et al., 2012). Here we found that AMH, at concentrations previously reported to be functional in other cell lines (Garrel et al., 2016), significantly increases the phosphorylation of ERK1/2 in GN11 cells within few minutes and in a dose-dependent manner (**Figure 55 b-c**).

Moreover, since AMH has been previously shown to induce migration of AMHR2-expressing cells from the coelomic epithelium into the Müllerian duct mesenchyme (Zhan et al., 2006) and

given the *in vivo* effects of AMHR2 invalidation on GnRH neuronal migration, we sought to determine whether AMH was a pro-motility factor for GN11 cells. Using transwell assays (**Figure 55d**), we showed that recombinant human AMH was able to significantly increase the motility of GN11 cells at all tested doses (50 ng/mL: 50.1 ± 7.2 cells per field, $P < 0.05$; 100 ng/mL 44.2 ± 7.4 cells per field, $P < 0.05$; 250 ng/mL 56.5 ± 8.0 cells per field, $P < 0.01$; n = 20 for all) compared to controls (serum free medium, SFM 11.8 ± 3.6 cells per field, n = 12; **Figure 5d**).

We next investigated which receptor complex was required for AMH-dependent cell migration in GN11 cells. This was achieved by targeted knockdown of type-1 and type-2 AMH receptors using a siRNA silencing approach. Silencing efficiency was first assessed, showing that siRNA transfection was able to reduce by 80% the mRNA expression of the target receptor genes (**Figure 55e**), compared to mock transfected cells.

Knockdown of individual AMH receptors led to distinct motility responses of GN11 cells to AMH stimulation (**Figure 55f**). As shown above (**Figure 55d**), this dose of recombinant AMH (50 ng/mL) was able to elicit a significant increase in GN11 cell motility (36.7 ± 2.6 cells per field, n = 31, Kruskal-Wallis test followed by Dunn's multiple comparison test) compared to cells exposed to SFM alone (17.4 ± 2.2 cells per field, n = 43). Silencing of *AcvR1* (32.2 ± 3.2 cells per field, n = 9), *BMPR1a* (47.2 ± 3.0 cells per field, n = 9) or *LNC* RNA (29.1 ± 2.5 cells per field, n = 34) did not affect the GN11 response to AMH treatment. In contrast, knockdown of *AMHR2* (10.6 ± 0.9 cells per field, n = 21) and *BMPR1b* (4.6 ± 1.3 cells per field, n = 21) resulted in significantly reduced GN11 cell motility in response to AMH (Mock vs. AMHR2 siRNA, $P < 0.01$; Mock vs. Bmpr1b siRNA, $P < 0.01$. Kruskal-Wallis test followed by Dunn's multiple comparison test). These data indicate that the AMH increased GN11 cell motility via an AMHR2/ BMPR1b signalling.

Figure 55. AMH promotes GnRH cell motility *in vitro* via AMHR2 and BMPR1B signalling.

AMH receptors are expressed by the immortalised murine GnRH cell lines GN11 and GT1-7 as determined by qRT-PCR, data normalised to GN11 expression (a). GN11 cells respond to AMH treatment by increasing the phosphorylation of MAPK in both a dose (b) and time (c) dependent manner, suggesting this pathway is active in these cells $n = 5$. Exogenous AMH is able to increase the motility of GN11 cells using a transwell motility assay, $n = 11$ for SFM, $n = 18$ for all other groups (d). In order to determine which AMH receptors were important for mediating this motility effect, the expression of each potential receptor was knocked down using targeted siRNAs. (e). Each siRNA was able to reduce the expression of its target RNA with no effect on the level of long non-coding RNA (*LNC*) $n = 3$ (e). Exogenous AMH was able to induce increased motility in control, *AcvR1*, *BMPR1a* and *LNC* siRNA treated groups. siRNA mediated knockdown of *AMHR2* and *BMPR1b* resulted in no change to the motility of GN11 cells compared to control when treated with AMH. (a, b) Data shown as mean ± SEM, * $P < 0.05$, ** $P < 0.01$, *** $P < 0.001$ by 1way ANOVA, Dunnett's post hoc test to compare multiple groups. (d-f) Data shown as median ± interquartile range, *a* = similar groups as determined by Kruskal-Wallis test followed by Dunn's multiple comparison test.

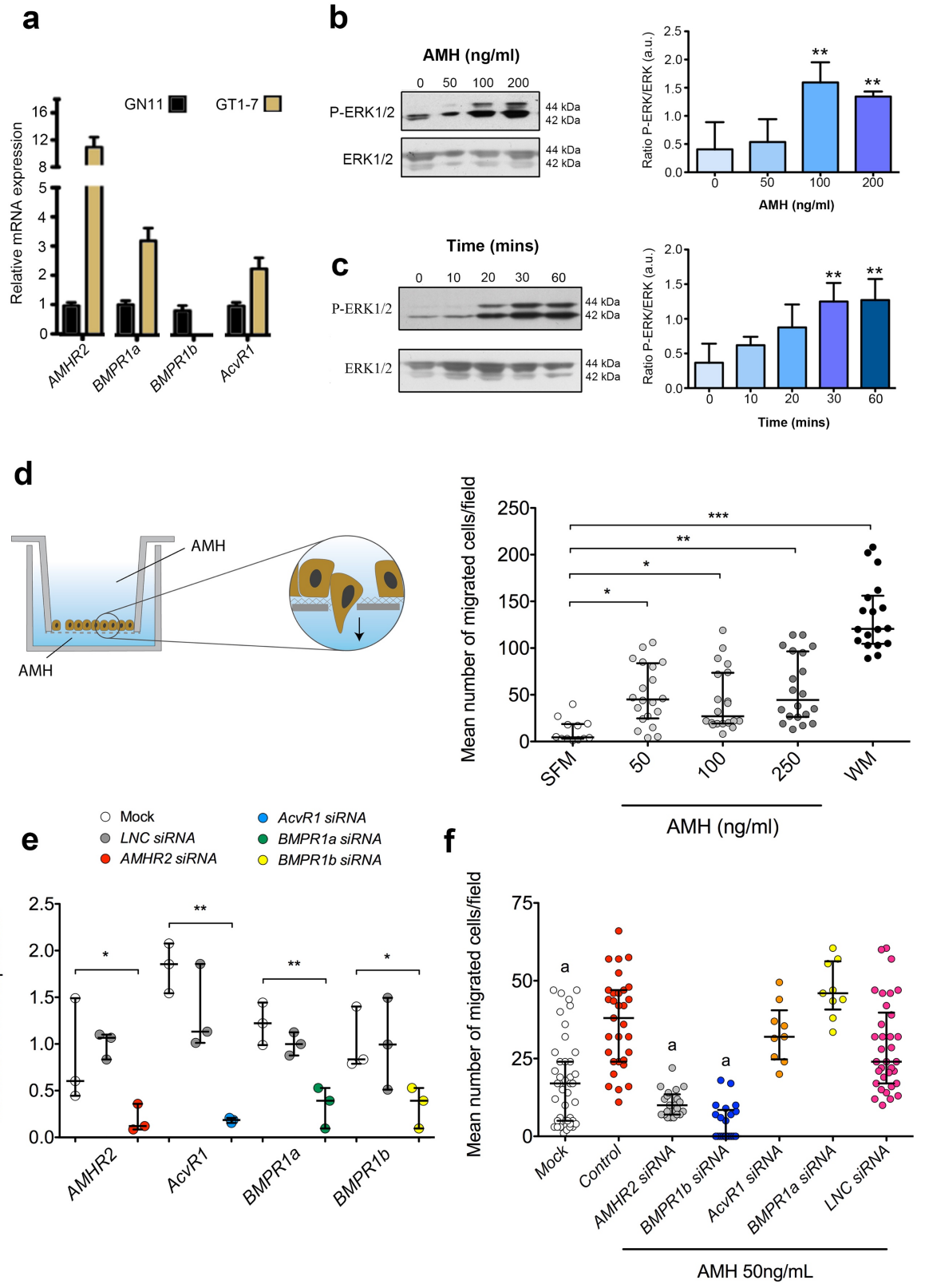
a
GN11
GT1-7
Relative mRNA expression
AMHR2
BMPR1a
BMPR1b
AcvR1
b
AMH (ng/ml)
0 50 100 200
P-ERK1/2
ERK1/2
44 kDa
42 kDa
Ratio P-ERK/ERK (a.u.)
AMH (ng/ml)
c
Time (mins)
0 10 20 30 60
Time (mins)
d
AMH
Mean number of migrated cells/field
SFM
50
100
250
WM
AMH (ng/ml)
e
Mock
LNC siRNA
AMHR2 siRNA
AcvR1 siRNA
BMPR1a siRNA
BMPR1b siRNA
f
Control
AMH 50ng/mL

8.5 AMH does not promote GnRH neuronal survival *in vitro*

Several papers have identified AMH as having positive effects on promoting neuronal cell survival (Lebeurrier et al., 2008; Wang et al., 2005). In order to determine whether the reduction in the size of the GnRH neuronal population in adult brains of *AMHR2*$^{-/-}$ mice was partially due to altered cell survival due to the lack of AMH signalling, we assessed the effect of AMH on GN11 and GT1-7 cell survival by flow cytometry (**Figure 56 a-b**). Here we tested whether exogenous AMH was able to rescue cells from TNF-α induced apoptosis in both cell lines. Previous studies have shown that GT1-7 cells express both high (TNFR1) and low (TNFR2) affinity TNF-α receptors, as determined by immunohistochemistry, flow cytometry and western blot analyses and TNF-α induces apoptosis in this cell line (Sortino et al., 1999). Additionally, TNF-α treatment of isolated GnRH cells from a 12 week human foetus resulted in NF-κB pathway activation and loss of GnRH expression (Sarchielli et al., 2017), suggesting embryonic GnRH cells are also capable of responding to TNFα signalling.

We used Alexa Fluor-conjugated anti-Annexin V and Propidium Iodide to distinguish between apoptotic and necrotic cells, respectively (**Figure 56 a-b**). Low levels of apoptotic (1.07 ± 0.67%) and necrotic (2.42 ± 1.22%) cells were detected in GN11 cells cultured in control medium, which was comparable to those seen when the cells were cultured with 250 ng/ml AMH alone (1.54 ± 1.03% of apoptotic cells and 2.47 ± 1.37% of necrotic cells). As expected, levels of apoptosis and necrosis increased by +18.21% and +1.93%, respectively, when GN11 cells were cultured with 10ng/mL TNF-α (**Figure 56a**). These values remained unchanged when cells were exposed to TNF-α together with AMH (at any concentration tested: 100, 250 or 500 ng/ml), indicating that AMH does not rescue GN11 cells from TNF-α-mediated cell death. Similar effects were also observed in GT1-7 cells as compared to GN11 cells (n = 3; **Figure 56b**).

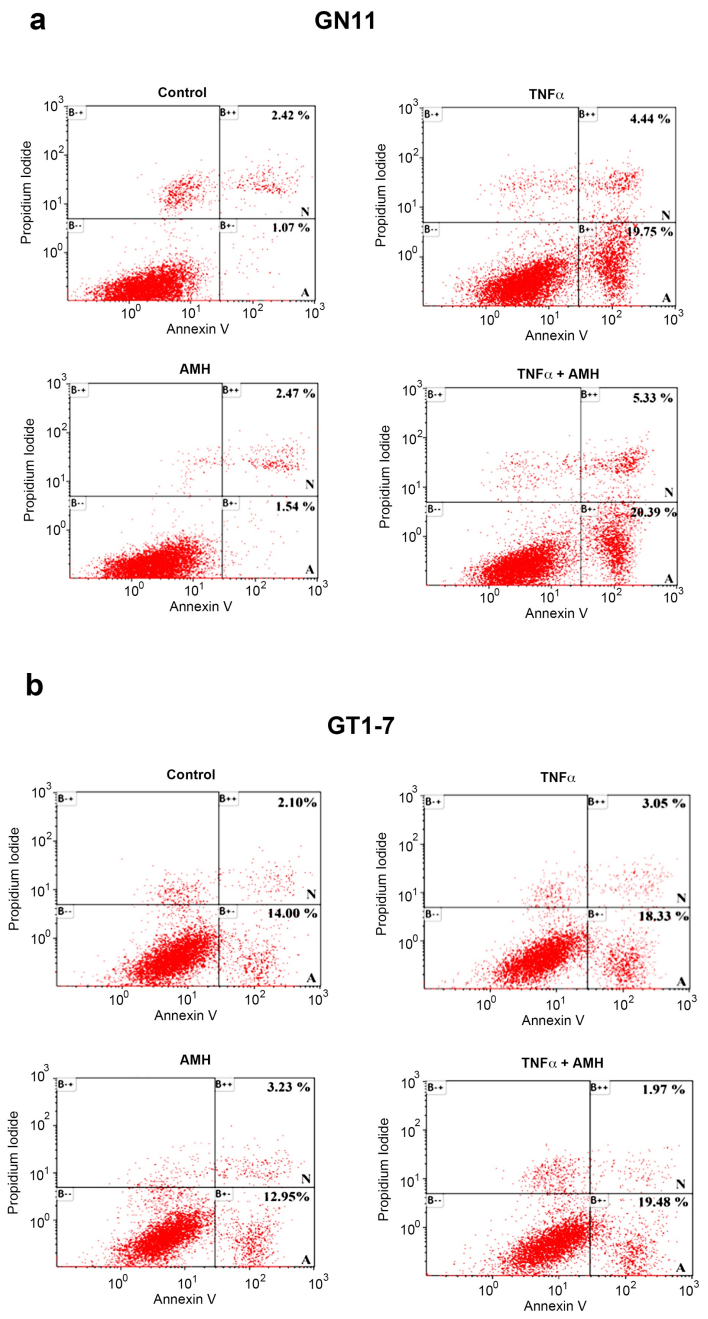

Figure 56. AMH is unable to rescue immortalised GnRH cells from TNF α induced apoptosis

(a) GN11 cells cultured in SFM show low levels of apoptotic and necrotic cells that is comparable to GN11 cells cultures with 100ng/mL of AMH. TNF α treatment causes significant increases in the proportion of apoptotic and necrotic cells as has been previously reported for other cell lines. Co-culture of TNF α and 100ng/mL AMH is unable to Increase GN11cell survival as compared to TNF α treatment alone. (b) the same pattern was observed for GT1-7 cells. Apoptotic cells single labelled with AnnexinV are labelled A, necrotic cells double positive for AnnexinV and Propidium Iodide are labelled N

8.6 *AMH* and *AMHR2* loss-of-function mutations in CHH patients

The KS-like phenotype that we reported in *AMHR2* null mice prompted us to ask whether insufficient AMH signalling through AMHR2 might also be involved in this human infertility syndrome. Therefore the group of Nelly Pitteloud (Lausanne, Switzerland) performed whole exome sequencing (WES) on a cohort of 70 KS and 43 nCHH patients. Several heterozygous nucleotide substitutions in *AMH* and *AMHR2* were identified in these cohorts (**Table 9** and **Table 10**; **Figure 51a**).

We identified eight coding variants in *AMH* and 2 in *AMHR2* in the CHH cohort. Four of the *AMH* variants (p.Arg116Gln, p.Pro151Ser, p.Asp238Glu, p.Glu160Asp) were identified in KS individuals and 4 were found in nCHH patients (p.Val12Gly, p.Thr99Ser, p.Ala519Val, p.Asp288Glu). Two variants in *AMH* were found to segregate with mutations in highly penetrant known KS- or nCHH-associated genes (*KAL1* [Franco et al., 1991; Legouis et al., 1991]; *TACR3* [Topaloglu et al., 2009]), suggesting that the CHH phenotypes associated to those variants could be explained *a priori* by the deleterious genetic defect in *KAL1* and *TACR3* rather than *AMH* polymorphisms.

Two of the *AMH* variants identified in our cohort of CHH cases (p.Val12Gly, p.Pro151Ser) have previously been identified in PMDS males (Picard et al., 2017). Interestingly, pelvic ultrasound of the two male CHH patients did not reveal signs of cryptorchidism nor PMDS, indicating that heterozygous mutations in AMH are not sufficient to trigger PMDS but they instead might contribute to the pathogenesis of CHH. The two variants in *AMHR2* were found in nCHH probands and one of the mutants (p.Tyr290Phe) was found to segregate with a mutation in *TACR3* (TACR3His148Leu/His148Leu).

Of note, we recently showed that AMH potently activates GnRH neuron firing in mice, resulting in GnRH and LH secretion (Cimino et al., 2016). Therefore, it is possible that mutations in *AMHR2* could affect GnRH secretion also in humans and contribute to the phenotype of nCHH. All of these missense variants are predicted by at least one protein prediction algorithm

as damaging to protein function and occur in conserved residues, suggesting these variants likely impact protein function (**Tables 9 and 10**).

To assess the biological activity of the variants, we tested their motility-inducing properties on GN11 cells (**Figure 57b**). We found that five of the six tested mutants were less effective at promoting GN11 motility as compared to WT AMH (**Figure 57b**). We next started to investigate the AMH secretory capacity of COS-7 cells transfected with 3 different AMH variants (p.Glu160Asp, p.Val12Gly, p.Asp288Glu), that reduce GN11 cell motility. Of these variants, only the AMH p.Asp288Glu, located in the fifth exon of the N-terminal domain, showed significantly reduced AMH secretion *in vitro* (**Figure 57c**). These results confirm that the identified AMH variants are indeed loss-of-function mutations, suggesting a pathogenic role in CHH patients and point towards a role for AMH in GnRH neuronal migration.

Table 9: Genotypes, functional prediction and clinical information of KS probands harbouring AMH variants.

						MAF Frequency (%)		Prediction			Conservation		Phenotype information				
Gene	Chromosome	Position	dbSNP number	Nucleotide Change	Amino acid Change	ExAC EUR	CoLaus	PPhen-2	SIFT	CADD (Cutoff>15)	GERP	Described in PMDS	Sex	Inheritance	Puberty	Olfactory phenotype	Mutations in other CHH genes (heterozygous)
AMH	19	2249678	-	c.347G > A	p.Arg116Gln	Pr	Pr	B	B	B	Mildly conserved	No	M	Fam	A	Subjective anosmia Absent OBs	None
	19	2250374	rs370532523	c.451C > T	p.Pro151Ser	0.0002	Pr	D	B	D	Conserved	Yes	M	S	A?	UPSIT 11/40	None
	19	2250897	-	c.714C > A	p.Asp238Glu	< 0.0001	Pr	B	B	D	Not conserved	No	F	Fam	P	Borderline (Sniffin'Sticks 12/16), father anosmic	None
AMH	19	2250403	-	c.480G > C	p.Glu160Asp	Pr	Pr	B	B	D	Mildly conserved	No	M	Fam	A		*KAL1* p.Cys86Ser

Table 10: Genotypes, functional prediction and clinical information of CHH probands (normal sense of smell or absence of formal test) harbouring AMH and AMHR2 variants.

						MAF Frequency (%)		Prediction			Conservation		Phenotype information				
Gene	Chromosome	Position	dbSNP number	Nucleotide Change	Amino acid Change	ExAC EUR	CoLaus	PPhen-2	SIFT	CADD (Cutoff>15)	GERP	Described in PMDS	Sex	Inheritance	Puberty	Olfactory phenotype	Mutations in other CHH genes (heterozygous)
AMH	19	2249366	rs149082963	c.35T > G	p.Val12Gly	0.0057	Pr	B	D	B	Mildly conserved	Yes	M	S	P	Not tested	None
	19	2249626	rs200226465	c.295A > T	p.Thr99Ser	0.0008	Pr	D	B	D	Conserved	No	M	Fam	P	Normosmic (Sniffin'Sticks)	*GNRHR* p.Gln106Arg *CCDC141* p.Lys1037Asn
	19	2251829	rs200031151	c.1556C > T	p.Ala519Val	0.0030	0.12	B	B	B	Mildly conserved	No	M	Fam	P	Normosmic (Sniffin'Sticks 15/16)	None
AMHR2	12	53823970	-	c.1332_1358del	p.Gly445_Leu453del	0.04	-	NA*	NA*	NA*	?	Yes	F	Fam*	A	Normosmic (Sniffin'Sticks)	None
AMH	19	2251137	rs199831511	c.864C > G	p.Asp288Glu	0.0031	Pr	D	B	D	Conserved	No	M	Fam	A	Formally tested	*TACR3* Trp275*/Trp275
AMHR2	12	53822696	-	c.869A > T	p.Tyr290Phe	-	-	B	B	B	Conserved	No	M	Fam	A	Normal formal smell test et OBs in MRI	*TACR3* His148Leu/His148Leu

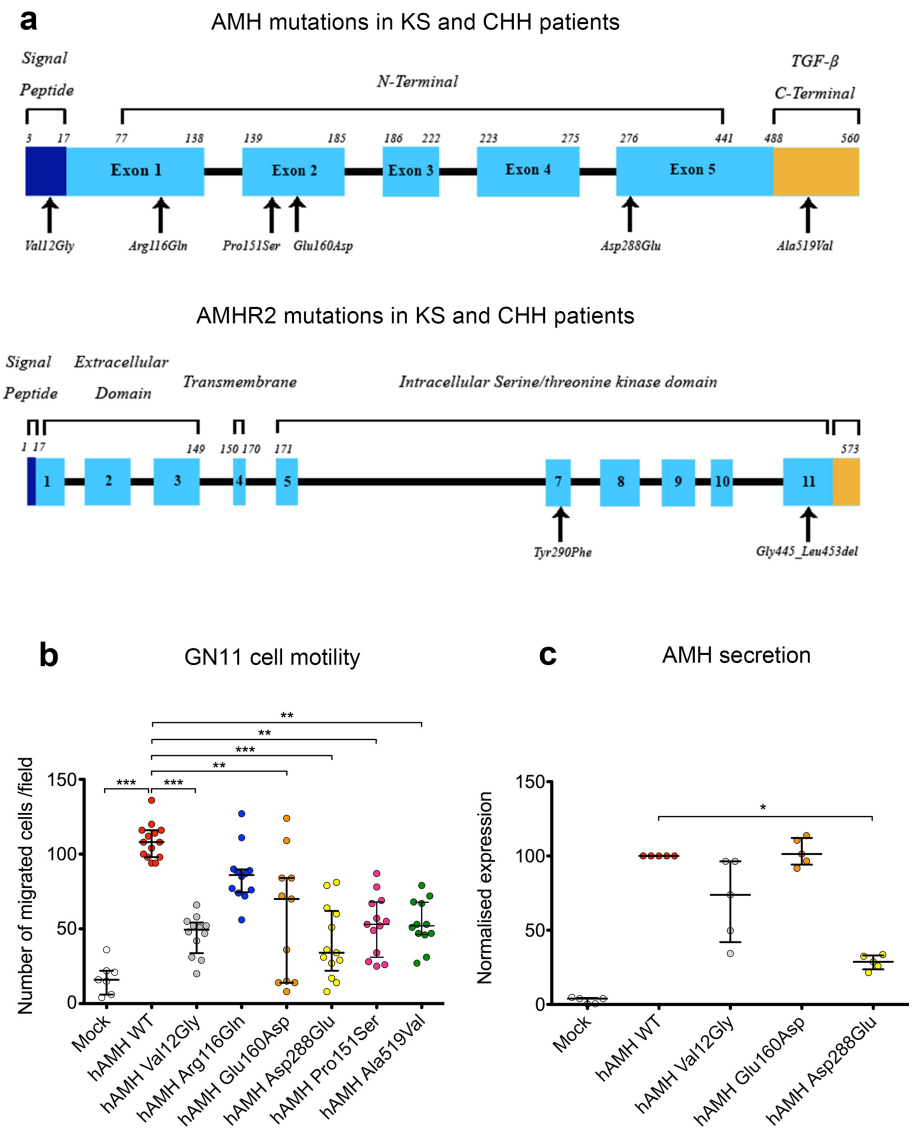

Figure 57. Functional validation of AMH mutations identified in CHH and KS patients

Whole exome sequencing of 70 KS and 43 nCHH probands and identified several heterozygous missense mutations in the AMH gene and in its receptors in both KS and nCHH individuals (a). Mutations were synthesised by targeted mutagenesis of the cloned wild type hAMH sequence. These mutated forms of AMH were tested for their ability to induce GN11 cell motility via transwell assay (b). The majority of mutated AMH isoforms were unable to induce the same level of motility as hAMH WT. Data represented as mean ± SD. $n > 7$ for all groups, * $P < 0.05$, ** $P < 0.01$, *** $P < 0.001$ by Kruskal–Wallis test followed by Dunn's multiple comparison test. In order to validate whether the mutated AMH isoforms were translated and secreted, an ELISA for hAMH was performed on the conditioned medium of transfected COS-7 cells (c). Several of the mutated forms of AMH differed in their level of secretion as determined by ELISA, but all were distinguishable from the mock medium that contains no AMH. Data represented as median ± interquartile range. * $P < 0.05$ by Kruskal–Wallis test followed by Dunn's multiple comparison test.

CHAPTER 9

Discussion

9.1 Application of Clearing Techniques to Study Human Embryology

Important progress has been made in the non-invasive medical imaging of embryos and foetuses *in utero* during pregnancy to detect congenital anomalies and malformations. This now includes 3D/4D obstetric ultrasonography which can generate holographic images of the embryo (Baken et al., 2015; Pooh et al., 2011) but mostly provide information about surface features and cavities, and 3D power Doppler which visualises the embryonic vasculature (Weisstanner et al., 2015). *In utero* magnetic resonance imaging (MRI) also provides a good appreciation of the development of the CNS (Weisstanner et al., 2015) in the foetus and diffusion tensor imaging (DTI) tractography is now used as a prenatal diagnostic of callosal dysgenesis as early as GW20 (Jakab et al., 2015).

The validation of these *in utero* 3D data is challenging as it currently relies on post-mortem evaluation of histological sections. Our method, which preserves the 3D organisation of the organs, should provide clinicians with a reliable spatial framework for the correlation of *in utero* and post-mortem imaging data. To this end, we created a dedicated database at https://transparent-human-embryo.com is available free for use of all human developmental data we have obtained and is fully updatable in the future for new results both from our lab or contributors around the World. The database currently contains over 1000 acquisitions of individual markers and tissues, comprising more than 1,500,000 optical sections relating to the development of various body systems including muscle, lung and limb development. Birth defects of a structural or functional origin affect more than 3% of live births (https://www.cdc.gov/ncbddd/birthdefects/data.html), presenting a serious emotional and healthcare burden to society and it is hoped that the continued expansion and use of our database for the analysis of embryos and foetuses with genetic diseases and malformations has the potential to improve their prenatal diagnosis and our understanding of their aetiologies.

9.2 Sexually Dimorphic Vascular Patterning of the Embryonic Gonads

An important observation made from this study is the differential vascularisation of the developing Müllerian ducts in males and females at GW10, with a total lack of capillaries surrounding these structures in males. This was also the case in a GW8 male embryo, an age preceding the onset of Sox9 expression – the first marker of male sex determination (Wilhelm et al., 2007). Although it has previously been shown that in some vertebrates, namely reptiles and birds (Oréal et al., 1998; Western et al., 1999), AMH expression precedes expression of Sox9 and contributes to male specific vascular patterning of the gonads in rat cultures (Ross et al., 2003).

Although, we did not obtain female embryos younger than GW10.5, our data suggest that the regression of the Müllerian ducts, which starts around GW10 could be linked to or facilitated by the lack of vascularisation of these ducts in males. By contrast, the Wolffian ducts are vascularised in both sexes. Intriguingly, work in mice has revealed a male specific vascular patterning of the gonadal vasculature can be induced in females by treatment with AMH (Ross et al., 2003). Specifically, the cells forming the *de novo* vessels were found to have originated in the mesonephros and migrated to the gonad, forming a coelomic vessel that extends beneath the coelomic epithelium of the gonad that only forms in normally virilised males and females treated with AMH. This supports previous reports of ovarian masculinisation in freemartin cattle (Jost et al., 1972) and in rat gonadal cultures *ex vivo* (Vigier et al., 1984). Whether this induction of male specific vascularisation is truly a consequence of direct AMH signalling is unclear however, as similar effects can be replicated by *in vitro* culture of the mesonephros in the presence of beads coated with either BMP2 or BMP4 (Ross et al., 2003). These results highlight the functional redundancy that can exist between members of the TGFβ signalling family, although it should be noted that neither BMP2 nor BMP4 are expressed in the gonads during this developmental window, so their physiological importance in regulating male vascular patterning is questionable.

This distal fused portion of the Müllerian ducts is distinct from the proximal region that expresses Pax2 (induced by the Wolffian ducts), whereas the fused portion is initially formed in Pax2 mutant mice (Torres et al., 1995) – indicating an autonomy of this region. Interestingly, our results suggest the distal fused part of the Müllerian ducts does not seem to regress and likely gives rise to the prostatic utricle as has been previously proposed (Jacob et al., 2012).

Although the paradigm originally established by Jost of active regression of the Müllerian ducts in males and the passive regression of the Wolffian ducts in females – due to a lack of androgen signalling to maintain them – has survived intact for over half a century, recent work (Zhao et al., 2017) has begun to raise important questions concerning its completeness. Zhao and colleagues found that the orphan nuclear receptor COUP–TF2 (chicken ovalbumin upstream promotor transcription factor 2) appears to play an active role in the regression of the Wolffian ducts, mediated by FGF signaling. Although intersex phenotypes in XY animals can be generated by genetic invalidation of factors involved at all levels of AMH signalling, the specific knockdown of *COUP–TF2* in the Wolffian duct mesenchyme ($Wt1^{CreRT2+};Couptf2^{f/f}$) is the first intersex model generated in XX mice. That the authors were able to exclude masculinisation of the ovary and the phenomena persisted independently of androgen activity raises important questions about how the development of the female genital tract could also be actively regulated.

9.3 GnRH Development in Humans: Old Confirmations & New Insights

The GnRH system is the master regulator of reproductive function in vertebrates, and alterations in GnRH signalling and/or neuronal development impair human reproduction. It is therefore critical to fully understand the mechanisms regulating the ontogenesis, differentiation and prenatal migration of GnRH neurons from the nose to the brain. Here we have conducted comprehensive anatomical studies of human embryos/foetuses, to get better insight into the development of GnRH neurons during the first trimester of gestation. The unprecedented use of whole-mount immunolabelling and 3DISCO technology coupled with LSM to carry out the high-resolution visualisation of markers for various cell and fibre types in whole embryos/foetuses has led to several novel observations concerning this system that could not have been achieved with conventional 2D histological analysis. These findings open new avenues in the study of human brain connectivity under physiological and pathological conditions. For instance, this study undertook the first quantitative analysis of GnRH neurons in human foetuses. We established that an average of 10,000 GnRH neurons are produced in humans during development. These cells are likely to survive through adulthood, considering that the number and anatomical distribution of neurons containing the GnRH transcript are similar in adult post-mortem brains (Rance et al., 1994). Indeed, these authors have reported that besides the hypothalamus, a great proportion of GnRH neurons in the adult human brain are scattered in extrahypothalamic regions including the magnocellular basal forebrain complex, extended amygdala, ventral pallidum, and putamen (Rance et al., 1994).

Our analysis also shows that GnRH neurons first appear in the vicinity of the presumptive VNO at CS 16 (approx. 39 days of gestation), several days earlier than previously reported (Schwanzel-Fukuda et al., 1996). The authors of this previous work examined human embryos at gestational days (GD) 28, 32, 42 and 46, and observed GnRH cells in the olfactory pit and the forebrain at GD 42, but not earlier (Schwanzel-Fukuda et al., 1996); intermediate stages between GD 32 and 42 were not analysed. At GD 39 (CS 16) we detected a total of 50 GnRH neurons in the embryo as a whole, all of which were located within the developing nasal region.

This distribution pattern and low cell number indicate that CS 16 corresponds to the birthdate of this neuroendocrine cell population.

It has been previously shown in other species that GnRH-expressing neurons migrate into the brain along branches of the VNN and TN (Schwanzel-Fukuda & Pfaff, 1989; Schwanzel-Fukuda et al., 1989; Wray et al., 1989), both of which emerge from the vomeronasal epithelium and run medially from the olfactory epithelium towards the dorsal region of the OB. However, their central entry point differs: the VNN reaches the AOB, whereas the TN projects ventrally and dorsally within the forebrain to target septal, hypothalamic and limbic areas (Pearson, 1941; Schwanzel-Fukuda & Pfaff, 1989; Schwanzel-Fukuda & Silverman, 1980; Verney et al., 2002; Wirsig-Wiechmann & Oka, 2002; Wray et al., 1989), involved in controlling innate behaviours and neuroendocrine responses. The issue of whether GnRH neurons in humans also reach their target areas using this axonal scaffold has been unknown.

Using whole-mount immunolabelling and 3DISCO, we found that GnRH neurons migrate into several hypothalamic and extrahypothalamic brain regions in tight association with peripherin-positive VNN/TN fibres. This observation indicates that the vomeronasal and terminal systems play important roles in the ontogenesis and migration of GnRH neurons in the human, similar to other mammals. This raises the possibility that some genetic forms of congenital hypogonadotropic hypogonadism in humans, characterised by GnRH deficiency and the failure of puberty onset, might be due to defective central projections of the TN, causing insufficient/aberrant GnRH migration. In agreement with this hypothesis, previous work from our laboratory has shown that intracranial projections of the VNN/TN, which express Neuropilin-1, the receptor for the guidance molecule Semaphorin3A, fail to enter the brain, instead accumulating at the dorsal surface of the cribriform plate in mice lacking a functional semaphorin-binding domain in Nrp1 (Nrp1sema/Sema mice) (Hanchate et al., 2012). Concordantly, deficient Semaphorin3A signalling appears to contribute to some human genetic reproductive disorders characterized by defective GnRH migration, such as Kallmann and CHARGE syndromes (Hanchate et al., 2012; Schulz et al., 2014; Young et al., 2012). Another striking finding is the existence of an evolutionarily conserved dorsal migratory path within the

brain for GnRH neurons. A similar observation was made in non-human primates twenty years ago (Quanbeck et al., 1997), but was not confirmed or extended to any other species. In the present study we identified GnRH neurons along the two migratory streams both in human and mouse embryos, and both species possessed unexpected GnRH neuronal populations in the neocortex and the developing piriform cortex, involved in olfaction.

An additional noteworthy and previously unreported observation in both species was the presence of a single-cell thick ring around each OB. The topography of these cells strikingly resembles that of a group of olfactory glomeruli called the "necklace" glomeruli, which surround the caudal end of the OBs (Shinoda et al., 1989). Interestingly, the necklace glomeruli have been implicated in detecting pheromones (Lin et al., 2004; Teicher et al., 1980), and our study shows that a significant number of GnRH neurons and fibres are still present during adulthood in the mouse OB and the AOB. This observation suggests that there may be some as-yet undetermined connective or functional link between the GnRH neurons in this structure and neurons involved in olfactory and/or pheromonal discrimination.

A structural and functional link between GnRH neuronal ontogenesis and pheromone detection could also come from our observations concerning the VNO. In humans and other mammals, odours represent relevant chemosensory cues in the establishment of early interactions between mothers and infants (Dulac et al., 2014), and several studies have identified behavioural responses to pheromonal compounds (Dulac et al., 2003). However, the issue of whether these responses are mediated by a functional VNO has been a matter of extensive debate. Here, we found that the anatomical site of presumptive VNO differentiation during early embryonic development in humans is defined, as in rodents, by the graded expression of the transcription factors AP-2α and PAX6. Previous studies have shown that a VNO is distinguishable in a great proportion of adult humans (Frasnelli et al., 2011). However, the neuronal connection between the VNO and the AOB has remained elusive. Here, we show that during human foetal development, the VNO and the AOB are indeed anatomically connected, since NRP-2-immunoreactive vomeronasal fibres project to the dorsal OB, as reported in rodents (Cloutier et al., 2002). The VNO also contains strongly Ki67- and SOX2-positive putative neurogenic

precursors, in agreement with the increase in volume of the human foetal VNO epithelium with age and its persistence at least until birth (Bhatnagar et al., 2001; Smith & Bhatnagar, 2000). Since it appears that GnRH neurons, olfactory ensheathing cells and other neurons belonging to the migratory mass emerge from the VNO, we hypothesize that these dividing VNO precursors might be the progenitors of one or all of the aforementioned cell types.

Finally, the computer-assisted 3D reconstruction of tissue sections immunolabelled for GnRH has allowed the generation of the first 3D atlas of GnRH cell bodies and fibres from GW 9 and 12 human foetuses. These mapping experiments have revealed the wide distribution of GnRH cells and terminals in several extrahypothalamic regions.

Altogether, these observations raise the intriguing possibility that GnRH neurons may also modulate as-yet unexplored non-reproductive functions. Indeed, the GnRH neuroendocrine system has been recently proposed to regulate systemic ageing (Zhang et al., 2013). The idea that turning down the hypothalamic release of modulators such as GnRH may accelerate aging is in line with recent findings that hypogonadal mice, which harbour a spontaneous mutation inactivating the GnRH gene (Mason et al., 1986), exhibit dementia-like changes during aging (Drummond et al., 2012). GnRH concentrations in the cerebrospinal fluid are proportional to those in the portal blood vessels which deliver the neurohormone to the anterior pituitary (Van Vugt et al., 1985). The cerebrospinal fluid may thus serve to transmit hypothalamic GnRH signals to GnRH-receptor-expressing neuronal populations in the hippocampus and/or other brain areas involved in cognition (Granger et al., 2004; Wilson et al., 2006).

9.4 AMH As A Novel Contributor To Hypogonadotropic Hypogonadisms

The only source of AMH described so far during embryonic development is the testis. The timing of AMH expression and secretion by the Sertoli cells is tightly regulated, as the Müllerian ducts only remain hormonally sensitive for a short period of time, outside of which the Müllerian ducts will fail to regress (Taguchi et al., 1984; Tsuji et al., 1992). This window is around E13/E14 in mice and appears to be determined by the expression of receptors able to bind AMH, with levels sharply decreased outside of the critical window (Josso et al., 2001).

In this report, we provide novel evidence that during embryonic development AMH is also expressed in extragonadal areas, namely in the nasal placode, with a spatiotemporal pattern likely to impact the GnRH/olfactory/vomeronasal system development. Using RT-PCR we found *AMH*, AMH receptors and *SMAD* transcripts to be expressed in the nasal regions of mouse embryos dissected at E11.5 and confirmed *AMH* mRNA expression in E12.5 GnRH-GFP neurons isolated through FACS. Immunohistochemistry coupled with confocal microscopy on nasal explants and in mouse embryo sections revealed that the majority of GnRH neurons located in the nasal compartment were AMH immunopositive. Furthermore, AMH was found to be expressed in the developing VNO and OE and along the olfactory/vomeronasal fibres during embryonic development.

We recently showed that migratory GnRH neurons and olfactory axons, both in mouse and human foetuses, express AMHR2 (Cimino et al., 2016). Thus, the spatiotemporal expression of AMH and its receptors in nasal regions correlates with migration of GnRH neurons toward the brain and the development of the olfactory/vomeronasal sensory systems through an autocrine/paracrine AMH/AMHR2 mechanism.

Here, we find that *in utero* injections of AMHR2-neutralising antibodies (AMHR2-NA) lead to deficits consistent with reduced migration of GnRH neurons. Most importantly, peripherin axonal labelling at E14.5 showed abnormal projection of the TN to the ventral forebrain in AMHR2-NA treated embryos. This projection forms the axonal scaffold for the intracerebral

migration of GnRH cells both in mice and humans (Casoni et al., 2016; Schwarting et al., 2001; Yoshida et al., 1995), suggesting that the defects in the targeting of these axons could contribute to the alteration in the GnRH migratory process detected in these animals.

3D imaging of solvent-cleared organs (3DISCO) is an organic solvent-based method used to reduce light scattering within samples, rendering them 'optically clear' and thereby allowing large volumes to be imaged without prior dissection (Erturk et al., 2012; 2013). This method has previously been combined with an immunolabelling protocol followed by light-sheet laser scanning microscopy (LSM) to study neuronal connectivity in mouse embryos and postnatal brains (Belle et al., 2014). Here, we used this technique to study the 3D organisation of the GnRH and olfactory system development in whole *AMHR2* $^{+/+}$ and *AMHR2* $^{-/-}$ embryos. Our experiments revealed that both acute neutralisation of AMHR2 or genetic invalidation of this receptor lead to the same phenotype with a strong accumulation of GnRH neurons in the nasal region and defects in both the olfactory targeting to the OBs and in the intracranial projections of the VNN/TN. These defects strongly resemble the phenotype previously described in pathohistological analyses of KS human foetuses (Schwanzel-Fukuda et al., 1996; Texeira et al., 2010).

Neuroanatomical analysis of *AMHR2* $^{-/-}$ adult brains showed a significant 40% reduction of the GnRH cell population compared to wild-type and heterozygous animals, suggesting that the GnRH cell migration defect observed in *AMHR2* $^{-/-}$ mouse embryos was not corrected during later development. Moreover, the decrease in the number of TH-immunopositive neurons in the olfactory bulbs of *AMHR2* $^{-/-}$ as compared to wild-type animals strongly suggests that it results from deficits of afferent projection from OSN during development and that these animals have probably olfactory impairments.

Given the *in vivo* effects of AMHR2 invalidation on GnRH neuronal migration, we sought to dissect whether AMH alters GnRH cell motility and to identify the cellular mechanisms governing this response. Our *in vitro* experiments demonstrated that AMH induces increased

cellular migration in GN11 cells and that this effect is mediated by the presence of both AMHR2 and BMPR1b and subsequent activation of the MAPK pathway.

The KS-like phenotype of *AMHR2*$^{-/-}$ mice, prompted us to ask whether insufficient AMH signalling might also be involved in the human CHH disorder. We performed whole-exome sequencing in a large cohort of CHH probands (n = 113) and their family members (when available) focusing on AMH and its exclusive binding receptor, AMHR2, identifying several missense mutations, all in the heterozygous state. The low penetrance of most CHH associated genes combined with variable phenotypic presentation among affected individuals carrying the same genetic defect, suggests that CHH is not a strictly monogenic disorder. Indeed, patients harbouring mutations in two or more CHH loci have been previously described (Pitteloud et al., 2007; Sykiotis et al., 2010).

Since AMH functions as a homodimer (di Clemente et al., 2010), we hypothesised that AMH variants in the heterozygous state might have a phenotypic impact on GnRH development/function via a dominant-negative interaction between a wild-type and variant AMH peptide.

Interestingly, we found that the conditioned medium from COS-7 cells transfected with the wild-type *AMH* cDNA significantly increased GN11 cell motility, whereas *AMHs* harbouring the p.Val12Gly, p.Glu160Asp, p.Asp288Glu, p.Pro151Ser, p.Ala519Val, missense mutations resulted in a 50% reduction of GN11 migration compared to the wild-type *AMH*. These results strongly indicate that the AMH mutations identified in CHH have a pathogenic effect. Moreover, since GN11 cells endogenously express AMH, these results also suggest that only a proportion of endogenous AMH dimers are able to achieve signalling capability *in vitro* and that the other fraction dimerizes with the mutant AMH deriving from the COS-7 conditioned medium, further substantiating the dominant-negative interaction model of the AMH variants.

AMH mutations affecting GN11 cell motility were found in both KS and nCHH affected individuals. We thus speculate that GnRH migratory defects might also occur in some forms of

nCHH. This hypothesis contrasts the current view of CHH pathogenesis, whereby defects in cell migration of GnRH neurons is thought to occur only in KS and not in nCHH patients (Boehm et al., 2015). However, histological examination of GnRH neurons in human foetuses carrying mutations in nCHH genes has never been performed.

We believe that the alterations of OB innervation and of GnRH migration, that characterise the KS pathogenesis, may not be inextricably linked events. Indeed, we recently showed using whole-mount immunolabelling and tissue-clearing (Casoni et al., 2016), that GnRH neurons in human foetuses migrate into their target brain regions in tight association with vomeronasal and terminal fibres only. This indicates that the vomeronasal and terminal systems play important roles in the ontogenesis and migration of GnRH neurons in humans and raises the intriguing possibility that some genetic forms of CHH in humans might be due to defective central projections of the terminal nerve, causing insufficient/aberrant GnRH migration, rather than being associated with defective olfactory axon targeting. In support of this, here we present evidence that both the terminal nerve projections as well as the migration of GnRH neurons were highly perturbed in mouse embryos when AMHR2 signalling was pharmacologically or genetically neutralised.

Similar defects in the projection of the vomeronasal/terminal nerves and migration of GnRH neurons have been previously reported in animal models harbouring mutations in known KS-associated genes, such as Sema3A (Cariboni et al., 2011; Hanchate et al., 2012; Young et al., 2012). Whilst other factors (e.g. Sema4D) have been shown to alter GnRH migratory activity with no effect on the development of OSNs (Giacobini et al., 2008).

In summary, this work provides insights into the molecular basis of AMH-dependent signalling in the correct establishment of the GnRH migratory process. Lack of this signalling pathway impairs the final size of the GnRH neuronal population in adulthood and the organisation of the OB.

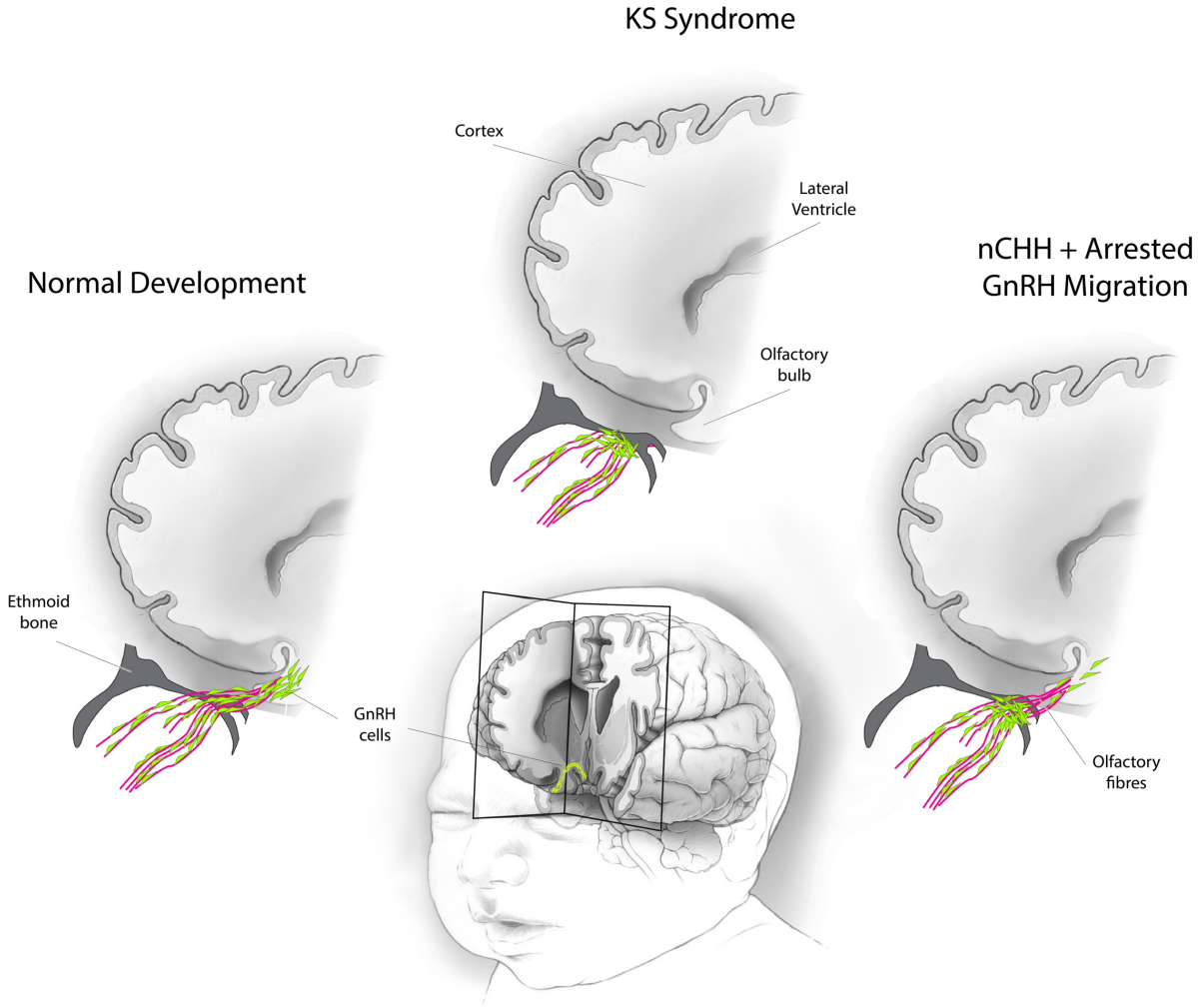

Figure 58. Proposed segregation of GnRH migratory defects between KS and nCHH syndromes

Alterations of OB innervation and of GnRH migration, that characterise KS pathogenesis, may not be inextricably linked events based on the data presented in this thesis. Although the development of the olfactory and GnRH systems are intimately linked, it appears that GnRH migration in humans occurs along terminal and VNN fibres only. Here we present evidence that both the terminal nerve projections as well as the migration of GnRH neurons were highly perturbed in mouse embryos when AMHR2 signalling was pharmacologically or genetically neutralised and supports the possibility that some genetic forms of nCHH in humans might be due to defective central projections of the terminal nerve, causing insufficient/aberrant GnRH migration, rather than being associated with defective olfactory axon targeting

CHAPTER 10

Conclusions

10.1 Conclusions

Generating a precise cellular and molecular cartography of the human embryo is essential to understand the mechanisms of organogenesis in normal and pathological conditions. Here, we combined whole-mount immunostaining, 3DISCO clearing and light-sheet imaging to make the first steps towards building a three-dimensional cellular map of human development during the first trimester of gestation. We provide 3D images at an unprecedented resolution of the several developing systems including the peripheral nervous system and the urogenital system. We present evidence for a differential vascularisation of male and female genital tracts concomitant to sex determination. This work paves the way for a cellular and molecular reference atlas of human cells which is critical to understanding human developmental disorders.

Additionally, the results described in the previous chapters help to elucidate several important morphological and functional aspects of the development of the GnRH-1 system in both mice and humans. We provide the first evidence of GnRH immunoreactivity at CS16, approximately 39 days of gestation, confirming the birth of this population occurs several days earlier than has previously been reported. Our quantification of the total number of GnRH cells present during human development is the first of its kind and suggests a rapid increase in the size of the population occurs between the 39th and 44th days of gestation, rising from 50 cells to an average of around 8,000 cells just a few days later. This number is highly likely to be an accurate representation of the total population as GnRH-1 mRNA has been shown to exhibit a very similar pattern of expression and in a similar number in adult post-mortem brains.

The confirmation of findings reported 20 years ago in rhesus macaques of a dorsal migratory pathway, leading to extra-hypothalamic populations of GnRH expressing neurons paves the way for exciting new scientific and clinical discoveries on the role of GnRH expression and release in human reproductive physiology, olfactory behaviour and cognitive processes.

Long considered a purely gonadal hormone, here we report that Anti-Müllerian Hormone is expressed during early embryonic development along the GnRH migratory pathway and that it regulates GnRH cell motility through AMHR2/BMPR1b heterodimerisation. Invalidation of AMH signalling *in vivo* results in defective development of the peripheral olfactory system and altered embryonic migration of the GnRH cells to the basal forebrain, resulting in a significant reduction of GnRH population size in adulthood and a KS-like phenotype.

These novel reports are supported by whole-exome sequencing of a cohort of 70 KS and 43 nCHH probands, that identified several heterozygous missense mutations in the AMH and AMHR2 genes in both KS and nCHH individuals. Biochemical validation revealed several mutated forms of AMH resulted in decreased GnRH cell motility and impaired secretion of AMH by transfected COS-7 cells, which strongly suggests that these variants have a pathogenic effect. Our findings highlight a novel role for AMH in the development and function of the GnRH neurons and indicate that AMH signalling insufficiency contributes to the pathogenesis of CHH.

In summary, this work provides insights into the molecular basis of AMH-dependent signalling in the correct establishment of the GnRH migratory process. Moreover, this work implicates AMH mutations in the pathophysiology of CHH consistent with the role of this gene in the correct development of GnRH neurons and supports overturning the idea that migratory defects of the GnRH population are exclusively restricted to KS and do not occur in nCHH conditions.

References

Abe H & Oka Y. Mechanisms of the modulation of pacemaker activity by GnRH peptides in the terminal nerve-GnRH neurons. Zool Sci. 19: 111-128 (2002)

Abe S et al., Expression of intermediate filaments at muscle insertions in human fetuses. J. Anat. 217: 167 - 173 (2010).

Abitua PB et al., The pre-vertebrate origins of neurogenic placodes. Nature. 524(7566): 462-5 (2015)

Abraham E et al., The zebrafish as a model system for forebrain GnRH neuronal development. General and comparative endocrinology. 164, 151-160. (2009).

Abraham E et al., Early development of forebrain gonadotrophin-releasing hormone (GnRH) neurones and the role of GnRH as an autocrine migration factor. J Neuroendocrinol. 20, 394-405. (2008).

Adams N. Is anti-mullerian hormone a hormone? Thesis, Doctor of Philosophy, University of Otago. (2012)

Adelman JP et al., Isolation of the gene and hypothalamic cDNA for the common precursor of gonadotropin-releasing hormone and prolactin release-inhibiting factor in human and rat. PNAS. 83: 179-83 (1986)

Akutsu S et al., Origin of luteinizing hormone-releasing hormone (LHRH) neurons in the chick embryo: effect of the olfactory placode ablation. Neuroscience letters 142, 241-244 (1992).

Al-Asaad I et al., Mullerian inhibiting substance in the caudate amphibian Pleurodeles waltl. Endocrinology 154(10): 3931-6. (2013)

Aleck K et al., True hermaphroditism with partial duplication of chromosome 22 and without SRY. Am J Med Gen. Part A 85(1): 2-4. (1999)

Allard S et al., Molecular mechanisms of hormone-mediated Mullerian duct regression: involvement of beta-catenin. Development. 127(15): 3349-60. (2000)

Amoss M et al., Purification, amino acid composition and N-terminus of the hypothalamic luteinizing hormone releasing factor (LRF) of ovine origin. Biochem & Biophys Res Comms. 44(1) 205-210. (1971)

Anderson C et al., Concentrations of AMH and inhibin-B in relation to follicular diameter in normal human small antral follicles. Human Reproduction. 25(5): 1282-1287. (2010)

Andersson AM et al., Serum inhibin B in healthy pubertal and adolescent boys: relation to age, stage of puberty, and follicle-stimulating hormone, luteinizing hormone, testosterone, and estradiol levels. J. Clin. Endocrinol. Metab. 82, 3976 - 3981 (1997).

Anttonen M et al., FOG-2 and GATA-4 are co-expressed in the mouse ovary and can modulate mullerian-inhibiting substance expression. Biol Reprod 68(4): 1333-40. (2003)

Arango NA et al., A mesenchymal perspective of mullerian duct differentiation and regression in Amhr2-lacZ mice. Mol Reprod Dev 75(7): 1154-62. (2008)

Arango NA et al., Targeted mutagenesis of the endogenous mouse Mis gene promoter: in vivo definition of genetic pathways of vertebrate sexual development. Cell 99(4): 409-19. (1999)

Aven, L & Ai X, Mechanisms of respiratory innervation during embryonic development. Organogenesis 9: 194 - 198 (2013)

Baarends WM et al., A novel member of the transmembrane serine/threonine kinase receptor family is specifically expressed in the gonads and in mesenchymal cells adjacent to the mullerian duct. Development 120, 189–197 (1994)
Baarends WM et al., Anti-Mullerian hormone and anti-Mullerian hormone type II receptor messenger ribonucleic acid expression during postnatal testis development and in the adult testis of the rat. Endocrinology 136(12): 5614–22. (1995)
Baarends WM et al., A novel member of the transmembrane serine/threonine kinase receptor family is specifically expressed in the gonads and in mesenchymal cells adjacent to the mullerian duct. Development 120, 189–197. (1994).
Baetens, D. et al. Extensive clinical, hormonal and genetic screening in a large consecutive series of 46XY neonates and infants with atypical sexual development. Orphanet J. Rare Dis. 9, 209 (2014)
Baken L et al., Design and validation of a 3D virtual reality desktop system for sonographic length and volume measurements in early pregnancy evaluation. J. Clin. Ultrasound 43, 164 – 170 (2015)
Baker H et al., Transneuronal regulation of tyrosine hydroxylase expression in olfactory bulb of mouse and rat. J Neurosci 3, 69–78 (1983).
Balland E et al., Hypothalamic tanycytes are an ERK-gated conduit for leptin into the brain. Cell metabolism. 19(2): 293–301. (2014)
Barbie TU et al., Mullerian Inhibiting Substance inhibits cervical cancer cell growth via a pathway involving p130 and p107. PNAS. 100(26): 15601– 15606. (2003)
Barraud P et al., Olfactory ensheathing glia are required for embryonic olfactory axon targeting and the migration of gonadotropin-releasing hormone neurons. Biology, 2:750–759, (2013).
Barry et al., Immunofluorescence study of the preoptico-terminal LRH tract in the female squirrel monkey during the estrous cycle. Cell Tissue Res. 198: 1–13 (1979)
Bastide P et al., Sox9 regulates cell proliferation and is required for Paneth cell differentiation in the intestinal epithelium. J. Cell Biol. 178: 635 – 648 (2007)
Bayer SA et al., Development of the preoptic area: time and site of origin, migratory routes, and settling patterns of its neurons. Journal of Comparative Neurology 265(1): 65–95. (1987)
Beau C et al., In vivo analysis of the regulation of the anti-Mullerian hormone, as a marker of Sertoli cell differentiation during testicular development, reveals a multi-step process. Mol Reprod Dev 59(3): 256–64. (2001)
Beauvillain JC & Tramu G. Immunocytochemical demonstration of LH-RH, somatostatin, and ACTH-like peptide in osmium-postfixed, resin-embedded median eminence. J Histochem Cytochem 28, 1014–1017 (1980).
Behar TN et al., Glutamate acting at NMDA receptors stimulates embryonic cortical neuronal migration. J Neurosci. 19(11): 4449–4461 (1999)
Behringer RR et al., Abnormal sexual development in transgenic mice chronically expressing mullerian inhibiting substance. Nature 345(6271): 167–70. (1990)
Behringer RR et al., Mullerian-inhibiting substance function during mammalian sexual development. Cell 79(3): 415–25 (1994)
Behringer RR et al., Mullerian-inhibiting substance function during mammalian sexual development. Cell 79, 415–425 (1994).
Belle M et al., A Simple Method for 3D Analysis of Immunolabeled Axonal Tracts in a Transparent Nervous System. Cell Rep. 9: 1191 – 1201 (2014)
Belle M et al., Tridimensional Visualization and Analysis of Early Human Development. Cell. 169, 161–173 e112 (2017).

Belville C et al., Role of type I receptors for anti-Mullerian hormone in the SMAT-1 Sertoli cell line. Oncogene 24(31): 4984-92. (2005)
Belville C et al., Mutations of the anti-mullerian hormone gene in patients with persistent mullerian duct syndrome: biosynthesis, secretion, and processing of the abnormal proteins and analysis using a three-dimensional model. Molecular endocrinology. 18, 708-721 (2004).
Belville C et al., Persistence of Mullerian derivatives in males. American journal of medical genetics 89, 218-223 (1999).
Bernard P et al., Wnt signaling in ovarian development inhibits Sf1 activation of Sox9 via the Tesco enhancer. Endocrinology 153(2): 901-12. (2012)
Betters E et al., Analysis of early human neural crest development. Dev. Biol. 344: 578 - 592 (2010)
Bhatnagar KP & Smith TD. The human vomeronasal organ. III. Postnatal development from infancy to the ninth decade. J Anat. 199, 289-302 (2001).
Bianco SD et al., The genetic and molecular basis of idiopathic hypogonadotropic hypogonadism. Nat. Rev. Endocrinol. 5, 569 - 576 (2009).
Blechschmidt, E. The Beginnings of Human Life (New York, NY: Springer New York). (1977)
Bless EP et al., Expression of a cell surface glycoconjugate in gonadotropin releasing hormone (GnRH) neurons in mice. Soc Neurosci Abstr. Vol. 26. (2001)
Boehm U et al., Expert consensus document: European Consensus Statement on congenital hypogonadotropic hypogonadism-pathogenesis, diagnosis and treatment. Nat Rev Endocrinol. 11, 547-564, (2015).
Bond C et al., The rat gonadotropin-releasing hormone: SH locus: structure and hypothalamic expression. Mol endocrinol 3, 1257-1262, (1989).
Bondurand N et al., Expression of the SOX10 gene during human development. FEBS Lett. 432: 168 - 172 (1998)
Bossy J. Development of olfactory and related structures in staged human embryos. Anatomy and embryology 161, 225-236 (1980).
Boukari K et al., Lack of androgen receptor expression in Sertoli cells accounts for the absence of anti-Mullerian hormone repression during early human testis development. J. Clin. Endocrinol. Metab. 94, 1818 - 1825. (2009)
Bourgeois F et al., A critical and previously unsuspected role for doublecortin at the neuromuscular junction in mouse and human. Neuromuscul. Disord. 25: 461 - 473 (2015)
Boyer A et al., WNT signaling in ovarian follicle biology and tumorigenesis. Trends in Endocrinology & Metabolism 21(1): 25-32. (2010)
Brennaman LH & Maness PF, NCAM in neuropsychiatric and neurodegenerative disorders. Structure and Function of the Neural Cell Adhesion Molecule NCAM. Springer New York, 299-317 (2010)
Brennan J et al., Divergent vascular mechanisms downstream of Sry establish the arterial system in the XY gonad. Dev. Biol. 244: 418 - 428 (2002)
Brown JW. The nervus terminalis in insectivorous bat embryos and notes on its presence during human ontogeny. Annals of the New York Academy of Sciences. 519, 184-200 (1987).
Bruder JM & Wierman ME, Evidence for transcriptional inhibition of GnRH gene expression by phorbol ester at a proximal promoter region. Mol Cell Endocrinol. 99(2):177-82 (1994)
Bruneau G et al., Prolonged neurogenesis during early development of gonadotropin-releasing hormone neurones in sheep (Ovis Aries): in vivo and in vitro studies. Neuroendocrinology 77, 177-186, (2003).

Brunjes PC & Frazier LL. Maturation and plasticity in the olfactory system of vertebrates. Brain Research Reviews 11(1): 1–45. (1986)
Brunjes PC et al., Olfactory bulb organization and development in Monodelphis domestica (grey short tailed opossum). J Comp Neurol. 320: 544–554 (1992)
Bulfone A et al., Spatially restricted expression of Dlx1, Dlx2 (Tes–1), Gbx2 and Wnt–3 in the embryonic day 12.5 mouse forebrain defines potential transverse and longitudinal segmental boundaries. J Neurosci. 1:3155 – 3172. (1993)
Burris T et al., Identification of a putative steroidogenic factor–1 response element in the DAX–1 promoter. Biochem biophys res comms. 214(2): 576–581. (1995)
Cain B et al., Distribution and colocalization of cholecystokinin with the prohormone convertase enzymes PC1, PC2, and PC5 in rat brain. J Comp Neurol. 467(3): 307–325. (2003)
Cameron H & Mckay R, Adult neurogenesis produces a large pool of new granule cells in the dentate gyrus. J Comp Neurol. 435(4): 406–417 (2001)
Campbell RE et al., Biocytin filling of adult gonadotropin–releasing hormone neurons in situ reveals extensive, spiny, dendritic processes. Endocrinology. 146(3):1163–9 (2005)
Campbell RE et al., Dendro–dendritic bundling and shared synapses between gonadotropin–releasing hormone neurons. PNAS. 106(26):10835–40 (2009)
Caraty A et al., Biphasic response in the secretion of gonadotrophin–releasing hormone in ovariectomized ewes injected with oestradiol. J Endocrinol. 1123(3):375–82 (1989)
Cariboni A & Maggi R, Kallmann's syndrome, a neuronal migration defect. Cellular and molecular life sciences 63(21): 2512–2526 (2006)
Cariboni A et al., Defective gonadotropin- releasing hormone neuron migration in mice lacking sema3a signalling through nrp1 and nrp2: Implications for the aetiology of hypogonadotropic hypogonadism. Hum Mol Genet. 20:336- 344. (2011)
Cariboni A et al., Dysfunctional SEMA3E signaling underlies gonadotropin–releasing hormone neuron deficiency in Kallmann syndrome. JCI. 125(6):2413–28 (2015)
Cariboni A et al., Neuropilins and their ligands are important in the migration of gonadotropin-releasing hormone neurons. J Neurosci. 27:2387-2395. (2007)
Cariboni A et al., Defective gonadotropin–releasing hormone neuron migration in mice lacking SEMA3A signalling through NRP1 and NRP2: implications for the aetiology of hypogonadotropic hypogonadism. Hum Mol Genet 20, 336–344 (2011).
Cariboni A et al., Slit2 and Robo3 modulate the migration of GnRH–secreting neurons. Development. 139(18): 3326–3331. (2012)
Carmeliet P et al., Biological Effects of Disruption of the Tissue-Type Plasminogen Activator, Urokinase-Type Plasminogen Activator, and Plasminogen Activator Inhibitor-1 Genes in Mice. Annals of the New York Academy of Sciences. 748(1): 367–381 (1994)
Casazza A et al., Semaphorin signals in cell adhesion and cell migration: Functional role and molecular mechanisms. Advances in experimental medicine and biology. 600:90-108. (2007)
Casoni F et al., Development of the neurons controlling fertility in humans: new insights from 3D imaging and transparent fetal brains. Development 143: 3969 – 3981 (2016)
Cate RL et al., Isolation of the bovine and human genes for müllerian inhibiting substance and expression of the human gene in animal cells. Cell. 45, 685 – 698. (1986)
Catlin EA et al., Mullerian inhibiting substance inhibits branching morphogenesis and induces apoptosis in fetal rat lung. Endocrinology, 138(2): 790–6. (1997)

Catlin EA et al., Sex-specific fetal lung development and mullerian inhibiting substance. Am. Rev. Respir. Dis. 141(2): 466-70. (1990)
Caton A et al., The branchial arches and HGF are growth-promoting and chemoattractant for cranial motor axons. Development. 127(8): 1751-1766 (2000)
Catteau-Jonard S & Dewailly D. Anti-Mullerian hormone and polycystic ovary syndrome. Gynecologie, obstetrique & fertilite 39(9): 514-517. (2011)
Chan E et al., for Canadian Association of Pediatric Surgeon Evidence-Based Resource. Ideal timing of orchiopexy: a systematic review. Pediatr. Surg. Int. 30, 87－97. (2014).
Chang H et al., Smad5 knockout mice die at mid-gestation due to multiple embryonic and extraembryonic defects. Development 126(8): 1631-1642. (1999)
Charlton H. Neural transplantation in hypogonadal (hpg) mice - physiology and neurobiology. Reproduction. 127: 3-12. (2004)
Chemes HE et al., Physiological androgen insensitivity of the fetal, neonatal, and early infantile testis is explained by the ontogeny of the androgen receptor expression in Sertoli cells. J. Clin. Endocrinol. Metab. 93, 4408－4412 (2008)
Chen P & Moenter SM, GABAergic transmission to gonadotropin-releasing hormone (GnRH) neurons is regulated by GnRH in a concentration-dependent manner engaging multiple signaling pathways. J Neurosci. 29(31): 9809-9818 (2009)
Chen YG et al., Mechanism of TGFbeta receptor inhibition by FKBP12. EMBO J. 16(13): 3866-76. (1997)
Chertow BS. The role of lysosomes and proteases in hormone secretion and degradation. Endocr Rev 2(2):137-73 (1981)
Christian CA & Moenter SM. The neurobiology of preovulatory and estradiol-induced gonadotropin-releasing hormone surges. Endocrine rev. 31, 544-577, (2010).
Chuah MI & Zheng DR. Olfactory marker protein is present in olfactory receptor cells of human fetuses. Neurosci 23, 363-370 (1987).
Chung AS & Ferrara N, Developmental and Pathological Angiogenesis. Annu. Rev. Cell Dev. Biol. 27: 563－584 (2011)
Cimino I et al., Novel role for anti-Müllerian hormone in the regulation of GnRH neuron excitability and hormone secretion. Nat Commun. 2016; 7: 10055 (2016)
Clarke IJ et al., GnRH-associated peptide (GAP) is cosecreted with GnRH into the hypophyseal portal blood of ovariectomized sheep. Biochem Biophys Res Commun. 143(2):665-71 (1987)
Clarke TY et al., Mullerian inhibiting substance signaling uses a bone morphogenetic protein (BMP)-like pathway mediated by ALK2 and induces SMAD6 expression. Mol Endocrinol 15(6): 946-59 (2001)
Clements A et al., Studies on human sexual development. III. Fetal pituitary and serum and amniotic fluid concentrations of LH, CG and FSH. J Clin Endocrinol Metab. 6(42): 9-19 (1976)
Clevers H & Nusse R. Wnt/β-catenin signaling and disease. Cell 149(6): 1192-1205. (2012)
Clipsham R & McCabe E. DAX1 and its network partners: exploring complexity in development. Molecular genetics and metabolism. 80(1): 81-120. (2003)
Cloutier JF et al., Neuropilin-2 mediates axonal fasciculation, zonal segregation, but not axonal convergence, of primary accessory olfactory neurons. Neuron 33, 877-892 (2002).
Cloutier JF et al., Differential requirements for semaphorin 3F and Slit-1 in axonal targeting, fasciculation, and segregation of olfactory sensory neuron projections. Journal of Neuroscience 24(41): 9087-9096. (2004)

Cogliati T et al., Pubertal impairment in Nhlh2 null mice is associated with hypothalamic and pituitary deficiencies. Mol Endocrinol. 21(12): 3013-27 (2007)
Cohen-Haguenuauer O et al., Mapping of the gene for anti-mullerian hormone to the short arm of human chromosome 19. Cytogenet Cell Genet 44(1): 2- 6. (1987)
Conrotto P et al., Sema4d induces angiogenesis through met recruitment by plexin b1. Blood. 105:4321-4329 (2005)
Corbier P et al., Changes in testicular weight and serum gonadotropin and testosterone levels before, during, and after birth in the perinatal rat. Endocrinology 103(6): 1985-1991. (1978)
Corbier P et al., Sex differences in serum luteinizing hormone and testosterone in the human neonate during the first few hours after birth. J Clin Endocrinol Metab. 71(5): 1344-1348. (1990)
Coveney D et al., Four-dimensional analysis of vascularization during primary development of an organ, the gonad. PNAS. 105: 7212-7217 (2008)
Crawford P et al., Nuclear receptor DAX-1 recruits nuclear receptor corepressor N-CoR to steroidogenic factor 1. Molecular and Cellular Biology. 18(5): 2949-2956. (1998)
Croizier S et al., Characterization of a mammalian prosencephalic functional plan. Frontiers in neuroanatomy. 8 (2014).
Croizier S et al., Development of posterior hypothalamic neurons enlightens a switch in the prosencephalic basic plan. PLoS One 6:e28574 (2011).
Daikoku S et al., Migration of LHRH neurons derived from the olfactory placode in rats. Archives of histology and cytology. 56(4): 353-370 (1993)
Dacquin R et al., Control of bone resorption by Semaphorin 4D is dependent on ovarian function. PLoS ONE. 6:e26627 (2011)
de Bakker BS et al., An interactive three-dimensional digital atlas and quantitative database of human development. Science 354: aag0053 (2016)
de Castro F et al., The adhesion molecule anosmin-1 in neurology: Kallmann syndrome and beyond. Adv Neurobiol. 8:273-92. (2014)
de Castro F et al., ANOS1: a unified nomenclature for Kallmann syndrome 1 gene (KAL1) and anosmin-1. Briefings in functional genomics 16(4): 205-210. (2016)
de Santa Barbara et al., Direct interaction of SRY-related protein SOX9 and steroidogenic factor 1 regulates transcription of the human anti-Mullerian hormone gene. Mol Cell Biol 18(11): 6653-65. (1998)
De Zegher et al., Pulsatile and sexually dimorphic secretion of luteinizing hormone in the human infant on the day of birth. Pediatr Res. 32: 605-7 (1992)
Deijck AH et al., Semaphorin signaling: molecular switches at the midline. Trends in cell biology. 20(9): 568-576. (2010)
Deiner MS & Sretavan DW, Altered midline axon pathways and ectopic neurons in the developing hypothalamus of netrin-1-and DCC-deficient mice. J Neurosci. 19.(2): 9900-9912 (1999)
Depmann M et al., Fluctuations in anti-Müllerian hormone levels throughout the menstrual cycle parallel fluctuations in the antral follicle count: a cohort study. Acta obstetricia et gynecologica Scandinavica 95(7): 820-828. (2016)
Des Portes V et al., Doublecortin is the major gene causing X-linked subcortical laminar heterotopia (SCLH). Hum. Mol. Genet. 7, 1063-1070. (1988)
Di Clemente N et al., Cloning, expression, and alternative splicing of the receptor for anti-Mullerian hormone. Mol. Endocrinol. 8, 1006-1020 (1994)

di Clemente N et al., Inhibitory effect of AMH upon the expression of aromatase and LH receptors by cultured granulosa cells of rat and porcine immature ovaries. Endocrine 2(6): 553–558. (1994)
di Clemente N et al., Processing of anti-mullerian hormone regulates receptor activation by a mechanism distinct from TGF-β. Molecular endocrinology. 24(11): 2193–2206. (2010)
Dodt H et al., Ultramicroscopy: three-dimensional visualization of neuronal networks in the whole mouse brain. Nat. Methods 4: 331－336 (2007)
Domínguez L et al., Patterns of hypothalamic regionalization in amphibians and reptiles: common traits revealed by a genoarchitectonic approach. Frontiers in neuroanatomy 9 (2015).
Drake R et al., Gray's Anatomy. Churchill Livingstone; 3 edition (March 7, 2010)
Dresser DW et al., The genes for a spliceosome protein (SAP62) and the anti-Mullerian hormone (AMH) are contiguous. Hum Mol Genet 4(9): 1613–8. (1995)
Drummond ES et al., Altered expression of Alzheimer's disease-related proteins in male hypogonadal mice. Endocrinology 153, 2789–2799 (2012).
Dulac C & Torello AT. Molecular detection of pheromone signals in mammals: from genes to behaviour. Nature reviews. Neuroscience 4, 551–562 (2003).
Dulac C et al., Neural control of maternal and paternal behaviors. Science. 345, 765–770 (2014).
Durlinger AL et al., Anti-Mullerian hormone attenuates the effects of FSH on follicle development in the mouse ovary. Endocrinology 142(11): 4891–9. (2001)
Durlinger AL et al., Anti-Mullerian hormone inhibits initiation of primordial follicle growth in the mouse ovary. Endocrinology 143(3): 1076–84. (2002)
Durlinger AL et al., Control of primordial follicle recruitment by anti-Mullerian hormone in the mouse ovary. Endocrinology 140(12): 5789–96. (1999)
Dwyer AA et al., Trial of recombinant follicle-stimulating hormone pretreatment for GnRH-induced fertility in patients with congenital hypogonadotropic hypogonadism. J. Clin. Endocrinol. Metab. 98, E1790－E1795 (2013).
Dwyer AA et al., Identifying the unmet health needs of patients with congenital hypogonadotropic hypogonadism using a web-based needs assessment: implications for online interventions and peer-to-peer support. Orphanet J. Rare Dis. 9, 83 (2014).
Ebling FJ. The neuroendocrine timing of puberty. Reproduction. 129(6): 675–83 (2005)
Eiraku M et al., Delta/notch-like epidermal growth factor (EGF)-related receptor, a novel EGF-like repeat-containing protein targeted to dendrites of developing and adult central nervous system neurons. J Biol Chem. 277, 25400–25407 (2002).
Eisthen HL et al., Neuromodulatory effects of gonadotropin releasing hormone on olfactory receptor neurons. J Neurosci. 20(11): 3947–55 (2000)
El Mestikawy S et al., From glutamate co-release to vesicular synergy: vesicular glutamate transporters. Nat rev. Neurosci. 12(4): 204 (2011)
Elima K et al., Molecular identification of PAL-E, a widely used endothelial cell marker. Hematology 106, 1－24. (2005)
Elmquist JK et al., Identifying hypothalamic pathways controlling food intake, body weight, and glucose homeostasis. J Comp Neurol. 493:63–71. (2005)
Ertürk A & Bradke F. High-resolution imaging of entire organs by 3-dimensional imaging of solvent cleared organs (3DISCO). Experimental neurology 242, 57–64, (2013).
Ertürk A et al., Three-dimensional imaging of solvent-cleared organs using 3DISCO. Nature protocols 7, 1983–1995 (2012).

Ertürk A et al., Three-dimensional imaging of the unsectioned adult spinal cord to assess axon regeneration and glial responses after injury. Nat. Med. 18, 166 – 171. (2012)
Espinasse PG. The development of the hypophysio-portal system in man. Journal of anatomy 68. Pt1: 11 (1933)
Espinosa-Medina I et al., Neurodevelopment. Parasympathetic ganglia derive from Schwann cell precursors. Science 345, 87 – 90. (2014)
Esteves A et al., Freemartinism in cattle. CECAV-Centro de Ciencia Animal e Veterinoria (2012).
Evans NP et al., Alterations in endogenous gonadotropin secretion and pituitary responsiveness to gonadotropin-releasing hormone in adult ewes, following indirect selection in prepubertal male lambs. Biol Reprod. 51(5):913-9 (1994)
Falardeau J et al., Decreased FGF8 signaling causes deficiency of gonadotropin-releasing hormone in humans and mice. J. Clin. Invest. 118, 2822 – 2831 (2008).
Fallat ME et al., Müllerian-inhibiting substance in follicular fluid and serum: a comparison of patients with tubal factor infertility, polycystic ovary syndrome, and endometriosis. Fertility and sterility. 67(5): 962-965. (1997)
Farikullah A et al., Persistent Müllerian duct syndrome: lessons learned from managing a series of eight patients over a 10-year period and review of literature regarding malignant risk from the Müllerian remnants. BJU international 110(11)c (2012)
Fenichel P et al., Anti-Mullerian hormone as a seminal marker for spermatogenesis in non-obstructive azoospermia. Human Reproduction. 14(8): 2020-2024. (1999)
Fernald RD & White RB. Gonadotropin-releasing hormone genes: phylogeny, structure, and functions. Front Neuroendocrinol. 20(3):224-40 (1999)
Fink G et al., Priming effect of luteinizing hormone releasing factor elicited by preoptic stimulation and by intravenous infusion and multiple injections of the synthetic decapeptide. J Endocrinol. 69(3): 359-372. (1976)
Forni PE et al., Neural crest and ectodermal cells intermix in the nasal placode to give rise to GnRH-1 neurons, sensory neurons, and olfactory ensheathing cells. J Neurosci. 31(18):6915-27 (2011)
Forni PE & Wray S, GnRH, anosmia and hypogonadotropic hypogonadism – Where are we? Frontiers in neuroendocrinology 36C, 165-177 (2015).
Foster JW et al., Campomelic dysplasia and autosomal sex reversal caused by mutations in an SRY-related gene. Nature. 372(6506): 525. (1994)
Franco B et al., A gene deleted in Kallmann's syndrome shares homology with neural cell adhesion and axonal path-finding molecules. Nature 353, 529-536 (1991).
Frasnelli J et al., The vomeronasal organ is not involved in the perception of endogenous odors. Hum Brain Mapp. 32(3):450-60 (2011)
Fritsch H et al., Molecular characteristics and alterations during early development of the human vagina. J. Anat. 220, 363 – 371. (2012)
Fryer HJL & Hockfield S. The role of polysialic acid and other carbohydrate polymers in neural structural plasticity. Current opinion in neurobiology. 6(1): 113-118 (1996)
Fueshko S & Wray S. LHRH cells migrate on peripherin fibers in embryonic olfactory explant cultures: an in vitro model for neurophilic neuronal migration. Dev biol 166, 331-348 (1994).
Fueshko SM et al., GABA inhibits migration of luteinizing hormone-releasing hormone neurons in embryonic olfactory explants. J Neurosci. 18(7): 2560-2569 (1998)
Fujimoto T. Nishimura's collection of human embryos and related publications. Congenit. Anom. (Kyoto). 41, 67 – 71. (2001)

Galambos C & Demello DE, Molecular mechanisms of pulmonary vascular development. Pediatr. Dev. Pathol. 10, 1－17. (2007)
Gamble JA et al., Disruption of ephrin signaling associates with disordered axophilic migration of the gonadotropin-releasing hormone neurons. Journal of Neuroscience 25(12): 3142-3150 (2005)
Garrel G et al., Anti-Mullerian hormone: a new actor of sexual dimorphism in pituitary gonadotrope activity before puberty. Sci Rep. 6:23790 (2016)
Garrosa, M et al., Developmental stages of the vomeronasal organ in the rat: a light and electron microscopic study. Journal fur Hirnforschung 33(2): 123-132 (1992)
Gasser RF, The development of the facial muscles in man. Am. J. Anat. 120, 357－375. (1967)
Gelman JS et al., Peptidomic analysis of human cell lines. J of proteome research. 10(4): 1583-1592. (2011)
Georgas KM et al., An illustrated anatomical ontology of the developing mouse lower urogenital tract. Development 142, 1893－1908. (2015)
Georgopoulos NA et al., Increased frequency of the anti-mullerian-inhibiting hormone receptor 2 (AMHR2) 482 A>G polymorphism in women with polycystic ovary syndrome: relationship to luteinizing hormone levels. J Clin Endocrinol Metab 98, E1866-1870 (2013)
Giacobini P et al., Hepatocyte growth factor/scatter factor facilitates migration of GN-11 immortalized LHRH neurons. Endocrinology. 143(9): 3306-3315 (2002)
Giacobini P et al., Semaphorin 4D regulates gonadotropin hormone-releasing hormone-1 neuronal migration through PlexinB1-Met complex. J Cell Biol. 183, 555-566 (2008).
Giacobini P et al., Cholecystokinin modulates migration of gonadotropin-releasing hormone-1 neurons. J Neurosci 24, 4737-4748 (2004).
Gilbert MS. The early development of the human diencephalon. J Comp Neurol. 62:81－116. (1935)
Gilmore TD. Introduction to NF-[kappa] B: players, pathways, perspectives. Oncogene 25(51): 6680. (2006)
Giuli G et al., The nuclear receptor SF-1 mediates sexually dimorphic expression of Mullerian Inhibiting Substance, in vivo. Development 124(9): 1799- 807. (1997)
Givens ML et al., Developmental regulation of gonadotropin-releasing hormone gene expression by the MSX and DLX homeodomain protein families. J Biol Chem 280(19): 19156-65 (2005)
Gleeson JG et al. Doublecortin, a brain-specific gene mutated in human X-linked lissencephaly and double cortex syndrome, encodes a putative signaling protein. Cell. 92, 63－72. (1998)
Gleeson JG et al., Doublecortin is a microtubule-associated protein and is expressed widely by migrating neurons. Neuron. 23, 257-271 (1999).
Goldsmith PC et al., Location of the neuroendocrine gonadotropin-releasing hormone neurons in the monkey hypothalamus by retrograde tracing and immunostaining. J Neuroendocrinol. 1;2(2):157-68 (1990)
Gonzalez-Martinez D et al., Ontogeny of GnRH and olfactory neuronal systems in man: novel insights from the investigation of inherited forms of Kallmann's syndrome. Frontiers in neuroendocrinology 25, 108-130 (2004).
Gore AC & Roberts JL, Regulation of gonadotropin-releasing hormone gene expression by the excitatory amino acids kainic acid and N-methyl-D,L-aspartate in the male rat. Endocrinology. 134(5):2026-31 (1994)
Gore AC & Roberts JL. Regulation of gonadotropin-releasing hormone gene expression in vivo and in vitro. Front Neuroendocrinol. 18(2):209-45 (1997)

Gorham JD et al., The expression of the neuronal intermediate filament protein peripherin in the rat embryo. Brain research. Developmental brain research 57, 235–248 (1990).
Gorham JD et al., Differential spatial and temporal expression of two type III intermediate filament proteins in olfactory receptor neurons. Neuron 7, 485–497 (1991).
Gouedard L et al., Engagement of bone morphogenetic protein type IB receptor and Smad1 signaling by anti–Mullerian hormone and its type II receptor. J. Biol. Chem. 275, 27973－27978. (2000)
Granger, A. et al. The promoter of the rat gonadotropin–releasing hormone receptor gene directs the expression of the human placental alkaline phosphatase reporter gene in gonadotrope cells in the anterior pituitary gland as well as in multiple extrapituitary tissues. Endocrinology 145, 983–993, (2004).
Griesinger G et al., Elimination half–life of Anti–Mullerian hormone. J. Clin. Endocrinol. Metab. 97(6): 2160–2163 (2012)
Grynnerup A et al., The role of anti-Müllerian hormone in female fertility and infertility－an overview. Acta obstetricia et gynecologica Scandinavica 91(11): 1252–1260. (2012)
Gubbay J et al. A gene mapping to the sex–determining region of the mouse Y chromosome is a member of a novel family of embryonically expressed genes. Nature. 346(6281): 245–250. (1990)
Gupta G et al., ID genes mediate tumor reinitiation during breast cancer lung metastasis PNAS. 104(49): 19506–19511. (2007)
Gustafson ML et al., Mullerian inhibiting substance in the diagnosis and management of intersex and gonadal abnormalities. J. Pediatr. Surg. 28(3): p. 439–44. (1993)
Gutierrez H et al., HGF regulates the development of cortical pyramidal dendrites. Development. 131(15): 3717–3726 (2004)
Halasz N et al., Immunohistochemical identification of two types of dopamine neuron in the rat olfactory bulb as seen by serial sectioning. J Neurocytol 10, 251–259 (1981).
Halpern M. The organization and function of the vomeronasal system. Annu Rev Neurosci. 10:325–62 (1987)
Hanchate NK et al., SEMA3A, a Gene Involved in Axonal Pathfinding, Is Mutated in Patients with Kallmann Syndrome. PLoS genetics 8, e1002896 (2012).
Hanley NA et al., SRY, SOX9, and DAX1 expression patterns during human sex determination and gonadal development. Mech. Dev. 91, 403－407. (2000).
Haqq CM et al., Molecular basis of mammalian sexual determination: activation of Müllerian inhibiting substance gene expression by SRY. Science. 266, 1494－1500. (1994)
Harris GW, Neural Control of the Pituitary Gland. London (1955)
Harris GW. Electrical stimulation of the hypothalamus and the mechanism of neural control of the adenohypophysis. J. Physiol. 107:418－29 (1948)
Harris GW. The induction of ovulation in the rabbit, by electrical stimulation of the hypothalamo–hypophysial mechanism. Proc. R. Soc. London Ser. B 122:374－94 (1937)
Harris GW. The induction of pseudopregnancy in the rat by electrical stimulation through the head. J. Physiol. 88:361－67 (1936)
Hashimoto, R. Development of the human Mullerian duct in the sexually undifferentiated stage. Anat. Rec. A. Discov. Mol. Cell. Evol. Biol. 272, 514－519. (2003)
Hayashi M et al., Osteoprotection by semaphorin 3A. Nature 485, 69－74 (2012).
Heanue TA & Pachnis V. Enteric nervous system development and Hirschsprung's disease: advances in genetic and stem cell studies. Nat. Rev. Neurosci. 8, 466－479. (2007)

Heger S et al., Overexpression of glutamic acid decarboxylase-67 (GAD-67) in gonadotropin-releasing hormone neurons disrupts migratory fate and female reproductive function in mice. Endocrinology. 144(6): 2566-2579 (2003)
Heldin C et al., TGF-beta signalling from cell membrane to nucleus through SMAD proteins. Nature 390(6659): 465. (1997)
Herbison AE et al., Gonadotropin-releasing hormone neuron requirements for puberty, ovulation, and fertility. Endocrinology. 149(2):597-604 (2008)
Herbison AE. Control of puberty onset and fertility by gonadotropin-releasing hormone neurons. Nat Rev Endocrinol. 12(8):452-66 (2016)
Herde MK & Herbison AE. Morphological Characterization of the Action Potential Initiation Segment in GnRH Neuron Dendrites and Axons of Male Mice. Endocrinology. 2015 156(11):4174-86 (2015)
Herde MK et al., GnRH neurons elaborate a long-range projection with shared axonal and dendritic functions. J Neurosci. 33(31):12689-97 (2013)
Herrick CJ, The morphology of the forebrain in amphibia and reptilia. J. comp. Neuro 20:413-546. (1910)l.
His W, Uber das frontale Ende des Gehirnrohrs. Arch Anat Entwickelungsges. Anatomische Abteilung des Arch f.Anat u. Physiol. 3:157-171 (1893a)
His W, Vorschlagezur Eintheilung des Gehirns. Arch Anat Entwickelungsges. Anatomische Abteilung des Arch f.Anat u. Physiol. 3:172-179. (1893b)
His W. Anatomie menschlicher Embryonen (Leipzig: Vogel). (1881)
Hodgkin AL & Huxley AF. A quantitative description of membrane current and its application to conduction and excitation in nerve. J Physiol. 117(4): 500-544. (1952)
Hoshiya Y et al., Mullerian Inhibiting Substance induces NFkB signaling in breast and prostate cancer cells. Mol. Cell. Endocrinol. 211(1-2): 43-9. (2003)
Hrabovszky E et al., Sexual dimorphism of kisspeptin and neurokinin B immunoreactive neurons in the infundibular nucleus of aged men and women. Frontiers in endocrinology 2, 80 (2011).
Hutchins IB et al., Calcium release-dependent actin flow in the leading process mediates axophilic migration. Journal of Neuroscience. 33(28): 11361-11371 (2013)
Imbeaud S et al., Insensitivity to anti-Müllerian hormone due to a mutation in the human anti-Müllerian hormone receptor. Nat. Genet. 11, 382-388. (1995)
Imhoff FM et al., The type 2 anti-Müllerian hormone receptor has splice variants that are dominant-negative inhibitors. FEBS letters. 587(12): 1749-1753. (2013)
Inai K et al., BMP-2 induces cell migration and periostin expression during atrioventricular valvulogenesis. Developmental biology 315(2): 383-396. (2008)
Incerti B et al., Kallmann syndrome gene on the X and Y chromosomes: implications for evolutionary divergence of human sex chromosomes. Nat Genet. 2:311-4. (1992)
Jacob M et al., Development, Differentiation and Derivatives of the Wolffian and Müllerian Ducts. In the Human Embryo, S. Yamada, ed. (InTech): 143-166. (2012)
Jadhav U et al., Hypogonadotropic hypogonadism in subjects with DAX1 mutations. Molecular and cellular endocrinology. 346(1): 65-73. (2011)
Jakab A et al., Disrupted developmental organization of the structural connectome in fetuses with corpus callosum agenesis. Neuroimage 111, 277-288. (2015)
Jamin SP et al., Genetic studies of the AMH/MIS signaling pathway for Mullerian duct regression. Mol. Cell. Endocrinol. 211, 15-19 (2003)

Jamin SP et al., Requirement of Bmpr1a for Müllerian duct regression during male sexual development. Nat. Genet. 32, 408－410. (2002)
Jamin SP et al., Requirement of Bmpr1a for Mullerian duct regression during male sexual development. Nature genetics 32, 408-410 (2002).
Jasoni CL et al., Anatomical location of mature GnRH neurons corresponds with their birthdate in the developing mouse. Developmental dynamics: an official publication of the American Association of Anatomists 238, 524-531 (2009).
Jimenez-Liñan et al., Examination of guinea pig luteinizing hormone-releasing hormone gene reveals a unique decapeptide and existence of two transcripts in the brain. Endocrinology. 138(10):4123-30 (1997)
Jongmans MC et al., CHD7 mutations in patients initially diagnosed with Kallmann syndrome—the clinical overlap with CHARGE syndrome. Clin. Genet. 75, 65－71 (2009)
Josso N et al., Clinical aspects and molecular genetics of the persistent Müllerian duct syndrome. Clinical endocrinology. 47(2): 137-144. (1997)
Josso N et al., Anti-Mullerian hormone and its receptors. Mol. Cell. Endocrinol. 179(1-2): p. 25-32. (2001)
Josso, N. & Clemente, N. Transduction pathway of anti-Mullerian hormone, a sex-specific member of the TGF-beta family. Trends in endocrinology and metabolism: TEM 14, 91-97 (2003).
Josso N et al., Anti-Mullerian hormone and its receptors. Molecular and cellular endocrinology 179, 25-32 (2001).
Jost A, Problems of fetal endocrinology - the gonadal and hypophyseal hormones. Recent Prog. Horm. Res. 8:379-418. (1953)
Jost A. The age factor in the castration of male rabbit fetuses. Proceedings of the Society for Experimental Biology and Medicine 66(2): 302-303. (1947)
Kallmann F et al., The genetic aspects of primary eunuchoidism. Am J Ment Defic. 48:33. (1944)
Kanahashi T et al., A Novel Strategy to Reveal the Latent Abnormalities in Human Embryonic Stages from a Large Embryo Collection. Anat. Rec. 299, 8－24. (2016)
Kansakoski J et al., Mutation screening of SEMA3A and SEMA7A in patients with congenital hypogonadotropic hypogonadism. Pediatr. Res. 75, 641－644 (2014).
Kaplan et al., The ontogenesis of pituitary hormones and hypothalamic factors in the human fetus: maturation of central nervous system regulation of anterior pituitary function. Recent Prog Horm Res. 32: 161-234 (1976)
Kapsimali M et al., Inhibition of Wnt/Axin/beta-catenin pathway activity promotes ventral CNS midline tissue to adopt hypothalamic rather than floorplate identity. Development. 131: 5923-33
Karagogeos D et al., Expression of the Cell Adhesion Proteins BEN / SC1 / DM-GRASP and TAG-1 Defines Early Steps of Axonogenesis in the Human Spinal Cord. J. Comp. Neurol. 427, 415－427. (1997)
Kashimada K & Koopman P, Sry: the master switch in mammalian sex determination. Development 137(23): 3921-30 (2010)
Kawagishi Y et al., Anti-Mullerian hormone signaling is influenced by Follistatin 288, but not 14 other transforming growth factor beta superfamily regulators. Mol Reprod Dev. 84(7): 626-37 (2017)
Kawagishi Y. Is Anti-Müllerian hormone regulated by TGFbeta Superfamily Binding Proteins? Thesis, Doctor of Philosophy, University of Otago. (2015)

Kawajiri K et al., Role of the LXXLL-motif and activation function 2 domain in subcellular localization of Dax-1 (dosage-sensitive sex reversal-adrenal hypoplasia congenita critical region on the X chromosome, gene 1). Molecular Endocrinology. 17(6): 994-1004. (2003)
Keibel F & Elze C, Normentafeln zur Entwicklungsgeschichte der Wirbeltiere. Achtes Heft. Des Menschen (Jena: Verlag von Gustav Fischer). (1908)
Keibel F & Mall FP, Manual of human embryology, Volume 1 (Philadelphia & London: Lippincott). (1910)
Kent J et al., A male-specific role for SOX9 in vertebrate sex determination. Development. 122(9): 2813-2822. (1996)
Kidd T et al., Slit is the midline repellent for the robo receptor in Drosophila. Cell. 96(6): 785-794. (1999)
Killeen MT & Sybingco SS, Netrin, Slit and Wnt receptors allow axons to choose the axis of migration. Develop biol. 323(2): 143-151 (2008)
Kim HG et al., Mutations in CHD7, encoding a chromatin-remodeling protein, cause idiopathic hypogonadotropic hypogonadism and Kallmann syndrome. Am. J. Hum. Genet. 83, 511-519 (2008).
Kim KH et al., Gonadotropin-releasing hormone immunoreactivity in the adult and fetal human olfactory system. Brain research 826, 220-229 (1999).
King DF & King LA, A brief historical note on staining by hematoxylin and eosin. Am. J. Dermatopathol. 8, 168. (1986)
King JC & Anthony EL, Biosynthesis of LHRH: inferences from immunocytochemical studies. Peptides. 4(6): 936-970 (1983)
King JC & Anthony EL, LHRH neurons and their projections in humans and other mammals: Species comparisons. Peptides. 5: 195-207 (1984)
King TR et al., Mapping anti-mullerian hormone (Amh) and related sequences in the mouse: identification of a new region of homology between MMU10 and HSA19p. Genomics 11(2): 273-83. (1991)
Klattig J et al., Wilms' tumor protein Wt1 is an activator of the anti-Mullerian hormone receptor gene Amhr2. Mol Cell Biol 27(12): 4355-64. (2007)
Kobayashi A & Behringer RR, Developmental genetics of the female reproductive tract in mammals. Nat. Rev. Genet. 4, 969-980. (2003)
Kobayashi M et al., Gonadotropin-releasing hormones of terminal nerve origin are not essential to ovarian development and ovulation in goldfish. Gen Comp Endocrinol. 95(2):192-200 (1994)
Kokoris GJ et al., Transplanted gonadotropin-releasing hormone neurons promote pulsatile luteinizing hormone secretion in congenitally hypogonadal (hpg) male mice. Neuroendocrinology. 48:45-52 (1988)
Komuro H & Rakic P, Modulation of neuronal migration by NMDA receptors. Science. 260: 95-95 (1993)
Komuro H & Rakic P, Orchestration of neuronal migration by activity of ion channels, neurotransmitter receptors, and intracellular Ca2+ fluctuations. Dev Neurobiol. 37(1): 110-130 (1998)
Kordon C et al., Role of classic and peptide neuromodulators in the neuroendocrine regulation of luteinzing hormone and prolactin. In: Knobil E, Neil JD, editors. Physiology of reproduction 2nd ed. New York: Raven; p. 1621-81 (1994)

Kramer PR & Wray S. Midline nasal tissue influences nestin expression in nasal-placode-derived luteinizing hormone-releasing hormone neurons during development. Dev Biol. 227(2):343-57 (2000)
Kramer PR et al., Transcription factor activator protein-2 is required for continued luteinizing hormone-releasing hormone expression in the forebrain of developing mice. Endocrinology. (5):1823-38 (2000)
Kraus DB & Fadem BH, Reproduction, development and physiology of the gray short-tailed opossum (monodelphis domestica). Lab Anim Sci. 37: 478-482 (1987)
Kreidberg JA et al., WT-1 is required for early kidney development. Cell 74(4): 679-91. (1993)
Krey JC & Silverman AJ. The luteinizing hormone-releasing hormone (LH-RH) neuronal networks of the guinea pig brain. II the regulation on gonadotropin secretion and the origin of the terminals in the median eminence. Brain Res. 157: 247-55 (1978)
Krueger S et al., Expression of neuroserpin, an inhibitor of tissue plasminogen activator, in the developing and adult nervous system of the mouse. J Neurosci. 17(23): 8984-8996. (1997)
Kruger RP et al., Semaphorins command cells to move. Nat Rev Mol Cell Biol. 6:789-800 (2005)
Krystosek A et al., Plasminogen activator release at the neuronal growth cone. Science. 213(4515): 1532-1534. (1981)
Kuiri-Hänninen T et al., Increased activity of the hypothalamic-pituitary-testicular axis in infancy results in increased androgen action in premature boys."The Journal of Clinical Endocrinology & Metabolism 96(1): 98-105. (2011a)
Kuiri-Hänninen T et al., Postnatal developmental changes in the pituitary-ovarian axis in preterm and term infant girls. The Journal of Clinical Endocrinology & Metabolism 96(11): 3432-3439. (2011b)
La Marca A et al., Anti-Mullerian hormone (AMH) as a predictive marker in assisted reproductive technology (ART). Hum Reprod Update 16: 113 - 130. (2010)
La Marca A et al., Anti-Mullerian hormone in premenopausal women and after spontaneous or surgically induced menopause. J. Soc. Gynecol. Investig. 12(7): p. 545-8. (2005)
Lahbib-Mansais Y et al., Mapping in pig of genes involved in sexual differentiation: AMH, WT1, FTZF1, SOX2, SOX9, AHC, and placental and embryonic CYP19. Cytogenet Cell Genet 76(1-2): 109-14. (1997)
Lalani SR et al., SEMA3E mutation in a patient with CHARGE syndrome. J Med Genetics. 41(7): e94. (2004)
Langlet et al., Tanycytic VEGF-A boosts blood-hypothalamus barrier plasticity and access of metabolic signals to the arcuate nucleus in response to fasting. Cell Metab 17:607 - 617 (2013a)
Langlet F et al., Tanycyte-like cells form a blood-cerebrospinal fluid barrier in the circumventricular organs of the mouse brain. J Comp Neurol. 521:3389-3405. (2013b)
Laurich VM et al., Mullerian inhibiting substance blocks the protein kinase A-induced expression of cytochrome p450 17alpha-hydroxylase/C(17- 20) lyase mRNA in a mouse Leydig cell line independent of cAMP responsive element binding protein phosphorylation. Endocrinology. 143(9): 3351-60 (2002)
Lebeurrier N et al., Anti-Mullerian-hormone-dependent regulation of the brain serine- protease inhibitor neuroserpin. J Cell Sci 121, 3357-3365 (2008)
Lechleider RJ et al., Targeted mutagenesis of Smad1 reveals an essential role in chorioallantoic fusion. Developmental biology 240(1): 157-167. (2001)

Lee K et al., Knockdown of GABAA receptor signaling in GnRH neurons has minimal effects upon fertility. Endocrinology. 151(9): 4428-4436 (2010)
Lee MM et al., Developmentally regulated polyadenylation of two discrete messenger ribonucleic acids for mullerian inhibiting substance. Endocrinology 130(2): 847-53 (1992)
Legouis R et al., The candidate gene for the X-linked Kallmann syndrome encodes a protein related to adhesion molecules. Cell. 67:423 - 35. (1991)
Levine JE & Duffy MT. Simultaneous measurement of luteinizing hormone (LH)-releasing hormone, LH, and follicle-stimulating hormone release in intact and short-term castrate rats. Endocrinology. 122(5): 2211-21 (1988)
Li L et al., A Dominant Negative Mutation at the ATP Binding Domain of AMHR2 Is Associated with a Defective Anti-Müllerian Hormone Signaling Pathway Mol Hum Reprod. 22(9), 669-678. (2016)
Li HS et al., Vertebrate slit, a secreted ligand for the transmembrane protein roundabout, is a repellent for olfactory bulb axons. Cell. 96(6): 807-818. (1999)
Lin W et al., Odors detected by mice deficient in cyclic nucleotide-gated channel subunit A2 stimulate the main olfactory system. J Neurosci. 24, 3703-3710, (2004).
Little MH et al., A high-resolution anatomical ontology of the developing murine genitourinary tract. Gene Expr. Patterns 7, 680 - 699. (2007)
Locher H et al., Neurosensory development and cell fate determination in the human cochlea. Neural Dev. 8, 20. (2013)
Long WQ et al., Detection of minimal levels of serum anti-Mullerian hormone during follow-up of patients with ovarian granulosa cell tumor by means of a highly sensitive enzyme-linked immunosorbent assay. J. Clin. Endocrinol. Metab. 85(2): p. 540-544. (2000)
Ludwig KS & Landmann L, Early development of the human mesonephros. Anat. Embryol. (Berl). 209, 439 - 447. (2005)
Luo X et al., A cell-specific nuclear receptor is essential for adrenal and gonadal development and sexual differentiation. Cell. 77(4): 481-490. (1994)
Luzzati F et al., Combining confocal laser scanning microscopy with serial section reconstruction in the study of adult neurogenesis. Frontiers in neuroscience. 5: 70, (2011).
Ly A et al., DSCAM is a netrin receptor that collaborates with DCC in mediating turning responses to netrin-1. Cell. 133(7): 1241-1254 (2008)
Maestre de San Juan A. Teratolagia: falta total de los nervios olfactorios con anosmia en un individuo en quien existia una atrofia congenita de los testiculos y miembro viril. El Siglo Medico. 3: 211 - 221. (1856)
Magre S & Jost A, Sertoli cells and testicular differentiation in the rat fetus. J Electron Microsc Tech 19(2): 172-88. (1991)
Main K et al., A possible role for reproductive hormones in newborn boys: progressive hypogonadism without the postnatal testosterone peak. J. Clin. Endocrinol. Metab. 85, 4905 - 4907 (2000)
Mansour S et al., A Clinical and Genetic-Study of Campomelic Dysplasia. J. Med. Genet. 32(6): p. 415-420 (1995)
Mantero V et al., Autoimmunity meets genetics: Multiple sclerosis in a patient with Kallmann syndrome. Journal of the neurological sciences 367: 256-257. (2016)
Markee JE et al., Activation of the anterior hypophysis by electrical stimulation in the rabbit. Endocrinology. 38:345 - 57(1946)

Mars W et al., Activation of hepatocyte growth factor by the plasminogen activators uPA and tPA. Am J Pathol. 143(3): 949 (1993)
Marusich MF & Weston JA, Identification of early neurogenic cells in the neural crest lineage. Developmental biology 149, 295-306 (1992).
Mason AJ et al., A deletion truncating the gonadotropin-releasing hormone gene is responsible for hypogonadism in the hpg mouse. Science. 234(4782) 1366-1371 (1986a)
Mason AJ et al., The hypogonadal mouse: reproductive functions restored by gene therapy. Science. 234(4782) 1372-1378 (1986b)
Matuso H et al., Structure of the porcine LH- and FSH- releasing hormone. The proposed amino acid sequence. Biochem & Biophys Res Comms. 43(6) 1334-1339 (1971)
Meier C et al., Persistent paramesonephric ducts (masculine uterus) in the male North American beaver (Castor canadensis). Canadian Journal of Zoology. 76(6): 1188-1193 (1998)
Meldrum BS, Glutamate as a neurotransmitter in the brain: review of physiology and pathology. The Journal of nutrition 130(4): 1007S-1015S (2000)
Mellon PL et al., Immortalization of hypothalamic GnRH neurons by genetically targeted tumorigenesis. Neuron 5, 1-10 (1990).
Merlo GR et al., The role of Dlx homeogenes in early development of the olfactory pathway. J Mol Histol. 38(4):347-58 (2007)
Messina A et al., A microRNA switch regulates the rise in hypothalamic GnRH production before puberty. Nature neuroscience 19, 835-844 (2016).
Messina A et al., Dysregulation of Semaphorin7A/beta1-integrin signaling leads to defective GnRH-1 cell migration, abnormal gonadal development and altered fertility. Hum Mol Genet 20, 4759-4774 (2011).
Miller NL et al., Necdin, a Prader-Willi syndrome candidate gene, regulates gonadotropin-releasing hormone neurons during development. Hum Mol Genet. 18(2):248-6 (2009)
Miller AM et al., Composition of the migratory mass during development of the olfactory nerve. The Journal of comparative neurology 518, 4825-4841 (2010).
Miraoui H et al., Role of fibroblast growth factor (FGF) signaling in the neuroendocrine control of human reproduction. Mol. Cell. Endocrinol. 346, 37 - 43 (2011).
Mishina Y et al., Genetic analysis of the Mullerian-inhibiting substance signal transduction pathway in mammalian sexual differentiation. Genes Dev 10(20): 2577-87. (1996)
Mishina Y et al., High specificity of Müllerian-inhibiting substance signaling in vivo. Endocrinology 140, 2084 - 2088. (1999)
Mitchell AL et al., Genetic basis and variable phenotypic expression of Kallmann syndrome: towards a unifying theory. Trends Endocrinol. Metab. 22, 249 - 258 (2011).
Miyamoyto et al., Identification of the second gonadotropin-releasing hormone in chicken hypothalamus: evidence that gonadotropin secretion is probably controlled by two distinct gonadotropin-releasing hormones in avian species. PNAS. 81(12) 3874-3878 (1984)
Montaner AD et al., Structure and biological activity of gonadotropin-releasing hormone isoforms isolated from rat and hamster brains. Neuroendocrinology. 74(3):202-12 (2001)
Moore KL & Persaud TV. The developing Human, 5th edition.300 (1993)
Moore KL et al., Clinically orientated anatomy. Lippincott Williams & Wilkins, (2006)
Moore SW et al., Netrins and their receptors. Axon Growth and Guidance. Springer New York. 17-31 (2007)

Morais da Silva S et al., Sox9 expression during gonadal development implies a conserved role for the gene in testis differentiation in mammals and birds. Nat. Genet. 14(1): p. 62-8 (1996)
Morales-Delgado et al., Regionalized differentiation of CRH, TRH, and GHRH peptidergic neurons in the mouse hypothalamus. Brain Struct Funct. 219(3):1083-111 (2014)
Morgan LM. Icons of Life: A Cultural History of Human Embryos (Berkeley: University of California Press). (2009)
Moustakas A & Heldin CH. The regulation of TGFβ signal transduction. Development. 136(22): 3699-3714. (2009)
Muller F & O'Rahilly R. Olfactory structures in staged human embryos. Cells, tissues, organs 178, 93-116 (2004).
Munsterberg A & Lovell-Badge R, Expression of the mouse anti-mullerian hormone gene suggests a role in both male and female sexual differentiation. Development 113, 613-624. (1991)
Murakami S & Arai Y. Direct evidence for the migration of LHRH neurons from the nasal region to the forebrain in the chick embryo: a carbocyanine dye analysis. Neuroscience research 19, 331-338 (1994).
Murakami S et al., The origin of the luteinizing hormone-releasing hormone (LHRH) neurons in newts (Cynops pyrrhogaster): the effect of olfactory placode ablation. Cell and tissue research 269, 21-27 (1992).
Murakami S et al., Netrin 1 provides a chemoattractive cue for the ventral migration of GnRH neurons in the chick forebrain. J Comp Neurol. 518(11): 2019-2034. (2010)
Muske LE & Moore FL. The nervus terminalis in amphibians: anatomy, chemistry and relationship with the hypothalamic gonadotropin-releasing hormone system. Brain, behavior and evolution 32, 141-150 (1988).
Muthu V et al., Rx3 and Shh direct anisotropic growth and specification in the zebrafish tuberal/anterior hypothalamus. Development. 143: 2651-63.
Nachtigal MW & Ingraham HA, Bioactivation of Mullerian inhibiting substance during gonadal development by a kex2/subtilisin-like endoprotease. PNAS. 93(15): 7711-6. (1996)
Nachtigal MW et al., Wilms' tumor 1 and Dax-1 modulate the orphan nuclear receptor SF-1 in sex-specific gene expression. Cell. 93, 445-454. (1998)
Nadi NS et al., Chemical deafferentation of the olfactory bulb: plasticity of the levels of tyrosine hydroxylase, dopamine and norepinephrine. Brain research 213, 365-377 (1981).
Nakao A et al., Identification of Smad7, a TGF-beta-inducible antagonist of TGF-beta signalling. Nature 389(6651): 631. (1997)
Naldini L et al., Extracellular proteolytic cleavage by urokinase is required for activation of hepatocyte growth factor/scatter factor. The EMBO journal. 11(13): 4825 (1992)
Nauta W & Gygax P. Silver impregnation of degenerating axons in the central nervous system a modified technique. Stain Technol. 29, 91-93 (1954)
Navarro VM et al., Regulation of gonadotropin-releasing hormone secretion by kisspeptin/dynorphin/neurokinin B neurons in the arcuate nucleus of the mouse. J Neurosci. 29(38):11859-66 (2009)
Neufeld G & Kessler O The semaphorins: Versatile regulators of tumour progression and tumour angiogenesis. Nat Rev Cancer. 8:632-645. (2008)
Niakan K et al., Novel role for the orphan nuclear receptor Dax1 in embryogenesis, different from steroidogenesis. Molecular genetics and metabolism. 88(3): 261-271. (2006)

Nicholls JG et al., Reflexes, fictive respiration and cell division in the brain and spinal cord of the newborn opossum, (monodelphis domestica), isolated and maintained in vitro. J Exp Biol. 152: 1-15 (1990)
Niemineva K. On the capillary net of the human cerebral hemispheres during the early fetal period. Annales medicinae experimentalis et biologiae Fenniae. Vol. 28. No. 3. (1949.)
Norgren RB & Gao C. LHRH neuronal subtypes have multiple origins in chickens. Developmental biology 165, 735-738 (1994).
Norman JR. Methods and technique of reconstruction. J. R. Microsc. Soc. 43, 37 - 56. (1923)
O'Brien LL et al., Differential regulation of mouse and human nephron progenitors by the Six family of transcriptional regulators. Development 143, 595 - 608. (2016)
O'Rahilly R & Muller F, Developmental Stages in Human Embryos. (1987)
O'Rahilly R. The timing and sequence of events in the development of the human reproductive system during the embryonic period proper. Anat. Embryol. (Berl). 166, 247 - 261. (1983)
Ogata T et al., Kallmann syndrome phenotype in a female patient with CHARGE syndrome and CHD7 mutation. Endocr J. 53(6): 741-3 (2006)
Oliveira M et al., Zika virus intrauterine infection causes fetal brain abnormality and microcephaly: Tip of the iceberg? Ultrasound Obstet. Gynecol. 47, 6 - 7. (2016)
Olsson N et al., Transforming growth factor- β -mediated mast cell migration depends on mitogen-activated protein kinase activity. Cellular signalling 13(7): 483-490. (2001)
Oreal EC et al., Early expression of AMH in chicken embryonic gonads precedes testicular SOX9 expression. Dev Dyn 212(4): 522-32. (1998)
Orvis GD & Behringer RR. Cellular mechanisms of Müllerian duct formation in the mouse. Dev. Biol. 306, 493 - 504. (2007)
Orvis GD et al., Functional redundancy of TGF-beta family type I receptors and receptor-Smads in mediating anti-Mullerian hormone-induced Mullerian duct regression in the mouse. Biol Reprod 78, 994-1001 (2008).
Otake T & Kuroiwa A, Molecular mechanism of male differentiation is conserved in the SRY-absent mammal, Tokudaia osimensis. Sci Rep. 6: 32874 (2016)
Palade G & Palay G. Electron microscope observations of interneuronal and neuromuscular synapses, the anatomical record 118 (2), 335-336 (1954).
Palevitch O. et al. Ontogeny of the GnRH systems in zebrafish brain: in situ hybridization and promoter-reporter expression analyses in intact animals. Cell and tissue research 327, 313-322 (2007).
Pan C et al., Shrinkage-mediated imaging of entire organs and organisms using uDISCO. Nat. Methods. (2016)
Pankhurst MW & McLennan IS. Human blood contains both the uncleaved precursor of anti-Müllerian hormone and a complex of the NH 2-and COOH-terminal peptides. American Journal of Physiology-Endocrinology and Metabolism. 305(10): E1241-E1247. (2013)
Park OK & Ramirez VD. Spontaneous changes in LHRH release during the rat estrous cycle, as measured with repetitive push-pull perfusions of the pituitary gland in the same female rats. Neuroendocrinology. 50(1):66-72. 1989
Parkash J et al., Suppression of β1-integrin in gonadotropin-releasing hormone cells disrupts migration and axonal extension resulting in severe reproductive alterations. J Neurosci. 32(47): 16992-17002. (2012)

Parr BA & McMahon AP. Sexually dimorphic development of the mammalian reproductive tract requires Wnt-7a. Nature. 395(6703): 707. (1998)
Parysek LM. A type III intermediate filament gene is expressed in mature neurons. Neuron 1, 395-401. (1988)
Parysek LM & Goldman RD. Distribution of a novel 57 kDa intermediate filament (IF) protein in the nervous system. J Neurosci 8, 555-563 (1988).
Pask AJ et al., Marsupial anti-Mullerian hormone gene structure, regulatory elements, and expression. Biol Reprod 70(1): 160-7. (2004)
Paulin C et al., Immunofluorescence study of LH-RH producing cells in the human fetal hypothalamus. Cell Tissue Res. 182, 341-345. (1977)
Pearlman AL et al., New directions for neuronal migration. Current opinion in neurobiology 8(1): 45-54. (1998)
Pearson CA & Placzek M. Development of the medial hypothalamus: forming a functional hypothalamic-neurohypophyseal interface. Curr. Top. Dev. Biol. 106, 49-88. (2013)
Pearson AA. The development of the nervus terminals in man. The Journal of comparative neurology 75, 39-66 (1941).
Penarrubia J et al., Basal and stimulation day 5 anti-Müllerian hormone serum concentrations as predictors of ovarian response and pregnancy in assisted reproductive technology cycles stimulated with gonadotropin-releasing hormone agonist-gonadotropin treatment. Human Reproduction. 20(4): 915-922. (2005)
Pepinsky RB et al., Proteolytic processing of mullerian inhibiting substance produces a transforming growth factor-beta-like fragment. J Biol Chem. 263(35): 18961-4. (1988)
Phillips et al., Immunocytochemical localization in rat brain of a prolactin release-inhibiting sequence of gonadotropin-releasing hormone prohormone. Nature. 316(6028):542-5 (1985)
Picard JY & Josso N. Purification of testicular anti-Mullerian hormone allowing direct visualization of the pure glycoprotein and determination of yield and purification factor. Mol Cell Endocrinol 34(1): 23-9. (1984)
Picard JY et al., Cloning and expression of cDNA for anti-müllerian hormone. PNAS. 83, 5464-5468. (1986)
Picard JY et al.,The Persistent Mullerian Duct Syndrome: An Update Based Upon a Personal Experience of 157 Cases. Sex Dev 11, 109-125 (2017).
Picon R, Action of the fetal testis on the development in vitro of the Mullerian ducts in the rat. Arch Anat Microsc Morphol Exp 58(1): 1-19. (1969)
Pitteloud, N., et al. Digenic mutations account for variable phenotypes in idiopathic hypogonadotropic hypogonadism. The Journal of clinical investigation 117, 457-463 (2007).
Pitteloud N et al., Loss-of-function mutation in the prokineticin 2 gene causes Kallmann syndrome and normosmic idiopathic hypogonadotropic hypogonadism. PNAS. 104(44): 17447-17452. (2007)
Polanco JC et al., Sox10 gain-of-function causes XX sex reversal in mice: implications for human 22q-linked disorders of sex development. Human molecular genetics 19(3): 506-516. (2009)
Pooh RK et al., Imaging of the human embryo with magnetic resonance imaging microscopy and high-resolution transvaginal 3-dimensional sonography: Human embryology in the 21st century. Am. J. Obstet. Gynecol. 204, 77: e1-77. (2011)
Prevot et al., Function-related structural plasticity of the GnRH system: a role for neuronal-glial-endothelial interactions. Front Neuroendocrinol. 31(3): 241-58 (2010)

Prince J et al., Robo-2 controls the segregation of a portion of basal vomeronasal sensory neuron axons to the posterior region of the accessory olfactory bulb. J Neurosci. 29(45): 14211-14222. (2009)
Prüger M et al., NSCL-1 and NSCL-2 synergistically determine the fate of GnRH-1 neurons and control necdin gene expression. EMBO J. 23(21):4353-64 (2004)
Puelles L & Ferran JL. Concept of neural genoarchitecture and its genomic fundament. Frontiers in neuroanatomy 6 (2012a).
Puelles L & Rubenstein JL. A new scenario of hypothalamic organization: rationale of new hypotheses introduced in the updated prosomeric model. Frontiers in neuroanatomy 9 (2015).
Puelles L et al., Gene maps and related histogenetic domains in the forebrain and midbrain. In: Paxinos G. ed. The Rat Nervous System, 3rd Edit. San Diego: Academic Press; (2004)
Puelles L et al., The hypothalamus. Academic press; Elsevier. (2012b)
Puelles, L. & Rubenstein, JL. A new scenario of hypothalamic organization: rationale of new hypotheses introduced in the updated prosomeric model. Front Neuroanat. 9:27. (2015)
Quanbeck C et al., Two populations of luteinizing hormone-releasing hormone neurons in the forebrain of the rhesus macaque during embryonic development. The Journal of comparative neurology 380, 293-309 (1997).
Quinton R. et al., Gonadotropin-releasing hormone immunoreactivity in the nasal epithelia of adults with Kallmann's syndrome and isolated hypogonadotropic hypogonadism and in the early midtrimester human fetus. The Journal of clinical endocrinology and metabolism 82, 309-314 (1997).
Racine C et al., Receptors for anti-Mullerian hormone on Leydig cells are responsible for its effects on steroidogenesis and cell differentiation. PNAS. 95(2): 594-9. (1998)
Radovick S et al., Migratory arrest of gonadotropin-releasing hormone neurons in transgenic mice. PNAS. 88, 3402-3406 (1991).
Rakic P. Principles of neural cell migration. Cellular and Molecular Life Sciences. 46(9): 882-891. (1990)
Rance N et al., Topography of neurons expressing luteinizing hormone-releasing hormone gene transcripts in the human hypothalamus and basal forebrain. J Comp Neurol. 339, 573-586, (1994).
Rangaraju NS et al., Pro-gonadotropin-releasing hormone protein is processed within hypothalamic neurosecretory granules. Neuroendocrinology. 53(1):20-8 (1991)
Renier N et al., iDISCO: A Simple, Rapid Method to Immunolabel Large Tissue Samples for Volume Imaging. Cell. 159, 1 – 15. (2014)
Renier N et al., Mapping of Brain Activity by Automated Volume Analysis of Immediate Early Genes. Cell. 165, 1789 – 1802. (2016)
Renu DB et al., Persistent mullerian duct syndrome. The Indian journal of radiology & imaging. 20(1): 72. (2010)
Rey R et al., Anti-Müllerian hormone in disorders of sex determination and differentiation. Arq. Bras. Endocrinol. Metabol. 49, 26 – 36. (2005)
Richardson DS & Lichtman JW. Clarifying Tissue Clearing. Cell 162, 246 – 257. (2015)
Rigon C et al., Association study of AMH and AMHRII polymorphisms with unexplained infertility. Fertility and sterility 94, 1244-1248 (2010).
Ritzen EM et al., Nordic consensus on treatment of undescended testes. Acta Paediatr. 96, 638 – 643 (2007).

Ronnekleiv OK & Resko JA, Ontogeny of gonadotropin-releasing hormone-containing neurons in early fetal development of rhesus macaques. Endocrinology 126, 498-511, doi:10.1210/endo-126-1-498 (1990).

Salhi I et al., The anti-Mullerian hormone type II receptor: insights into the binding domains recognized by a monoclonal antibody and the natural ligand. Biochemical Journal. 379(3): 785-793. (2004)

Santos-Durán GN et al., Prosomeric organization of the hypothalamus in an elasmobranch, the catshark Scyliorhinus canicula. Front Neuroanat. 9:37 (2015)

Sarchielli E et al., Tumor Necrosis Factor-alpha Impairs Kisspeptin Signaling in Human Gonadotropin-Releasing Hormone Primary Neurons. The Journal of clinical endocrinology and metabolism 102, 46-56 (2017).

Sarkar A & Hochedlinger K, The Sox Family of Transcription Factors: Versatile Regulators of Stem and Progenitor Cell Fate. Cell Stem Cell. 12, 15－30. (2013)

Sarkar DK et al., Gonadotropin-releasing hormone surge in pro-oestrous rats. Nature. 264(5585): 461-463. (1976)

Schepers G et al., SOX8 is expressed during testis differentiation in mice and synergizes with SF1 to activate the Amh promoter in vitro. Journal of Biological Chemistry. 278(30): 28101-28108 (2003)

Schepers G et al., Twenty pairs of sox: extent, homology, and nomenclature of the mouse and human sox transcription factor gene families. Developmental cell. 3(2): 167-170. (2002)

Schille C et al., Differential requirement of bone morphogenetic protein receptors Ia (ALK3) and Ib (ALK6) in early embryonic patterning and neural crest development. BMC developmental biology 16(1): 1. (2016)

Schmidt H & Schwarz HP, Serum concentrations of LH and FSH in the healthy newborn. Eur J Endocrinol. 143: 213-5 (2000)

Schmierer B & Hill CS. TGF [beta]-SMAD signal transduction: molecular specificity and functional flexibility. Nature reviews. Molecular cell biology. 8(12): 970. (2007)

Schulz RWJ et al., Estrogen-induced alterations in amh and dmrt1 expression signal for disruption in male sexual development in the zebrafish. Environ Sci Technol 41(17): 6305-10. (2007)

Schulz, Y. et al. CHD7, the gene mutated in CHARGE syndrome, regulates genes involved in neural crest cell guidance. Human genetics, doi:10.1007/s00439-014-1444-2 (2014).

Schwanzel-Fukuda M & Pfaff DW, Origin of luteinizing hormone-releasing hormone neurons. Nature 338, 161-164 (1989).

Schwanzel-Fukuda M & Silverman AJ, The nervus terminalis of the guinea pig: a new luteinizing hormone-releasing hormone (LHRH) neuronal system. The Journal of comparative neurology 191, 213-225 (1980).

Schwanzel-Fukuda M et al., Migration of luteinizing hormone-releasing hormone (LHRH) neurons in early human embryos. The Journal of comparative neurology 366, 547-557 (1996).

Schwanzel-Fukuda M et al., Luteinizing hormone-releasing hormone (LHRH)-expressing cells do not migrate normally in an inherited hypogonadal (Kallmann) syndrome. Brain Res Mol Brain Res. 6, 311-326 (1989).

Schwarting GA et al., Deleted in colorectal cancer (DCC) regulates the migration of luteinizing hormone-releasing hormone neurons to the basal forebrain. J Neurosci. 21, 911-919 (2001).

Schwarting GA et al., Netrin 1-mediated chemoattraction regulates the migratory pathway of LHRH neurons." European Journal of Neuroscience 19(1): 11-20. (2004)

Seeburg PH & Adelman JP, Characterization of cDNA precursor of human luteinizing hormone releasing hormone. Nature. 311: 666-8 (1984)
Segarra J et al., Combined signaling through ERK, PI3K/AKT, and RAC1/p38 is required for met-triggered cortical neuron migration. J Biol Chem. 281(8): 4771-4778 (2006)
Segev DL et al., Mullerian inhibiting substance regulates NFkB signaling and growth of mammary epithelial cells in vivo. J. Biol. Chem. 276(29): 26799-806. (2001)
Selmanoff M et al., Single cell levels of hypothalamic messenger ribonucleic acid encoding luteinizing hormone-releasing hormone in intact, castrated, and hyperprolactinemic male rats. Endocrinology. 128(1):459-66 (1991)
Seminara SB et al., Gonadotropin-releasing hormone deficiency in the human (idiopathic hypogonadotropic hypogonadism and Kallmann's syndrome): Pathophysiological and genetic considerations. Endocr. Rev. 19, 521 - 539. (1998)
Sharif A et al., Role of glia in the regulation of gonadotropin-releasing hormone neuronal activity and secretion. Neuroendocrinology. 98(1):1-15 (2013)
Shen WH et al., Nuclear receptor steroidogenic factor 1 regulates the mullerian inhibiting substance gene: a link to the sex determination cascade. Cell. 77(5): 651-61. (1994)
Sherwood N et al., Characterization of a teleost gonadotropin-releasing hormone. PNAS. 80(9):2794-8 (1983)
Shi Y et al., Crystal structure of a Smad MH1 domain bound to DNA: insights on DNA binding in TGF-β signaling. Cell 94(5): 585-594. (1998)
Shinoda K et al., "Necklace olfactory glomeruli" form unique components of the rat primary olfactory system. J Comp Neurol. 284, 362-373, (1989).
Silverman AJ et al., Intrahypothalamic injection of a cell line secreting gonadotropin-releasing hormone results in cellular differentiation and reversal of hypogonadism in mutant mice. PNAS. 89 10668 - 10672 (1992)
Silverman AJ et al., Localization of luteinizing hormone-releasing hormone (LHRH) neurons that project to the median eminence. J Neurosci. 7(8):2312-9 (1987)
Silverman AJ et al., The luteinizing hormone-releasing hormone pathways in rhesus (Macaca mulata) and pigtailed (Macaca nemestrina) monkeys: new observations on thick, unembedded sections. J Comp Neurol. 2111: 309-17 (1982)
Silverman AJ et al., Light and electron microscopic immunocytochemical analysis of antibodies directed against GnRH and its precursor in hypothalamic neurons. Journal of Histochemistry & Cytochemistry. 38(6): 803-813. (1990)
Simonian S & Herbison AE, Differing, spatially restricted roles of ionotropic glutamate receptors in regulating the migration of GnRH neurons during embryogenesis. Journal of Neuroscience. 21(3): 934-943 (2001)
Sinclair AH et al., A gene from the human sex-determining region encodes a protein with homology to a conserved DNA-binding motif. Nature. 346(6281): 240-244. (1990)
Siow Y et al., Mullerian inhibiting substance improves longevity of motility and viability of fresh and cryopreserved sperm. Journal of andrology. 19(5): 568-572. (1998)
Sisk CL & Foster DL. The neural basis of puberty and adolescence. Nature Neurosci. 7:1040-1047 (2004)
Skrapits K et al., Lateral hypothalamic orexin and melanin-concentrating hormone neurons provide direct input to gonadotropin-releasing hormone neurons in the human. Front Cell Neurosci. 9:348 (2015)

Smith PE. The disabilities caused by hypophysectomy and their repair. The tuberal (hypothalamic) syndrome in the rat. JAMA. 88:158－61 (1927)
Smith TD & Bhatnagar KP, The human vomeronasal organ. Part II: prenatal development. Journal of anatomy 197 Pt 3, 421-436 (2000).
Song et al., GnRH-prohormone-containing neurons in the primate brain: immunostaining for the GnRH-associated peptide. Peptides. 8(2):335-46 (1987)
Sonnenberg E et al., Expression of the met-receptor and its ligand, HGF-SF during mouse embryogenesis. Exs 65: 381-394 (1993)
Sorrentino A et al., The type I TGF-[beta] receptor engages TRAF6 to activate TAK1 in a receptor kinase-independent manner. Nature cell biology. 10(1): 1199. (2008)
Sortino MA et al., Tumor necrosis factor-alpha induces apoptosis in immortalized hypothalamic neurons: involvement of ceramide-generating pathways. Endocrinology. 140, 4841-4849 (1999).
Spergel DJ et al., GABA- and glutamate-activated channels in green fluorescent protein-tagged gonadotropin-releasing hormone neurons in transgenic mice. J Neurosci. 19(6):2037-50. (1999)
Spergel DJ et al., GABA- and glutamate-activated channels in green fluorescent protein-tagged gonadotropin-releasing hormone neurons in transgenic mice. J Neurosci 19, 2037-2050 (1999).
Starling, EH. "The Croonian Lectures." Lancet. 26: 579-583. (1905)
Stein E & Tessier-Lavigne M. Hierarchical organization of guidance receptors: silencing of netrin attraction by slit through a Robo/DCC receptor complex. Science. 291(5510): 1928-1938. (2001)
Su Z & He C, Olfactory ensheathing cells: biology in neural development and regeneration. Progress in Neurobiol. 92(4): 517-32 (2010)
Sun KL et al., Netrins: versatile extracellular cues with diverse functions. Development 138(11): 2153-2169 (2011)
Suter KJ et al., Genetic targeting of green fluorescent protein to gonadotropin-releasing hormone neurons: characterization of whole-cell electrophysiological properties and morphology. Endocrinology. 141(1):412-9 (2000)
Swain A et al., Dax1 antagonizes Sry action in mammalian sex determination." Nature 391.6669 (1998): 761. (1998)
Sykiotis GP et al., Oligogenic basis of isolated gonadotropin-releasing hormone deficiency. Proc. Natl Acad. Sci. USA 107, 15140－15144 (2010).
Tabarin A et al., A novel mutation in DAX1 causes delayed-onset adrenal insufficiency and incomplete hypogonadotropic hypogonadism. JCI. 105(3): 321. (2000)
Taguchi O et al., Timing and irreversibility of Mullerian duct inhibition in the embryonic reproductive tract of the human male. Developmental biology 106, 394-398 (1984).
Takayanagi Y & Onaka T, Roles of prolactin-releasing peptide and RFamide related peptides in the control of stress and food intake. The FEBS journal. 277(24): 4998-5005. (2010)
Tarozzo et al., Development and migration of olfactory neurones in the nervous system of the neonatal opossum. Proc Biol Sci. 262(1363):95-101 (1995)
Taylor AE et al., Determinants of abnormal gonadotropin secretion in clinically defined women with polycystic ovary syndrome. J Clin Endocrinol Metab. 82, 2248-2256 (1997)
Teicher M et al., Suckling pheromone stimulation of a modified glomerular region in the developing rat olfactory bulb revealed by the 2-deoxyglucose method. Brain research 194, 530-535 (1980).
Teixeira J et al., Developmental expression of a candidate müllerian inhibiting substance type II receptor. Endocrinology 137, 160－165. (1996)

Teixeira J et al., Mullerian inhibiting substance: an instructive developmental hormone with diagnostic and possible therapeutic applications. Endocr. Rev. 22, 657－674. (2001)
Teixeira L., et al. Defective migration of neuroendocrine GnRH cells in human arrhinencephalic conditions. The Journal of clinical investigation 120, 3668-3672 (2010).
Tellier AL et al., Expression of the PAX2 gene in human embryos and exclusion in the CHARGE syndrome. Am. J. Med. Genet. 93, 85－88. (2000)
Temple JL et al., An evolutionarily conserved form of gonadotropin-releasing hormone coordinates energy and reproductive behavior. Endocrinology. 144(1): 13-9 (2003)
Terasawa E. Developmental changes in the positive feedback effect of estrogen on luteinizing hormone release in ovariectomized female rhesus monkeys. Endocrinology. 117(6):2490-7 (1985)
Tessmar-Raible K et al., Conserved sensory-neurosecretory cell types in annelid and fish forebrain: insights into hypothalamus evolution. Cell. 129(7): 1389-1400. (2007)
Thewke DP & Seeds NW, Expression of hepatocyte growth factor/scatter factor, its receptor, c-met, and tissue-type plasminogen activator during development of the murine olfactory system. J Neurosci. 16(21): 6933-6944 (1996)
Tobet SA & Schwarting GA, Recent progress in gonadotropin-releasing hormone neuronal migration. Endocrinology. 147(3):1159-65 (2006)
Tobet SA et al., Expression of gamma-aminobutyric acid and gonadotropin-releasing hormone during neuronal migration through the olfactory system. Endocrinology 137(12): 5415-5420 (1996a)
Tobet SA et al., Migration of neurons containing gonadotropin releasing hormone (GnRH) in slices from embryonic nasal compartment and forebrain. Developmental brain research 97(2): 287-292 (1996b)
Topaloglu AK et al., TAC3 and TACR3 mutations in familial hypogonadotropic hypogonadism reveal a key role for Neurokinin B in the central control of reproduction. Nature genetics 41, 354-358 (2009).
Tornberg J et al., Heparan sulfate 6-O-sulfotransferase 1, a gene involved in extracellular sugar modifications, is mutated in patients with idiopathic hypogonadotrophic hypogonadism. Proc. Natl Acad. Sci. USA 108, 11524－11529 (2011).
Tran D et al., Anti-Mullerian hormone is a functional marker of foetal Sertoli cells. Nature 269(5627): 411-2 (1977)
Tremblay JJ et al., Modulation of endogenous GATA-4 activity reveals its dual contribution to Mullerian inhibiting substance gene transcription in Sertoli cells. Mol Endocrinol 15(9): 1636-50. (2001)
Tsai PS et al., Targeted expression of a dominant-negative fibroblast growth factor (FGF) receptor in gonadotropin-releasing hormone (GnRH) neurons reduces FGF responsiveness and the size of GnRH neuronal population. Mol Endocrinol. 19(1):225-36 (2005)
Tsuji M et al., Effect of human recombinant mullerian inhibiting substance on isolated epithelial and mesenchymal cells during mullerian duct regression in the rat. Endocrinology 131(3): 1481-1488. (1992)
Tuttelmann F et al., Anti-Müllerian hormone in men with normal and reduced sperm concentration and men with maldescended testes. Fertility and sterility. 91(5): 1812-1819. (2009)
Twan WH et al., The presence and ancestral role of gonadotropin-releasing hormone in the reproduction of scleractinian coral, Euphyllia ancora. Endocrinology. 147(1): 397-406. (2006)

Valverde F et al., Formation of an olfactory glomerulus: morphological aspects of development and organization. Neuroscience 49, 255-275 (1992).
van Rooij IA et al., Serum anti-Mullerian hormone levels: a novel measure of ovarian reserve. Hum Reprod 17(12): 3065-71. (2002)
Van Vugt DA et al., Gonadotropin-releasing hormone pulses in third ventricular cerebrospinal fluid of ovariectomized rhesus monkeys: correlation with luteinizing hormone pulses. Endocrinology 117, 1550-1558 (1985).
Verney C et al., Changing distribution of monoaminergic markers in the developing human cerebral cortex with special emphasis on the serotonin transporter. The Anatomical record 267, 87-93 (2002).
Verrijn S et al., An amino-terminal DAX1 (NROB1) missense mutation associated with isolated mineralocorticoid deficiency. J Clin Endocrinol Metab. 92(3): 755-761. (2007)
Vigier RS et al., Transcription factor GATA-4 is expressed in a sexually dimorphic pattern during mouse gonadal development and is a potent activator of the Müllerian inhibiting substance promoter. Dev. Camb. Engl. 125, 2665－2675. (1998)
Vilensky JA, The neglected cranial nerve: nervus terminalis (cranial nerve N). Clinical anatomy 27, 46-53 (2014).
Visser JA et al., The Serine/Threonine Transmembrane Receptor ALK2 Mediates Müllerian Inhibiting Substance Signaling. Mol. Endocrinol. 15, 936－945 (2001)
Visser JA, AMH signaling: from receptor to target gene. Mol. Cell. Endocrinol. 211, 65－73. (2003)
Visser JA. Shaping up the function of anti-Müllerian hormone in ovaries of mono-ovulatory species. Human Reprod. 31(7): 1403-1405. (2016)
Vissers Lisenka ELM et al., Mutations in a new member of the chromodomain gene family cause CHARGE syndrome. Nature genetics 36(9): 955. (2004)
Wang HJ et al., Increased GnRH mRNA in the GnRH neurons expressing cFos during the proestrous LH surge. Endocrinology. 136(8):3673-6 (1995)
Wang P et al., Mullerian Inhibiting Substance acts as a motor neuron survival factor in vitro. PNAS. 102, 16421－16425. (2005)
Wang P et al., Mullerian inhibiting substance contributes to sex-linked biases in the brain and behavior. PNAS. 106, 7203－7208. (2009)
Watabe T & Miyazono K. Roles of TGF-[beta] family signaling in stem cell renewal and differentiation. Cell research. 19(1): 103. (2009)
Watanabe M et al., GABAA receptors mediate excitation in adult rat GnRH neurons. Biol of reprod. 81(2): 327-332 (2009)
Weiss A & Attisano L. The TGFbeta superfamily signaling pathway. Wiley Interdisciplinary Reviews: Developmental Biology. 2(1): 47-63. (2013)
Weisstanner C et al., MRI of the Fetal Brain. Clin. Neuroradiol. 25, 189－196. (2015)
Western PS et al., Temperature-dependent sex determination in the American alligator: AMH precedes SOX9 expression. Dev Dyn 216(4-5): 411-9. (1999)
Whitlock KE et al., Gonadotropin-releasing hormone (GnRH) cells arise from cranial neural crest and adenohypophyseal regions of the neural plate in the zebrafish, Danio rerio. Dev Biol. 257(1):140-52 (2003)
Wilhelm D et al., Sex determination and gonadal development in mammals. Physiol. Rev. 87, 1－28. (2007)

Wilson AC et al., Human neurons express type I GnRH receptor and respond to GnRH I by increasing luteinizing hormone expression. The Journal of endocrinology 191, 651-663, (2006).
Wilson CA et al., Mullerian inhibiting substance requires its N-terminal domain for maintenance of biological activity, a novel finding within the transforming growth factor-beta superfamily. Mol. Endocrinol. 7, 247-257. (1993)
Winter JSD et al., Pituitary-gonadal relations in infancy. 2. Patterns of serum gonadal steroid concentraions in man from birth to two years of age. J Clin Endocrinol Metab. 42: 679-86 (1976)
Wirsig-Wiechmann CR et al., Pheromonal activation of vomeronasal neurons in plethodontid salamanders. Brain Res. 952(2): 335-44 (2002)
Wirsig-Wiechmann CR & Oka Y, The terminal nerve ganglion cells project to the olfactory mucosa in the dwarf gourami. Neuroscience research 44, 337-341 (2002).
Wise PM et al., Menopause: the aging of multiple pacemakers. Science. 5;273(5271):67-70. (1996)
Witkin JW & Silverman AJ, Luteinizing hormone-releasing hormone (LHRH) in rat olfactory systems. J Comp Neurol. 218, 426-432, (1983).
Wrana JL. Regulation of Smad activity. Cell 10(2): 189-192. (2000)
Wray S et al., A subset of peripherin positive olfactory axons delineates the luteinizing hormone releasing hormone neuronal migratory pathway in developing mouse. Dev Biol. 166, 349-354 (1994).
Wray S et al., Evidence that cells expressing luteinizing hormone-releasing hormone mRNA in the mouse are derived from progenitor cells in the olfactory placode. PNAS. 86, 8132-8136 (1989).
Wray S, Development of Luteinizing hormone releasing hormone neurones. J of Neuroendocrinol. 13(1): 3-11 (2001)
Wray S, From Nose to Brain: Development of Gonadotropin-releasing hormone -1 Neurons. J Neuroendocrinol. 22(7): 743-53 (2010)
Wu X et al., Mullerian inhibiting substance recruits ALK3 to regulate Leydig cell differentiation. Endocrinology 153(10): 4929-37. (2012)
Wu X et al., Pubertal and adult Leydig cell function in Mullerian inhibiting substance-deficient mice. Endocrinology 146(2): 589-95. (2005)
Wu W et al., Directional guidance of neuronal migration in the olfactory system by the protein Slit. Nature 400(6742): 331. (1999(
Xu N et al., A mutation in the fibroblast growth factor receptor 1 gene causes fully penetrant normosmic isolated hypogonadotropic hypogonadism. J. Clin. Endocrinol. Metab. 92, 1155-1158 (2007).
Yabe T et al., Bone morphogenetic proteins BMP-6 and BMP-7 have differential effects on survival and neurite outgrowth of cerebellar granule cell neurons. Journal of neuroscience research. 68(2): 161-168. (2002)
Yamada S et al., Developmental atlas of the early first trimester human embryo. Dev. Dyn. 239, 1585-1595. (2010)
Yamashita Y et al., Activation of PKA, p38 MAPK and ERK1/2 by gonadotropins in cumulus cells is critical for induction of EGF-like factor and TACE/ADAM17 gene expression during in vitro maturation of porcine COCs. J Ovarian Res. 2(1): 20. (2009)
Yamauchi Y et al., Two Y genes can replace the entire Y chromosome for assisted reproduction in the mouse. Science 343(6166): 69-72. (2014)
Yeo TT et al., Characterization of gonadotropin-releasing hormone gene transcripts in a mouse hypothalamic neuronal GT1 cell line. Brain Res Mol Brain Res.42(2):255-62 (1996)

Yepes M et al., Regulation of seizure spreading by neuroserpin and tissue-type plasminogen activator is plasminogen-independent. JCI. 109(12): 1571. (2002)
Yi S et al., The type I BMP receptor BmprIB is essential for female reproductive function. PNAS. 98(14): 7994-9. (2001)
Yin W & Gore AC. Neuroendocrine control of reproductive aging: roles of GnRH neurons. Reproduction. 232(3): 403-14 (2006)
Yoshida K et al., The migration of luteinizing hormone-releasing hormone neurons in the developing rat is associated with a transient, caudal projection of the vomeronasal nerve. J Neurosci 15, 7769-7777 (1995).
Young J et al., SEMA3A deletion in a family with Kallmann syndrome validates the role of semaphorin 3A in human puberty and olfactory system development. Human reproduction 27, 1460-1465 (2012).
Yu RN et al., Role of Ahch in gonadal development and gametogenesis. Nature genetics. 20(4): 353-57 (1998)
Zhan Y et al., Mullerian inhibiting substance regulates its receptor/SMAD signaling and causes mesenchymal transition of the coelomic epithelial cells early in Mullerian duct regression. Development 133, 2359-2369 (2006).
Zhang YE. Non-Smad pathways in TGF-β signaling. Cell research 19(1): 128. (2009)
Zhang G et al., Hypothalamic programming of systemic ageing involving IKK-beta, NF-kappaB and GnRH. Nature 497, 211-216 (2013).
Zhao F et al., Elimination of the male reproductive tract in the female embryo is promoted by COUP-TFII in mice. Science. 357(6352): 717-720. (2017)
Zhou Y et al., Semaphorin signaling: progress made and promises ahead. Trends in biochemical sciences. 33(4): 161-170. (2008)

ANNEX 1

Cranial nerves

	Name	Cranial exit	Modality	Function
CN N	Terminal n.	Cribriform plate	Sensory?	Unknown in humans
CN I	Olfactory n.	Cribriform plate	Sensory (SSS)	Smell
CN II	Optic n.	Optic canal	Sensory (SVS)	Vision
CN III	Occulomtor n.	Sup. Orbital fissure	Motor (GSM & GVM)	Extrinsic eye muscles & *levator palpebrae superioris m.* Pupillary sphincter
CN IV	Trochlear n.	Sup. Orbital fissure	Motor (GSM)	Superior oblique m.
CN V	Trigeminal n.			
V_1	Opthalmic	Sup. Orbital fissure	GSS	Scalp, forehead and nose
V_2	Maxillary	*Foramen rotundum*	GSS	Cheeks, lower eye lid, nasal mucosa, upper lip, upper teeth and palate
V_3	Mandibular	Foramen ovale	Both Sensory (GSS) Motor (SVM)	GSS: anterior 2/3 tongue, skin over mandible and lower teeth SVM: muscles of mastication
CN VI	Abducens n.	*Sup.* Orbital fissure	Motor (GSM)	Lateral rectus m.
CN VII	Facial n.	Int. acoustic meatus, stylomastoid foramen	Both Sensory (GSS & SVS) Motor (GVM & GVM)	GSS: sensation to part of ext. ear SVS: taste from ant. 2/3 tongue, hard and soft palate. GSM: muscles of facial expression GVM: lacrimal, submandibular, sublingual glands and mucous glands of mouth and nose
CN VIII	Vestibulocochlear n.	Int. acoustic meatus	Sensory (SSS)	Hearing & balance
CN IX	Glossopharyngeal n.	Jugular foramen	Both Sensory (GSS, GVS, SVS) Motor (GVM & SVM)	GSS: post. 1/3 tongue, ext. ear, and middle ear cavity GVS: carotid body and sinus SVS: taste from post. 1/3 tongue GVM: parotic gland. SVM: stylopharyngeus m.

CN X	Vagus n.	Jugular foramen	Both Sensory (GSS GVS SVS) Motor (GVM & SVM)	GSS: ext. ear, larynx and pharynx. GVS: larynx, pharynx and, thoracic & abdominal viscera. SVS: taste from epiglottis region of tongue GVM: smooth muscles of pharynx, larynx and most of the gastrointestinal tract SVM: most muscles of pharynx and larynx
CN XI	Accessory n.	Jugular foramen	Motor (GSM & SVM)	GSM: trapezius and sternocleidomastoid SVM: a few fibres run with CN X to viscera
CN XII	Hypoglossal n.	Hypoglossal canal	Motor (GSM)	Intrinsic and extrinsic tongue muscles (except the palatoglossus m.)

Table 11. Anatomical features of the cranial nerves

The olfactory nerve (CN I) and optic nerve (CN II) originate from the cerebrum

Midbrain – pontine junction – CN III
Pons – CN V
Medulla Oblongata – posterior to the olive: CN IX–XI.
Midbrain – posterior midbrain CN IV
Pontine–medulla junction – CNVI–VIII
Anterior to the olive: CN XII

Sensory (afferent) Modalities

General somatic sensory (GSS) – general sensation from skin.
General visceral sensory (GVS) – general sensation from viscera.
Special somatic sensory (SSS) – senses derived from ectoderm (sight, sound, balance).
Special visceral sensory (SVS) – senses derived from endoderm (taste).

Motor (efferent) Modalities

General somatic motor (GSM) – skeletal muscles.
General visceral motor (GVM) – smooth muscles of gut and autonomic motor. Reference: Moore et al., 2006

Étude anatomique, moléculaire et génétique de migration des neurones à GnRH chez la souris et l'homme

Résumé

Chez les mammifères, le contrôle de la reproduction est médié par un réseau hypothalamique qui intègre divers stimuli pour réguler la sécrétion de la Gonadotropin Releasing Hormone (GnRH). Ces neurones à GnRH naissent dans la placode olfactive et migrent vers le cerveau le long des axones vomeronasaux et terminaux au cours du développement embryonnaire. Bien que ce processus a bien été étudié chez les rongeurs, sa caractérisation complète chez l'homme reste inachevée. Il est largement admis que des perturbations dans le développement ou dans la sécrétion de GnRH sont associées chez l'homme à un hypogonadisme hypogonadotrope congénital (CHH), qui est un trouble caractérisé par un retard ou une absence de la puberté conduisant à l'infertilité. Les systèmes GnRH et olfactif ont des liens complexes au cours du développement, le syndrome de Kallmann (KS) représente un trouble qui associe l'hypogonadisme dû à une déficience en GnRH et l'anosmie. Le CHH et le KS sont des troubles oligogéniques, les mutations génétiques sous-jacentes n'expliquent que 50% des cas cliniques. Dans cette étude, nous avons entrepris une caractérisation complète du processus migratoire des neurones à GnRH au cours du premier trimestre de gestation sur une grande série d'embryons et de fœtus humains, ce qui nous a permis d'élaborer le premier atlas chronologique et quantitatif de la distribution de GnRH. En effet, l'utilisation d'une nouvelle approche de transparisation des tissus embryologiques humains par de solvants organiques, a permis d'établir pour la première fois, une véritable représentation des neurones dans leur contexte natal in vivo. De plus, les résultats de cette étude ont non seulement révélé que le nombre de neurones GnRH chez l'homme était significativement plus élevé que prévu, mais aussi que ces derniers migrent vers plusieurs régions du cerveau extra-hypothalamique, en plus de l'hypothalamus. Leur présence dans ces régions soulève l'hypothèse qu'ils pourraient exercer des rôles non reproductifs, créant de nouvelles pistes pour la recherche sur les fonctions du système GnRH dans les processus cognitifs, comportementaux et physiologiques. Le second objectif de ce travail a visé à caractériser un nouveau gène candidat impliqué dans le développement du système GnRH: L'hormone Anti-Müllerienne (AMH), connue pour son rôle dans la différenciation de la gonade bipotentielle chez les mâles. Néanmoins, une récente étude menée par notre équipe a mis en évidence son rôle extragonadique sur les neurones à GnRH en période post-natale. Le séquençage complet d'une large cohorte de patients européens a révélé plusieurs nouvelles mutations faux-sens dans le gène de l'AMH chez les patients atteints de CHH et KS, non retrouvés dans la cohorte des témoins. L'évaluation de la pertinence fonctionnelle de ces mutations a ensuite été effectuée par diverses analyses biochimiques in vitro de la bioactivité des mutations, ainsi que par la caractérisation d'une lignée de souris transgénique. Ce qui a entraîné une diminution de la sécrétion de l'AMH et une diminution de la bioactivité de la protéine sécrétée dans les études in vitro; Conduisant à une éventuelle réduction de la capacité migratoire. Cela suggère fortement que ces mutations pourraient avoir un effet pathogène. En outre,nous montrons que le récepteur AMHR2 est exprimé le long des fibres olfactives et par les neurones à GnRH pendant le processus migratoire GnRH. L'analyse pathohistologique des souris Amhr2$^{-/-}$ a révélé une altération de la migration embryonnaire des neurones à GnRH vers le cerveau antérieur basal, entraînant une réduction significative du nombre total de neurones GnRH dans les cerveaux adultes de ces animaux, conduisant à une fertilité réduite. L'ensemble de ces travaux indiquent que l'insuffisance de signalisation AMH contribuerait à la pathogenèse des troubles de CHH chez l'homme, et met en évidence un nouveau rôle de l'AMH dans développement et la fonction des neurones GnRH.